Use of Gaseous Ozone to Prevent Post-harvest Microbial Spoilage of Leafy Produce

Shreya Baldev Wani

Doctor of Philosophy

School of Biology
Newcastle University

29 September 2015

Declaration

I, Shreya Wani declare that this thesis and the work presented in it are my own and have been generated by me as the result of my own original research. Where other sources of information have been used, they have been duly acknowledged.

Shreya B. Wani

“Forces of nature act in a mysterious manner. We can but solve the mystery by deducing the unknown result from the known results of similar events”

Mahatma Gandhi

Abstract

Fresh leafy salads suffer from post-harvest microbial contamination and decay. Due to increasing pesticide resistance and consumer pressures, residue free alternatives, such as ozone, are being actively explored and encouraged to reduce microbial loads of crops in storage/transit. Previous work has demonstrated that long-term exposure to low concentrations of ozone can be effective in retarding the degradation of some fruit and vegetable. Much less is known about the potential of ozone-exposure to protect leafy produce. The first goal of this project was to determine ozone exposure levels that did not damage produce, but reduced microbial loads significantly. Different produce types exhibited varying abilities to resist ozone damage, e.g. coriander and rocket were relatively resistant to ozone (10 ppm for 10 min); while spinach, watercress and lettuce were more sensitive (1 ppm for 10 min). These ozone exposure levels reduced bacterial loads by at least 1-log. Confocal microscopy confirmed that some bacterial cells (1−10%) survived ozone treatment. These visual observations demonstrated heterogeneity in the resistance of the leaf surface microflora to ozone treatment. It was tested if colony age and/or stress (e.g. cold) may be responsible for the variation in ozone resistance observed. Stressed cells of *Pseudomonas* sp. isolated from coriander exhibited greater resistance to ozone than control cells. Subsequent gene expression analysis using RNA-Seq technology of stressed cells showed significant changes in the expression of genes related to stress resistance compared to controls. In particular, it was observed that in aged colonies, about 90% of the changes in gene expression mapped to one gene, a non-coding RNA that is part of RNase P. Many of the genes showing differential expression were involved in energy production and transport, motility or cell wall/membrane integrity. This improved mechanistic understanding of ozone resistance may lead to novel anti-microbial treatments.

As there are growing concerns about the contamination of leafy products with pathogens resulting in food poisoning the final part of this work focused on the potential of ozone to inactivate food pathogens on leafy produce. Results showed that this treatment significantly reduced *E. coli* and *Listeria* spp. on spinach, and the pathogens did not re-grow after treatment over a 9-day storage period.

It was concluded that gaseous ozone treatment is worthy of further exploration as a potential commercial tool to improve the safety of fresh leafy salads and herbs, and reduce microbial spoilage.

Keywords: gaseous ozone treatment, fresh produce, spinach, coriander, watercress, lettuce, rocket, microbial spoilage, *Pseudomonas* sp., food-pathogens, *Escherichia coli, Listeria spp.*

Acknowledgements

I would first like to thank my PhD supervisors, Dr Ian Singleton and Professor Jeremy Barnes, for their help, advice, support and encouragement throughout the project, and especially for giving me the opportunity to conduct such an interesting investigation. Extended thanks to my industrial representatives Dr Steve Rothwell from Vitacress Salads Ltd and Thane Goodrich from Intercrop Ltd for their valuable inputs and continued interest in the progression of the project. Thanks to HDC (Horticultural Development Company) for funding my PhD Studentship in conjunction with Vitacress Salads Ltd, Intercrop Ltd, Geneius Laboratories Ltd and Biofresh Ltd. The assistance and training provided by my colleagues was invaluable to the success of my project, and I would like to thank every PhD student and member of staff, past and present, for their friendship and encouragement. Particular thanks to Dr Matthew Peake for his continued effort in keeping the lab running smoothly and training in microbiological and molecular techniques. Thanks to Trevor Booth at medical department for helping me with confocal microscopy for producing LIVE/DEAD bacterial images on leaves and his enthusiasm for my research. Thanks to Illinois University for performing RNA Sequencing on my samples and providing me with bioinformatics data. Special thanks to Alan Craig for maintaining and calibrating my ozone unit in lab routinely. My fellow PhD students in the School of Biology, particularly Dalal Al-baijan, Aayush Sharma, Hartati, Sammy Logan, David Smith and Ashly Chessher, deserve special mention for their friendship. My overwhelming gratitude goes to Jagpreet Kaur Maker for assisting and helping me during my project and also editing/formatting my thesis and manuscripts for journal publications.

I would like to thank all of my family and my brother, Monil for their support, for listening and for their unshakeable faith in me throughout the numerous ups and downs of research. Immense thanks to my parents, Leena and Baldev; for their love, support, blessings and giving me such an excellent start in life, without which I would never have achieved all that I have so far in my life and career.

Finally, to my husband, then fiancé, Sagar Basutkar for being patient and holding my hand, keeping my spirits up and always making me smile even when things were tough.

Lastly, I would like to thank God for what He has given me in my life.

Publications

1) Wani S, Maker J, Thompson J, Barnes J, Singleton I (2015) Effect of Ozone Treatment on Inactivation of *Escherichia coli* and *Listeria* sp. on Spinach. Agriculture 5 (2):155-169. doi:10.3390/agriculture5020155 (Appendix E)

2) Wani S, Barnes J, Singleton I (2016) Investigation of potential reasons for bacterial survival on 'ready-to-eat' leafy produce during exposure to gaseous ozone. Postharvest Biology and Technology 111:185-190. doi:10.1016/j.postharvbio.2015.08.007 (Appendix F)

Table of Contents

List of Figures

Chapter 1

Chapter 2

Chapter 3

Chapter 4

Chapter 5

List of Tables

Chapter 1

Chapter 2

Chapter 3

Chapter 4

Chapter 5

Abbreviations

ALOA	Agar Listeria according to Ottaviani and Agosti
BLAST	Basic Local Alignment Search Tool
BOD	Biological oxygen demand
BPW	Buffered Peptone Water
CA	California
cDNA	Complementary DNA
CFC	Cephaloridin Fucidin Centrimide
CFU	Colony forming unit
CFU/g	Colony forming unit per gram
COD	Chemical oxygen demand
COG	Cluster of orthologous groups
CSLM	Confocal scanning laser microscopy
CsrA	carbon storage regulator
DBP	Disinfection by-product
DEG/DEGs	Differentially expressed genes
DNA	Deoxyribonucleic acid
dNTP	Deoxynucleotide nucleoside triphosphate
DRBC	Dichloran Rose Bengal Chloramphenicol
EAW	Electrolysed acidic water
EC	Enzyme Commision
EHEC	Enterohaemorrhagic
EOL	End of life
EPA	Environmental Protection Agency
EPS	Exopolysaccharides
EW	Electrolysed water

FDA	Food and Drug Administration
FDR	False discovery rate
Fig.	Figure
FITC	Fluorescein isothiocyanate
GRAS	Generally Recognized As Safe
HAAs	Haloacetic acids
HSP	Heat-shock protein
HTST	High temperature for short time
HUS	Haemolytic uremic syndrome
LB	Luria-Bertani
Log	Logarithm
LPS	Lipopolysaccharides
MA	Modified atmosphere
MHB	Mueller Hinton Broth
MRD	Maximum recovery diluent
mRNA	Messenger RNA
NA	Nutrient agar
NCBI	National Center for Biotechnology Information
NEW	Neutral electrolysed water
NGS	Next generation sequencing
NIOSH	National Institute of Occupational Safety and Health
Nt	Nucleotides
OSHA	Occupational Safety and Health Administration
PA	Peroxyacetic acid
PBS	Phosphate buffer soltion
PCA	Plate Count Agar
PCR	Polymerase chain reaction

PI	Propidium iodide
PMTs	Photomultiplier tube detectors
POD	Peroxidase
PPO	Polyphenol oxidase
qPCR	Quantitative PCR
RNA	Ribonucleic acid
ROS	Reactive oxygen species
rRNA	Ribosomal ribonucleic acid
RsmA	repressor of stationary-phase metabolites
RT	Reverse transcription
RTE	Ready-to-Eat
RT-PCR	Real-time polymerase chain reaction
SAGE	Serial analysis of gene expression
SEM	Scanning electron microscopy
SOL	Start of life
TBX	Tryptone Bile X-Glucuronide
TCA	Tricarboxylic acid
TEM	Transmission electron microscopy
THMs	Trihalomethanes
tRNA	Total RNA
TVC/TVCs	Total Viable Counts
UK	United Kingdom
USA	United States of America
US-FDA	United States Food and Drug Administration
UV	Ultraviolet
VTEC	Verocytotoxigenic Escherichia coli
WHO	World Health Orgonisation

Chapter 1 General Introduction

1.1 General introduction

The increasing popularity of fresh produce as a food source is due to its accepted importance as a source of vitamins, fibre and nutrients (Olaimat and Holley 2012). Production of leafy produce has grown rapidly in the past few decades due to increases in year-round consumption and rising demand for worldwide distribution (Little and Gillespie 2008). Research suggests that a low fat and high fibre diet, which mainly includes abundant consumption of fruits and vegetables, is protective against illness such as cancers and cardiovascular diseases (Mercanoglu Taban and Halkman 2011). Increased consumption of leafy produce is predominantly encouraged by the trend of healthier lifestyles and the '5 A DAY – live well' concept promoted world-wide by Governments and independent health authorities (Little and Gillespie 2008).

Fresh leafy produce typically has a limited shelf-life due to microbial spoilage, receives minimum processing and is generally consumed raw (Naito and Takahara 2006). Minimal processing means that there is an increased risk of microbial food-borne disease to the consumer; therefore, research into methods of reducing microbial contamination to prevent both spoilage and reduce the risk of food-borne disease to consumers is important (Naito and Takahara 2006). Spoilage of produce is caused by numerous microbial species by either breaking the protective cover of the leaf or by entering the plant tissue through wounds (Tournas 2005b). It appears that microbial contamination can arise at any stage from production to consumer consumption and this contamination can occur from animal, environmental or human sources (Olaimat and Holley 2012). The microbial communities found on leafy produce are commonly dominated by bacteria from the *Enterobacteriaceae* and *Pseudomonadaceae* families and the total microbial population commonly ranges from 10^5–10^7 CFU cm^{-2} (Ragaert et al. 2007). Generally, the microbial populations present do not affect foliage in the field, but after harvesting and storage, certain bacteria such as *Pseudomonas* spp., *Bacillus* spp. and *Erwinia* spp. can begin to cause soft rot of the produce (Saranraj 2012). The proteolytic and pectinolytic activities that cause soft rot can be carried out by these microbes at storage temperatures as low as 0.2°C (Saranraj 2012). For example, a total of 8,000 tonnes of processed vegetables and salad was wasted in 2012

in the UK due to microbial contamination and the cost of this waste was approximately £23 million (WRAP 2012).

In addition to spoilage, microbes present on leafy produce have also been implicated in human disease. All types of leafy produce have the potential to harbour pathogens, such as *Escherichia coli*, *Listeria monocytogenes*, *Shigella* spp. and *Salmonella* spp., which are ultimately responsible for the majority of food-borne illnesses (Abadias et al. 2008). A multi-state outbreak of *E. coli* O157:H7 emerging from spinach was reported in the United States in 2006, resulting in 276 cases of food-borne illness and three deaths (Goodburn and Wallace 2013). A total of 88 outbreaks with more 3435 cases of illness were reported in the United Kingdom between 1996 and 2006 relating to fresh produce (Goodburn and Wallace 2013). Verotoxigenic *E. coli* (VTEC) O104 outbreak in Europe, traced to sprouting salad seed consumption, resulted ultimately in 56 deaths (Da Silva Felicio et al. 2015). Microbial contamination of fresh produce by pathogenic microbes not only poses significant risk to public health but also affects the industry financially by resulting in costly product recalls. For example, the recent Shiga toxin-producing *E. coli* O157 outbreak in watercress is estimated to have required the recall of two hundred thousand items from retailers in the United Kingdom (Launders 2013).

The safety of leafy produce is considered a high priority from an international perspective by the World Health Organisation (WHO) (Goodburn and Wallace 2013). To reduce contamination, leafy produce is often treated with various chemical compounds including ethanol, chlorine, sodium hypochlorite and/or organic acids (Naito and Takahara 2006). However, high dosage and repeated usage of these compounds potentially results in tainting of the produce and results in residues of concern on the surface of the treated leaves and equipment (Naito and Takahara 2006). Hence, there is a major commercial interest in developing alternative treatment methods to reduce losses of leafy salads by microbial spoilage. Given the importance of controlling microbial spoilage and pathogen contamination, the present study concentrates on optimizing an alternative treatment—gaseous ozone—to reduce microbial spoilage and inactivate food-borne pathogens on the surface of the leafy produce without causing physical damage to the produce.

1.2 Microbial contamination of leafy salads

1.2.1 Action of spoilage micro-flora

Almost all leafy salads provide a suitable environment for the growth and survival of various types of microbes (Saranraj 2012; Mohamed Mahroop Raja 2012) encouraged by the nearly neutral pH, high levels of nutrient availability and the wetness of phylloplane environment (Ragaert et al. 2007; Tournas 2005b; Mohamed Mahroop Raja 2012). Leaves primarily consist of polysaccharides including pectin, cellulose and hemicellulose and lignin, with starch being the major storage polymer (Saranraj 2012; Tournas 2005b; Lee et al. 2013). The leaf surface thus provides a carbon and nutrient-rich environment in which microbes may flourish. Moreover, leaves are exposed to various stresses before, during and/or after harvest due to adverse weather conditions, birds, pests, rodents, harvesting and processing which could cause physical injury (Ragaert et al. 2007). Damaged areas on leaves provide a refuge for bacterial growth (Ragaert et al. 2007). For example, levels of *Pseudomonas fluorescens* contamination are directly proportional to the quantity of sugars present on the leaves (Mercier and Lindow 2000). Spoilage micro-organisms grow and survive on hosts by producing lytic enzymes that degrade plant polymers to release nutrients and water (Saranraj 2012). The glucosidic bond of pectin (major structural leaf component) is split by pectinolytic enzymes, resulting in liquefaction and softening of the leafy produce (Lee et al. 2013). Pectin degradation is considered to be the initial stage of spoilage and cellulose is degraded by cellulase enzymes produced by some microbes, however, cellulose degradation is believed to follow the breakdown of pectins (Tournas, 2005b).

Once microbes have gained entry to the leaf, they then have access to internal nutrient sources. For example, during spoilage, amylase breaks down starch to maltose and maltose is further hydrolysed into two glucose molecules. All micro-organisms use glucose as their main source of carbon, but some microbes use other sugars such as sucrose, fructose, mannitol, cellobiose and rhamnose. Through glycolysis, glucose is metabolised to generate pyruvic acid which may further be converted into acetic acid. This acetic acid is then broken down to water and carbon dioxide via the tricarboxylic acid (TCA) cycle. This is how microbes metabolise glucose aerobically. Many microbes are capable of metabolizing pyruvic acid through anaerobic pathways by converting it to

acetaldehyde or lactic acid (Jacxsens et al. 2003). Further, alcohol dehydrogenase converts acetaldehyde to ethanol (this is termed anaerobic fermentation). Relatively few filamentous fungal (mould) species can ferment glucose, but many bacteria and yeast have this ability. The metabolic pathway selected during spoilage of the produce completely depends upon the organisms involved (Tournas 2005a). For example, *Leuconostoc* spp. convert carbohydrates into ethyl alcohol, lactic acid and carbon dioxide, whereas *E. coli* metabolizes carbohydrate into formic acid, lactic acid, acetic acid, carbon dioxide and hydrogen (Sathe et al. 2007). Carbohydrate breakdown of produce sometimes contributes to unpleasant flavours and odours, which in conjunction with discolouration and softening, result in product that is unacceptable for human consumption (Tournas 2005a). Vitamins and minerals may also subject to microbial degradation, thereby reducing the nutritional value of the product (Tournas 2005a).

1.2.2 Types of Spoilage micro-flora

A wide variety of microbes, including both Gram-positive and Gram-negative bacteria, lactic acid bacteria, pectinolytic organism, yeasts and moulds, can be responsible for spoilage of the leafy produce, resulting in high economic losses (Barth et al. 2009; Tournas 2005a). The slimy and watery appearance of decayed produce is typical of bacterial spoilage, whereas some fungal rots can also cause a soft and watery appearance. However, fungal spoilage is easily distinguished by the occurrence of fungal mycelia and spore-forming structures (Tournas 2005a). A summary of the spoilage organisms commonly involved in the spoilage of leafy produce is shown in Table 1.1.

Table 1. 1: Predominant spoilage microflora contaminating leafy salads

Spoilage organism	Type of spoilage	Reference
Bacteria		
Erwinia carotovora	Bacterial soft rot	Tournas 2005a
Erwinia herbiccola	Bacterial soft roft	Ragaert et al. 2007
Pseudomonas chicorii	Bacterial zonate spot	Tournas 2005a
P. marginalis group	Soft rot of leafy vegetables	Tournas 2005a
P. fluorescens	Bacterial soft rot	Tournas 2005a
P. putida	Bacterial soft rot	Tournas 2005a
Rahnella aquatilis	Soft rot	Ragaert et al. 2007
Xanthomonas campestris	Black rot	Tournas 2005a
		Tournas 2005a
Fungi		
Alternaria brassicola	Alternaria rot	Tournas 2005a
Botrytis cinerea	Grey mould rot	Tournas 2005a
Geotrichum candidum	Sour rot	Tournas 2005a
Rhizoctonia spp.	Slimy brown rot	Tournas 2005a

Counts of bacteria on 'Ready-to-Eat' packaged salads bags have found varying microbial population levels: 5.4×10^6, 1.5×10^7 and 3.7×10^7 CFU/g within 24 h of packing (Goodburn and Wallace 2013). High yeast and mould counts from several 'Ready-to-Eat' packaged salad bags were also detected (Barth et al. 2009). The dominant genera of bacteria involved in spoilage of produce at low temperature consists of species belonging to *Enterobacteriaceae, Rahnella aquatilis and Erwinia herbicola and Pseudomonadaceae* (especially *P. fluorescens*) (Ragaert et al. 2007). These organisms are capable of fermenting many sugars and alcohols that are not used by other species (Tournas 2005a). Lactic acid bacteria, especially *Leuconostoc mesenteroides, Lactobacilli and Lactic streptococci,* are also associated with decomposition of the produce (Ragaert et al. 2007). Phytopathogenic organisms like *Burkholderia cepacia* (similar to *Pseudomonas* spp.) and *Pantoea agglomerans* (similar to *Enterobacter* and *Erwinia* spp.) are also commonly isolated (Barth et al. 2009). Numerous yeast species have been identified as contaminants of fresh leafy salads including *Cryptococcus, Torulaspora, Candida, Rhodotorula and Pichia* (Ragaert et al.

2007). The most common moulds (filamentous fungi) isolated from salads include *Alternaria, Aspergillus, Fusarium, Cladosporium, Mycosphaerella and Penicillium* (Barth et al. 2009), but these are not generally reported to cause spoilage when compared with bacteria and yeast (Barth et al. 2009).

1.2.3 Food pathogens

Although spoilage bacteria, yeasts and moulds dominate on fresh produce, food-borne pathogens may also be present (Olaimat and Holley 2012). Hence, fresh produce is known as a possible vehicle for food-borne outbreaks due to pathogens such as *E. coli* O157:H7, *Salmonella* spp., *Cryptosporidium*, *Cyclospora* spp., *L. monocytogenes*, *Shigella* spp., Norovirus and *Clostridium botulinum* (Warning and Datta 2013; Brandl 2006).

Contamination of fresh produce with pathogens can occur either pre-harvest and/or post-harvest. Pre-harvest sources of pathogens generally include organic fertilizers, irrigation water and soil (Fig. 1.1), whereas post-harvest sources are mainly unhygienic human handling of equipment, transport vehicles, containers, etc. (Olaimat and Holley 2012).

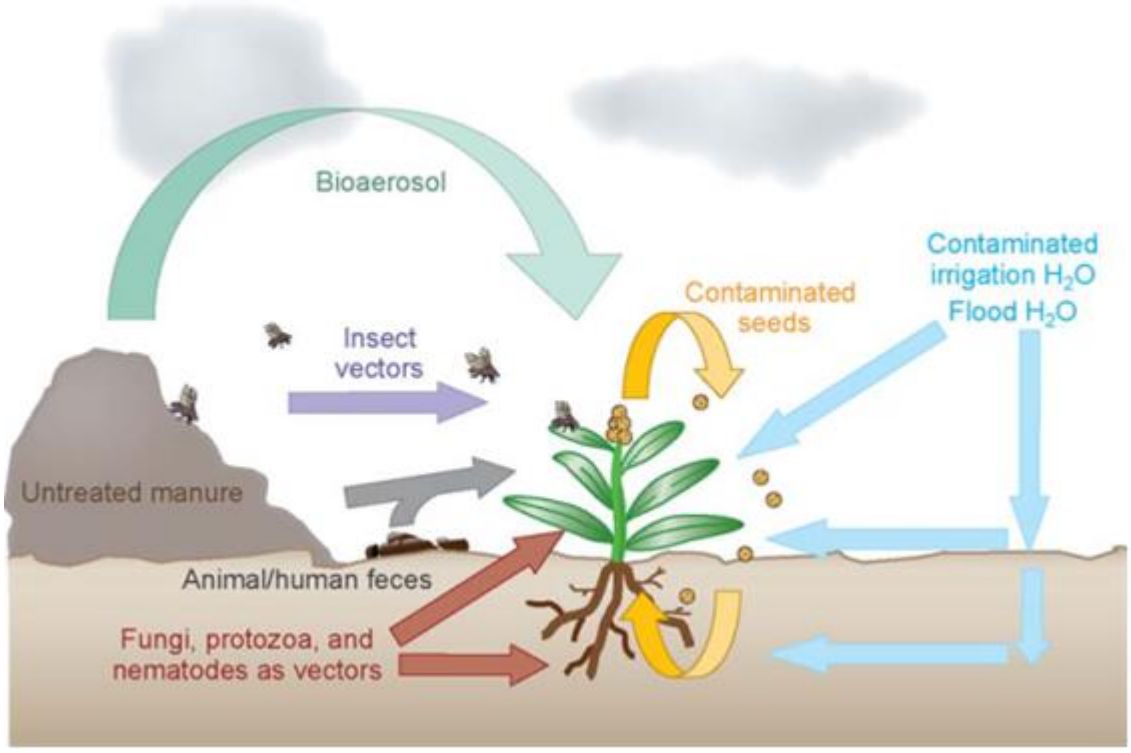

Figure 1. 1: Schematic illustration of factors that can contribute to the contamination of produce with pathogens in the field (adapted from Brandl 2006).

Application of organic fertilizers like animal manures, sewage waste, slurries and sludge in the field can directly introduce pathogens that can potentially contaminate leafy produce (Heaton and Jones 2008). Annually in the UK, approximately 90 million tonnes of organic fertilizers are applied to land (Food Standards Agency 2004a, Aviation House, London, UK).

Pathogens may be naturally present in soil, but they can also be introduced from organic wastes added as fertilizer. Produce can become contaminated by microbes present in soil when water spray irrigation or heavy rain causes leaf splash. The possibility of produce contamination depends on the survival strategy of the pathogen in the environment and its viability during harvest and through to consumption. Primarily, the microbes are able to survive in the soil or in organic matter applied to the land before the produce is planted. The survival criteria depends on the type of soil, nutrients, temperature, moisture content and source of contamination (Olaimat and Holley 2012). The survival periods of some enteropathogens are listed in Table 1.2. The survival period of the pathogen is usually variable depending on the environment and organic waste treatments (Heaton and Jones 2008). The application of animal manure on land results in an increased load of enteric pathogens due to their ability to survive in soil for several months or years (Martínez-Vaz et al. 2014). Slurry, faeces and manure may naturally contain pathogens like *E. coli* and *Salmonella* spp. ranging between 10^2–10^7 CFU/g (Olaimat and Holley 2012). The method in which organic matter is applied to the land may also increase survival time of pathogens. For example, inoculation of liquid manure or clumps of matter above ground can protect microbes from high temperature and desiccation (Hutchison et al. 2004). Exposure of bacteria to stresses at this phase may enhance survival by inducing bacterial survival strategies. *Salmonella* and *E. coli* are capable of surviving stressed conditions by producing stress proteins which decrease the impact of adverse abiotic conditions (Heaton and Jones 2008).

Table 1. 2: Survival periods of enteropathgens in the field environment (Adopted from Heaton and Jones 2008)

Pathogen	Environment	Survival (day)
Escherichia coli O157: H7	Soil + animal manure	30
E. coli O157: H7	Soil + animal manure	99
E. coli O157: H7	Animal manure	60
E. coli O157: H7	Slurries	60
E. coli O157: H7	Abattoir waste	60
E. coli O157: H7	Sewage waste	60
E. coli O157: H7	Non-aerated ovine manure	>365
E. coli O157: H7	Aerated ovine manure	120
E. coli O157: H7	Non-aerated slurry	600
E. coli O157: H7	Aerated slurry	30
E. coli	Slurry + dirty water	90
Salmonella	Soil	968
Salmonella	Soil + bovine slurry	300
Salmonella	Soil + animal manure	30
Salmonella	Slurry + dirty water	90
Campylobacter	Soil + animal manure	30
Campylobacter	Slurry + dirty water	90
Listeria	Soil + animal manure	30
Listeria	Slurry + dirty water	180
L. monocytogenes	Soil + sewage sludge	56
Hepatitis A	Water	>365
Hepatitis A	Soil	96

Modified atmosphere cultivated seed, contaminated with *E. coli* and *Salmonella*, has shown internalization of these organisms in spinach and lettuce (Martínez-Vaz et al. 2014). It has been suggested that internalization of pathogens can occur by two different mechanisms: entry via natural openings on the plant surface (such as stomata, physical damage and lenticels) or entry via the root system (Martínez-Vaz et al. 2014).

The presence of particular pathogens has also been linked to seasonal variation, e.g. increased levels of *E. coli* are encountered during spring and summer, whereas

Campylobacter levels are highest in spring and autumn. Pre-harvest treatments are not always sufficient to control the incidence of pathogenic bacteria on leafy greens, and hence, post-harvest treatments need to be applied to safeguard the product (Heaton and Jones 2008).

1.2.4 Sources of microbial pathogens in leafy produce: Irrigation water quality

Irrigation water quality is generally affected by the presence of enteropathogens which are introduced in watercourses due to soil, faecal matter and material from sewage (Heaton and Jones 2008). When contaminated water contacts the surface of leafy produce, it can result in the internalization of the pathogen into plants (Martínez-Vaz et al. 2014). Increased occurrence of pathogens is observed when produce is irrigated with wastewater due to the cost and unavailability of potable water in some areas (Fonseca et al. 2011a; Olaimat and Holley 2012). In the UK, approximately 71% of irrigation water is obtained from treated sewage wastewater (Tyrell and George 2006). In developing countries, untreated waste-water is used for irrigation which results in much-enhanced risks of microbial contamination (Heaton and Jones 2008). The risk of pathogenic contamination through reclaimed water differs between produce, for example, lettuce is known to pose a higher risk compared with other produce (Fonseca et al. 2011a). The possibility of pathogens surviving after packaging depends upon the interval between irrigation and harvest of the produce (Tyrell and George 2006).

The use of contaminated irrigation water has given rise to number of pathogenic outbreaks. In 2005, an outbreak of *Salmonella typhimurium* was experienced in the UK and Finland due to lettuce imported from Spain that had been irrigated with contaminated wastewater (Heaton and Jones 2008).

1.3 Leafy produce – from farm to fork

For growing leafy salads in the UK, seeds are first grown in temperature-controlled greenhouses for approximately 3 weeks and then planted into the field (British Leafy Salads Association 2014). Temperatures of 12–18°C combined with sufficient moisture and good soil offer the best conditions for growing leafy salads (British Leafy Salads Association 2014). For maintaining the quality of the salad leaves, appropriate nutrients

and irrigation are provided while they are growing (Luo et al. 2010). Leafy produce is harvested either mechanically or by hand depending upon the type of leaf. For example, whole head lettuce is cut and wrapped by hand, whereas baby leaves are harvested by machine (British Leafy Salads Association 2014). After cutting, fresh produce is rapidly cooled to 3°C (within 3 h of harvesting) by vacuum cooling, hydro-vacuum cooling or forced-air cooling. Following cooling, fresh produce is commonly stored at 2–4°C to transportation to the processing plant where leaves are sorted, washed and dried, and finally packed prior to distribution to retail/food service sector outlets (Caponigro et al. 2010). A schematic representation of the food production chain from farm to fork and potential sources of contamination is shown in Fig. 1.2.

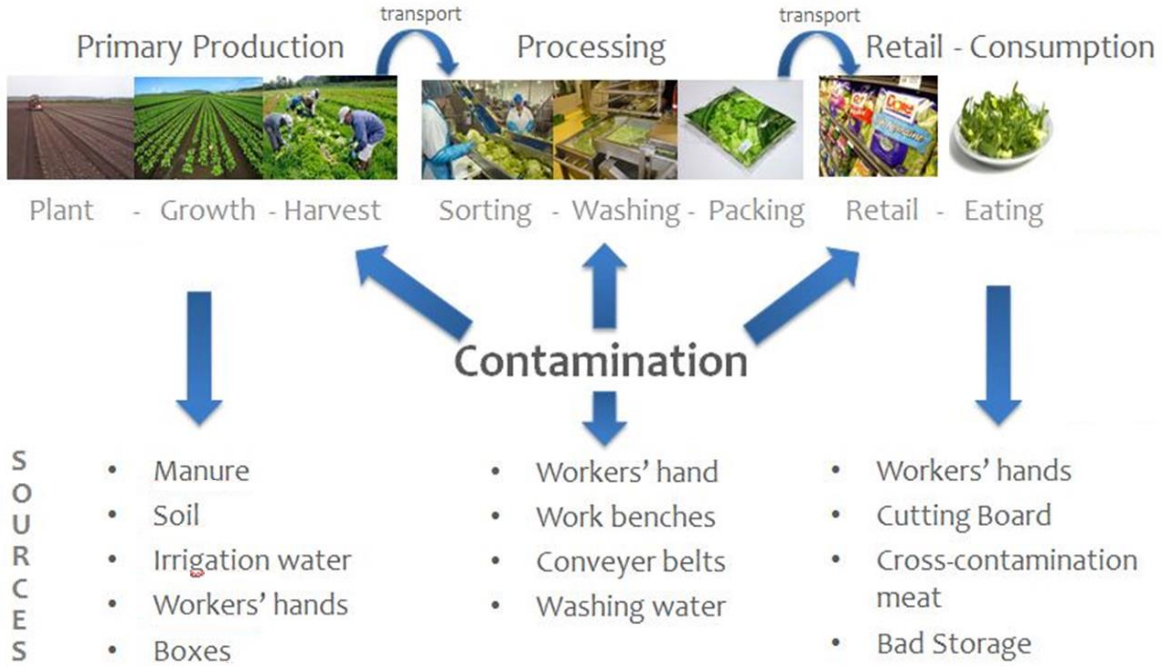

Figure 1. 2: Schematic diagram of food production chain from farm to fork and potential sources of contamination (source: **http://www.enbichem.ugent.be/content/qmrafreshcut**). Additional sources of contamination will include bioaerosols, insects, contaminated seeds and human/animal feces (Brandl 2006).

In 'Ready-to-Eat' leafy salads, rapid removal of field heat is one of the most important processes for extending the shelf-life of the produce, as excessive heat can cause immediate deterioration. Vacuum cooling is most commonly used to remove field heat within 30 min of harvesting (McDonald 2000). The principle of this process is to quickly evaporate water from the produce at very low vacuum; this is achieved by lowering the pressure in the vacuum tunnel causing the boiling temperature of free

water in the produce to decrease. In order to achieve target cooling temperatures, the water vapour generated during evaporation is removed using cooling coils to avoid water accumulation inside the system (Sun and Zheng 2006). Another significant factor is storage temperature as this affects the bacterial growth and sensory quality of the produce. Storage at lower temperature reduces microbial activity and sensory disorders (Jacxsens 2002). Hence, leaves are maintained in cold storage (4°C or less) before processing. A schematic representation of the processing line is shown in Fig. 1.3. The trimming and cutting procedures are performed in temperature-controlled (5°C to 10°C), segregated and hygienic factory sectors (Artes 2005). During this process, the inedible parts like damaged leaves, stalks, top and calyx are removed to reduce the over-all contamination on fresh produce before down-stream processing (Artes 2005). After this process, the leaves are conveyed to a washing area where the produce is either sprayed or bathed with spring, potable water or disinfectant. If the product is treated with disinfectant (for example, hypochlorite), then the produce must be rinsed with cold water and checked for the residual levels of the disinfectant on the leaves (Artes 2005). After drying, the leaves are then transferred to pack houses where they are packed into permeable plastic packaging which induce atmosphere modification (Caponigro et al. 2010). The technique requires modifying the internal gaseous environment of a package to a formation dissimilar from that of air (Rico et al. 2007). This is often done by physically reducing the amount of oxygen (O_2) and increasing levels of carbon dioxide (CO_2) (Ramos et al. 2013). A typical modified atmosphere storage condition commonly employed as a mild preservation technique for fresh produce is 1–5 kPa O_2 in combination with 3–10 kPa CO_2. This can potentially reduce respiration rate, delay enzymatic browning and slow down leaf metabolism (mainly oxidation) to retain its freshness and good shelf life (Caponigro et al. 2010; Jacxsens et al. 2003; Jacxsens 2002; Cui et al. 2009).

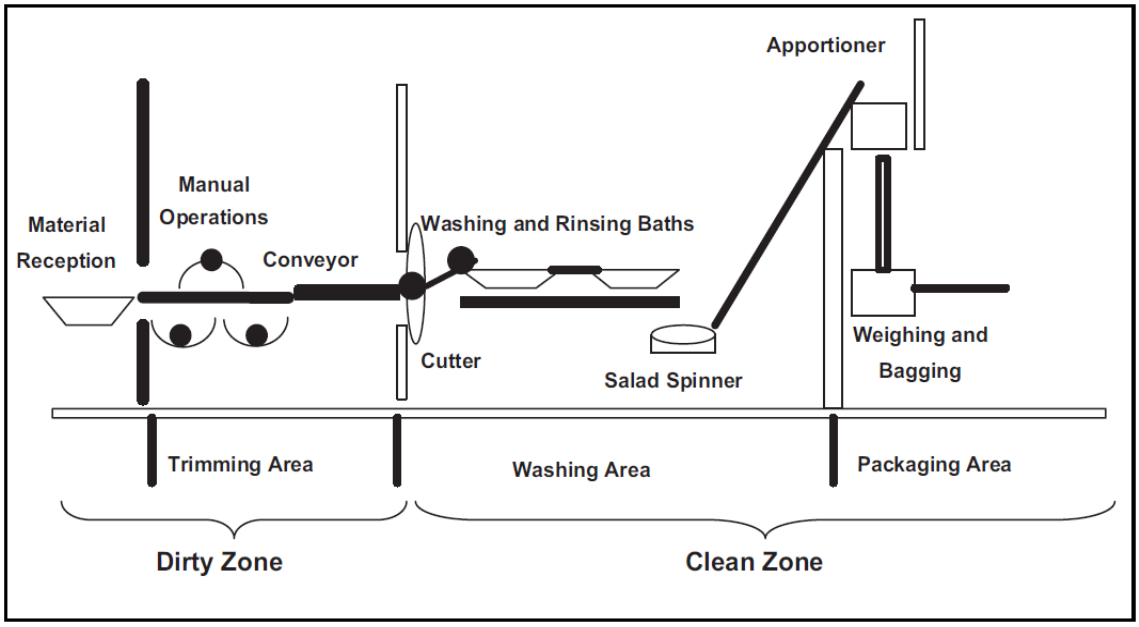

Figure 1. 3: Schematic representation of the leafy produce processing line (adapted from Artes 2005).

1.3.1 Shelf life of leafy salads

The shelf life of a product is defined as an acceptable loss in quality corresponding to a certain timeframe (days) but the range of days depends upon the type of shelf life: microbiological shelf life, food safety shelf life, marketing shelf life or sensory shelf life (Barth et al. 2009). Usually fresh produce is labelled by use-by-date, best use-by-day or sell-by-date, and this is not necessarily the same as microbiological or sensory shelf life (Barth et al. 2009). Large differences in bacterial counts have been reported between produce type and batches of the produce, but the count typically ranges from 10^3 to 10^9 CFU/g after processing, and despite such high counts, the quality of the produce is often acceptable (Jacxsens 2002; Rico et al. 2007).

1.4 Chemical disinfectants

There are numerous post-harvest treatments used commercially to eliminate microbes on fresh leafy produce (Ramos et al. 2013). The primary aim is to reduce microbial contamination and the use of methods that lower pathogen levels is vital for preventing food-borne epidemics (Corbo et al. 2006). Some of the novel chemical agents that have recently gained attention include chlorine dioxide, organic acids, hydrogen peroxide,

electrolyzed water and peroxyacetic acid. Commonly used chemical treatments (such as chlorine-based products) have proved reasonably effective in reducing microbial populations and pathogens on leafy salads. However, these disinfectants do not usually reduce microbial contamination by more than 2–3 $\log_{10}$ units (Artes 2005). Table 1.3 evaluates the different chemical technologies and their efficacies for microbial reduction and practicality for use in an industrial setting.

Table 1. 3: Chemical disinfectants used to reduce microbial contamination on leafy produce (modified from Rico et al. 2007, Ölmez and Kretzschmar 2009 and Ramos et al. 2013)

Method	Advantages	Limitations
Chlorine (hypochlorite)	- Cost effective - Easily available - Long history of use	- Formation of chlorinated by-products causing potential adverse health effects - Banned in some European countries - Ineffective on some bacterial spores - Maximum 1–2 log unit bacterial reduction achieved on many produce types - Corrosive - Sensitive to air, temperature, light and organic matter - pH dependent
Chlorine dioxide	- Better antimicrobial activity than chlorine at neutral pH - Less chlorinated by-product formation - Less corrosive - Higher penetration ability	- Not efficient for fresh produce at permitted concentration level - Explosive - Requires monitoring in indoor facility - Lethality affected by temperature, humidity, gas concentration and exposure time
Organic acids	- Easy to use - Cost-effective, depending on type of acid applied	- Antimicrobial activity depends upon type of acid and strain of micro-organisms - Time consuming - Hinders with the sensory quality - High level of COD and BOD

		count produced in the wasterwater generated from the fresh produce processing
Hydrogen peroxide	- No toxic production - Non-corrosive at permitted levels - Easy to use - Cost effective	- Phytotoxic, impact on produce quality - Less effective against micro-organisms at permitted levels - Long exposure time
Electrolyzed water	- High antimicrobial activity	- Interferes with overall quality of the leafy produce
Peroxyacetic acid	- Non-toxic - Non corrosive at permitted levels - High antimicrobial activity at low temperatures and pH range (5–8)	- Not effective at permitted levels

1.4.1 Chlorine (Hypochlorite)

Chlorine-based chemicals are the most commonly-adopted sanitizers for the treatment of fresh leafy produce employing concentrations ranging from 50 to 200 ppm and a contact time of not more than 5 min (Rico et al. 2007; Ramos et al. 2013). An industrial survey reported that approximately 76% of companies use hypochlorite as a disinfectant, and thus, without chlorine-based chemicals, there possibly would not be a market for fresh salads and vegetables (Gil et al. 2009). Despite chlorine being more active at low pH levels, chlorine-based chemicals are generally used at neutral pH (varying from 6.0 to 7.5) to reduce equipment corrosion (Rico et al. 2007). Depending on chlorine concentration, target micro-organism, contact time and processing technique, microbial counts are commonly reduced by 1–3.15 log CFU/g (Ramos et al. 2013). Although chlorine is the most commonly applied treatment in the fresh produce industry, it is known to react with natural organic material resulting in the formation of carcinogenic bi-products, such as trihalomethanes (THMs) and haloacetic acids (HAAs), which are potentially hazardous to human health (Ölmez and Kretzschmar 2009; Ramos et al. 2013). In addition, chlorine-based treatments produce high volumes of wastewater with a very high biological oxygen demand (BOD) and chlorine-based products are banned in organic systems throughout Europe (Ölmez and Kretzschmar

2009). A few European countries including Belgium, Germany, Switzerland and The Netherlands have also banned the use of chlorine-based disinfectants for conventional production (Rico et al. 2007; Ölmez and Kretzschmar 2009). Future regulations may eliminate chlorine use in the fresh produce industry, and therefore, processing sectors are seeking efficient alternatives to ensure produce safety while maintaining sensory attributes (Rico et al. 2007; Ölmez and Kretzschmar 2009).

1.4.2 Chlorine dioxide

Chlorine dioxide is used as an alternative disinfectant in product processing as it is less reactive to organic materials, ammonia or nitrogen-containing compounds (which results in reduced production of harmful chloramine substances) and has approximately 2.5-times the oxidizing capacity of chlorine (Goodburn and Wallace 2013; Rico et al. 2007). Chlorine dioxide must therefore be generated on site and has the downside that it is explosive (Ölmez and Kretzschmar 2009). Chlorine dioxide has been accepted as a sanitizer due to its antimicrobial activity, and it is highly effective against pathogens like *E.* coli O157:H7, *L. monocytogenes* and *S. typhimurium* (Rico et al. 2007). Many factors like chlorine dioxide concentration, exposure time, temperature and relative humidity can affect the efficacy of the treatment. The main drawback is that it is not so efficient on fresh produce because it requires higher concentration levels to reduce microbial load than accepted by regulations (Ramos et al. 2013). Some studies have also indicated an adverse effect of treatment on the sensory attributes of the produce (Ölmez and Kretzschmar 2009).

1.4.3 Organic acids

Organic acids primarily include lactic, ascorbic, acetic and citric acids, which are known for their antimicrobial activity against mesophilic and psychrophilic organisms and have been given Generally Recognized As Safe (GRAS) status in the US (Ölmez and Kretzschmar 2009). Their antimicrobial activity is related to disruption of cell membrane permeability and/or transport, anion accumulation, pH reduction in the environment, or decrease in internal cellular pH (Ramos et al. 2013). The antimicrobial action of organic acids mainly depends upon the type of the acid; thus, treatments generally incorporate a cocktail of organic acids (Ölmez and Kretzschmar 2009).

Organic acid treatments may cause unacceptable off taints and souring of the produce. In addition, organic acids are known to produce high levels of COD and BOD in the resulting wastewater and can result in additional clean-up costs in a commercial environment (Ölmez and Kretzschmar 2009).

1.4.4 Hydrogen peroxide

Hydrogen peroxide (H_2O_2) is capable of both bactericidal and bacteriostatic activity because of its strong oxidizing capacity and production of cytotoxic species such as superoxide and hydroxyl radicals (Ölmez and Kretzschmar 2009). The sporicidal activity of H_2O_2 combined with quick breakdown makes it a potential attractive sanitizer in the food industry (Parish 2003). Catalases and peroxidases in cells decompose H_2O_2 into oxygen and water, thus resulting in no residues on the surface of the treated produce (Rico et al. 2007; Ölmez and Kretzschmar 2009).

To date, H_2O_2 has not been commonly used commercially. The main limitation is its phytotoxicity against some products like lettuce, where it quickly results in browning, and it must be applied in conjunction with antibrowning agents such as ascorbic acid and citric acid (Ölmez and Kretzschmar 2009). Moreover, H_2O_2 concentrations of 2–4% should be applied for efficient results. Lower concentrations (1–2%) are not effective in reducing the microbial load, whereas higher concentrations (4–5%) affect the overall quality attributes of the produce (Ramos et al. 2013).

1.4.5 Electrolysed water

Electrolysed water (EW) is produced by electrolysing aqueous sodium chloride (0.5–1.0% NaCl) to generate electrolysed acidic water (EAW) at the anode and neutral electrolysed water (NEW) at the cathode as shown in Fig. 1.4 (Rico et al. 2007). Acidic electrolysed water (pH 2.1–4.5) has high oxidation reduction potential and generates presence of powerful oxidizing agents including superoxide and peroxide (Artés et al. 2009). Neutral electrolysed water (pH 5.0–8.5) also has a strong bactericidal effect due to its high oxidation reduction potential and exhibits an advantage over EAW as it does not affect the pH or visual appearance of the treated produce (Rico et al. 2007; Ramos et al. 2013). However, use of this method has shown a negative effect on nutrient content and sometimes results in unacceptable browning and organoleptic changes in treated produce (Goodburn and Wallace 2013).

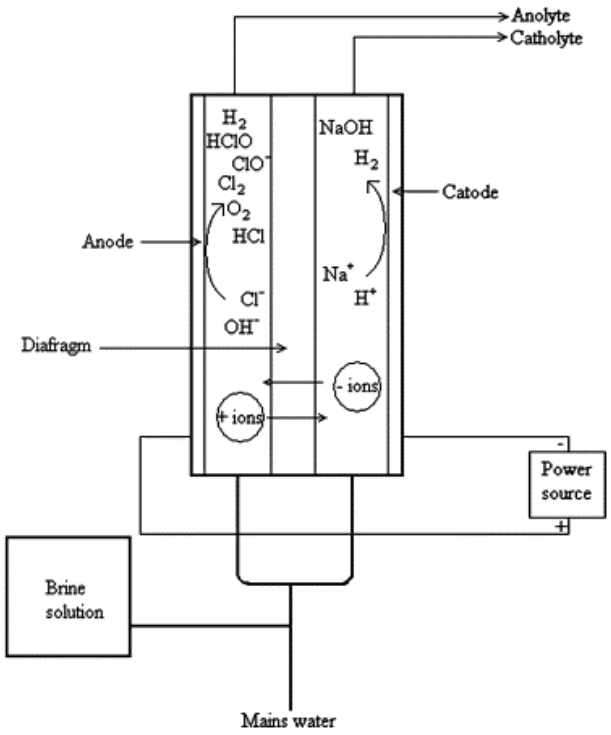

Figure 1. 4: Production of electrolysed water (Adopted from Rico et al. 2007).

1.4.6 Peroxyacetic acid

Peroxyacetic acid (PA) is also known as peracetic acid and is an aqueous combination of peracetic acid (CH_3CO_3H) and H_2O_2. Peroxyacetic acid is capable of tolerating some factors like pH ranging from 1–8, soil contamination and temperature; hence, it is used in food processing (Artés et al. 2009). It is a powerful oxidizing agent capable of effectively inactivating food pathogens, and therefore, it is applied to food products in recommended formulation mixture of 15% CH_3CO_3H and 11% H_2O_2 in concentrations up to 80 ppm. However, 80 ppm is insufficient to achieve significant reduction of bacterial load of leafy produce (Ramos et al. 2013).

1.5 Other non-chemical disinfection methods

In addition to the chemical disinfectants, there are a number of other sanitizing agents (non-chemical) that are approved and have been evaluated in laboratory-scale investigations for leafy produce. Table 1.4 evaluates other non-chemical disinfectants and their efficacies for microbial reduction.

Table 1. 4: Other non-chemical disinfectants used to reduce microbial contamination on leafy produce (modified from Rico et al. 2007, Ölmez and Kretzschmar 2009 and Ramos et al. 2013)

Method	Advantages	Limitations
Ultraviolet (UV) light	- No residual toxicity - Relatively inexpensive - Easy to use - Can delay deterioration process	- Difficulty in measuring the UV dose accurately - Requirement of pre-treatment - Poor penetration depth - Restricted application on opaque produce surface - Affects colour of the produce
Irradiation	- Cost effective - Increases shelf-life of the produce - Can be conducted at room temperature - Can be applied after packaging	- Variable efficacy against foodborne pathogens - Overall produce quality affected at high doses - Alters produce texture - Acceptance by consumers
Thermal treatments	- Good efficiency to inactive micro-organism	- Affect the colour and texture of fresh produce - Might affect nutrients in the produce - Requires high power - Generates waste
Cold plasma	- No detectable residue - Great efficiency - Relatively better penetration - Could be used during packaging process - Treats produce uniformly	- Mode of action is unclear - Inactivation depends upon the type of micro-organisms - May interfere with the produce quality - Limited evidence about the stability of the plasma for commercial setting

1.5.1 Ultraviolet light

There are three types of ultraviolet (UV) radiation based on wavelength of exposure: near UV radiation, which is known as UV-A ranging from 315 to 400 nm; mid-range UV radiation, which is known as UV-B ranging from 280 to 315 nm and far UV radiation, which is known as UV-C ranging from 200 to 280 nm (Prakash 2000). UV-C is frequently used in the fresh food industry and is known to act directly as an antimicrobial agent damaging bacterial DNA or inducing resistance mechanisms (such as stilbenoids and anthocyanins) in different produce against food pathogens (Rico et al. 2007; Ramos et al. 2013). This method is comparatively less expensive and easy to use in processing but it is difficult to measure the UV dose accurately and direct exposure of all surfaces to the treatment is vital to achieve an effective result (i.e. shadow effects can be a problem) (Thomas Bintsis 2000). Moreover, a high dose of UV-C radiation is capable of damaging produce (Rico et al. 2007; Ramos et al. 2013).

1.5.2 Irradiation

Ionizing radiation such as that administered by X-ray, electron beams and Gamma-rays produces ions, electronically charged atoms or molecules (Ramos et al. 2013). Low-dose gamma irradiation is capable of reducing bacterial, protozoan and parasitic pathogens by delaying maturation of treated produce (Prakash 2000; Lu et al. 2005). Ionizing radiation uses water as the main target to produce free radicals, which react with and deactivate microbial components (Rico et al. 2007). This method has been approved by the FDA for direct application on fruits and vegetables at a maximum level of 1.0 kGy (Parish 2003). In some cases, the quality of produce is extended, whereas in others, it results in undesirable changes (Rico et al. 2007). In iceberg lettuce and spinach, a maximum dose of 4.0 kGy can be applied according to a petition evaluated by the US FDA, which was filed by the Food Irradiation Coalition to ensure safety of fresh produce (Ramos et al. 2013).

1.5.3 Thermal treatments i.e. heat-shock and blanching

Thermal treatments are broadly used in the food industry to prepare and preserve food, but this can lead to undesirable changes in produce in terms of freshness, nutrients, texture and flavour (Rico et al. 2007). This method was modified for leafy produce by

applying high temperature for short time (HTST), minimising undesirable changes. This concept is based on the fact that high temperature inactivates bacterial growth, whereas exposing produce for a short time to high temperature may reduce the chances of altering produce quality. However, it is crucial to control the process if product quality is to be maintained (Ohlsson and Bengtsson 2002).

Blanching is routinely used in minimally processed produce industries as a decontaminating technique (Arroqui et al. 2003). In this treatment, produce is washed in water at high temperature (85–100°C) with infrared radiation or steam. During storage, the rate of degradation can be reduced if the produce is exposed only for short time. Blanching can reduce the microbiological counts on fresh leafy produce by more than 3-$\log_{10}$ CFU/g and *Enterobacteriaceae* counts by less than 1-$\log_{10}$ CFU/g (Rico et al. 2007). The limitation of this method is that it can affect the colour and texture of fresh produce and may damage nutrients through thermal degradation. Finally, blanching requires high power and generates a significant amount of waste (Song et al. 2003).

1.5.4 Cold plasma

Cold plasma, also known as non-thermal ionized gas, is an evolving antimicrobial technique for disinfecting surfaces. Plasma is made up of gas molecules, which have been separated by an energy input. It is created by negative and positive ions, electrons, photons, atoms, excited or non-excited molecules and free radicals, and altogether, it is capable of inactivating microbes (Fernandez et al. 2012).

Cold plasma is reported to be highly effective in eliminating food pathogens like *Salmonella* spp. and *E. coli* O157:H7 on the surface of the produce (Fernandez et al. 2012; Schluter et al. 2013; Niemira 2012). The amount of inactivation is dependent upon bacterial loading, type of bacteria, gas flow, physiological state of cells and gas mixture (Bermúdez-Aguirre et al. 2013). However, there is not sufficient information regarding physicochemical changes that might happen in the produce because of the interaction between charged particles from plasma with the food product (Ramos et al. 2013).

1.6 Alternative treatment: Ozone

Ozone is a triatomic oxygen molecule (O_3) that is arranged to form an obtuse angle, whereby a central oxygen atom is attached to two equidistant oxygen atoms (Miller et al. 2013). Ozone is relatively unstable and is generally produced naturally by high-voltage electric discharge such as thunderstorms or ultraviolet rays emitted from the sun that separates molecular oxygen (O_2) into two O atoms (Fig. 1.5). These single O atoms quickly combine with available O_2 to form O_3 (Mahapatra et al. 2005; Nogales 2008).

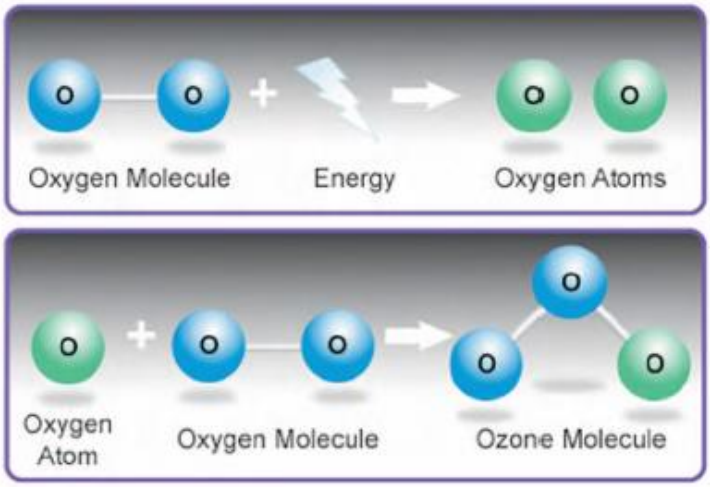

Figure 1. 5: Natural production of ozone. Adapted from Nogales (2008).

Ozone is a blue coloured gas with a pungent characteristic odour described as "fresh air after a thunderstorm" at room and lower temperatures (Perry and Yousef 2011). It is a powerful oxidising agent because of its relatively high electrochemical potential (E°, Volt) of 2.07 V (Miller et al. 2013; Mahapatra et al. 2005). The main physical properties of ozone are summarized in Table 1.5.

Table 1. 5: Main physical properties of ozone. Adapted from Guzel – Seydim et al. (2004) and Goncalves (2009)

Physical properties	Liquid phase	Gaseous phase
Molecular weight	47.98 g mol^{-1}	
Density	1,352 kg m^{-3} (at –112°C)	2.141 kg m^{-3} (at 1.013 bar and 0°C)
Boiling point	−111.3°C	
Melting point	−192.5°C	
Critical temperature	−12.2°C	−12.2°C
Critical pressure	55.73 bar	55.73 bar
Critical density	540 kg m^{-3}	540 kg m^{-3}

Gaseous ozone is commercially produced by one of three methods: corona (electrical) discharge, electrochemical discharge or ultraviolet (UV) radiation (Miller et al. 2013). Although the corona discharge method consumes a large amount of electricity, it is usually the preferred method because it generates high ozone concentrations and is cost effective (Perry and Yousef 2011). Corona discharge involves two electrodes (high tension electrode and low tension electrode) that are separated by a dielectric material such as glass (Mahapatra et al. 2005). Dried oxygen (or air, but this will result in low levels of production and contamination by nitrogenous contaminants) is converted into ozone when it is passed through these electrodes subjected to high voltage (Fig. 1.6). To maximize output and purity, dried oxygen should be applied in preference to dried air (Miller et al. 2013; Mahapatra et al. 2005). Gaseous ozone cannot be stored as it rapidly decomposes into oxygen (Guzel – Seydim et al. 2004).

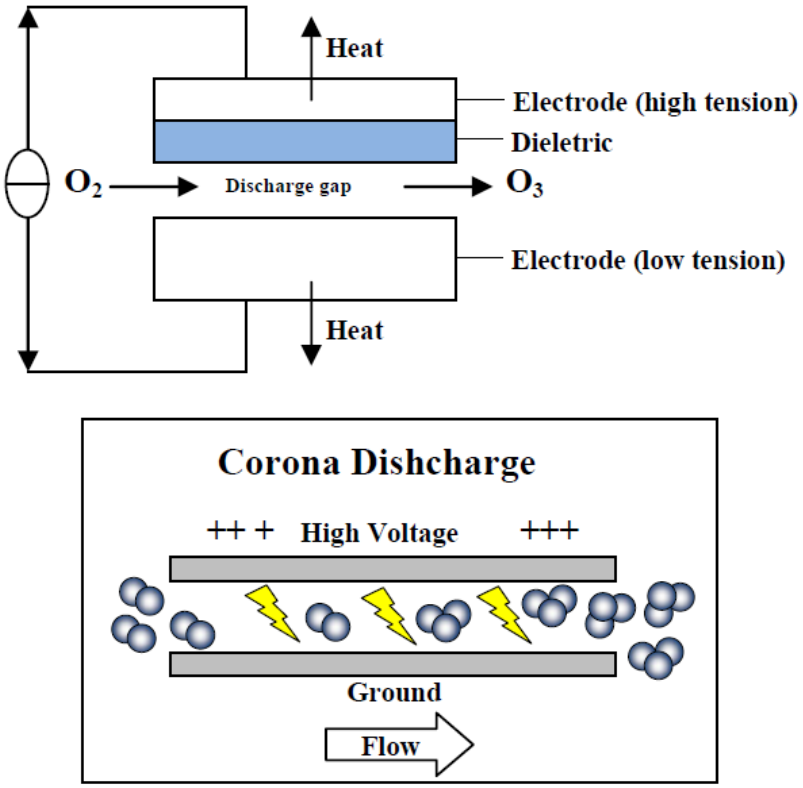

Figure 1. 6: Corono discharge method. Adapted from Goncalves (2009a).

Using the electrochemical method, ozone is formed through an electric current applied between a cathode and anode in an electrolytic solution comprising water and a solution of highly electronegative anions (Mahapatra et al. 2005). A combination of oxygen and ozone is generated at the anode (Miller et al. 2013).

Ozone production by UV radiation is based on exposure of oxygen to UV light at a wavelength of 140–190 nm as shown in Fig. 1.7 (Mahapatra et al. 2005).

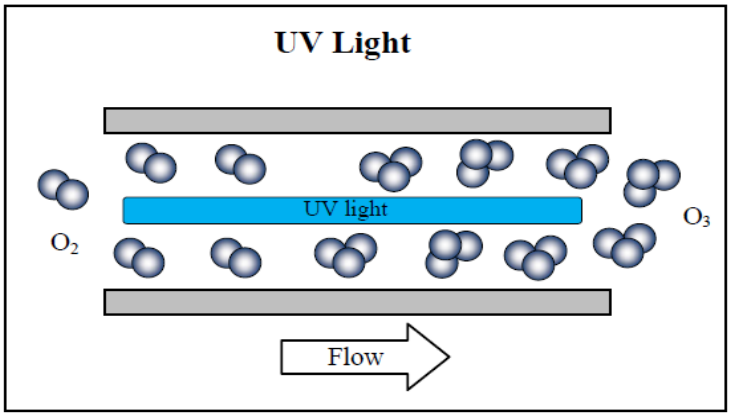

Figure 1. 7: Ultra-violet radiation method of ozone generation. Adapted from Goncalves (2009a).

The strong oxidizing action of ozone is capable of inactivating micro-organisms including both Gram positive and Gram negative bacteria, bacterial spores, fungi, fungal spores, viruses and protozoa (Goncalves 2009a). The third oxygen atom in ozone is electrophilic, and hence, it is attracted to other molecules with unbalanced charge to balance itself electrically. Therefore, ozone is attracted to diseased cells, detrimental bacteria and pathogens as they carry such a charge (Mahapatra et al. 2005). It has been suggested that on interaction, ozone acts on the cell wall before the gas and or its dissolution products penetrate microbes and attack various cellular components such as proteins, nucleic acids, lipids and enzymes, and ultimately results in degradation of the DNA and/or RNA content of the cell (Joshi et al. 2013; Khadre 2001; Miller et al. 2013). Once cell membranes are damaged by ozone exposure, it causes leakage of cell content which results in gradual cell inactivation and death (Perry and Yousef 2011). Ozone is destroyed and decomposes into oxygen and additional reactive oxygen species (ROS) when reacting with other components (Goncalves 2009a).

Ozone has been used as a key disinfectant to treat municipal and drinking water since the late 19th century, but has lately gained the attention of food and agriculture industries. However, application of higher ozone exposure levels must be taken into consideration as it may cause harmful human health effects and damage the produce being treated (Horvitz and Cantalejo 2014). The recommended ozone exposure levels are given in Table 1.6.

Table 1. 6: Recommended ozone exposure levels. Adapted from Goncalves (2009a)

Institution	Maximum concentration (ppm) in air	Limits for human exposure
Food and Drug Administration (FDA)	0.05	8h
Occupational Safety and Health Administration (OSHA)	0.10	8h
National Institute of Occupational Safety and Health (NIOSH)	0.10	Permanent
Environmental Protection Agency (EPA)	0.08	8h
Ministry of Labor and Employment (Brazil) – Portaria 3214/78	0.08	48h/week

Other than meeting health and safety requirements, there are no limitations on the adoption of ozone treatment for commercial crops. Use of ozone has been permitted in many Asian and European countries. In addition, the gas holds Generally Recognised as Safe status in the USA and is approved by US-FDA as a 'direct contact food sanitizing agent' since 2003 (Karaca and Velioglu 2007). The fresh produce sector is most likely to profit from current developments in ozone decontamination technology and several researchers have started exploring the use of aqueous and gaseous ozone to treat fresh produce.

1.7 Conclusion

Conventionally used chemical disinfectants such as chlorine and chlorine dioxide have been evaluated for use as sanitizing agents in produce. However, the use of chlorine has been associated with the formation of carcinogenic compounds in the last few years, and some pathogens have exhibited resistance to the lethal action of the compounds. Some of the novel technologies of disinfection methods include the use of organic acids, irradiation, cold plasma and ultraviolet light, but these approaches affect the quality of the produce such as colour, texture and nutrient content. Given the significance of controlling microbial contamination of fresh leafy produce and increasing consumer pressures over residues resulting from the use of biocides, residue free alternatives are being actively explored and encouraged to reduce microbial loads and curb spoilage of crops in storage/transit. This thesis focuses on exploring use of ozone due to numerous reasons: it is readily accessible, demonstrates strong anti-microbial activity, is cost-effective and can be produced on site. The multi-functionality of ozone makes it a promising sanitizing agent. More importantly, excess ozone rapidly decomposes into oxygen and thus leaves no residues in treated produce from its decomposition. In particular, the US-FDA's rulings on ozone usage in food processing industry have resulted in increased interest in potential applications worldwide.

1.8 Aims

The main aim of this thesis is to study the potential offered by gaseous ozone as an alternative to traditional post-harvest treatments to improve the shelf-life and safety of some types of leafy produce.

Objectives:

1. To identify key spoilage microbes present on the surface of selected leafy produce
2. To study the impact of gaseous ozone on key post-harvest microbes present on leafy salads

3. To investigate potential reasons for bacterial survival on leaf surfaces after ozone exposure

4. To determine if pre-exposure to stress results in increased bacterial resistance to ozone treatment and explore the mechanistic nature of this phenomenon using next generation sequencing (RNA-Seq)

5. To examine the effect of ozone treatment on the inactivation of *E. coli* and *Listeria* spp. on spinach

Chapter 2 Impacts of Gaseous Ozone on Key Post-harvest Microbes Present on Leafy Salads

2.1 Introduction

Previous work has demonstrated that long-term exposure to low atmospheric concentrations of ozone can be effective in some crops (e.g. kiwi, avocado, berries) in significantly reducing mould proliferation, but less work has been done on leafy produce. Ozone has been successfully used as a principal sanitizer for treating drinking and municipal waters for 100 years but has recently gained attention for agri-food applications (Mahapatra et al. 2005). It is well known for its strong oxidizing capacity and has been recognized as a powerful antimicrobial agent, reacting with organic substances approximately 3,000 times quicker than chlorine (Singh et al. 2002). In 1997, the United States Food and Drug Administration (US-FDA), in union with an expert panel, granted ozone GRAS status (Tzortzakis et al. 2007), and later, in 2003, it received formal approval from the US-FDA as a 'direct contact food sanitizing agent' (Karaca and Velioglu 2007). One of the major advantages of ozone treatment is the fact the gas leaves no detectable residues in/on treated products, because ozone rapidly decomposes into oxygen unlike other sanitizers used in the food processing industry (Mahapatra et al. 2005). Moreover, the gas can cheaply and quickly be generated on site and is readily applicable for a variety of commercial applications. Hence, it has been hypothesized that ozone treatment will significantly reduce dominant post-harvest microbial spoilage on leafy produce without causing physical damage to the treated produce.

Aim: To investigate the impact of gaseous ozone on key spoilage micro-organism present on the surface of the leafy salads

Objectives:

- To identify the key post-harvest micro-organisms present on the surface of the leafy produce
- To determine the optimum ozone exposure limit to treat leafy salads while maintaining physical integrity of the produce
- To determine the impact of ozone treatment on dominant micro-organisms present on the surface of the leafy produce

- To optimize ozone fumigation to achieve higher bacterial kills

2.2 Materials and Methods

2.2.1 Characterization of the principal microbial population present on leafy salads: Enumeration of principal microbial population

The principal microbial population present on leafy salads were enumerated and characterized using standard industrial technique (culture-dependent technique). Two packets of organic Italian style salad (lettuce, wild rocket and spinach), watercress & rocket, organic spinach & coriander were purchased from a local retailer and the microflora that developed over the shelf-life of the product was examined. Products were stored at 4^{o}C in the dark as directed on the packaging and tested at the start of life (SOL) and on the sell-by-date i.e. end of life (EOL). The 'SOL' and 'EOL' samples were subject to bacterial enumeration and principal organisms were identified (at Geneius Laboratories, 44 Colbourne Crescent, Nelson Park, Cramlington, NE23 1WB). The samples (25 g) were stomached in 200 mL of sterile BPW using Stomacher® 400 circulator. The stomaching technique gives nearly 100 % efficiency in recovering viable bacteria. This technique is UKAS accredited and it is tested regularly by use of standard samples provided by an external company. The total viable count (TVC), yeast and moulds were determined on Plate Count Agar (PCA) and Dichloran Rose Bengal Chloramphenicol (DRBC) agar plates, respectively, using standard spread plate techniques. PCA and DRBC agar plates were incubated at 30°C for 3 days and 25°C for 5 days, respectively, after serial dilution in maximum recovery diluent (MRD). The low concentration of peptone in MRD reduces micro-organism multiplication in the sample for at least one hour during the dilution stage and minimizes physiological shock experienced by organism upon inoculation.

2.2.2 Characterization of the principal microbial population present on leafy salads: DNA extraction, PCR amplification and sequencing

Discrete colonies of the morphologically dominant microbial types from 'SOL' samples were subsequently re-cultured for microbial identification (Geneius microID®) using 16S (for bacteria) and 28S (for moulds and yeast) rRNA gene sequence. Total DNA from agar grown cells was extracted using a QIAGEN kit and extracted DNA was

stored at −20°C. Using the universal primers, (27F) (5′-AGAGTTTGATCMTGGCTCAG-3′) and (1525R) (5′-AAGGAGGTGWTCCARCC-3′) and (63F) (5′-GCATATCAATAAGCGGAGGAAAAG-3′) and (635R) (5′-GGTCCGTGTTTCAAGACG-3′), a segment of the bacterial 16S rRNA gene and 28S rRNA gene, respectively, was amplified using a Hybaid PCR Express thermal cycler; PCR cycles were performed at 94°C for 3 min, 94°C for 30 s, 55°C for 30 s and 72°C for 30 s. A total of 30 cycles were performed with a final extension step at 72°C for 5 min. PCR amplification was performed using reaction mixtures (final volume 10 µL) consisting of 2 ng template, buffer incubation mix with 1.5 mM $MgCl_2$, 0.2 mM dNTP (Qiagen), 0.5 mM primer 27F, 0.5 mM primer 1525R, and 2.5 U of DreamTaq proof-reading DNA Polymerase (Fermentas). Amplification of PCR products was confirmed by capillary electrophoresis and visualised using a Qiaxcel transilluminator. PCR products were then purified using Exonuclease 1 & Alkaline phosphatase prior to sequencing (ABI 3730, 96 capillary array sequencer). The sequences were assembled by aligning the forward and reverse sequences using ABI MicroSeq software to form a consensus sequence. This consensus sequence was then compared with sequences in the US-FDA approved ABI MicroSeq® database as well as with sequences in the BLAST nucleotide database (NCBI) (sees Appendix A).

2.2.3 Ozone fumigation system

A purpose designed ozone fumigation system constructed of stainless steel (diameter of 35 cm) was housed in a fume hood (Fig. 2.1). An inlet pipe was used to add ozone generated by electric discharge from oxygen (model SGA01 Pacific Ozone Technology Inc., Brentwood, California, USA), and the introduction of ozone was manually controlled via stainless steel needle valves/gap flow meters. Once the desired ozone concentration was achieved, Petri plates/leafy produce to be exposed to ozone were placed at the bottom of the treatment chamber and the fumigation system sealed with a Pyrex cover (Fig. 2.1). The ozone concentration in the system was recorded using a photometric analyzer (model 450, manufactured by Advanced Pollution Instrumentation Division, 9480 Carroll Park Drive, San Diego CA 92121-5201). The ozone monitor employed in these studies was serviced weekly and calibrated routinely against standards using a Dasibi 1008PC calibration unit.

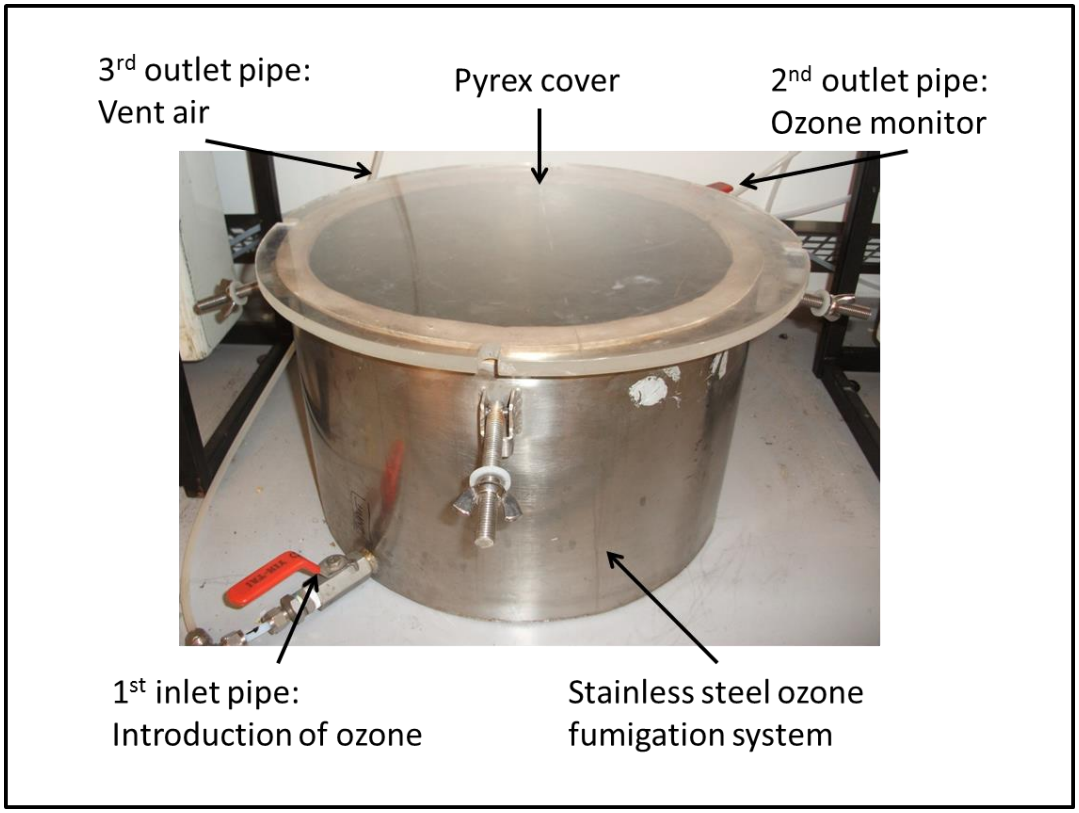

Figure 2. 1: Ozone fumigation system

2.2.4 Assessing the impact of ozone treatment on key classes of microbes isolated from fresh produce in vitro

The principal bacteria, yeast and mold identified on leafy produce were isolated from coriander samples and were sub-cultured on Cephaloridin Fucidin Centrimide (CFC) and DRBC agar plates, respectively. A single colony was isolated from each culture plate after incubation of 25°C for 2 days and 5 days, respectively, and transferred to MRD. A standardized concentration 10^4 cells per mL of each culture was spread (100 µL) onto sterile CFC and DRBC agar plates, respectively. These plates were then either exposed to 1, 10, 50 ppm ozone or 'clean air' (controls) produced in a sterile laminar flow cabinet for 10 min. After treatment, CFC agar plates and DRBC agar plates were incubated at 25°C for 2 days and 5 days, respectively. The number of colonies propagated on non-exposed control plates were compared with the numbers found on ozone-treated plates based on three replicate observations.

To examine whether ozone affected media constituents and reduced microbial growth indirectly, additional CFC and DRBC plates were pre-exposed to either 10 ppm ozone or 'clean' air for 10 min before performing the inoculation step as mentioned above.

2.2.5 Optimisation of ozone exposure levels (concentration and duration) to treat leafy salads without causing visual damage to produce

This experiment focused on optimizing the concentration and duration of ozone exposure to which fresh produce could be exposed without causing visible damage/deterioration. To determine the impact on visual quality of the produce, fresh leafy produce including baby spinach, watercress, coriander, lettuce and rocket were received from Intercrop Ltd. (UK) and Vitacress Ltd. (UK) and then exposed to 1, 10, 25, 50 ppm ozone or 'clean air' (controls) for varying periods of time (1 to 60 min). Following exposure to ozone, the produce was then packed in a sterile self-seal bag and maintained at 4°C in dark conditions. Ozone injury was assessed visually by comparing twenty ozone-exposed leaves with non-exposed control leaves every alternate day for 7 days.

2.2.6 The impact of ozone treatment on the microbes present on targeted leaves in vivo

Once ozone exposure levels that didn't cause visual damage were determined (from section 2.2.5), these same concentrations were used to examine reduction of microbial load on the surface of the targeted salad leaves. Baby spinach, coriander, watercress, rocket and lettuce were purchased from a local retailer and the total viable count of each was assessed at day 0 (labelled as 'SOL' – start of life) by exposing a whole packet of produce (240 g) to either 0 (clean air), 1 or 10 ppm ozone for 10 min. After the treatment, samples were collected by Geneius Laboratories for immediate enumeration. The samples (25 g) were stomached in 200 mL of sterile BPW using Stomacher® 400 circulator and the total viable count (CFU/g), *Pseudomonas* spp, yeast and moulds were determined after growth on PCA, CFC or DRBC agar plates respectively using standard spread plate technique. PCA, CFC and DRBC agar plates were incubated at 30°C for 3 days and 25°C for 2 and 5 days, respectively, after serial dilution in MRD.

2.2.7 The importance of ozone gas accessibility to reduce microbial load on the surface of the leafy produce in vivo

In this study, individual leaves of each targeted produce was used unlike a whole packet (240 g) of each targeted produce to investigate the importance of ozone gas accessibility to reduce microbial load on the surface of the leafy produce. Single leaves of organic

baby spinach, Iceberg lettuce, wild rocket, coriander and watercress were treated with 0, 1 or 10 ppm ozone for 10 min. After treatment, each leaf was vigorously vortexed for 2 min in 2 mL of MRD. Colony counts were made of each sample using standard PCA in Petri-dishes after serial dilution in MRD. Incubation of PCA plates was at 30°C for 3 days.

2.2.8 Modified ozone fumigation system – delivery of high ozone concentrations for short time durations (seconds)

The fumigation system was modified to improve application of ozone to the surface of produce and reduce the time required to build up the desired ozone concentration. The aim was to develop a system allowing application of higher ozone concentrations for shorter durations to achieve better bacterial kill without damaging the produce, and likely better reproduce the type of system facilitating commercialization. The modified ozone exposure apparatus was constructed from 20 cm^2 × 20 cm^2 Perspex. Produce was placed on a steel mesh in a 2 cm deep drawer that was introduced in to the box and the produce then exposed to ozone (Fig. 2.2). An inlet pipe was used to add ozone generated by electric discharge from oxygen, with the introduction of ozone controlled manually. The ozone fumigation box and the steel mesh were sterilised with 70% ethanol prior to its use. The ozone concentration was recorded by a photometric analyzer (model 450, manufactured by Advanced Pollution Instrumentation Inc.).

Figure 2. 2: Modified ozone fumigation system.

2.2.9 Exploration of higher ozone exposure levels to treat leafy produce without causing visual damage

This experiment aimed to determine the highest ozone concentration and exposure time that could be used to treat organic baby spinach, Iceberg lettuce, wild rocket, coriander and watercress without causing visible damage/deterioration to the produce. Produce was exposed to 10, 15, 20, 25 ppm ozone or 'clean air' (controls) for varying periods of time ranging from 30 s to 2 min. Following exposure to ozone, produce was then packed in a sterile self-seal bag and maintained at 4°C in the dark. Ozone injury was assessed visually by comparing twenty ozone exposed produce with non-exposed control produce every alternate day for 7 days.

2.2.10 Use of the highest ozone exposure levels to reduce microbial load present on the surface of leafy produce (in vivo)

When the highest ozone exposure levels that did not cause produce damage were determined (Section 2.2.9 and 2.3.6), the same concentrations were used to examine reduction of microbial load on the surface of the leafy produce. Organic baby spinach, Iceberg lettuce, wild rocket, coriander and watercress were treated with either 10 ppm ozone for 2 min, 15 ppm ozone for 30 s or untreated in ozone box as mentioned in Section 2.2.9. After treatment, total viable counts (CFU/g) were enumerated using standard PCA in Petri-dishes and incubated at 30°C for 3 days after serial dilution in MRD.

2.2.11 Statistical analysis

Data were analysed using SPSS (IBM SPSS Statistics 19 64Bit) and graphs were produced using Microsoft Office Excel 2010 and SigmaPlot 12.5. Data distribution was tested using Normality test and significant differences between mean values were verified using LSD ($P< 0.05$) following one-way ANOVA.

2.2.12 Log reduction

Microbial log reduction was calculated as follows:

$$\text{Log reduction} = \log_{10}(A) - \log_{10}(B) \text{ or Log reduction} = \log_{10}(A \div B)$$

Where A is the number of viable microorganism before treatment and B is the number of viable microorganism after treatment.

2.3 Results

2.3.1 Microbial genera present on leafy salads

The range of micro-organisms found to be present and their respective counts are shown in Table 2.1. The microbial count ranged from 10^5 to 10^9 CFU/g. An increase in microbiological counts was observed over the course of shelf-life (i.e. with prolonged incubation). The most numerous microbial genera identified at start of life 'SOL' were *Pseudomonas* spp., *Bacillus* spp., *Debaryomyces* spp., *Penicillium* spp. and *Alternaria* spp.

Table 2. 1: The dominant genera of microbiota present at SOL of packed leafy produce with their total bacterial and fungi count (CFU/g) at 'SOL' – start of life and 'EOL' – end of life

Specimen source	**Total bacterial counts (CFU/g)**		**Dominant Bacteria**	**Total Fungi counts (CFU/g)**		**Dominant Fungi**
	SOL	**EOL**		**SOL**	**EOL**	
Coriander	2×10^6	2×10^9	*Pseudomonas* *Bacillus*	1.4×10^5	9×10^6	*Alternaria* *Phaesophaeria*
Organic Spinach	1.6×10^8	2×10^8	*Pseudomonas*	1.8×10^6	8×10^7	*Penicillium* *Alternaria*
Rocket/ Watercress	1.6×10^7	5×10^7	*Pseudomonas* *Aeromonas*	1.8×10^5	2×10^6	*Cryptococcus* *Debaryomyces*
Lettuce, wild rocket & spinach	1×10^7	3×10^8	*Rahnella* *Aeromonas* *Exiguobacterium*	1.4×10^5	9×10^6	*Crytococcus* *Cladosporium* *Debaryomyces*

2.3.2 The impact of ozone treatment on key classes of microbes isolated from fresh produce in vitro

Colony numbers (CFU) of *Pseudomonas* spp. (bacterial model species), *Alternaria alternata* (fungal model species) and *Debaryomyces hansenii* (yeast model species) were significantly reduced ($P < 0.05$) by *in vitro* ozone treatment (Fig. 2.3 & 2.4), even at extremely low dosages (1 ppm for 10 min). After 10 min exposure to ozone concentrations of 10 ppm and 50 ppm, a highly significant reduction in counts of all the tested microbes, *Psuedomonas* spp., *A. alternata* and *D. hansenii*, was obtained.

There was no significant difference in colony count reductions between 10 ppm and 50 ppm ozone treatments for *Psuedomonas* spp. and *D. hansenii*.

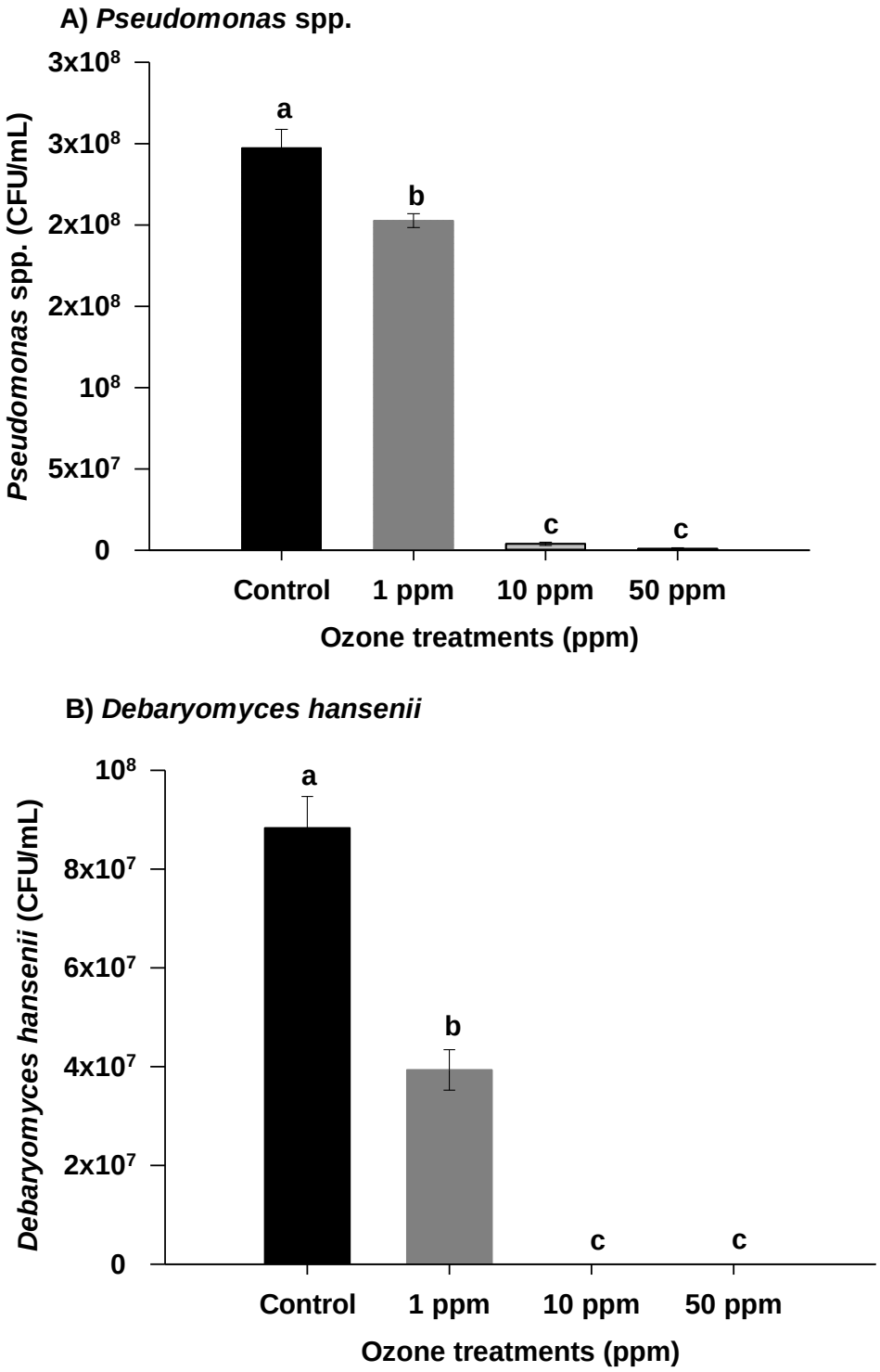

Figure 2. 3: Impacts of ozone treatment on A) *Pseudomonas* spp. and B) *D. hansenii* (CFU/mL). The treatment chamber was ventilated with 1, 10 or 50 ppm ozone for 10 min. Controls were exposed to 'clean air'. Values represent the mean (±Standard Error) of measurements made on three independent plates per treatment. Bars with different letters are statistically significantly different ($P < 0.05$).

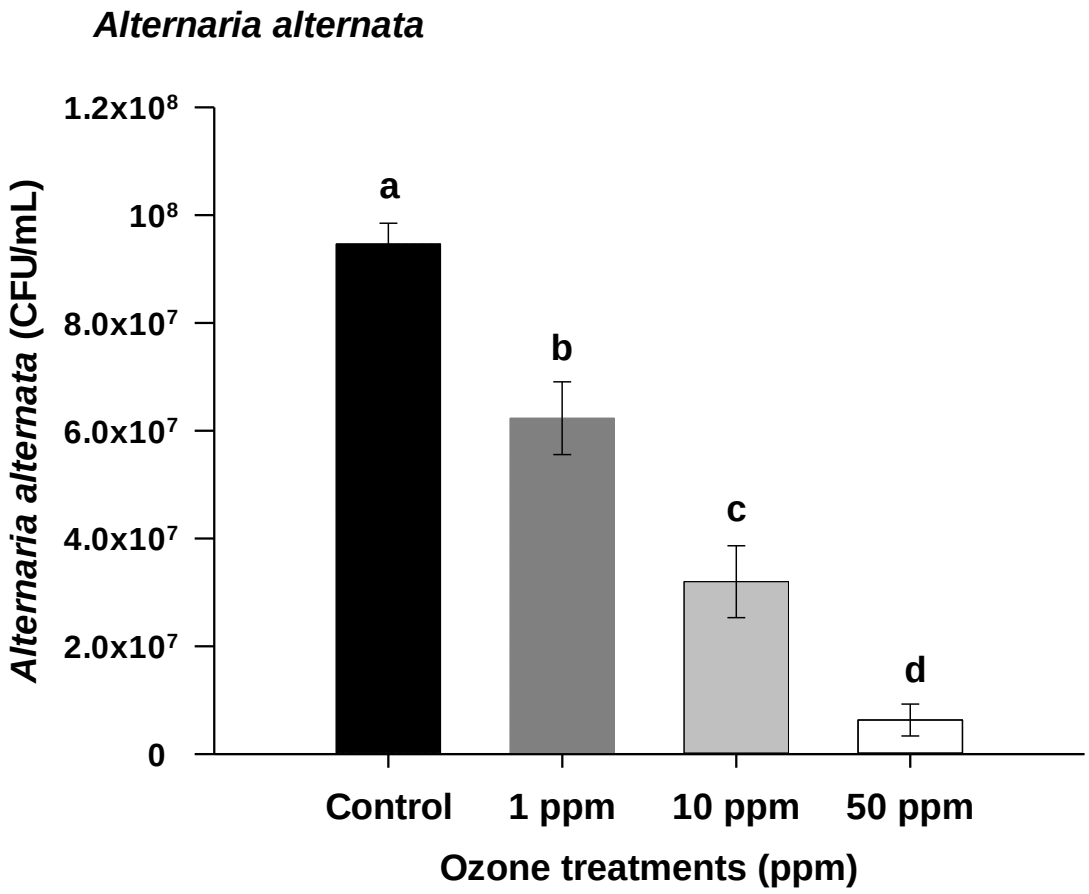

Figure 2. 4: Impacts of ozone treatment on *A. alternata* (CFU/mL). The treatment chamber was ventilated with 1, 10 or 50 ppm ozone for 10 min. Controls were exposed to 'clean air'. Values represent the mean (±Standard Error) of measurements made on three independent plates per treatment. Bars with different letters are statistically significantly different ($P < 0.05$).

Potential impacts of direct media exposure to ozone on subsequent colony development *in vitro* were determined just in case ozone affected media constituents and reduced microbial growth indirectly. No significant difference was observed between the treatments ($P < 0.05$); therefore, impact of ozone on the media used to culture the organisms was not the reason for the observed impact of ozone on microbial growth *in vitro* (Fig. 2.5 & 2.6).

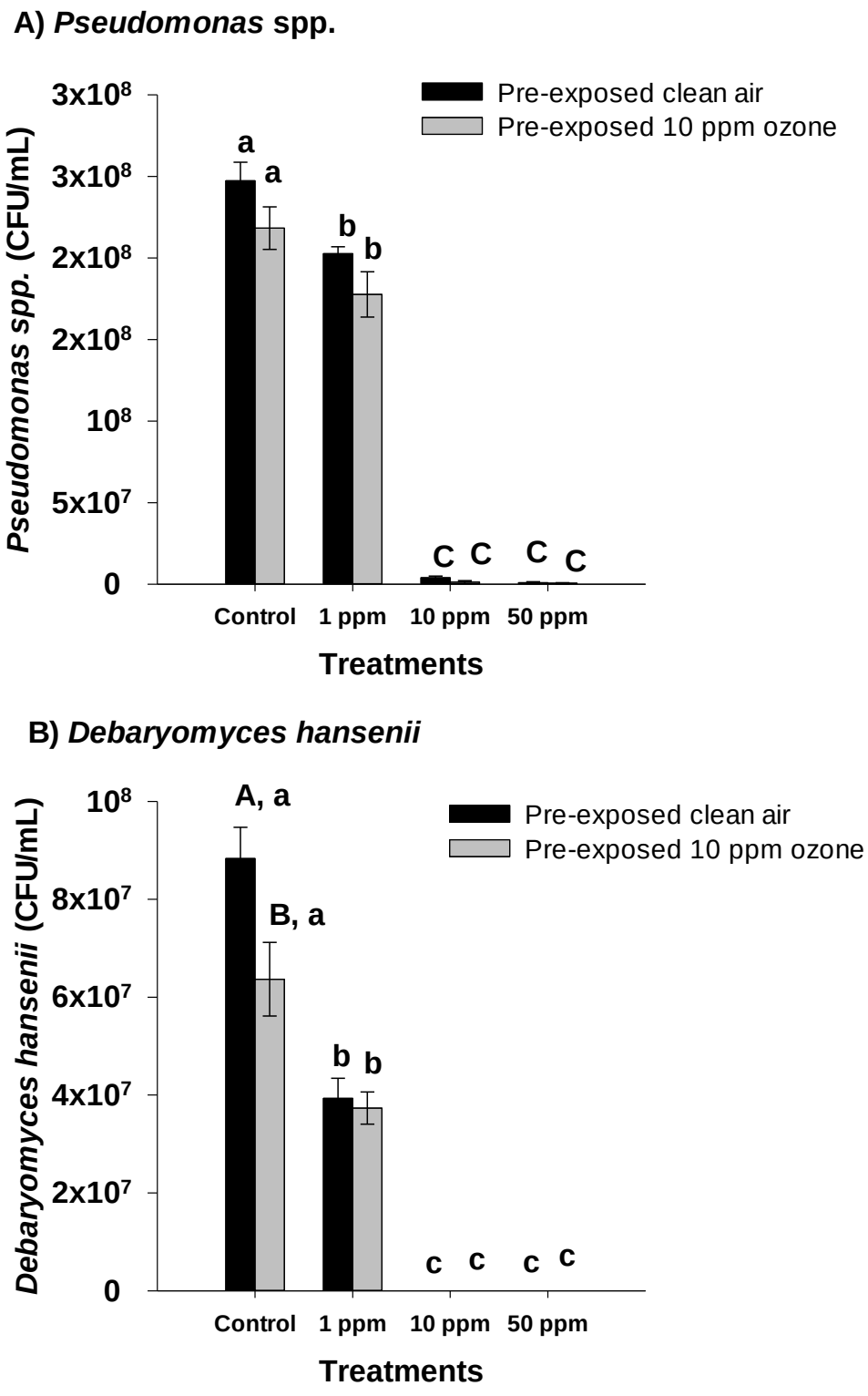

Figure 2. 5: Impacts of ozone treatment on A) *Pseudomonas* spp. and B) *D. hansenii* (CFU/mL). CFC and DBRC agar plates were either pre-exposed to clean air or 10 ppm ozone for 10 min. The treatment chamber was ventilated with 1, 10 or 50 ppm ozone for 10 min. Controls were exposed to 'clean air'. Values represent the mean (±Standard Error) of measurements made on three independent plates per treatment. Bars on the graph within ozone level and pre-exposed treatments with same letters are not statistically significantly different ($P < 0.05$).

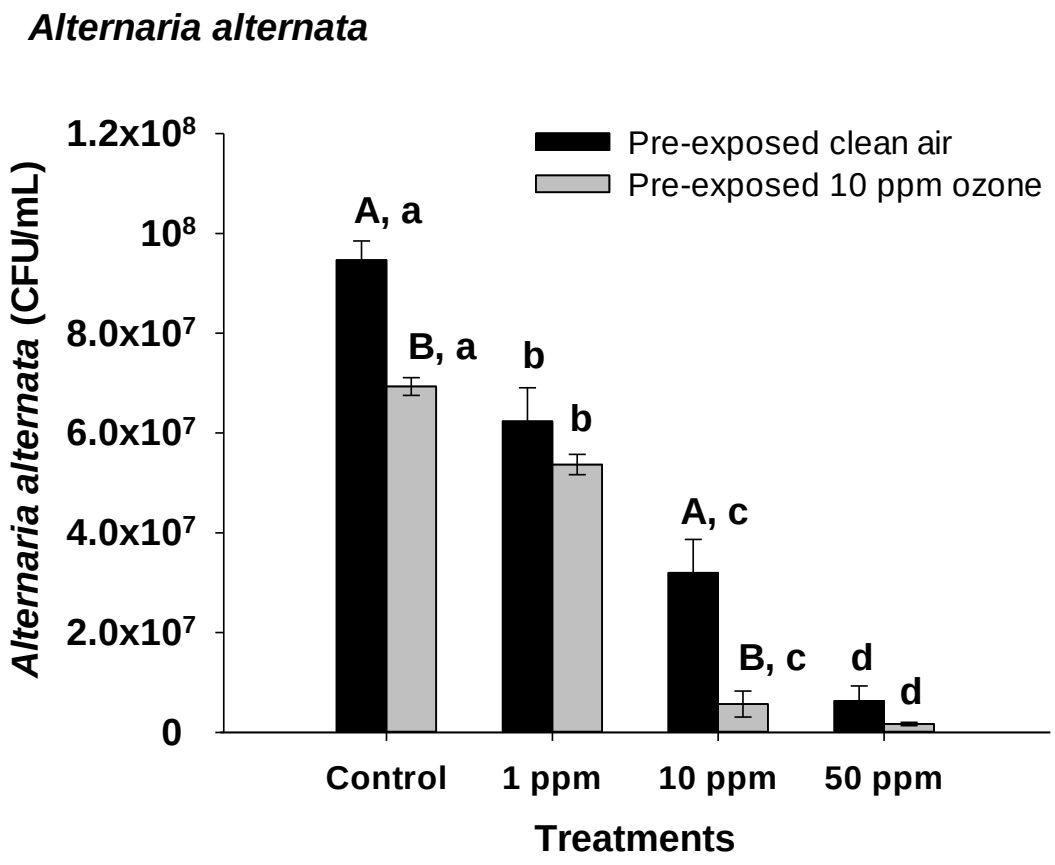

Figure 2. 6: Impacts of ozone treatment on *Alternaria alternata* (CFU/mL). DBRC agar plates were either pre-exposed to clean air or 10 ppm ozone for 10 min. The treatment chamber was ventilated with 1, 10 or 50 ppm ozone for 10 min. Controls were exposed to 'clean air'. Values represent the mean (±Standard Error) of measurements made on three independent plates per treatment. Bars on the graph within ozone level and pre-exposed treatments with same letters are not statistically significantly different ($P < 0.05$).

2.3.3 Optimisation of the concentration and duration of ozone exposure levels to treat leafy salads without causing visual damage

No differences in visual colour, texture or freshness of appearance was observed when targeted leafy produce were exposed to 1 ppm ozone for 10 min (Table 2.2). In contrast, only coriander and rocket retained their appearance when exposed to 10 ppm ozone for 10 min. Ozone treated leafy produce visually looked as fresh as the control (Fig. 2.7) Fig. 2.8 illustrates ozone injury/ visual damage on spinach when exposed to 10 ppm for 10 min. Ozone injury/visible damage were observed on all produce when exposed to 25 and 50 ppm ozone concentration (data not shown).

Table 2. 2: Maximum ozone exposure levels of different types of leafy produce (ozone exposure levels that did not cause visual damage)

Target produce	Ozone exposure limit	
	Concentration of ozone exposure (ppm)	Duration of ozone exposure (min)
Baby spinach	**1**	**10**
Watercress	**1**	**10**
Coriander	**10**	**10**
Lettuce	**1**	**10**
Rocket	**10**	**10**

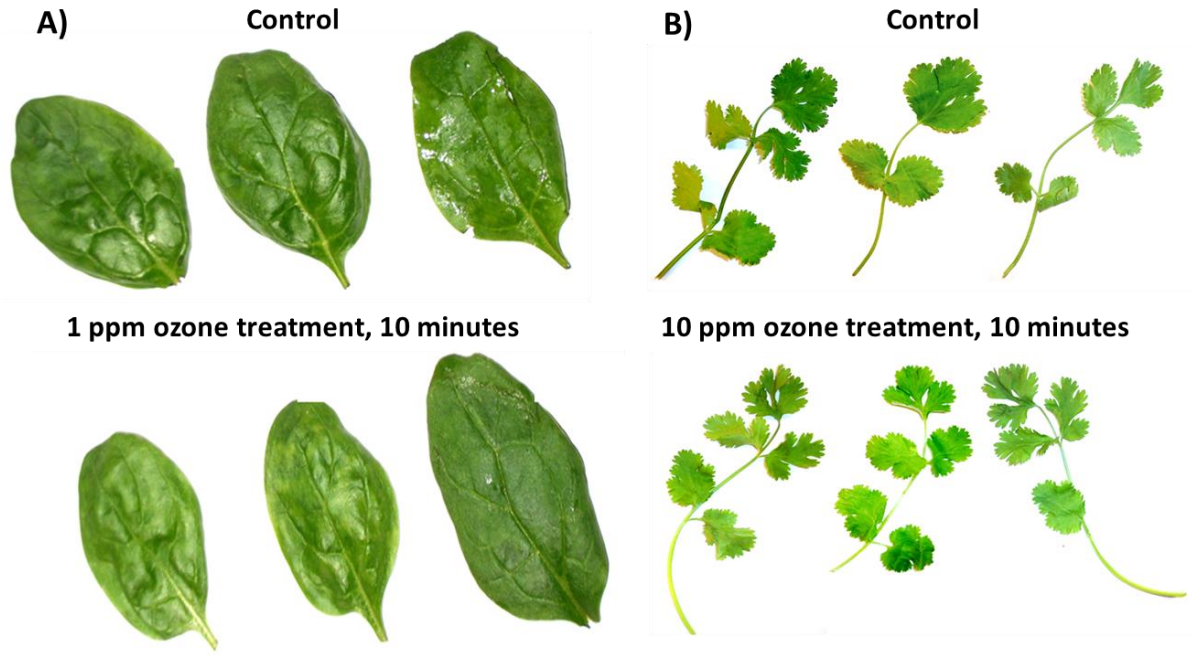

Figure 2. 7: Representative cases of ozone treated leafy produce (e.g. A) spinach and B) coriander) showing no obvious difference between controls and ozone treatment after 7 days of storage.

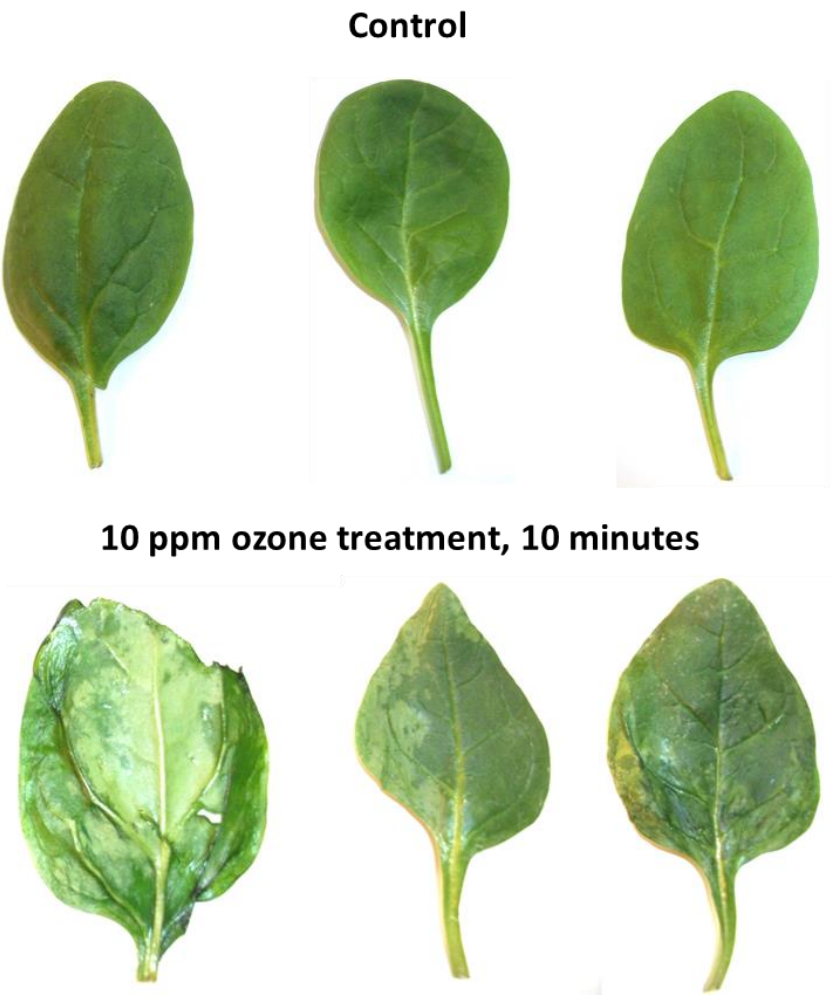

Figure 2. 8: Representative case of ozone injury/visual damage on spinach when exposed to 10 ppm ozone for 10 min. Ozone damage included yellowing, paling, wilting and physical lesions on the leaf surfaces.

2.3.4 Impact of ozone treatment on the microbes present on a variety of produce in vivo

The initial total viable count (TVC) and *Pseudomonas* spp. count on the targeted produce was 10^6–10^7 CFU/g while initial yeast levels were low (Fig. 2.9, 2.10 & 2.11). Exposure of produce (240 g of each produce type) to ozone treatments that gave reduced counts when microbes were treated *(in vitro)* on plates (Fig. 2.3 & 2.4) interestingly resulted in no significant reduction ($P < 0.05$) in TVC, *Pseudomonas* spp., moulds and yeasts. This suggested that ozone gas was not penetrating efficiently through a large amount of produce and so it was decided to test the effect of ozone gas exposure on single leaves; this would allow ozone gas to access the leaf surface efficiently.

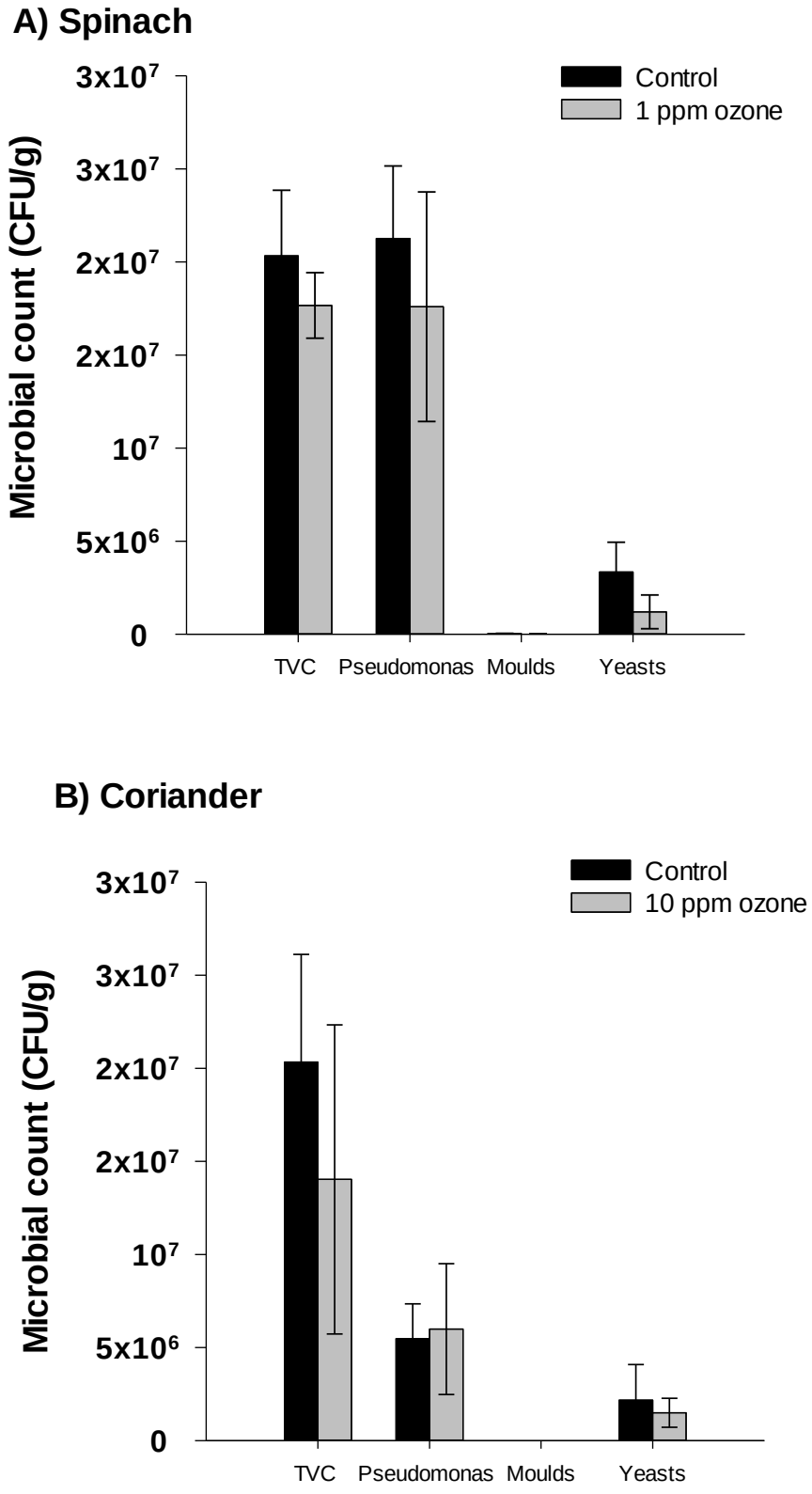

Figure 2. 9: Impact of ozone treatment on microbial flora present on the surface of A) spinach and B) coriander leaves. Produce were either exposed to 1 ppm or 10 ppm ozone (grey bar) or 'clean' air (black bar) for 10 min. Values represent means (±Standard Error) of measurements made on three independent packets of targeted produce per treatment.

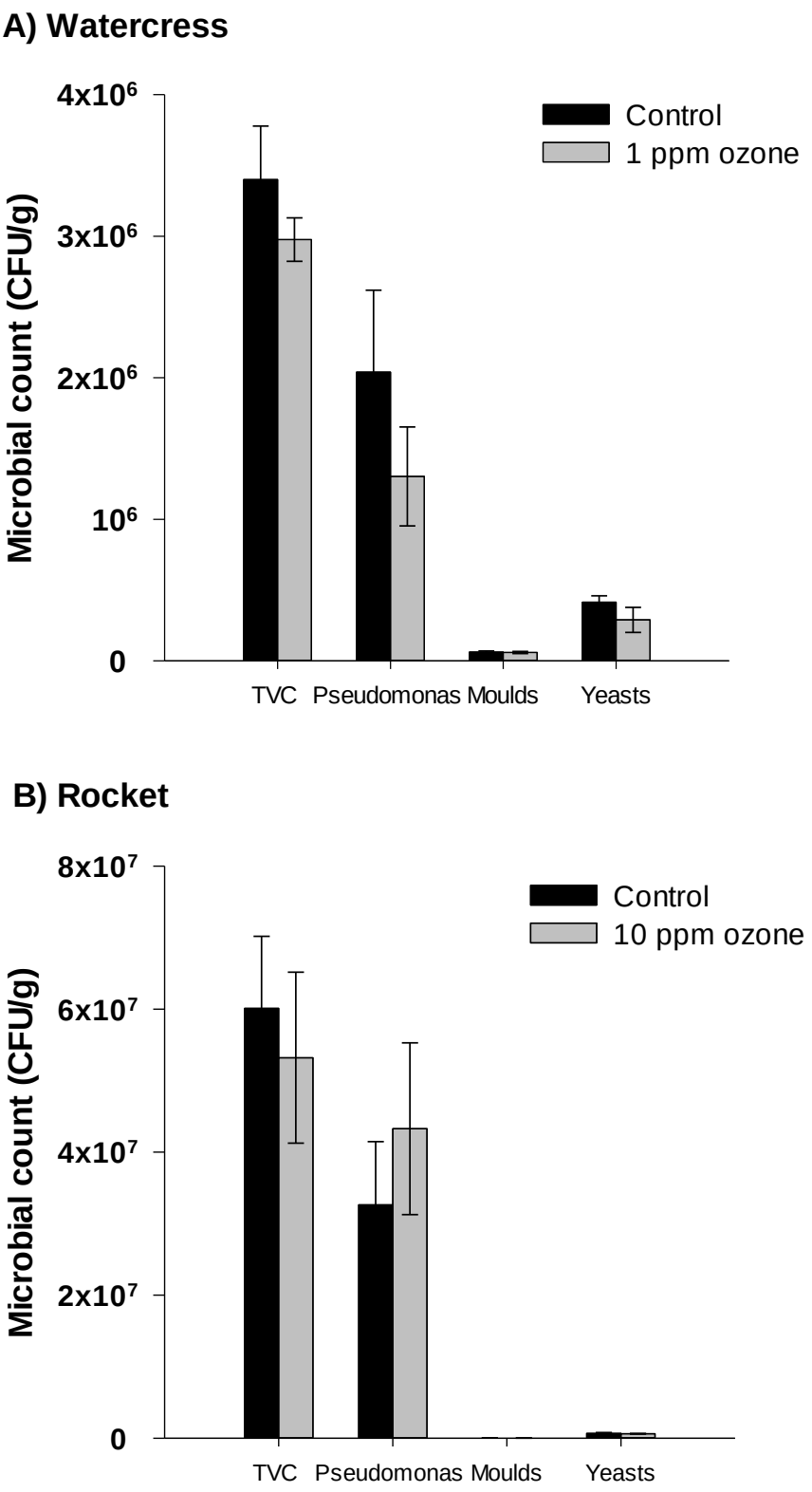

Figure 2. 10: Impact of ozone treatment on microbial flora present on the surface of A) watercress and B) rocket leaves. Produce were either exposed to 1 ppm or 10 ppm ozone (grey bar) or 'clean' air (black bar) for 10 min. Values represent means (±Standard Error) of measurements made on three independent packets of targeted produce per treatment.

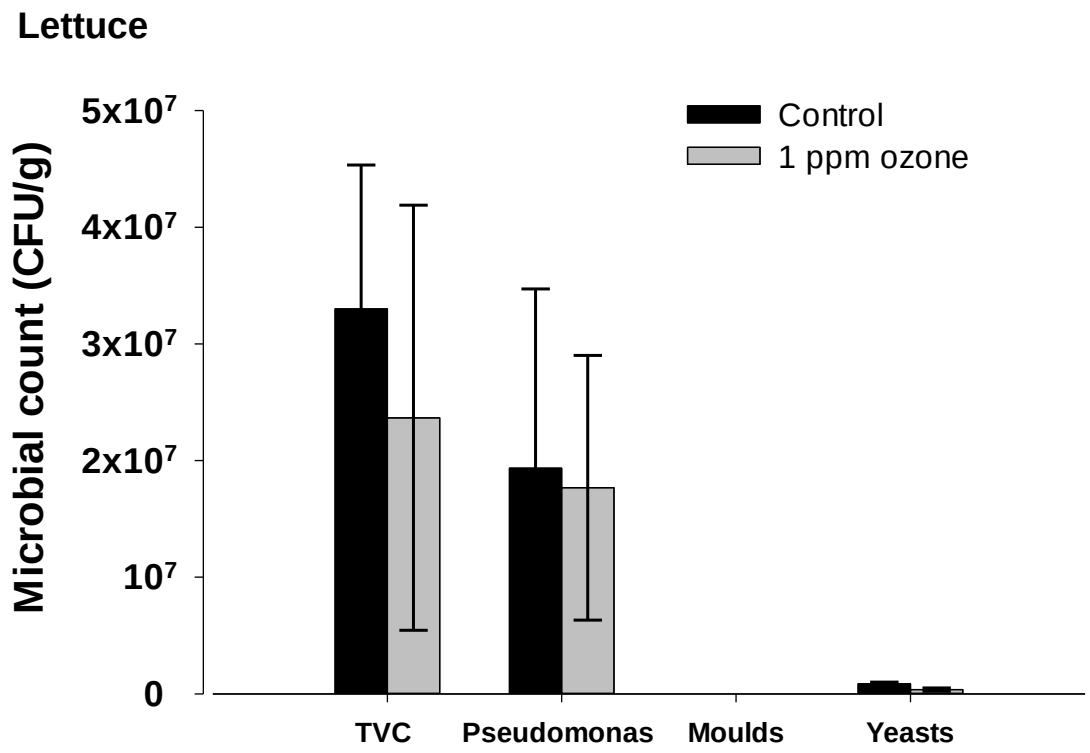

Figure 2. 11: Impact of ozone treatment on microbial flora present on the surface lettuce leaves exposed to 1 ppm ozone concentration (grey bar) or 'clean' air (black bar) for 10 min. Values represent means (± Standard Error) of measurements made on three independent packets of targeted produce per treatment

2.3.5 To determine the importance of ozone accessibility to reduce microbial load on the surface of the leafy produce in vivo

Gaseous ozone was effective in significantly reducing microbial load on a single targeted leaf (Fig. 2.12). A maximum of 2.1 log microbial reduction on coriander leaves was observed by ozone treatment (Table 2.3).

Table 2. 3: Microbial log reduction achieved by ozone treatment on leafy produce

Targeted leafy produce	Log reduction
Spinach	**1.8**
Coriander	**2.1**
Watercress	**1.5**
Rocket	**1**
Lettuce	**1.7**

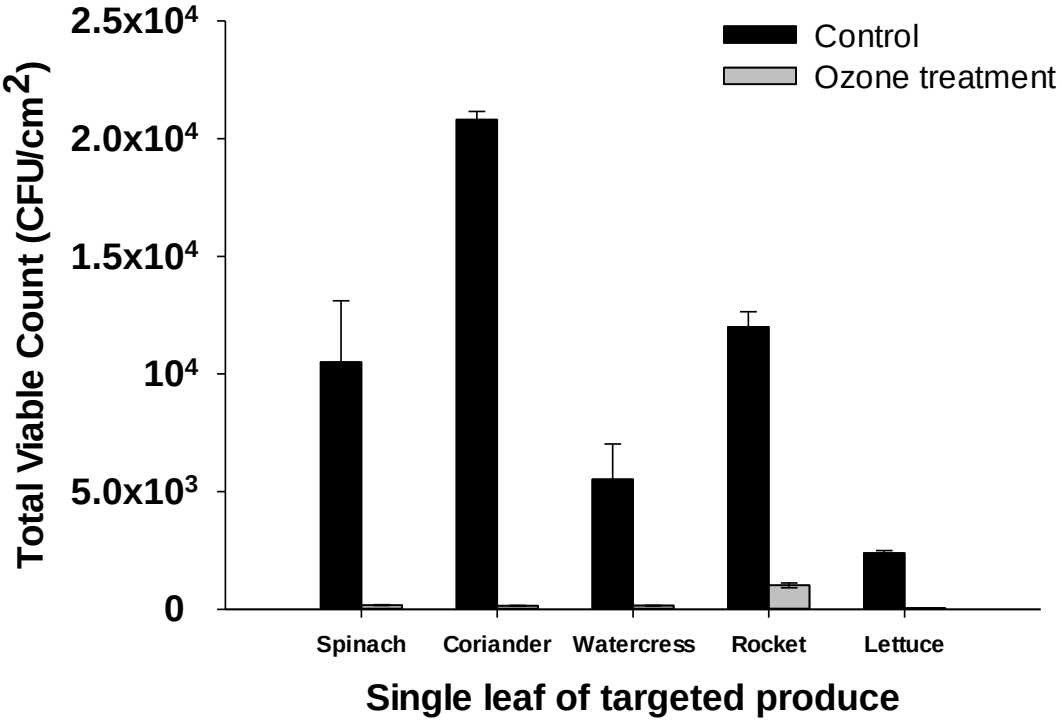

Figure 2. 12: Total Viable Count (CFU/cm^2) of spinach, watercress and lettuce when treated with 1 ppm while coriander and rocket treated with 10 ppm ozone concentration (grey bar) or untreated (black bar) for 10 min obtained using standard plate count method. Values represent means (+/−Standard Error) of measurements made on three independent single leaves per treatment.

2.3.6 Exploration of higher ozone exposure levels to treat leafy produce without causing visual damage

No visual ozone damage was observed when leafy produce was exposed to higher concentrations such as 10, 15 and 20 ppm ozone for shorter durations (Table 2.4). Ozone treated produce visually looked as fresh as untreated produce (control) after 7 days of storage as shown in Fig. 2.13. Ozone injury/visible damage were observed on all produce when exposed to 25 ppm ozone concentration.

Table 2. 4: The maximum ozone exposure levels that can be applied on the targeted produce without causing visible damage over 7 day shelf life

	Duration of the exposure of targeted leafy produce				
	Spinach	**Rocket**	**Watercress**	**Lettuce**	**Coriander**
10 ppm	**2 min**	**2 min**	**2 min**	**2 min**	**2 min**
15 ppm	**45 s**	**45 s**	**30 s**	**30 s**	**30 s**
20 ppm	**30 s**	**30 s**	**15 s**	**15 s**	**30 s**
25 ppm	**0**	**0**	**0**	**0**	**0**

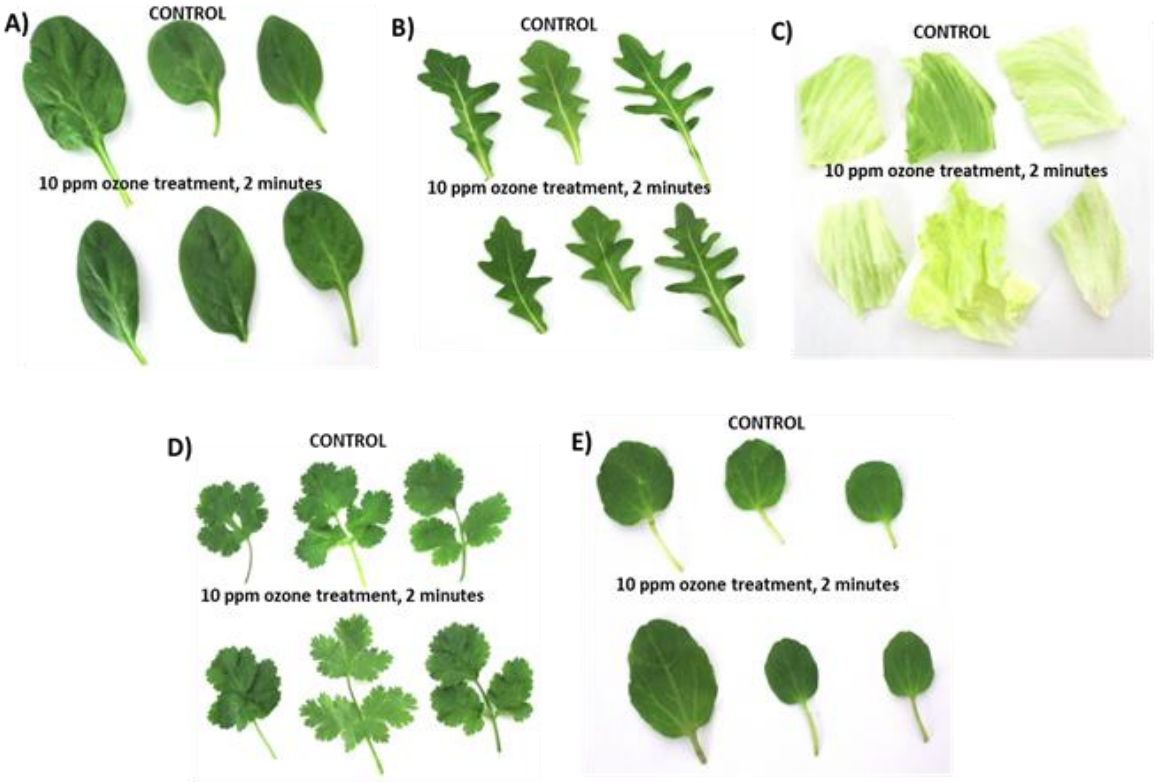

Figure 2. 13: Impact of the highest ozone exposure levels on visual quality of A) spinach, B) rocket, C) lettuce, D) coriander and E) watercress after 7 days of storage.

2.3.7 Impact of the highest ozone exposure levels to reduce microbial load present on the surface of leafy produce (in vivo)

The impact of high ozone concentration on microbes present on the surface of the spinach, rocket, lettuce, coriander and watercress leaves is shown in Fig. 2.14, 2.15, & 2.16. Microbial log reduction of the produce when subjected to 10 and 15 ppm ozone as

compared to control is shown in table 2.5. However, there was no significant difference between 10 and 15 ppm ozone treatments in numbers of colonies impacted.

Table 2. 5: Microbial log reduction achieved by ozone treatment on leafy produce

Targeted leafy produce	10 ppm ozone	15 ppm ozone
Spinach	**1.1**	**1.1**
Coriander	**1**	**1.1**
Watercress	**1**	**1.2**
Rocket	**2.2**	**2.1**
Lettuce	**0.8**	**0.9**

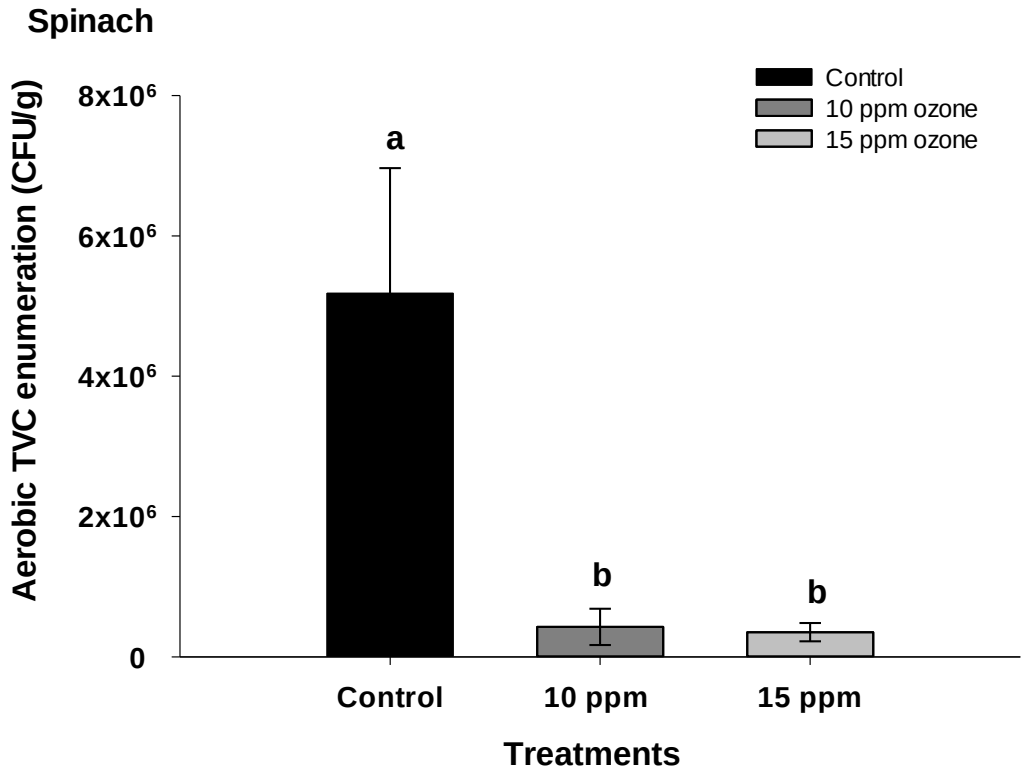

Figure 2. 14: Impacts of high ozone treatment on microbial flora present on surface of spinach exposed to 10 ppm ozone concentration (grey bar) for 2 min, 15 ppm ozone concentration (dark grey bar) for 30 s or 'clean' air (black bar).Values represent means (±Standard Error) of measurements made on three independent targeted produce per treatment. Bars with different letters are statistically significantly different ($P < 0.05$).

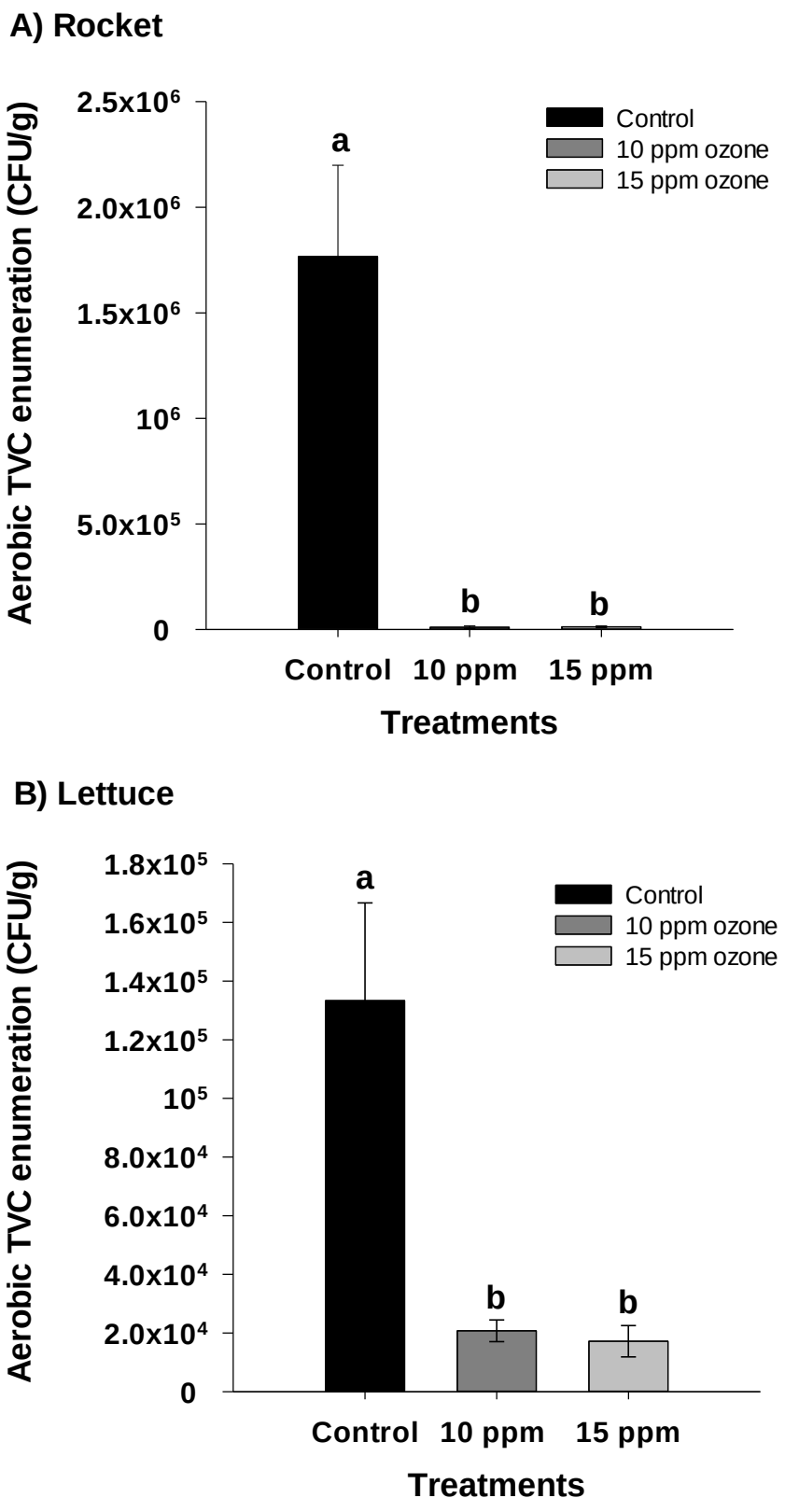

Figure 2. 15: Impacts of high ozone treatment on microbial flora present on surface of A) rocket and B) lettuce exposed to 10 ppm ozone (grey bar) for 2 min, 15 ppm ozone concentration (dark grey bar) for 30 s or 'clean' air (black bar).Values represent means (±Standard Error) of measurements made on three independent targeted produce per treatment. Bars with different letters are statistically significantly different ($P < 0.05$).

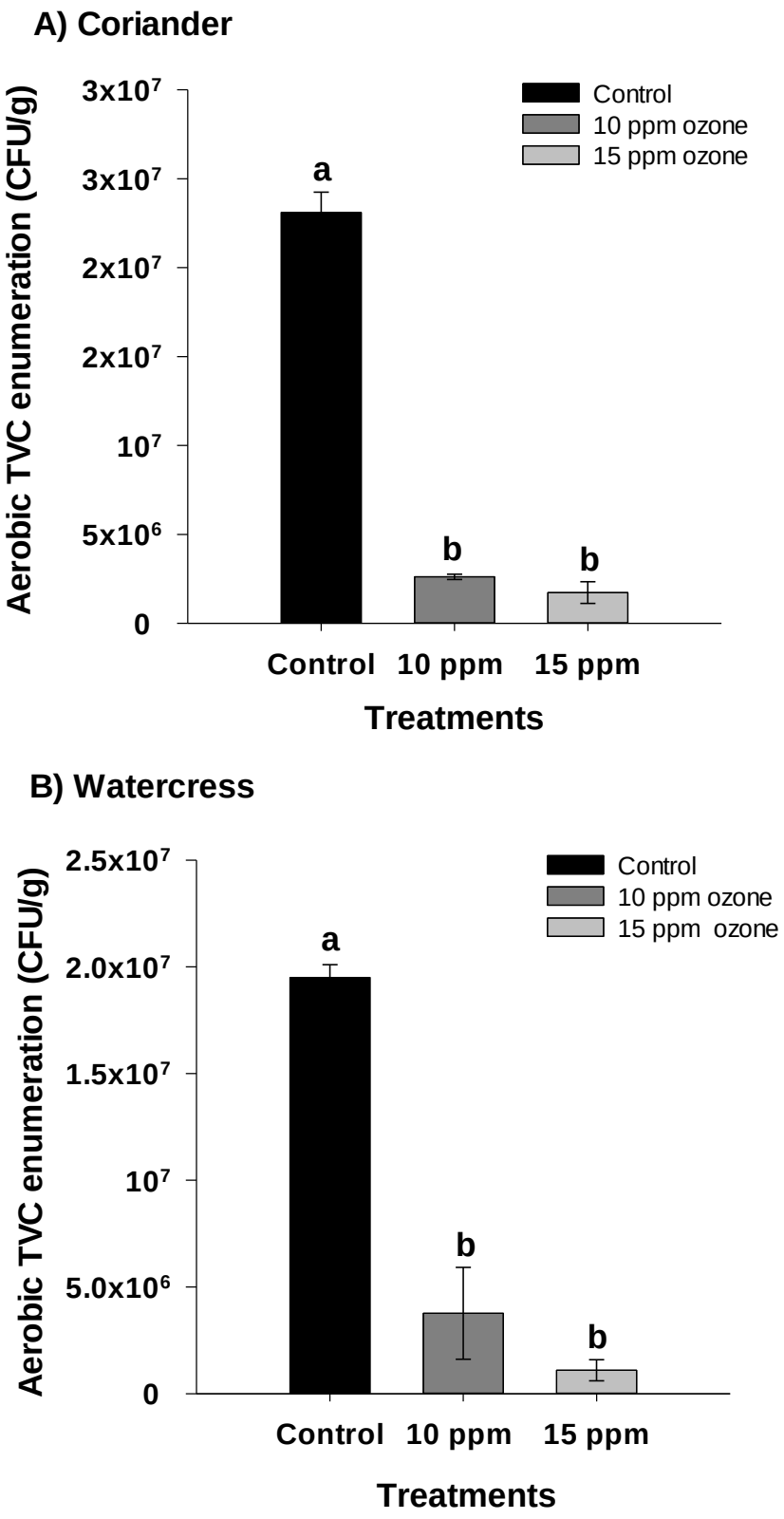

Figure 2. 16: Impacts of high ozone treatment on microbial flora present on surface of A) coriander and B) watercress. Produce were either exposed to 10 ppm ozone (grey bar) for 2 min, 15 ppm ozone (dark grey bar) for 30 s or 'clean' air (black bar).Values represent means (±Standard Error) of measurements made on three targeted produce per treatment. Bars with different letters are statistically significantly different ($P < 0.05$).

2.4 Discussion

2.4.1 The key microbial population present on the leafy salads

Salad leaves were found to be colonized by a variety of culturable bacteria, yeasts and moulds ranging in number from 10^5 to 10^9 CFU/g, similar to levels found in previous studies (Lindow et al. 2003). The most numerous microbial genera included *Pseudomonas* spp., *Alternaria alernata* and *Debaryomyces hansenii*. *Massilia* and *Arthrobacter* are also usually recognized and reported from lettuce and spinach (Rastogi et al. 2012). However, members of the genus *Massilia* have been identified only through culture-independent techniques (Rastogi et al. 2012). The microbial population was, however, dominated by Gram-negative bacteria. *Pseudomonas* spp. was present in all leafy produce types investigated at levels of more than 10^6 CFU/g. This result is consistent with Jacxsens and colleagues' (2002) conclusions that *Pseudomonas* was the principal determinant of the shelf-life of lettuce and other minimally processed leafy salads. Another experiment conducted by Rastogi and colleagues' (2012) observed the presence of *Pseudomonas* in field-grown lettuce at all their sampling location, based on culture-dependent and culture-independent analysis.

Alternaria is one the most commonly identified moulds on/in fresh and minimally processed produce (Tournas 2005a). However, only low levels of contamination were observed in the present study. This result is similar to the findings of Thournas (2005a). This may be because field-grown leafy salad production methods favour bacterial and yeast growth over mould development and/or fundamental properties of the produce like slightly acidic to neutral pH suppress mould development (Ragaert et al. 2007). In addition, moulds are mainly present as spores which makes it transient inhabitant of leaf surface (Lindow and Brandl 2003).

In the present study, microbial genera have been characterized by using culture-based approaches and hence much of the work on produce-associated bacteria has focused on a small number of spoilage bacteria. Culture-dependent approaches will not include bacteria that are not able to grow on standard artificial media or are slow growing (Dees et al. 2015). This limits the understanding of the bacterial community's genetics and physiology (Dees et al. 2015). The introduction of culture-independent tecniques, in

particular, microbial profiling using high-throughput sequencing has revealed more complexity and diversity of the leaf microbiota (Muller and Ruppel 2014).

2.4.2 The impact of ozone treatment on key classes of microbes isolated from fresh produce in vitro

The antimicrobial activity of ozone was tested on three dominant microbes isolated from produce: *Pseudomonas* spp., *Alternaria alternata* and *Debaryomyces hansenii* in an *in vitro* experiment. The results from the study show that overall ozone treatment resulted in a 1–2 $\log_{10}$ reduction in microbial count and *D. hansenii* was more sensitive to ozone exposure than the other genera. The degree of microbial inactivation by ozone treatment depends on its physiological state and various factors like strain of micro-organism, age of the culture, concentration of the treated population (Fan et al. 2007). Furthermore researchers have reported variable sensitivity of different microbes to ozone treatment (Khadre 2001). It is noteworthy, however, that in the present study it was observed that all microbes were inactivated by 10 min exposure to ozone concentrations above 10 ppm and pre-exposure of media to ozone didn't impact colony development *in vitro*.

2.4.3 Optimisation of the concentration and duration of ozone exposure levels to treat leafy salads without causing visual damage

The visual appearance and freshness of leafy produce have been the main judging criteria for quality distinction at purchase or consumption (Rico et al. 2007). No visual ozone damage was observed when leafy produce was treated with 1 ppm gaseous ozone, however, higher levels (e.g. 10 ppm for 10 min) caused visual damage to spinach, watercress and lettuce. Similar results were previously observed on fresh produce like lettuce, spinach and rocket leaves when treated with different ozone concentrations (Alexopoulos et al. 2013). Lack of visual damage may be due to the inhibitory action of ozone on the enzymes such as peroxidase (POD) and polyphenol oxidase (PPO) which are responsible for browning (Ölmez and Akbas 2009) or simply representative of the fact that some leaves display lower stomatal conductance than others and thus absorb less ozone (Dumont et al. 2013). Only coriander and rocket leaves retained their fresh appearance when exposed to 10 ppm ozone treatment. Damage was observed when higher ozone dosage was applied. It is evident that the impact of ozone treatment on the

quality of leafy produce is dependent on concentration; it may be beneficial up to a certain level to apply ozone, whereas after a critical level, it may accelerate browning responses resulting in inferior quality.

2.4.4 Impact of ozone treatment on the microbes present on targeted leaves in vivo

In contrast to the ozone-induced reduction in microbial counts observed *in vitro*, equivalent ozone exposure resulted in no effects when a packet of targeted produce was treated *per se*. Both the exposure time and the ozone concentration were not found to be significant in terms of microbial reduction. This is an interesting observation and could suggest that there are fundamental differences between the phenotype of the microbes under investigation in culture and on the surface of produce. Bacterial culture grown under laboratory conditions are inactivated more easily than bacteria present on organic matter or attached to carbon particles (Jin-Gab Kim 1998). There are different findings reported on the efficacy of ozone treatment against micro-organisms. In a similar study, a 6-log reduction in total microbial load was observed in spinach and lettuce when treated with different ozone concentrations (Selma et al. 2008) . It was also reported that moulds and yeasts were reduced by 2- and 3-log respectively (Selma et al. 2008). Alternatively, the result may simply reflect the inability of ozone to penetrate to the leaf surface under such fumigation conditions.

2.4.5 The importance of ozone accessibility to reduce microbial load on the surface of the leafy produce in vivo

To evaluate the importance of ozone accessibility to reduce microbial load on the surface of the leafy produce, single leaves were treated with ozone. A significant microbial reduction (1–2 log) was observed. Similarly, some researchers have also observed 1–2 log microbial reductions on leafy produce when gaseous ozone was used at 0.5–4.5 ppm for 10 min (Glowacz et al. 2014). Achiving higher log reductions than observed in this study may be difficult due to numerous reasons. One of them could be due to the extremely uneven and rough surfaces of the leafy produce, e.g. leaf margins could provide shelter to the microbial population (Alexopoulos et al. 2013).

2.4.6 Exploration of higher ozone exposure levels to treat leafy produce without causing visual damage

No visual damage was observed on leafy produce when exposed to higher ozone exposure concentration such as 10, 15 and 20 ppm for shorter duration of exposure, but different produce types had different ozone tolerance levels and change in overall visual quality was observed after the maximum ozone exposure limit. This could be due to the fact that ozone being a powerful oxidising agent acts on the tissue of the targeted produce promoting enzymatic activity and action of ozone could vary depending upon the enzymatic composition, pigments and other compounds that affect the colour of the targeted produce (Bermúdez-Aguirre and Barbosa-Cánovas 2013). All leafy produce visually appeared to be as fresh as untreated control produce when exposed to its maximum ozone concentration. However, ozone concentration higher than 20 ppm damaged leafy produce indicating that it was not suitable for commercial use.

2.4.7 Impact of highest ozone exposure levels to reduce microbial load present on the surface of leafy produce (in vivo)

A significant decrease in microbial count was observed on the surface of the targeted leafy salads when treated with high ozone concentration for shorter duration of exposure using the modified ozone fumigation system. However, 1–10% of surface bacteria survived ozone treatment. It may be due to exopolysaccharides (EPS) which are responsible for protecting bacterial cells against stress (Monier and Lindow 2003). Therefore, the ‘naked’ cells of identical physiological state may not have retained adequate EPS to confer protection against ozone treatment. This indicates metabolic differences between the cells present on the surface of leaves. Overall, the results indicate that although the vast majority of bacteria are killed by ozone, there are a number of cells that survive. Reasons for this observation which could be due to a combination of physical protection in a micro-colony and increased stress resistance in certain cells due to environmental conditions. This was further investigated in Chapter 3.

2.5 Conclusion

The first aim of this study was to determine the dominant culturable microbial group present on the surface of leafy produce. *Pseudomonas* spp., *Alternaria alernata* and *Debaryomyces hansenii* were the dominant genera present on the surface of produce.

Ozone exposure levels that did not damage produce, but reduced microbial loads significantly were determined. Different produce types had different abilities to resist ozone damage e.g. coriander and rocket were resistant to ozone (10 ppm for 10 min), whereas spinach, watercress and lettuce were more sensitive (1 ppm for 10 min). All ozone exposures used reduced bacterial loads *in vitro* but equivalent ozone exposure resulted in no effects when a packet of targeted produce was treated *per se*. Neither the exposure time nor the ozone concentration were found to be significant in terms of microbial reduction. Hence, a modified ozone fumigation system was engineered to improve application of ozone to produce surfaces and to reduce the time required to build up the desired ozone concentrations needed for produce treatment. High ozone exposure levels for shorter duration (10 ppm for 2 min and 15 ppm for 30 s) were determined that did not damage the produce visually and significantly reduced surface microflora. However, 1–10% of surface bacteria survived this ozone treatment. Therefore, the next stage of this study will focus on visualising microbes on leaf surfaces before and after ozone treatment using confocal microscopy in conjunction with appropriate staining techniques, and further investigate potential factors responsible for the ozone resistance in bacteria.

Chapter 3 Investigation of Potential Reasons for Bacterial Survival on Salad Leaves during Exposure to Gaseous Ozone

3.1 Introduction

Bacteria on fresh produce were not completely inactivated by optimal ozone treatment as reported in Chapter 2. Typically, 1–10% of the bacteria remained viable on the leaf surface (as estimated by viable counts). This may be due to a combination of physical protection of cells (e.g. micro-colonies) and/or increased ozone resistance induced by parallel factors such as refrigeration (Finkel 2006). To determine if cells were being protected in micro-colonies, it was necessary to develop a method to observe cells directly on leaf surfaces following ozone exposure.

Traditional plate count techniques detect only culturable bacteria which can result in underestimation of cell viability, but culture independent methods such as fluorescence microscopy allow quick and direct assessment of microbial colonization of plant surfaces. Cells can be observed using both conventional transmission electron microscopy (TEM) and scanning electron microscopy (SEM; Seo et al. 1998). However, the dehydration and fixation techniques involved in sample preparation result in visual artefacts which present a serious limitation to these approaches (Little 1991). The problems can be overcome by using cryo-staged confocal scanning laser microscopy (CSLM) which allows samples to be observed in a completely hydrated state (Seo et al. 1998). CSLM produces sharp, in-focus images from three dimensional specimens without the need for actually splicing the object (Ferrando and Spiess 2000). Moreover, live bacterial cells can be observed by selective labelling since samples are prepared non-invasively (Ferrando and Spiess 2000).

CSLM is a modified version of conventional light microscopy, where a laser is used as a light source instead of a lamp. It also features complex photomultiplier tube detectors (PMTs), and computerization to manage the scanning mirrors and view collected images. Specific software is used to store and analyse images (Paddock 2000). A schematic representation of confocal microscopy is shown in Fig. 3.1. A focused spot of light is used to scan the specimen while a photomultiplier records the light released through the interaction of the scanning light with focused areas (Evans and Donahue 2008). A dichroic mirror reflects the excited beam of light from the laser which is focused by the objective lens to a limited spot in the sample (Ferrando and Spiess 2000). The irradiated spot emits fluorescent light which passes through the dichroic

mirror and adjustable pinhole aperture (which is positioned optically in relation to the illumination aperture), and is gathered by a photomultiplier (Ferrando and Spiess 2000). The rapid reaction of the light detector of the scan should be shown with the same spatial position and reasonable brightness on the computer screen at all points (Paddock 2000). Spatial filtering by a small detector pinhole aperture is most significant to achieve maximum resolutions and optical sectioning (Park and Kihm 2006). Three-dimensional images of the specimen can be created by moving the microscope stage in axial (Z) plane which allows a series of optical sections to be made and also processing together slices of each point of light recorded throughout (Evans and Donahue 2008).

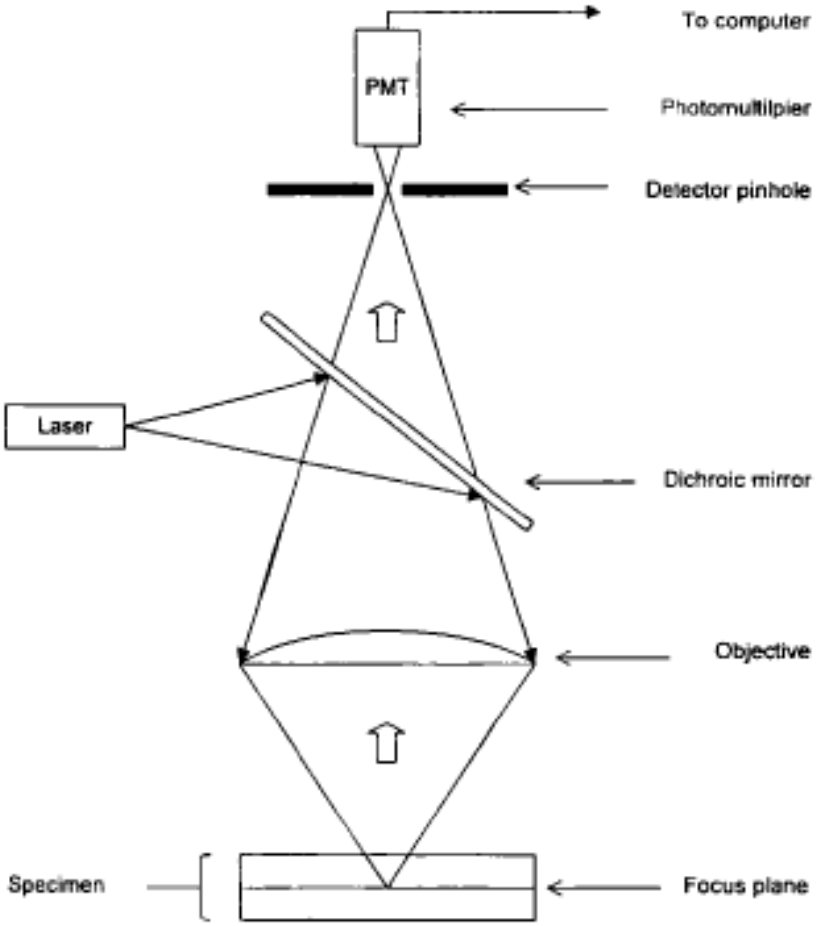

Figure 3. 1: A schematic representation of confocal microscopy. Adapted from Paddock, 2000.

The use of a laser in confocal microscopy is important to overcome the limitations of emission wavelength and the minimum intensity requirements for fluorescence microscopy. Selection of a laser mainly depends on wavelengths of emission, stability, power at each wavelength and cost. Most commercially used wave gas lasers are

helium–cadmium (He/Cd), helium–neon (He/Ne) and argon ion or krypton ion or sometimes a mixture of both gases (Ferrando and Spiess 2000).

A staining method, the LIVE/DEAD BacLight viability kit (Invitrogen/Molecular Probes, Eugene, Oregon, USA), is commonly used for enumeration of bacteria, archaea or eukaryotic cells, such as yeast. This kit comprises two fluorescent nucleic acid stains, SYTO®9 and propidium iodide (PI) (Berney et al. 2007; Little 1991). SYTO®9 is a green fluorescent stain that penetrates all cell membranes, whereas PI is a red fluorescent stain which penetrates only damaged cell membranes (Leuko et al. 2004). The discharge properties of the stain mixture bound to DNA changes because of the displacement of green fluorescent SYTO®9 stain by the red fluorescent PI stain (Berney et al. 2007). Although this kit only allows differentiation between intact and damaged cell membranes, it is frequently inferred to reflect active and dead cells as it appears appropriate to consider membrane-compromised cells as dead (Berney et al. 2007). Therefore, microscopic evaluation of LIVE/DEAD stained cells using the above approach is generally simplified to either green labelled as 'live' cells or red labelled as 'dead' cells (Leuko et al. 2004).

Epiphytic bacteria, i.e. bacteria present on the surface of a leaf, are exposed to numerous environmental stresses in nature, such as nutrient stress, water stress, variable weather conditions and exposure to UV radiation (Capozzi et al. 2009). Surviving and growing in these stressful conditions may pose a difficult challenge (Beattie 1995). However, bacteria are capable of adapting to and growing under stressful conditions (Beattie 1999) and initiating stress response mechanisms (Capozzi et al. 2009).

In this chapter, CSLM was used to differentiate between live and dead bacteria on the surface of a range of leafy salads and herbs (spinach, rocket, watercress, coriander and lettuce) in the presence and absence of ozone treatment. It also provided an opportunity to test the hypothesis that prior exposure to stress (cold) and increasing colny age enhances cell resistance to ozone exposure, using a *Pseudomonas* species isolated from coriander. *Pseudomonas* sp. was used as a model in this work, as species from this genera are known to be involved in the microbial proteolytic and pectinolytic activities that cause soft rot of fresh produce at storage temperatures as low as 0.2°C (Saranraj 2012) and were shown to be abundant on the leaf surfaces examined. The material in this chapter has been published in the paper (Wani et al. 2016).

Aim:

To investigate potential reasons for bacterial survival on leafy produce surfaces during exposure to gaseous ozone

Objectives:

- To develop a CLSM technique to visualize natural bacterial flora on leaves
- To develop a method for differential staining of 'live' and 'dead' bacterial cells to evaluate the efficacy of ozone treatment
- To determine if colony age and pre-exposure to cold stress affect the ozone resistance of a typical spoilage bacterium (*Pseudomonas* sp.)

3.2 Materials and Methods

3.2.1 Leafy produce

Packets of 'Ready-to-Eat' organic baby spinach, Iceberg lettuce, wild rocket, coriander and watercress were purchased from a local retailer and stored at 4°C until the use-by-date, i.e. 'EOL' (end of life). The leaves were then aseptically cut into discs using a sterile cork borer delivering 1.13 cm^2 for visualization of cell viability and enumeration of natural flora bacteria.

3.2.2 Bacterial staining and visualisation for cell viability assessment on leafy produce

Cell viability stains were separately prepared as per the manufacturer's instructions. This protocol utilizes green-fluorescent SYTO®9 stain to label live bacterial cells green, whereas red-fluorescent propidium iodide stains dead cells red. The staining solutions were prepared in Mueller Hinton Broth (MHB) and filter-sterilized using a syringe-mounted membrane filter of 0.2 µm pore size prior to use. The BacLight stains were added directly to the leaf surfaces which were placed onto sterile glass slides in 250 µL aliquots before placing a coverslip on top. The stained leaf was then incubated in the dark for 30 min before viewing with CSLM (Leica TCS SP2, Leica Microsystems, GMBH, Heidelberg, Germany). The samples were scanned with a 488 nm Argon laser for the SYTO®9-stained bacteria using emission wavelengths collected at 500–550 nm,

whereas a 543 nm Helium/Neon laser for the propidium iodide-stained bacteria using emission wavelengths collected at 574–714 nm. The microscope was equipped with either 40× HCX Plan (numerical aperture = 0.85) or 63× oil immersion objective (numerical aperture = 1.32) to image the leaf surfaces.

3.2.3 Direct enumeration of bacteria on leafy produce after ozone treatment using confocal microscopy

'Ready-to-Eat' organic baby spinach leaves, Iceberg lettuce, wild rocket, coriander and watercress were aseptically cut into discs using a sterile cork borer and placed onto sterile glass slides. Produce was treated with either 0, (charcoal filtered air), 1 (spinach, lettuce and watercress) or 10 (rocket and coriander) ppm ozone for 10 min. The leaf surface bacterial staining procedure as described in Section 3.2.2 was then performed. Images were captured at 40× magnification. Three replicates (leaf discs) of each product per treatment were used for enumeration of viable cells (stained green). Bacteria from 20 microscopic fields were counted on each replicate leaf for each type of fresh produce using image J software (Selinummi et al. 2005), and results were expressed as average numbers of bacteria per square centimeter (cm^{-2}) of leaf.

3.2.4 Investigating potential reasons for bacterial survival during ozone treatment: Isolation and identification of Pseudomonas sp.

The effect of stress on ozone resistance was determined on a *Pseudomonas* isolated from coriander. The isolation and identification of *Pseudomonas* sp. was performed as described in Section 2.2.1 & 2.2.2. The nucleotide sequence for the isolate employed in this study has been deposited in GenBank (NCBI) under the accession number: KR067481.

3.2.5 Investigating potential reasons for bacterial survival during ozone treatment: Effect of temperature on ozone resistance of Pseudomonas sp. in vitro

To find potential reasons for the ozone resistance observed by individual bacteria, it was hypothesised that both previous stress exposure and colony age contribute to ozone resistance.

To determine the effect of prior cold exposure on ozone resistance *in vitro*, a colony of *Pseudomonas* sp. (isolated from coriander) was sub-cultured on to CFC plates and

incubated at optimum conditions, i.e. 25°C for 48 h (control) and 4°C (test) to mimic produce storage conditions for 7 days. A colony of *Pseudomonas* sp. from each temperature plate was serially diluted to a standard concentration of 10^4 cells per mL (maintaining respective temperature conditions) in MRD and 100 µL of the cell suspension spread on to CFC agar plates. Each plate (containing either bacteria grown at 4°C or 25°C) was then treated with either 1 ppm ozone or 'clean air' for 10 min. Colony count was determined after incubating all plates at 25°C for 48 h.

3.2.6 Investigating potential reasons for bacterial survival during ozone treatment: Colony age effects on ozone resistance of Pseudomonas sp. in vitro

To determine whether colony age affected the ozone resistance of the bacteria, a colony of *Pseudomonas* sp. was sub-cultured onto CFC plates and incubated at 25°C for up to 12 days. A single colony was isolated on the 2^{nd}, 4^{th}, 7^{th}, 10^{th} and 12^{th} day of incubation and transferred to MRD. A standardized concentration of 10^4 cells per mL of each colony age was spread (100 µL) onto sterile CFC plates and these plates were then exposed to either 1 ppm ozone or 'clean air' for 10 min. Colony count was determined after incubating CFC plates at 25°C for 48 h. The percent survival of *Pseudomonas* sp. was calculated by comparing the ozone treated colonies to the control colonies (not ozone treated).

3.2.7 Statistical analysis

Data were analysed using SPSS (IBM SPSS Statistics 19 64Bit) and graphs were produced using Microsoft Office Excel 2010 and SigmaPlot 12.5. Data distribution was tested using Normality test and significant differences between mean values were verified using LSD ($P < 0.05$) following one-way ANOVA.

3.2.8 Log reduction

Microbial log reduction was calculated as follows:

$$\text{Log reduction} = \log_{10}(A) - \log_{10}(B) \text{ or Log reduction} = \log_{10}(A \div B)$$

Where A is the number of viable microorganism before treatment and B is the number of viable microorganism after treatment.

3.3 Results

3.3.1 Confocal microscopy: Visualization of bacteria on leaves

Spinach leaves were observed using CSLM together with LIVE/DEAD® BacLight™ Viability Kit to determine if the bacteria that survived ozone treatment were typically present in colonies or individual cells. Bacteria were attached mainly to the leaf epidermal cell margins and observed at 20× magnification, scale bar = 47.6 µm (Fig. 3.2)

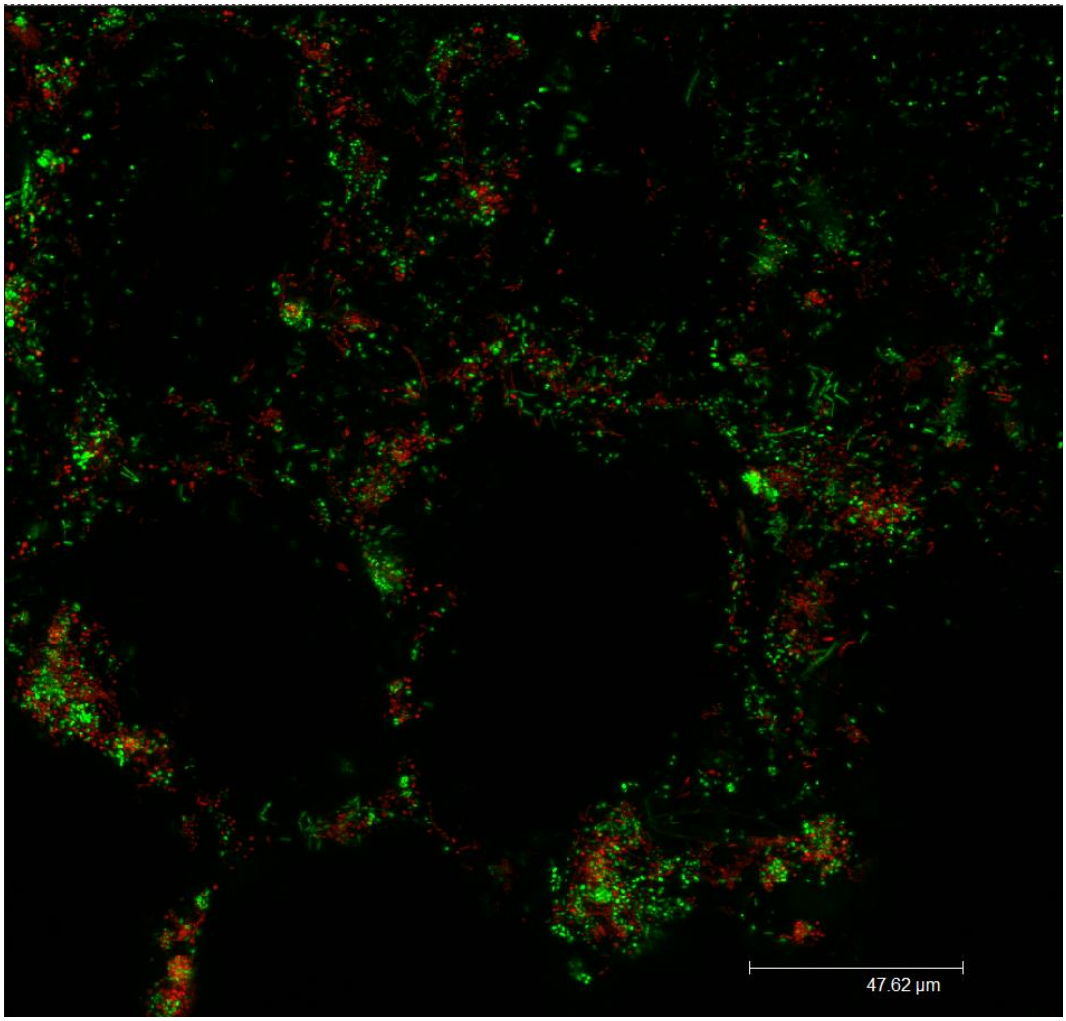

Figure 3. 2: Confocal microscopy image of a control (not exposed to ozone) baby spinach leaf. Bacteria were stained with green-fluorescent SYTO®9 to label live bacterial cells green and with red-fluorescent propidium iodide to label dead bacterial cells red. Bacteria appeared to attach preferentially to the epidermal cell margins. Scale bar = 47.6 µm.

3.3.2 Direct enumeration of bacteria on leafy produce after ozone treatment using confocal microscopy

Bacterial viability on non-ozone exposed control leaves was nearly 90% (Fig. 3.3A & B), whereas only 10% of bacteria on ozone-treated leaf surfaces appeared viable. On control leaves, large aggregations of live cells stained green are visible (see Fig. 3.3A indicated by the blue arrow). Micro-colonies and cells in twos/threes, as indicated by the orange arrow (Fig. 3.3A – spinach leaf as an example), were frequent. Individual dead cells stained red are visible in Fig. 3.3A (indicated by a white arrow). Similar bacterial aggregates were also observed on watercress, coriander, rocket and lettuce leaf surfaces (Fig. 3.4). In Fig 3.3B, yellow arrows indicate individual bacteria surviving ozone treatment. Enumeration of bacterial viability after ozone exposure showed at least 1-log reduction in all targeted produce (Table 3.1, Fig. 3.5).

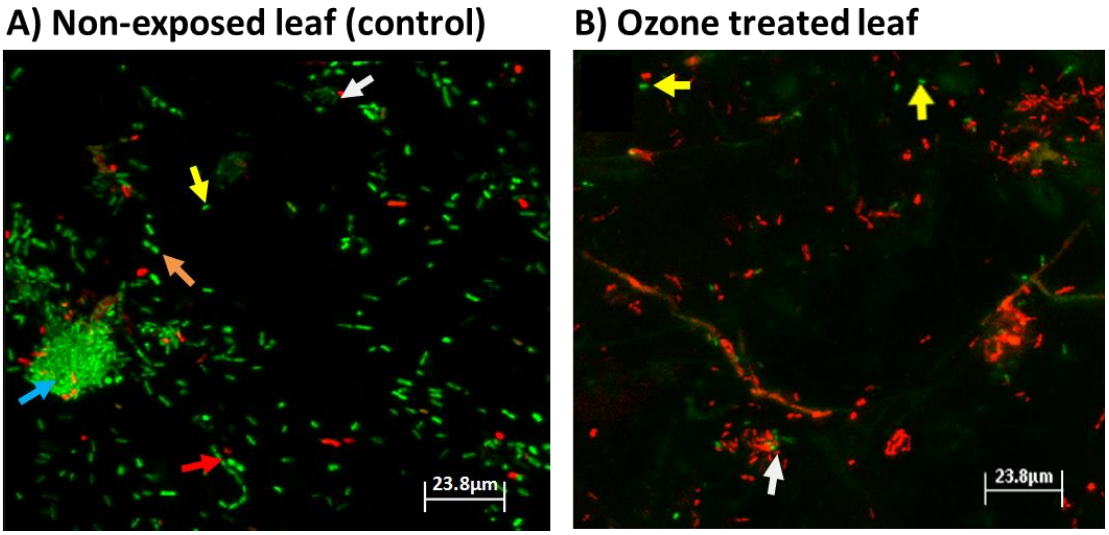

Figure 3. 3: fluorescent SYTO®9 to label live bacterial cells green and with red-fluorescent propidium iodide to label dead bacterial cells red. Scale bar = 23.8 µm (A) Non-ozone exposed leaf (control). Blue arrow indicates large aggregates of live cells, orange arrow indicates small colonies in two/threes, red arrow indicates bacteria in chains and yellow arrow indicates individual cells present on a leaf surface and white arrow indicates individual dead cell (B) Leaf treated with 1ppm ozone for 10 min. White arrow indicates live cell present in micro-colony of dead cells and yellow arrows indicate individual live cells surviving ozone treatment

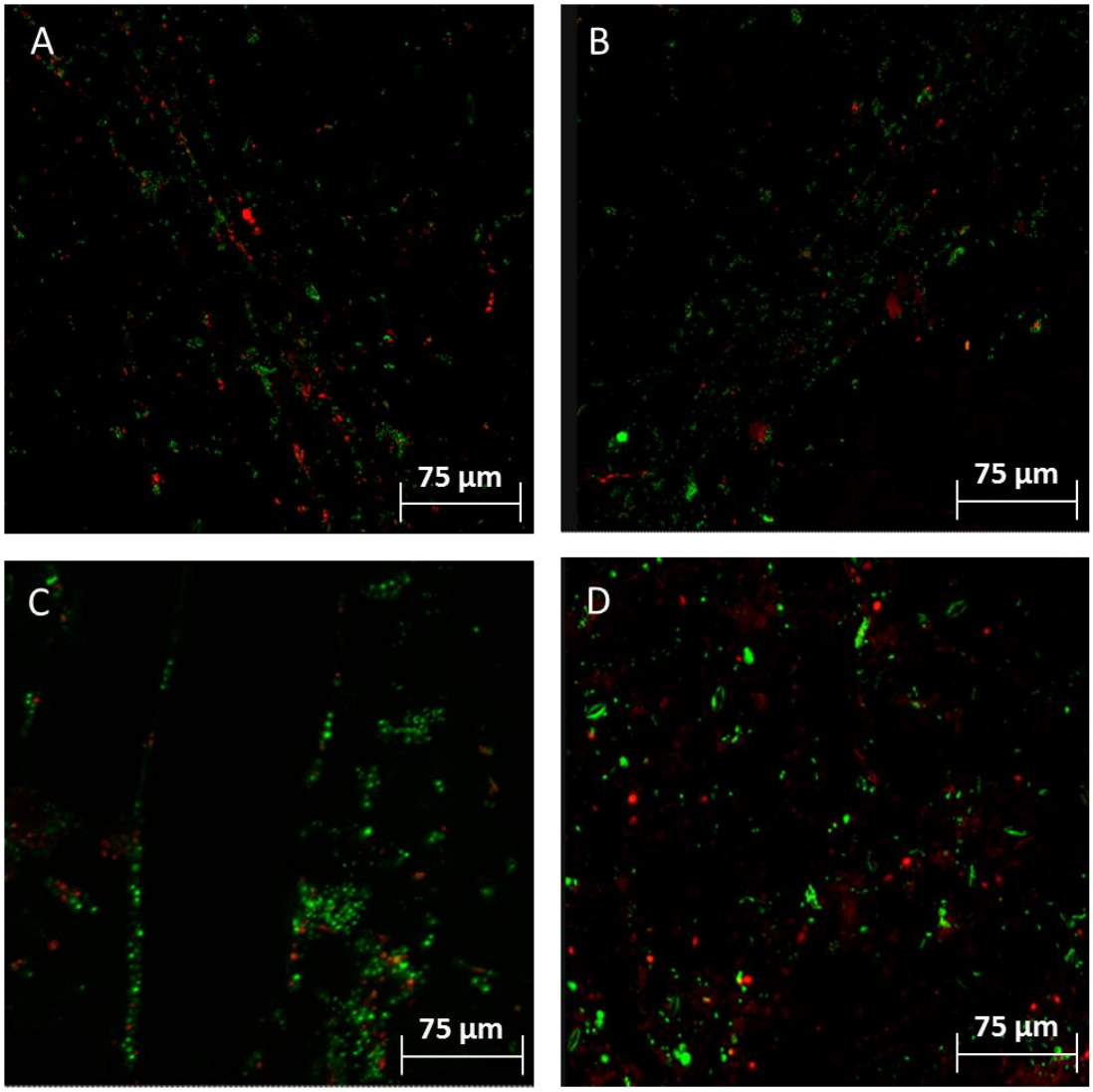

Figure 3. 4: Confocal microscopy image of the A) watercress B) coriander C) rocket and D) lettuce leaf surfaces before ozone treatment at x40 magnification. Bacteria were stained with green-fluorescent SYTO®9 to label live bacterial cells green and with red-fluorescent propidium iodide to label dead bacterial cells red**,** scale bar = 75 µm

Table 3. 1: Microbial log reduction achieved by ozone treatment on leafy produce

Targeted leafy produce	Log reduction
Spinach	**0.8**
Coriander	**1**
Watercress	**1.4**
Rocket	**1.1**
Lettuce	**1.3**

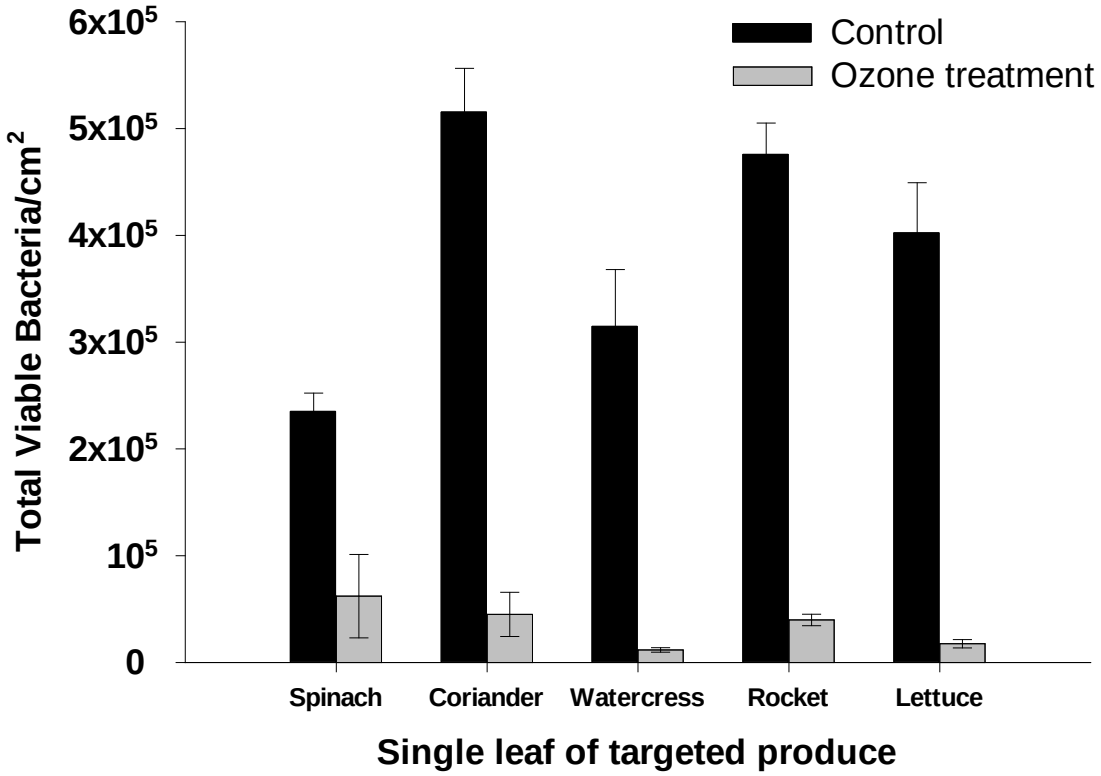

Figure 3. 5: Total viable bacterial count from the spinach, watercress and lettuce leaves treated with 1 ppm ozone and coriander and rocket treated with 10 ppm (grey bar) versus leaves not treated with ozone and maintained in 'clean air' for an equivalent period (black bars) for 10 min. Data derived from microscopic counts of SYTO®9/PI stained bacteria on leaves. Values represent means (±Standard Error) of measurements made on three independent leaves per treatment

3.3.3 Investigating potential reasons for bacterial survival on leaf surfaces after ozone treatment: Effect of temperature on ozone resistance of Pseudomonas sp. in vitro

Colony numbers (CFU) of *Pseudomonas* sp. maintained in optimum conditions (25°C) *in vitro* were significantly reduced by ozone treatment ($P < 0.05$; Fig. 3.6). In contrast, colony numbers of *Pseudomonas* sp. maintained in cold conditions (i.e. stored at 4°C) *in vitro* were not significantly reduced by ozone enrichment ($P < 0.05$; Fig. 3.6) implying that bacteria submitted to refrigerated conditions show enhanced resistance to ozone.

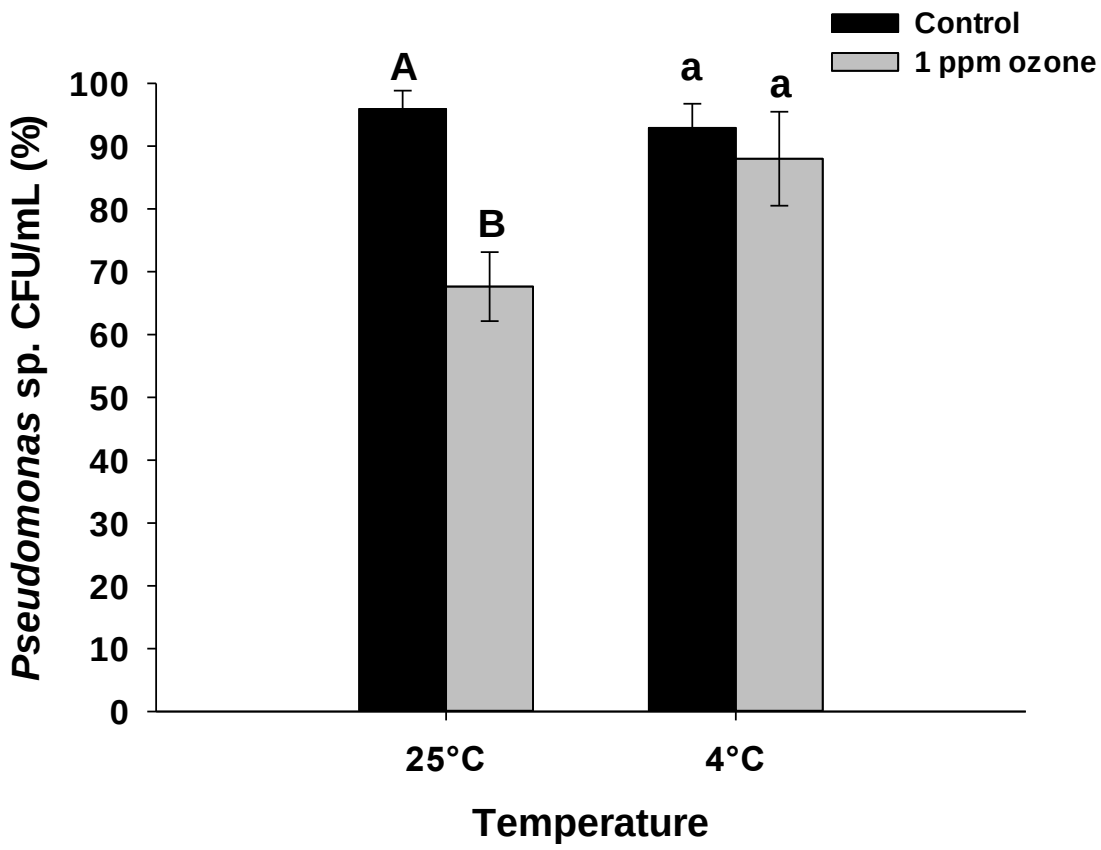

Figure 3. 6: Impacts of ozone-exposure (1 ppm for 10 min) on *Pseudomonas* sp. grown at 25°C and 4°C and then exposed to either 1 ppm ozone concentration (grey bar) or 'clean' air (black bar) for 10 min. After the treatment, the plates were either incubated at optimum temperature i.e. 25°C for 24 h. Values represent means (±Standard Error) of measurements made on three independent plates per treatment. Bars with different letters are statistically significantly different ($P < 0.05$).

3.3.4 Investigating potential reasons for bacterial survival on leaf surfaces after ozone treatment: Effect of age on ozone resistance of the leaf surface bacteria in vitro

Pseudomonas cells derived from 7-, 10- and 12-day-old colonies showed approximately 40% greater survival to ozone treatment than those from 2- and 4-day-old colonies (Fig. 3.7), suggesting that cells from older bacterial colonies are more ozone resistant than cells from younger colonies. The increase in survival was statistically significant ($P < 0.05$).

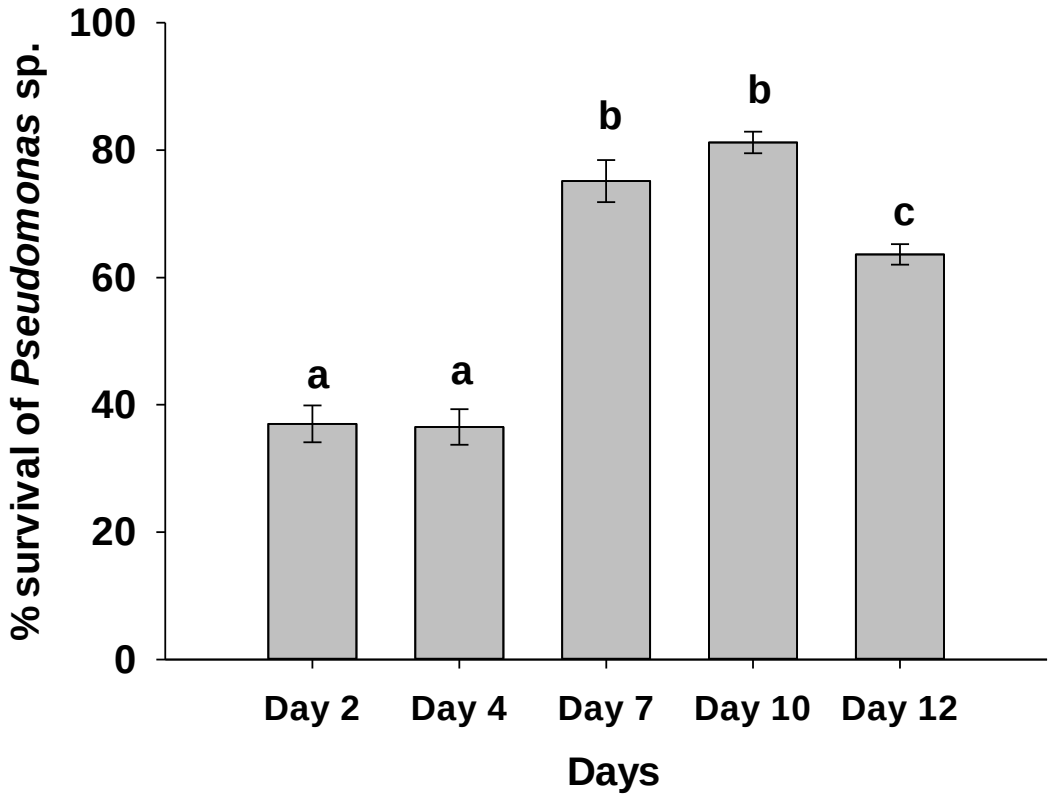

Figure 3. 7: Survival of *Pseudomonas* sp obtained from different colony ages exposed to 1 ppm ozone concentration for 10 min. After ozone exposure, the culture plates were maintained at 25°C for 12 days. Bars with different letters are statistically significantly different ($P < 0.05$).

3.4 Discussion

3.4.1 Potential reasons for bacterial resistance to ozone treatment: Survival in micro-colonies

Confocal microscopy revealed that bacteria were mainly attached to plant cell margins, consistent with the report by Romantschuk et al. (1996). SYTO®9/PI staining in conjunction with CSLM allowed *in situ* observation of bacteria on untreated leaf surfaces (control), and they appeared to be present as small micro-colonies and as individual cells (Fig. 3.3A). Similar observations were obtained by Carmichael et al. (1999), who used fluorescein isothiocyanate (FITC) staining together with confocal imaging techniques to observe both clusters and individual bacteria on the surface of lettuce leaves.

The data presented here indicate that although ozone treatment significantly reduced bacterial viable counts on the leaf surface, approximately 1−10% of the bacterial flora exhibited resistance to the ozone treatment employed. Confocal images of ozone treated leaves revealed that 2-3 live cells survived in micro-colonies (surrounded by dead cells). Micro-colonies and biofilms are formed on leaf surfaces due to bacterial attachment and production of exopolymeric substances (Mah 2001). This motivates microbial cells to stimulate activities unachievable alone or outside of micro-colonies. The possible benefits of micro-colonies or biofilms are protection from UV, desiccation and predation, and the facilitation of genetic exchange, gene transfer and synergistic interaction between cells (Morris and Monier 2003). Biofilms allow microbes to remain in close contact and communicate by quorum sensing, and thus, combat anti-microbial treatments as a community (Jahid and Ha 2012). The survival of bacteria to ozone exposure could also be due to the presence of a small sub-population of persister cells. These cells are invulnerable cells that neither grow nor die, which may enter a highly-protected state exhibiting intense resistance, and develop more commonly in micro-colonies or biofilm (Van Houdt and Michiels 2010; Bridier et al. 2011).

Therefore, cells in micro-colonies/biofilms on leaf surfaces may resist ozone treatment by both physical protection (i.e. surrounding cells are killed but the cells in the centre of a colony are physically protected) or by the biofilm bacteria having inherent enhanced resistance mechanisms.

3.4.2 Potential reasons for bacterial resistance to ozone treatment: Survival of individual cells

Some individual cells on the leaf surface appeared to survive ozone treatment (Fig. 3.3B) suggesting that they also exhibit inherent resistance mechanisms. It was hypothesised that the survival of the individual bacteria on the leaf surface after ozone exposure is due to colony ageing or prior exposure to cold (Wani et al. 2015; Johnson 2008).

During growth in the field, the bacteria present on the surface of leaves are continually subjected to changes in temperature, nutrient availability and osmotic pressure (Lindow 1995). In addition, to prevent microbial spoilage and contamination by pathogens, cumulative mild processing steps are employed during the production of fresh produce

increasing chances of additional stress and potentially developing hardy bacteria that are able to resist any further applied treatments such as ozone exposure (Capozzi et al. 2009).

A number of stresses have been shown to induce such 'cross protection', and in this study, cold stress was used as a model to determine if prior stress exposure enhanced the ozone resistance of a typical leaf surface bacterium. Results suggest that pre-exposure of bacteria (*Pseudomonas* sp.) to cold stress enhanced ozone resistance *in vitro*. Survival of these bacteria in stressed conditions is a combination of cell responses designed to minimise the lethal effects or repair damage (Jozefczuk et al. 2010). When repairing damage, the presence of cold shock proteins in bacteria overcomes growth-limiting effects by either altering redox status or increasing stability of RNA and DNA secondary structures (Reva et al. 2006). Cold shock acclimation proteins are produced in high abundance during low temperature and have been identified in *Pseudomonas* spp. (Reva et al. 2006). Our results indicate that such stress-related temperature responses may also help bacteria to survive subsequent ozone exposure.

It was also hypothesised that colony age is a factor contributing to the ozone resistance of individual leaf surface bacteria (Wani et al. 2015). Fresh produce takes weeks to grow in the field and is then subject to harvest and transportation; any cells present on the leaf surface could easily have been present and persist for a prolonged period (Wani et al. 2016). Here, results clearly demonstrated that cells derived from older colonies were more resistant to ozone than cells from younger colonies, and this observation is strengthened by previous work showing that older biofilm cells of *Pseudomonas aeruginosa* exhibit greater resistance to biocides than younger cells (Bridier et al. 2011) and older cells show increased expression of RpoS genes.

Saint-Ruf and colleague (2014) examined diversification in aging colonies of *E. coli*. They observed that most of the cells in colonies on the first day of incubation were actively dividing while on day 4 and 7 of incubation, there were fewer dividing cells in aging colonies. Further, it was deomstrated that clusters of cells with different phenotypes started to appear inside *E. coli* colonies grown on LB agar plates after seven days (Saint-Ruf C 2014). These aged colonies showed enhanced adaptive radiation to stress response which could have possibly resulted from the generation of mutants during colony growth (Saint-Ruf C 2014). A variety of molecular mechanisms are

responsible for mutation in againg colonies: a) the formation of mutants could be generated late in colony development (Saint-Ruf C 2014); b) some mutants might require the presence of other mutants that scavenge toxins or provide nutrients for growth (Katz and Hershberg 2013) and c), mutants may only begin growing or may grow better when local microenvironmental conditions become favorable. For example, dead cells could provide nutrients to colony founders (Katz and Hershberg 2013).

Therefore, further understanding of the molecular basis of ozone resistance of leaf surface bacteria is required. A detailed understanding of the resistance mechanisms involved may help to develop novel methods to control the contamination of fresh produce.

3.5 Conclusion

This work focused on visualising microbes on leaf surfaces after ozone treatment by using confocal scanning microscopy and investigating potential reasons for ozone resistance in leaf surface bacteria. Confocal microscopy demonstrated that bacterial cells able to survive ozone exposure occurred both in micro-colonies and as individuals on the leaf surface. This suggested that bacterial ozone resistance was likely due to a number of factors e.g. physical protection in small colonies and inherent resistance of individual cells. Subsequent results suggested that colony age and prior exposure to cold stress of a typical leaf surface bacterium (*Pseudomonas* sp.) enhances ozone resistance *in vitro*. Therefore, transcriptomic approaches were designed for further investigation on understanding the mechanisms of ozone resistance in aged colonies and cold stressed cells of *Pseudomonas* sp.; this may lead to methods that can overcome resistance. Such applications could deliver immense potential for commercial applications.

Chapter 4 Investigating Reasons for Bacterial Ozone Resistance: a Gene Expression Study using RNA-Seq

4.1 Introduction

Results from Chapter 3 demonstrated that aged colonies and cold-stressed cells of *Pseudomonas* sp. isolated from coriander exhibited higher ozone resistance than control (2-day-old) cells. This implies that common crop growth and/or storage conditions may enhance bacterial resistance to treatments applied. To try and understand the potential mechanisms responsible for ozone resistance, it was decided to conduct a detailed comparison of gene expression in aged colonies and cold-stressed *Pseudomonas* cells compared with untreated controls using RNA-Seq technology.

By definition, a group of all the transcripts (RNAs) present in a cell assessed quantitatively and qualitatively at a specific instant of cell growth or during a particular physiological state is called the transcriptome (Pinto et al. 2011). The transcriptome denotes a vital association between information encoded in DNA and the phenotype (Malone and Oliver 2011). To date, knowledge of how the transcriptome varies in cold-stressed and ageing bacteria remains poor. In the present study, it was aimed to identify differentially expressed genes (DEGs) and pathways under stressed conditions to develop a better understanding of ozone resistance mechanisms in bacteria – employing *Pseudomonas* as a model to do so. Various techniques to study differentially expressed genes (DEGs) are available, including Northern blotting; nuclease protection assay; serial analysis of gene expression (SAGE) and quantitative real-time polymerase chain reaction (RT)-PCR; hybridization methodology (microarrays) and tiling array technology (Xia et al. 2013; Pinto et al. 2011). These approaches are relatively inexpensive, but they all have inherent technical limitations (Pinto et al. 2011). For example, in array technology, the accuracy of the expression measurements depends to a significant extent on the amount of transcripts present. If these are in low abundance, the accuracy of expression measurements is compromised (Zhoa 2014). In addition, probes used in microarrays vary significantly in their hybridization properties, and are restricted to examining only those genes for which probes are specifically designed (Zhoa 2014).

Next-generation sequencing (NGS) of RNA (i.e. RNA-Seq) is currently considered a novel and better tool to study gene expression patterns and the approach has gained credence in all areas of genomic study, including transcriptomics (Xia et al. 2013). This

revolutionary technique was initially developed for identifying the transcriptional map of eukaryotic organisms as it is easier to isolate their mRNAs with poly-A tails, but the technology is also now being applied to the study of prokaryotes, predominantly bacteria (Pinto et al. 2011). RNA sequencing is capable of capturing majority of the expressed transcripts (Chen et al. 2011; Malone and Oliver 2011; Sorek and Cossart 2010). This makes the technique ideal to develop further understanding of potential ozone resistance mechanisms in aged/stressed bacteria. Total RNA (tRNA) is typically extracted and then converted into a cDNA library by reverse transcription (RT) with adaptors attached to either one or both ends of cDNA fragments (Sorek and Cossart 2010; Wang 2009). Each molecule is then sequenced, and the output of RNA-Seq generally consists of millions of short sequence reads from one end (single-end sequencing) or both ends (pair-end sequencing), which denotes the fragments of RNA (Pinto et al. 2011; Wang 2009). This is performed by direct sequencing on any of the new sequencing technologies such as Roche 454, Applied Biosystems' SOLiD platforms and the Illumina Genome Analyzer (Wang 2009; Wilhelm and Landry 2009). The transcribed sequences are either aligned to a reference genome or assembled *de novo* without the genomic sequence (Malone and Oliver 2011; Wang 2009). The level of gene expression is evaluated by counting the reads that map back to the reference and the number of mapped reads signifies the amount of expression level for that particular gene (Sorek and Cossart 2010). A basic flowchart for obtaining a bacterial transcriptome using RNA-Seq technology is illustrated in Fig. 4.1.

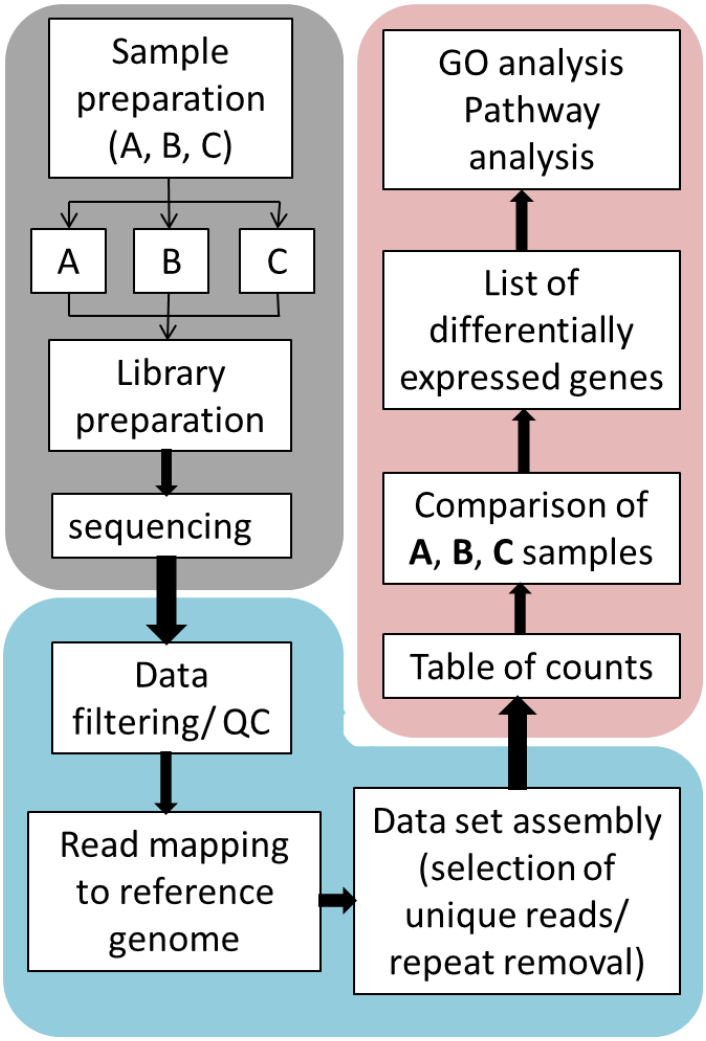

Figure 4. 1: Basic flowchart of RNA-Seq. A typical analysis stream for three theoretical biological samples (A, B and C) is shown with the various sections colour coded as wet-lab work (grey), creation of the filtered data sets (cyan), and data analysis (pink). Key: QC = Quality Control & GO = Gene Ontology (Modified from Wilhelm and Landry 2009).

In addition, RNA-Seq has almost no background noise as compared with microarray and requires less RNA per sample. It also gives high coverage of the transcripts and sequence data are reproducible (Pinto et al. 2011). Unlike microarrays, this system can be used on species for which a full genome sequence is not available as it provides direct access to the sequence. RNA-Seq does not rely upon hybridization, which eliminates the possibility of potential cross-hybridization (McCormick et al 2011). Overall, it is the first technique that allows quantitative and accurate analysis of the entire transcriptome in less time and is relatively cost effective when compared with large-scale Sanger sequencing or arrays (Wang 2009).

This chapter focuses on determining the potential molecular mechanisms by which bacteria are able to resist ozone treatment. Better understanding of these mechanisms may allow future development of novel more effective treatments for the control of bacteria and such teatments may be applicable in a wide range of commercial situations. It was hypothesized that RNA-Seq will show increased expression of RpoS gene and accumulation of cold-shock protein in aged colonies and cold-stressed cells respectively.

Aim: To investigate potential mechanisms for bacterial ozone resistance in aged and cold-stressed cells using next-generation sequencing (RNA-Seq)

Objectives:

- To isolate total RNA from aged colonies, cold stress treated and control *Pseudomonas* sp. for RNA sequencing
- To evaluate the level of gene expression by counting the reads that map back to a selected reference genome
- To determine if the modification in cellular pathways are the most affected by aged colony and cold-stress e.g. cellular component, molecular function and biological process

4.2 Materials & Methods

4.2.1 Bacterial culture: preparation of control, aged and cold-stressed cells

Results from Chapter 3 revealed that aged colonies or cold-stressed cells of *Pseudomonas* sp. (isolated from coriander) showed higher ozone resistance than untreated control cells. In order to examine the mechanisms involved, gene expression in stressed bacteria and control cells were compared using RNA-Seq. To examine responses of cold-stressed cultures, a colony of *Pseudomonas* sp. isolated from coriander was inoculated in 9 mL of sterile MRD and serial diluted to a standardized concentration 10^4 cells per mL. This inoculum (100 µL) was spread onto sterile CFC plates and maintained at 4°C (in a bid to mimick cold storage conditions) for 7 days. For examining aged colonies responses, the plates were incubated at 25°C for 10 days. Control (young) cultures were incubated at 25°C for 48 h.

4.2.2 RNA extraction

After incubation, colonies of bacteria from all CFC plates (cold-stressed, aged and control cells) were transferred into a three-fold buffer/PBS solution (150 mL 1 × PBS + 300 mL nutrient broth) using a sterile loop and diluted to obtain equal amounts of cells from each treatment (i.e. 10^4 cells per mL). Cold conditions were maintained throughout (i.e. cells were added to pre-chilled solutions) for the cold-stressed cultures. The cells were then lysed to release RNA; RNase-away treated glass beads 2 mm in diameter were added and samples shaken in a bead-beater (Qiagen TissueLyser II) at 30 Hz (hertz) for 20 s.

Three biological replicates were used for all RNA-Seq experiments from each treatment type. The total RNA from the bacterial cells was extracted using an ISOLATE RNA kit (Bioline). All procedures were performed according to the manufacturer's protocol and guidelines. This protocol involved filtration of cell lysate in a column. DNase I reaction mixture was used to digest DNA followed by washing and drying of silica membrane prior to eluting the RNA with 60 µL RNase-free water. The integrity and quality of the total RNA was determined by a NanoDrop 1000 spectrophotometer and Agilent's 2100 Bioanalyzer using the Agilent RNA 6000 (Appendix B) Nano kit. All nine samples were stored in RNAStable columns (Biomatrica) according to the manufacturer's protocol and shipped to Illinois University (University of Illinois Keck Center, 1201 W. Gregory Dr., 334 ERML, Urbana, IL 61801, USA) for sequencing and down-stream analysis. The following protocols were conducted by Illinois University.

4.2.3 Construction of RNA-Seq libraries enriched for bacterial mRNA

RNA-Seq libraries were constructed using the TruSeq Stranded RNA Sample Preparation Kit (Illumina San Diego, CA). In brief, total RNA was recovered from the RNAStable columns according to the manufacturer's protocol. RNA was DNAsed and then quantified by Qubit (Life Technologies, Grand Island, NY) and checked for integrity on a 1% eGel (Life Technologies). Ribosomal RNA was removed from 1 µg of total RNA using the Ribo-Zero™ Magnetic Bacteria kit (Illumina, CA). First-strand synthesis was synthesized with a random hexamer and SuperScript II (Life Technologies). Double stranded DNA was blunt-ended, 3′-end A-tailed and ligated to indexed adaptors. The adaptor-ligated double-stranded cDNA was amplified by PCR for 12 cycles with the Kapa HiFi polymerase (Kapa Biosystems, Woburn, MA). The final

libraries were quantitated on Qubit and the average size determined on an Agilent bioanalyzer DNA7500 DNA chip (Agilent Technologies, Wilmington, DE) and diluted to 10 nM final concentration. The 10 nM dilution was further quantitated by qPCR on a BioRad CFX Connect Real-Time System (Bio-Rad Laboratories, Inc. CA), which resulted in high accuracy that results in consistent pooling of barcoded libraries and maximization of number of clusters in the flowcell.

4.2.4 Sequencing on an Illumina HiSeq2000

The pooled libraries were loaded onto one lane of an 8-lane flowcell for cluster formation on cBOT and sequenced on an Illumina HiSeq2000 from one end of the molecules for a total read length of 100 nucleotides (nt) from that end. The typical output from a lane with version 3 sequencing reagents and Casava1.8.2 is 150 to 200 million reads; 192M reads were generated from this run. The run generated .bcl files which were converted into demultiplexed compressed fastq files using Casava 1.8.2 (Illumina, CA). A secondary pipeline decompressed the fastq files, generated plots with quality scores using FastX Tool Kit, removed perfect matches to reads that contain only adaptor and generated a report with the number of reads per sample/library. Demultiplexed fastq files were .tgz compressed.

4.2.5 RNA-Seq alignment

Raw FASTQ data were subjected to a head crop of 1 base due to a fair number of low-quality bases at positions 2-3, then quality-trimmed from both 3′ and 5′ ends using the program Trimmomatic v 0.30 (Lohse et al. 2012), using a minimal phred33 quality score of 20 and a minimal length of 15. Sequences were then aligned using Novoalign v3.00.05, Novocraft using the default parameters for single-end reads and the *Pseudomonas* sp. GM60 genome (Genbank: AKJI00000000.1) from NCBI as the reference genome. The raw read counts were tabulated for each sample using the GFF gene model file from NCBI and htseq-count, from HTSeq v0.6.1 using parameters -m intersection-nonempty -s reverse -t gene -i Name.

The raw read counts were input into R v3.1.1 (R Core Team 2013) for data pre-processing and statistical analysis using packages from Bioconductor (Carey et al. 2005) as indicated below. Of the genes expressed, 2207 out of 5943 did not have at least 1 count per million mapped reads in at least 2 samples and were filtered out. The

remaining 3736 genes were analyzed for differential expression using edgeR v3.6.8 (Robinson et al 2010). The raw count values were used in a negative binomial model (Robinson and Smyth 2007) that accounted for the total library size for each sample and an extra TMM normalization factor (Robinson and Oshlack 2010) for any biases due to changes in total RNA composition of the samples, along with qCML tagwise dispersion estimates. Pairwise comparisons of cold-stressed (4C) vs control (C) and aged (D10) vs C were calculated using exact tests, and a False Discovery Rate (FDR) correction (Benjamini and Hochberg 1995) was performed separately for each comparison. All clustering of samples was performed using normalized individual sample expression levels obtained from edgeR's cpm function, which adjusts for the total number of reads and the extra TMM normalization factor, plus adds a proportional constant (0.25 average) to avoid zero values, then transforms to the $\log_2$ scale.

Annotation information for the genes was obtained from the Integrated Microbial Genomes system [10] (Taxon ID: 2511231018, last Modified Date: 2014-08-05) for the following annotation types: cluster of orthologous groups (COG) categories and individual COG terms, Enzyme Commision (EC) IDs. For each annotation category, over-representation testing for each category/ID was performed by comparing the frequency of the category/ID among genes with FDR p-values < 0.05 (4C vs Control: 1132 genes, D10 vs Control: 1124 genes) to the frequency found in the 3736 tested genes. P-values were calculated in two ways: theoretically using the traditional hyper-geometric test and empirically by bootstrapping 10,000 samplings of X genes from Y background (X = number of significant genes in each comparison that mapped to any term in the annotation category and Y = number of the 3736 tested genes that mapped to any term in the annotation category). Next, the proportion of the 10,000 samplings that had the number of genes for a particular category/ID equal to or larger than the actual significant number of genes for that category/ID was calculated.

4.3 Results

4.3.1 Illumina sequencing and sequence mapping

Raw sequence output generated 192 million reads, each with a length of 100nt. Those reads mapping to the most suitable reference genome (*Pseudomonas* sp. GM60) were first categorized into three classes (Table 4.1). Uniquely mapped reads are those that

map to only one position in the genome, and gapped alignment are those that have a (limited) mismatch as compared with the reference genome. Unmapped reads did not (share sufficient sequence similarity to) map to any position in the reference genome.

Table 4. 1: Number of reads sequenced and mapped

Sample	Read Sequences	Unique Alignment	Gapped Alignment	Unmapped reads
4C_I	25,748,666	17,053,980	2,922,953	8,688,761
4C_II	21,949,529	15,677,275	2,848,392	6,267,351
4C_III	21,107,733	15,729,041	3,018,542	5,374,059
C_I	19,333,104	14,605,701	2,389,820	4,724,414
C_II	19,842,086	15,181,454	2,724,031	4,657,447
C_III	21,722,592	16,535,963	2,435,825	5,183,392
D10_I	20,758,340	14,542,190	1,213,218	6,215,488
D10_II	19,940,059	14,311,523	1,169,298	5,627,645
D10_III	21,465,952	16,539,000	1,122,241	4,925,913

4C, 10D and C stand for cold-stressed, aged and control samples, respectively. Numbers I, II and III indicate the three biological replicates.

The assembled transcripts were then classified into two main categories (Table 4.2): unique aligned transcripts and unmapped transcipts.

Table 4. 2: Classification of transcripts

Sample	Aligned (%)	Unmapped (%)
4C_I	66.16	33.09
4C_II	71.33	27.27
4C_III	74.40	24.33
C_I	75.51	22.86
C_II	76.54	21.79
C_III	76.07	22.10
D10_I	70.70	15.71
D10_II	72.26	17.20
D10_III	77.37	16.23

1 million reads aligned to *Pseudomonas* sp. GM60

4.3.2 Gene expression analysis

After the alignment of the sequence and statistical analysis, the genes differentially expressed between aged cultures (D10) and control (C) as well as between cold-stressed cultures (4C) and their respective control were identified. Overall, the three biological replicates in each sample were similar to each other in terms of differential gene

expression. At the level of the treatments, cold-stressed (4C) and control (C) samples were more comparable with each other than the aged (D10) sample (Fig. 4.2).

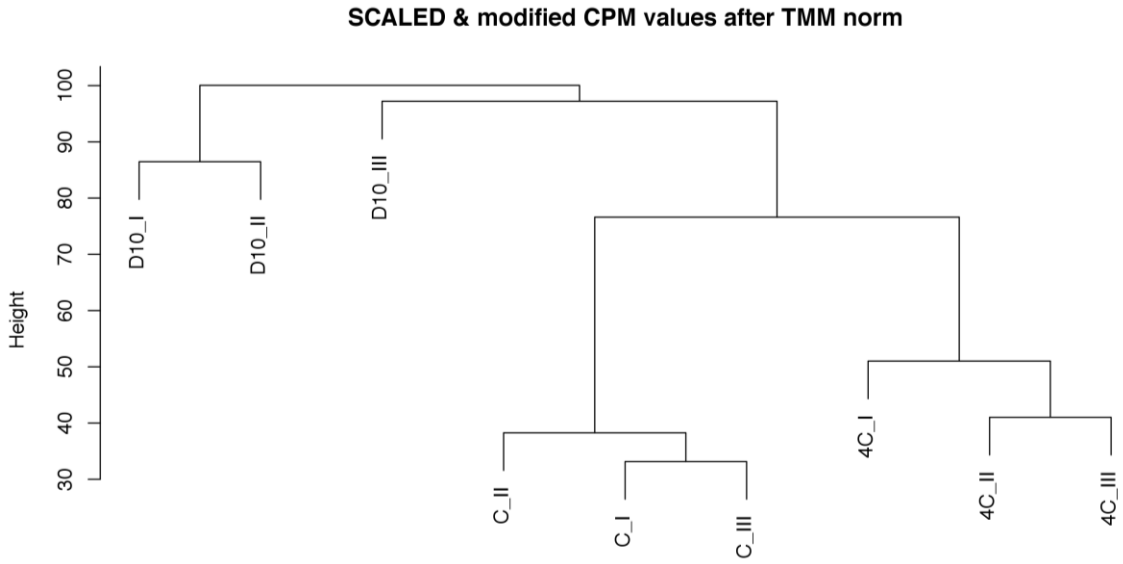

Figure 4. 2: Overview of gene expression in all three bacterial samples. 4C, 10D and C stand for cold-stressed, aged and control samples, respectively. Numbers I, II and III indicate the three biological replicates (Source: Illinois University) .

The analysis of differentially expressed genes (DEGs) revealed that very few genes in aged colonies (D10) were responsible for the observed differences as compared with cold-stressed (4C) and control (C) samples. Fig. 4.3 illustrates that approximately 98% (Y-axis) of the reads were assigned to <5% of the genes (x-axis) in aged colonies (D10). In addition, >90% of the reads map to one gene in all three aged (D10) samples, subsequently characterised to be a non-coding RNA which is a component of RNaseP.

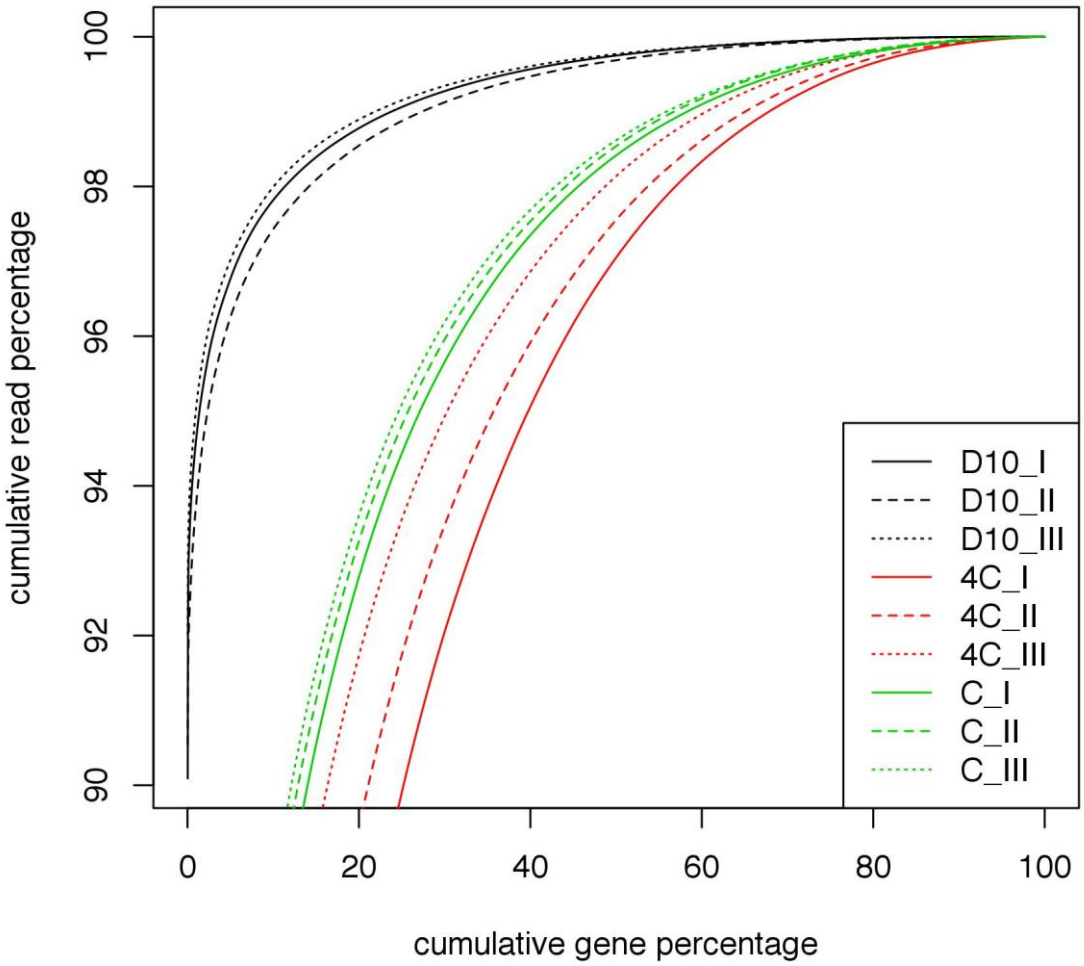

Figure 4. 3: Cumulative gene percentage graph of all three samples (Source: Illinois University).

The heatmap shows some complex patterns of expression, with two distinct groups (clusters) of genes in each pairwise comparison (Fig. 4.4 & 4.5). Within these clusters, control (C) and cold-stressed (4C) samples show limited variation in expression, whereas expression in aged colonies (D10) was observed to be more variable.

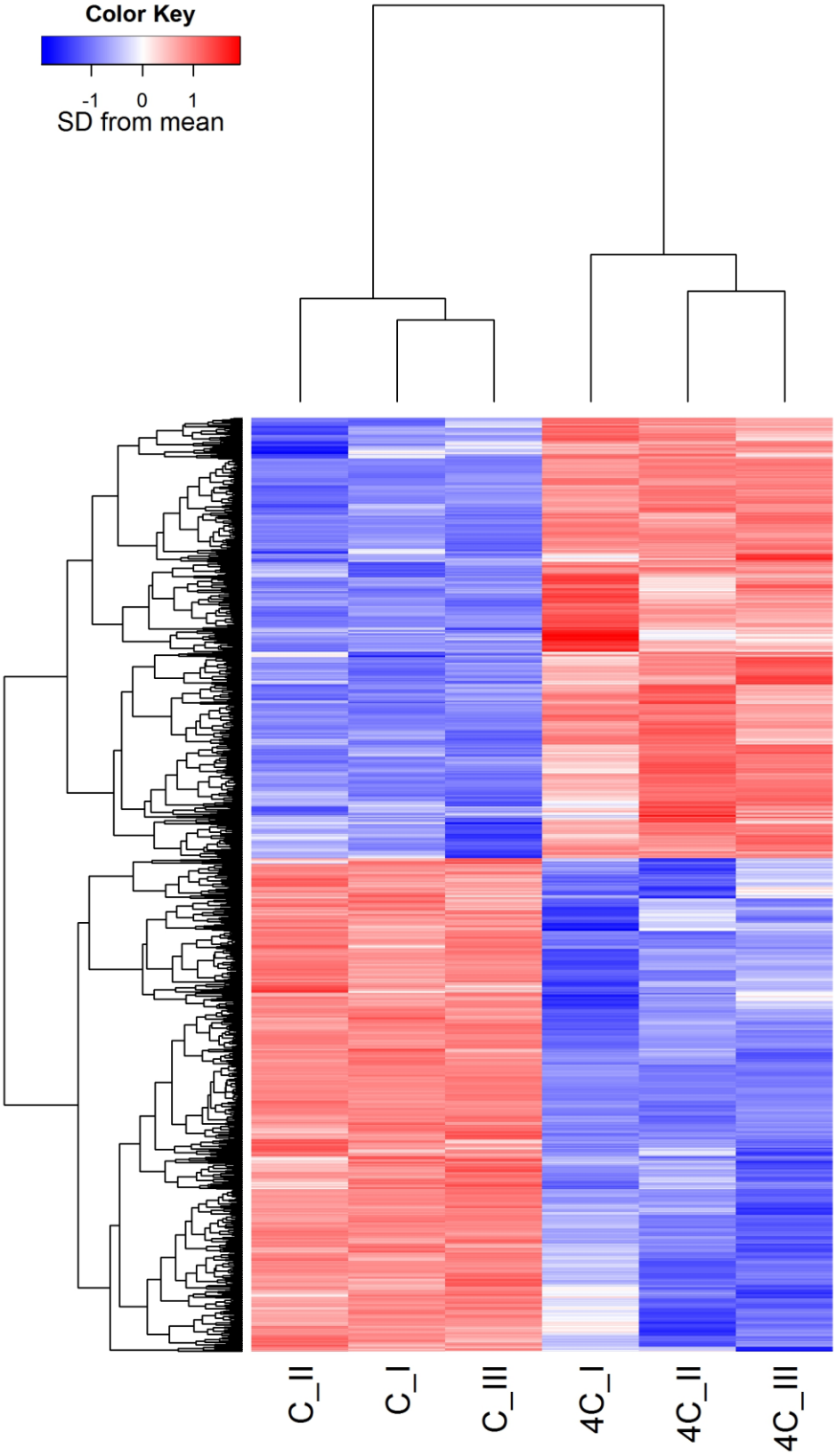

Figure 4. 4: Heat maps showing differential gene expression patterns in control bacteria (C) v/s cells subject to cold- stress (4C). Red denotes a relative increase in gene expression (upregulation) and blue denotes a relative decrease in gene expression (down regulation) (Source: Illinois University).

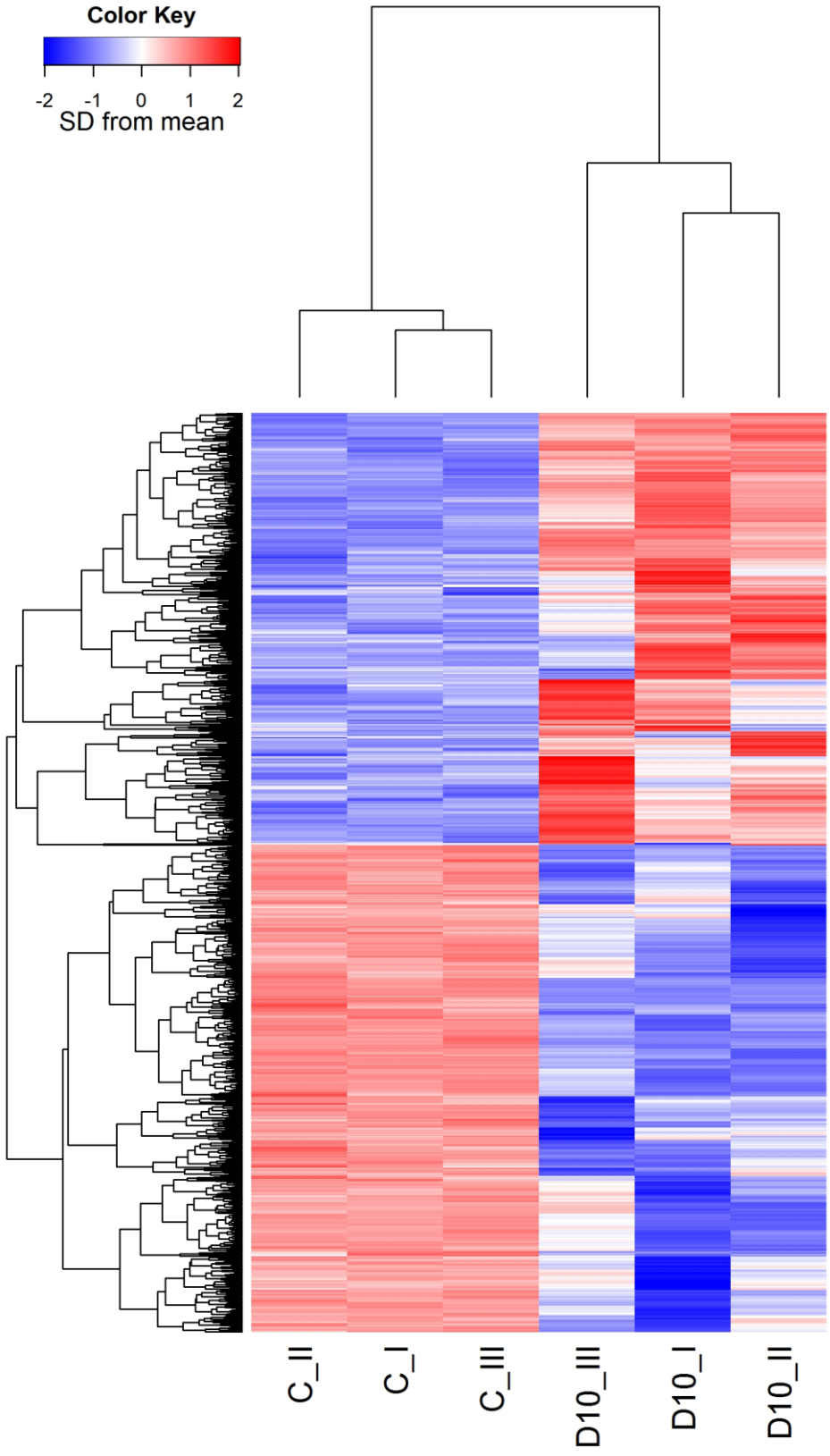

Figure 4. 5: Heat maps showing differential gene expression patterns in control bacteria (C) v/s aged colonies (10D). Red denotes a relative increase in gene expression (upregulation) and blue denotes a relative decrease in gene expression (down regulation) (Source: Illinois University).

4.3.3 Identification of differentially expressed genes

Gene expression was measured using exact tests, and a False Discovery Rate correction (FDR) was done separately for each comparison i.e. cold-stressed samples vs control and aged colonies vs control. Differential gene expression for stressed samples compared with control were calculated using the $\log_2$ (fold change) of stressed vs control for each gene. At a statistically significant value ($P < 0.05$), 2256 out of 3736 genes showing substantial changes were detected. Of those, pairwise comparisons yielded the statistically significant ($P < 0.05$) up-regulation of 535 genes and the down-regulation of 597 genes in cold-stressed bacteria. Cells from aged colonies yielded 530 up-regulated genes and 594 down-regulated genes compared with control cells. Among those 1132 DEGs in cold-stressed *Pseudomonas* sp. compared with control, the ten most up-regulated and the ten most down regulated expressed genes are shown in Table 4.3. Glycine/D-amino acid oxidases (deaminating) and molecular chaperone (small heat shock protein) were the most expressed genes. In aged colonies of *Pseudomonas* sp. compared with the control, the ten most up-regulated and the ten most down regulated expressed genes are listed in Table 4.4. 23S rRNA, Bacterial LSU and purine-cytosine permease and related proteins were the most expressed genes. For a complete list of differentially expressed genes in both aged and cold-stressed bacteria compared to control samples see Appendix C and D.

Table 4. 3: Top ten up- and down-regulated DEGs in cold-stressed *Pseudomonas* sp. compared with control (Source: Illinois University)

Gene ID	Log_2 (FC)	Description
Top 10 up-regulated genes		
PMI32_01763	4.62174	Glycine/D-amino acid oxidases (deaminating)
PMI32_00477	4.17795	Coenzyme PQQ biosynthesis protein B
PMI32_01765	4.13081	Glutamine synthetase
PMI32_04694	3.98571	Hypothetical protein
PMI32_00487	3.87063	Histidine kinase-, DNA gyrase B- and HSP90-like ATPase. /Histidine kinase./HAMP domain.
PMI32_00491	3.83721	ABC transporter, ATP-binding subunit, PQQ-dependent alcohol dehydrogenase system
PMI32_00485	3.8013	Uncharacterized low-complexity proteins
PMI32_00426	3.75132	Agmatinase
PMI32_01766	3.56562	Predicted glutamine amidotransferases
PMI32_04286	3.49382	PAS domain S-box/diguanylate cyclase (GGDEF) domain
PMI32_02731	3.45087	NADH dehydrogenase, FAD-containing subunit
Top 10 down- regulated genes		
PMI32_02330	−6.744927	Molecular chaperone (small heat shock protein)
PMI32_01419	−4.11551	ABC-type sugar transport system, periplasmic component
PMI32_05381	−3.457111	Response regulator containing CheY-like receiver, AAA-type ATPase, and DNA-binding domains
PMI32_03032	−3.31562	NAD-dependent aldehyde dehydrogenases
PMI32_03117	−3.293417	Hypothetical protein
PMI32_01791	−3.203104	Ferredoxin
PMI32_02716	−3.110358	Muconolactone delta-isomerase
PMI32_03729	−2.964031	Peroxiredoxin
PMI32_01773	−2.821	Uncharacterized conserved protein
PMI32_00892	−2.804881	Predicted secreted protein

Table 4. 4: Top ten up- and down-regulated DEGs in aged colonies of *Pseudomonas* sp. compared with control (Source: Illinois University)

Gene ID	Log_2 (FC)	Description
Top 10 up-regulated genes		
PMI32_02062	4.8026	23S rRNA. Bacterial LSU
PMI32_02059	4.34645	16S rRNA. Bacterial SSU
PMI32_01179	4.10422	Copper-(or silver)-translocating P-type ATPase
PMI32_04093	4.02374	Tellurite resistance protein and related permeases
PMI32_02731	3.78444	NADH dehydrogenase, FAD-containing subunit
PMI32_04612	3.33074	Pirin-related protein
PMI32_03547	3.20364	Transcriptional regulator
PMI32_02043	3.19504	Tryptophan synthase, beta subunit
PMI32_04280	3.1467	5-methyltetrahydropteroyltriglutamate--homocysteine S-methyltransferase
PMI32_01112	3.14066	Bacterial RNase P class A
Top 10 down-regulated genes		
PMI32_00678	−5.94385	Transcriptional regulators
PMI32_03776	−5.838476	Predicted acetyltransferases and hydrolases with the alpha/beta hydrolase fold
PMI32_02945	−5.602532	tRNA_Undet_???
PMI32_03927	−5.344614	Transcriptional regulators
PMI32_02406	−5.334854	Uncharacterized copper-binding protein
PMI32_01054	−5.282105	Uncharacterized conserved protein
PMI32_02270	−4.980973	Uncharacterized protein conserved in bacteria
PMI32_03777	−4.741894	EamA-like transporter family.
PMI32_01580	−4.728343	Uncharacterized homolog of the cytoplasmic domain of flagellar protein FhlB
PMI32_01747	−4.720232	Purine-cytosine permease and related proteins

4.3.4 Interaction among DEGs in response to different stress conditions

It was observed that many DEGs responded similarly in both the treatments i.e. aged colonies and cold stress, which may indicate that gene interactions or shared pathways are involved in these cells. A Venn diagram (Fig. 4.6) illustrates the overlap among genes differentially expressed in the different treatments. Ninety differentially expressed genes were found to be up-regulated in both aged colonies and cold-stressed bacteria, whereas one hundred and eighty-two differentially expressed genes were found to be down-regulated in both aged colonies and cold-stressed bacteria. In addition, fifty-two DEGs that were up-regulated in cold-stressed bacteria were observed to be down-regulated in aged colonies, whereas eighty-seven DEGs which were down-regulated in cold stress bacteria were observed to be up-regulated in aged bacteria.

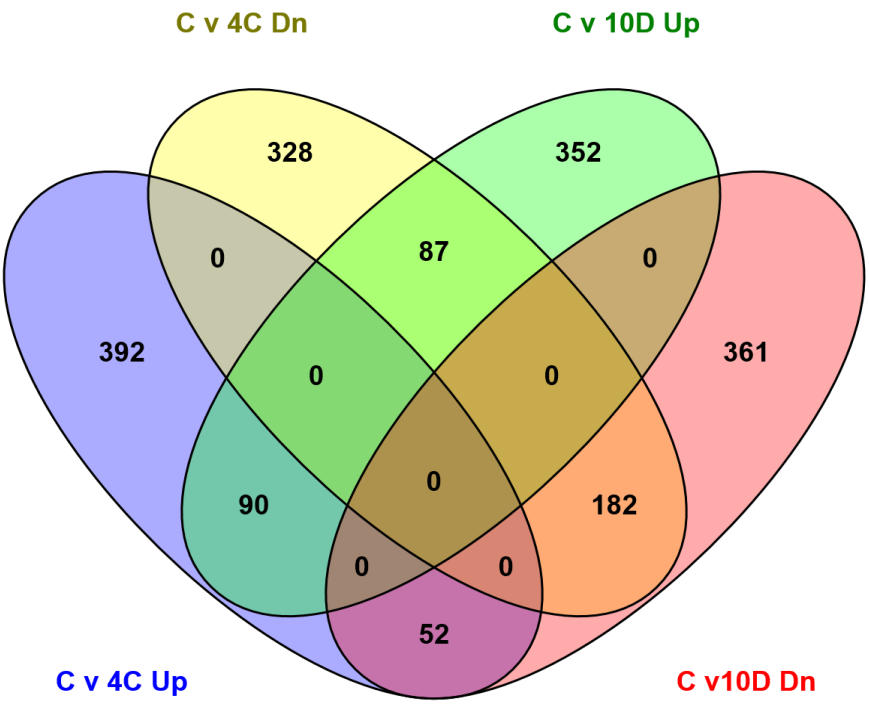

Figure 4. 6: Venn diagram describing overlaps among differentially expressed genes in cold-stressed (4C) and aged (10D) bacteria. All DEGs were divided into two groups i.e. up-regulated (Up) and down-regulated (Dn) within each group and were compared with each other.

4.3.5 Pathway analysis – COG category

Pathway-based analysis can help in further understanding the biological function. To identify the biological pathways that are active in cold-stress, aged colonies and control bacteria (*Pseudomonas* sp.), all expressed genes were mapped to the reference pathways in COG category. These pathways belonged to 23 clades. Among them, 'Inorganic ion transport and metabolism', 'Amino acid transport and metabolism' and 'Coenzyme transport and metabolism' were over-represented in cold-stressed bacteria, whereas 'Carbohydrate transport and metabolism', 'Cell cycle control, cell division, chromosome partitioning' and 'Post-translational modification, protein turnover, chaperones' were over-represented in aged colonies (Fig. 4.7). 'Energy production and conversion' was over-represented in both cold-stressed and aged bacteria.

'Cell cycle control, cell division, chromosome partitioning', 'Translational, ribosomal structure and biogenesis', 'Replication, recombination and repair' and 'Cell wall/membrane/envelope biogenesis' were under-represented in cold-stressed bacteria, whereas 'General function prediction only' and 'Intracellular trafficking, secretion, and

vesicular transport' were under-represented in aged colonies (Fig. 4.7). 'Cell motility' was under-represented in both cold-stressed and aged colonies.

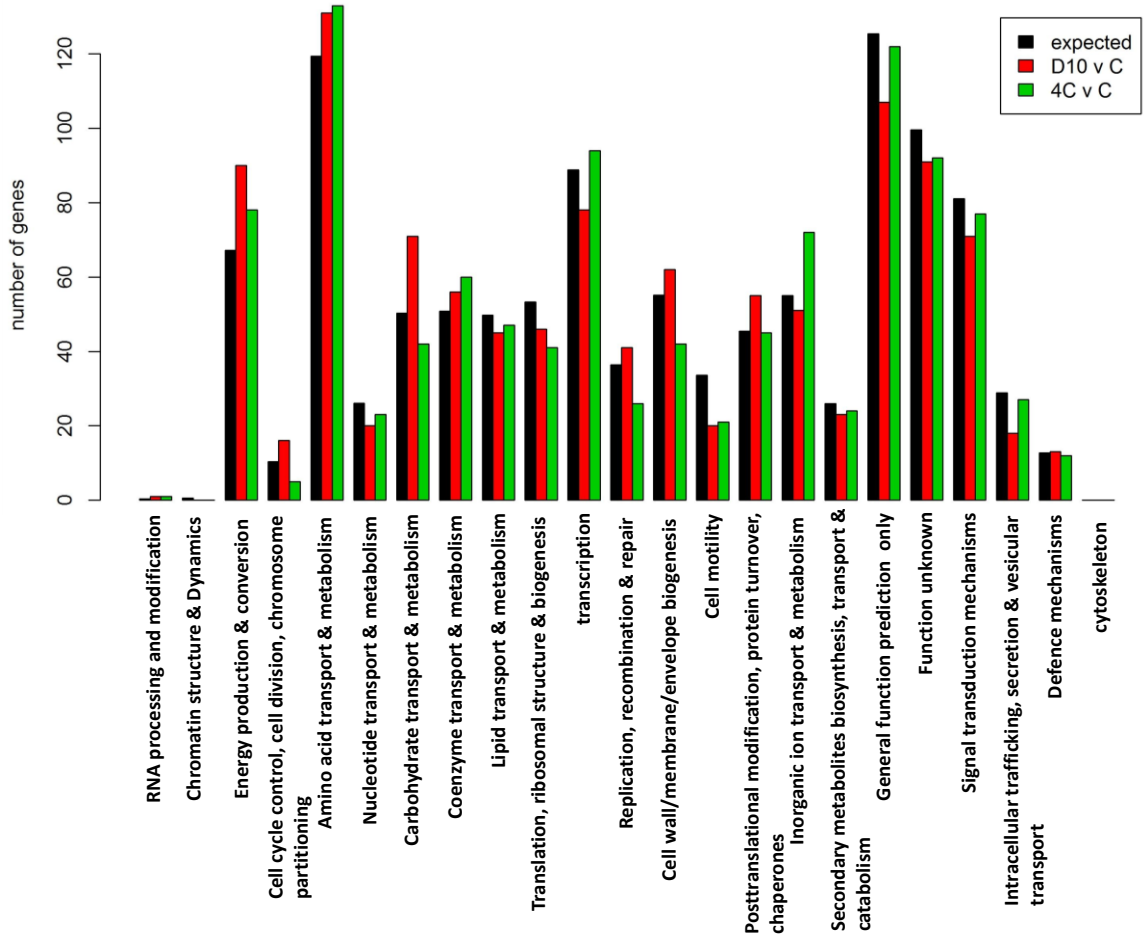

Figure 4. 7: COG category classification of number of genes detected in aged colonies (10 D), cold-stressed (4°C) and control (C) bacteria (Source: Illinois University).

4.4 Discussion

4.4.1 Illumina sequencing and sequence mapping to the reference genome

Transcriptome sequencing using Illumina technology generated a total of 192 million raw sequencing reads with a length of 100nt. The analysis of the treated *Pseudomonas* sp. culture led to average of 73% of the assembled reads matched to known transcripts, i.e. *Pseudomonas* GM 60, as predicted by genome sequencing and annotation (Table 4.1 & 4.2). The remaining transcripts comprised approximately 27% of unmapped reads. The percentage of unmapped reads is commonly observed to be between 5 and 40% during high-throughput RNA-Seq and it is assumed to possibly comprise novel genes

(Rubio et al. 2015). This suggests that 27 % of unmapped reads might be new gene sequences present in our isolate (Xia et al. 2013).

4.4.2 Pattern of differentially expressed genes

To obtain a general view of differentially expressed gene (DEG) expression patterns, pairwise comparison of expression was explored. This showed that genes were differentially expressed between the age/stress treatments and the control. In particular, it was observed that in aged colonies, approximately 90% of genes expressed mapped to one gene i.e. a non-coding RNA that is part of RNase P. RNase P consists of a catalytic RNA subunit and a protein subunit (C5), and together it controls the activity of the bacterial cell; however, in one case, it has been proposed that RNA was absent and cell activity was entirely controlled by proteins (Collins et al. 2000). Previous research performed with different substrates and RNA, in the absence or presence of protein subunit, showed that in the presence of protein subunit' RNase P was a more effective and adaptable enzyme (Gopalan 1997) and the general consensus appears to be that both RNA and the C5 protein subunit have to be present for the 'ribozyme' to be active. RNase P is an important ribonucleoprotein enzyme accountable for the maturation of the 5′-end of tRNAs which is essential for bacterial growth and survival (Gruegelsiepe et al. 2006). Interestingly in this study, genes (PMI32_00689, PMI32_01521, PMI32_00687, PMI32_00688, PMI32_04760) encoding for C5 proteins were down-regulated in aged colonies. These genes are involved in 'Intracellular trafficking, secretion, vesicular transport' metabolism which were under-represented in aged colonies. In addition, other genes such as 'Lysine efflux permease' encoding for C5 protein was under-represented in 'General function only' metabolism. Overall, it would appear that the aged colonies are accumulating the RNA sub-unit of RNase P without the accompanying C5 protein, implying that the activity of this important gene regulator is very different in aged colonies when compared with cold-stressed and younger control cells. Using RNA-Seq, RNase P along with other non-coding RNAs has been detected in *P. putida* DOT-T1E (a strain isolated from wastewater treatment plant), which exhibits resistance to a wide range of toxic compounds (Gomez-Lozano et al. 2015). Greugelsiepe and colleagues demonstrated growth inhibition of *E. coli* cells by targeting RNase P using anti-sense oligomer specific to catalytic RNase P. Recent advances in genomics and next generation technology have also demonstrated that non-

coding RNA's are crucial in controlling various levels of gene expression in physiology and development of cell adaptations to environmental change (Mattick and Makunin 2006). Especially in prokaryotes, non-coding RNAs are extremely regulated and often expressed as part of major stress response regulatory systems (Gottesman 2005). They exert their effects by base-pairing with cellular mRNA resulting into changes in translation and/or stability of the mRNA (Gottesman 2005; Repoila and Darfeuille 2009). Fluctuations in stability of the mRNA may significantly affect protein synthesis that contribute to bacterial adaptation and survival under stressful conditions (Takayama 2000). For example, in *P. aeruginosa*, a non-coding RNA, CsrA (carbon storage regulator)/RsmA (repressor of stationary-phase metabolites) controls extracellular rhamnolipid and lipase production known to initiate colonization, eventually resulting into biofilm formation (Lucchetti-Miganeh et al. 2008; Romeo et al. 2013). CsrA activates or represses genes to regulate numerous cellular functions like biofilm formation, quorum sensing, carbon metabolism, environmental stress resistance, motility, production of secondary metabolites and production of cytotoxic factor by preventing translation or by stabilizing mRNA (Lucchetti-Miganeh et al. 2008). In addition, it is suggested that the existence of a trivial population of extremely resistant cells in a micro-colony may be responsible for biofilm resistance in response to applied stress (Coenye 2010). This suggests that a few bacterial cells in micro-colonies surviving ozone treatment might be exhibiting resistance due to the presence of non-coding RNA which is part of RNase P in aged colonies as compared with cells from younger colonies. One such mechanism, identified as persistence, is commonly observed in several pathogens like *P. aeruginosa*, *L. monocytogenes*, *E. coli* and *S. enterica* that develop resistance to antibiotics (Stepanyan et al. 2015). In this state, a small population of cells within a biofilm/micro-colony switch into a dormant state, enabling tolerance to high doses of antibiotics (Romling and Balsalobre 2012). In *E. coli*, a reduced level of persister cells was observed when expression of a transcriptional regulator, antitoxin MqsA was repressed (Romling and Balsalobre 2012). The identification of such regulators in aged colonies might help to control the switch between antimicrobial-susceptible and ozone-resistant forms. However, this is purely hypothetical as very little research has previously focused on the role of non-coding RNA in aged cells and their adaptation to stress.

4.4.3 Differentially expressed genes (DEGs)

Overall, approximately 500 DEGs were significantly up-regulated and approximately 500 DEGs were down-regulated. These clear expression patterns show that genes were expressed differentially between treatments. The observed values for DEGs are higher than those in a previous *P. aeruginosa* study based on RNA-Seq used to evaluate gene expression between mature *P. aeruginosa* and planktonic culture, in which 227 up-regulated and 46 down-regulated genes were observed (Dotsch et al. 2012).

Genes such as Glycine/D-amino acid oxidases (deaminating), PMI32_04694 and PMI32_00487 (Table 4.3), which encode for amino acid metabolism, were up-regulated in cold-stressed cell. These amino acids produce proteins that enhance fluidity of cell membrane during low temperature (Frank et al. 2011). This result was also observed in *P. putida* KT2440 growing at 10°C (Frank et al. 2011). Down-regulation of molecular chaperone (heat-shock protein; HSP) was observed in cold-stressed cells. This is commonly observed in numerous psychrophilic organism (Feller 2013). 'NADH dehydrogenase', 'Ferredoxin', Peroxiredoxin' and 'ATPase & DNA-binding' gene down-regulated in cold-stressed bacteria were also identified to have reduced expression in *P. putida* KT2440 grown at 4°C using Southern hybridization analysis (Reva et al. 2006). Genes such as 'NADH dehydrogenase' and 'Pirin related protein' were up—regulated in aged bacteria which are involved in energy metabolism. Genes like 'flagellar protein FlhB' were down-regulated in aged colonies which encode for flagellar motility. This result was also observed in *P. aeruginosa* involved in biofilm formation (Beloin and Ghigo 2005).

Out of 1132 and 1124 DEGs genes, 160 and 164 genes in cold-stressed and aged bacteria, respectively, represented 'hypothetical proteins' and 'uncharacterized conserved protein'. These genes are potentially good candidates for identifying novel functions relevant to stress resistance in bacteria.

4.4.4 Interaction among DEGs in response to different stress conditions

Further, comparison of up-regulated and down-regulated genes between cold-stressed and aged colonies revealed overlaps. Overlap between 90 up-regulated and 182 down-regulated genes were observed between cold-stressed and aged colonies. For example, few genes like 'universal stress protein UspA and related nucleotide binding protein',

'dihydroxy-acid dehydratase', 'Acyl-CoA dehydrogenases', 'RNA polymerase sigma factor', 'drug resistance transporter', 'Signal transduction histidine kinase' and 'NADH deydrogenase' were up-regulated, whereas 'ribonuclease R', 'ATP synthase', 'peroxiredoxin', 'superoxide dismutase', 'flagellar biosynthesis' and 'pirin related proteins' were down-regulated in both the stress conditions. This suggests that some common genes are involved in combating environmental stress, and inhibiting/targeting these genes will potentially decrease acquired resistance of bacteria to a range of applied stresses.

4.4.5 COG classification of differentially regulated genes of cold-stressed or/and aged colonies: Cold-stressed cells

Pseudomonas sp. grown at optimum temperature appeared to mainly use amino acids and short peptides as its carbon and nitrogen sources (Fonseca et al. 2011b). The cells grown at low temperature (4°C) led to an increase in the expression of genes corresponding to amino acid, inorganic ion and co-enzyme transport and metabolism. Enzymes such as polyhydroxyalkanoates and carbonic anhydrase, which are highly stable enzymes required for cold-adaptation, were observed to be up-regulated in cold-stressed cells (Feller 2013). Genes annotated as amino acid permeases, which are a well-characterized part of amino acid transport systems, were up-regulated in cold-stressed cells (Moreno and Rojo 2014). The stronger expression of these amino acid uptake systems was paralleled by the increased expression of the genes involved in the assimilation of proline (PMI32_00243, PMI32_00244, PM132_00241, PMI32_04860, PMI32_00604), valine (PMI32_04780, PMI32_04778) and leucine (PM132_01191). In summary, the expression of genes corresponding to the transport and/or metabolism of proline, valine, leucine, tyrosine, phenylalanine, glutamate and isoleucine were up-regulated in cold-stressed cells. This higher expression of the genes in cold-stressed bacteria may result in an increase in the metabolism of these amino acids (Fonseca et al. 2011b, 2013).

Changes were also observed in genes involved in the bacterial cell wall/membrane/envelope. The cell membrane plays a vital role in response to various stress including cold, pH, osmotic and toxic compounds because it acts as a barrier between the cell and environment (Reva et al. 2006; Frank et al. 2011). Enzymes of lipopolysaccharides (LPS) biosynthesis and lipid metabolism are generally considered

to be key essentials of the outer membrane of bacteria and responses to environmental stresses (Reva et al. 2006). The phosphatidylglycerophosphate synthase and related enzymes, which are crucial for phospholipid production, were up-regulated in cold-stressed bacteria. One LPS biosynthesis gene, predicted acyl-COA transferases was identified in cold-stressed *Pseudomonas* sp. which is required to cope with cold conditions (Moreno and Rojo 2014). This gene was also identified in *P. putida to* cope with acid, benzoate and cold stresses (Reva et al. 2006). Lipid A plays a crucial role in innate immune system signaling as well as in modulation in Gram-negative bacteria (Thaipisuttikul et al. 2014). It also controls external membrane fluidity and permeability (Thaipisuttikul et al. 2014). Lipid A in *Pseudomonas* sp. is either penta-, hexa- or heptaacylated; R-3-hydroxy and/or up to five fatty acid residues are attached to the glucosamine disaccharide backbone directly, whereas other two fatty acids are attached to the R-3-hydroxy groups of the R-3-hydroxy fatty acid residues. The main intermediate $(KDO)_2$-lipid IV_A is consecutively acylated with fatty acids in the later step of the lipid A biosynthetic pathway (Reva et al. 2006). The expression of lipid-A acyl-CoA transferases that encode lipid A fatty acyl transferases was down-regulated in cold-stressed bacteria. The lower expression of this gene might be part of the adaptation process that facilitates the growth of *Pseudomonas* bacteria at low temperature.

Taurine catabolism dioxygenase Tau D, TfdA family which encode for protein LapA was down-regulated in cold-stressed cells. Protein LapA is essential for biofilm formation and for coping with urea stress (Reva et al. 2006). Another important metabolic activity, i.e. replication, recombination and repair, was under-expressed in cold-stressed bacteria. It was found that at low temperatures, the bacteria increases the stability of the secondary structures of their nucleic acid by halting DNA replication and related metabolism (Moreno and Rojo 2014).

4.4.6 COG classification of differentially regulated genes of cold-stressed or/and aged colonies: Aged colonies

Of the functional classes, ‘carbohydrate transport and metabolism’, ‘cell cycle control, cell division’ and ‘post-translational modification’ were over-expressed in aged colonies. Majority of genes in ‘carbohydrate transport and metabolism’ play roles in the accumulation and breakdown of storage materials like glycogen. For example, 1, 4-alpha glucan branching enzyme encodes enzymes with putative roles in glycogen

synthesis and degradation. Such genes were also observed in *P. aeruginosa* in stationary phase conditions but were not expressed in planktonic cultures (Waite et al. 2006). Genes such as ATPases involved in chromosome partitioning, cell division protein and SOS-response cell division inhibitor were up-regulated in aged colonies. These genes are involved in slowing cellular growth and inhibiting cell division. These cells might enter into a dormant state to survive stressed conditions. According to Waite and colleagues (2006), these genes were not expressed in planktonic culture/younger cells of *P. aeruginosa*, making it susceptible to survive in stressed conditions.

Genes involved in flagella (e.g. PMI32_04720, PMI32_03992) and type IV pili (pilZ, pilE) were down-regulated in aged bacterial colonies. Similar result was observed in matured *P. aeruginosa* using RNA Sequencing (Beloin and Ghigo 2005). The flagellar motility is normally required in the initial phase of micro-colony/biofilm formation and numerous reports show that flagella might not be required within a mature biofilm which is capable for coping with environmental stress (Beloin and Ghigo 2005).

4.4.7 COG classification of differentially regulated genes of cold-stressed or/and aged colonies: Cold-stressed and aged colonies

The central metabolic pathways of energy production and conversion play key roles in coping with environmental stress (Moreno and Rojo 2014). In the work herein, energy production and conversion was over-represented in cold-stressed as well as aged bacteria. Enzymes such as phosphoenolpyruvate carboxykinase (ATP) and phosphoenolpyruvate carboxylase were up-regulated in both cold-stressed and aged colonies. Inhibition of these enzymes in bacteria might make them less/non-resistant to environmental stress conditions (Reva et al. 2006).

This study has provided new insight into the mechanism by which cold-stressed and aged bacterial colonies demonstrate resistance. Altogether, the study suggests that 'Inorganic ion transport and metabolism', 'Energy production and conversion', 'Amino acid transport and metabolism', 'Coenzyme transport and metabolism', 'Carbohydrate transport and metabolism', 'cell cycle control, cell division', 'post-translational modification' and 'motility' contribute to resistance in *Pseudomonas* sp. Further, quantitative RT-PCR (q-PCR) analysis to confirm gene expression revealed by RNA-

Seq is required. In addition, detailed analysis of the differentially expressed genes present in both treatments might lead to methods which will be beneficial commercially.

4.5 Conclusion

Transcriptome analysis using RNA-Sequencing of aged colonies or cold-stressed cells showed significant changes in the expression of genes related to stress resistance compared with controls. In particular, it was observed that in aged colonies, approximately 90% of the changes in gene expression mapped to one gene (a non-coding RNA that is part of RNase P). This gene interacts with cellular mRNA transcripts to control bacterial growth in response to environmental stress conditions. Many of the genes showing differential expression were involved in energy production, transport, motility or cell wall/membrane integrity. Several changes appeared directed towards neutralizing problems created by low temperature or ageing, such as increased stability of RNA/DNA structures, changes in protein folding and reduced growth rate (persistence). Future work will involve validating RNA-Seq observations using targeted Quantitative or Real-time PCR.

Chapter 5 Effect of Ozone Treatment for Inactivating *Escherichia coli* and *Listeria* spp. on Spinach

5.1 Introduction

In addition to resulting in the postharvest spoilage, there has been an increased incidence of outbreaks of disorders and deaths as a result of the consumption of pathogen-contaminated raw leafy produce (Beuchat 2000). All fresh produce, including leafy salads and herbs, has the potential to harbour food-borne pathogens such as *E. coli*, *L. monocytogenes*, *Shigell*a spp. and *Salmonella* (Abadias et al. 2008; Velusamy et al. 2010). Contamination of fresh produce with pathogens can occur either pre-harvest and/or post-harvest. Pre-harvest sources of pathogens generally include organic fertilizers, irrigation water and soil, whereas post-harvest sources mainly result from handling procedures including equipment, transport vehicles and containers (Critzer and Doyle 2010).

Investigation of leafy products on sale showed greater frequency in the detection of *E. coli* and *L. monocytogenes* than anticipated (Engels 2012). *E. coli* is a Gram-negative, facultative anaerobe and member of the *Enterobacteriaceae* family. It is commonly present in gastrointestinal tract of humans and animals including deer, cattle and pigs (Griffin 1991). Most *E. coli* are harmless to humans, but epidemiological research has documented that intake of leafy produce contaminated with *E .coli* O157:H7 can pose detrimental effects on human health at doses as low as the ingestion of 10 cells (Tomas-Callejas et al. 2011). *E. coli* strains that cause disease are categorized on the basis of pathogenicity, virulence and clinical syndrome. *E. coli* O157:H7 belongs to a enterohaemorrhagic (EHEC) group (Coia 1998). Infection with *E. coli* O157:H7 causes major outbreaks particularly associated with raw leafy produce (Engels 2012). It causes symptoms ranging from mild diarrhoea to haemorrhagic colitis and life-threatening haemolytic uremic syndrome (HUS), especially in babies and aged individuals (Tomas-Callejas et al. 2011). Although leaf surfaces are not a perfect environment for *E. coli* to flourish, it can survive harsh conditions in the field and during storage/transit of produce (Engels 2012).

L. monocytogenes is a Gram-positive, facultative anaerobic, non-spore forming rod-shaped bacilli which is capable of growing at low temperatures. This pathogen is widely present in soil, plant and water surfaces (Farber 1991). It causes less than one percent of food-borne diseases but it is responsible for causing listeriosis in humans which

commonly results in symptoms requiring hospitalization (Todd 2011). For healthy individuals, the main symptoms are fever and diarrhoea, whereas for pregnant women, it may cause septicaemia, meningitis, abortion or stillbirth (Todd 2011; Engels 2012). *L. monocytogenes* is capable of growing at refrigeration temperatures and surviving within food/fresh produce-processing sites (Engels 2012). A list of symptoms caused by pathogenic micro-organisms responsible for food-borne illnesses is given in Table 5.1

Table 5. 1: Symptoms caused by *E. coli* and *L. monocytogenes* following consumption by humans (modified from Velusamy et al. 2010)

Microorganism	**Infective dose (no. of organisms)**	**Incubation period**	**Symptoms**	**Name of the disease**
E. coli	<10	2 to 4 days	Stomach pain, diarrhoea, nausea, chills, fever and headache	Haemorrhagic colitis
L. monocytogenes	<1000	2 days to 3 weeks	Fever, chills, headache, backache, sometimes abdominal pain and diarrhoea	Listeriosis

Microbial contamination of fresh produce not only poses significant risks to public health but also affects the industry financially by resulting in costly product recalls. For example, the recent Shiga toxin-producing *E. coli* O157 outbreak in watercress is estimated to have required the recall of two hundred thousand items in the United Kingdom (Launders 2013). Food-borne outbreaks are common in many countries. This could be due to the pathogens developing resistance to traditional sanitizing agents, and thus, posing a hazard to the safety of the food supply (Bower 1999).

Given the importance of controlling pathogen contamination of leafy fresh produce, the present study aimed to determine the antimicrobial effects of ozone for the control of different strains of *E. coli* and *Listeria* spp. and to observe the regrowth of these pathogenic bacteria on ozone-treated produce during storage of produce for 9 days at 4°C. Spinach was artificially contaminated by inoculating with *E. coli* or *Listeria* spp. before ozone treatment. Six different strains of non-pathogenic *E. coli* were used as a representative model for *E. coli* O157:H7, as there have been no reports suggesting significant differences in growth pattern and survival strategy between non-pathogenic *E. coli* and pathogenic *E. coli* O157:H7 (Gleeson 2005). In addition, *L. innocua* and *L. seeligeri* were used in lieu of *L. monocytogenes* because it has been accepted as a safe non-pathogenic alternative for *L. monocytogenes* due to its similar growth characteristics and behaviour on leafy produce (O'Beirne 1998; Fan et al. 2007). The material in this chapter has been published in the paper (Wani et al. 2015).

Aim: To study the effect of ozone treatment on foodborne pathogens inoculated onto spinach

Objectives:

- To determine the impact of ozone treatment on different strains of *E. coli* and *Listeria* spp. inoculated onto spinach
- To determine the impact of ozone on pathogen recovery after 9-days' storage mimicking a commercial storage environment
- To determine if colony age affects ozone resistance of non-pathogen *E. coli* O157:K88a

5.2 Materials and Method

5.2.1 Assessing the impact of ozone treatment on food pathogens: E. coli and L. innocua in vitro

E. coli K12 and *L. innocua* were obtained from a culture collection maintained by Geneius Laboratories Ltd. These cultures were sub-cultured by spread plating on Nutrient agar (NA) and Agar Listeria according to Ottaviani and Agosti (ALOA) agar plates, respectively. A single colony was isolated from each culture plate after incubation at 37°C for 24 h and 30°C for 48 h, respectively and transferred to MRD. A standardized concentration 10^4 cells per mL (100 µL) of each culture was spread onto sterile NA and ALOA agar plates respectively. These plates were then either exposed to 1, 10 or 50 ppm ozone or charcoal filtered 'clean air' (controls) for 10 min at room temperature. After treatment, NA and ALOA agar plates were incubated at 37°C for 24 h and 30°C for 48 h respectively. The number of colonies produced on control plates (non-ozone exposed) were compared with the numbers found on ozone-treated plates based on three replicate observations.

5.2.2 Ozone resistance of different strains of E. coli: Inoculation of E. coli onto spinach leaves and ozone exposure conditions

Six strains of *E. coli* (*E. coli* O157:K88a, *E. coli* O25:H4, *E. coli* O128:K67, *E. coli* K12, *E. coli* O55:K59 and *E. coli* O104:H12) were obtained from a culture collection maintained by Geneius Laboratories Ltd. Cultures were stored at 4°C on Luria-Bertani (LB) agar plates and activated in LB broth at 37°C. Baby-leaf spinach was purchased from a local retailer and aseptically cut into discs measuring 1.13 cm^2 using a sterile cork borer. A suspension of *E. coli* (overnight culture, 10^8–10^9 CFU/mL LB broth) was applied directly to the leaf disc in 300 µL aliquots and then the inoculated leaves were stored overnight at 7°C to mimic produce storage conditions and to allow attachment of *E. coli* to the leaf surface. Inoculated leaves were either exposed to 1 ppm ozone or charcoal filtered 'clean air' for 10 min at room temperature. To determine the number of *E. coli* remaining (control and ozone exposed), the leaf discs were vigorously shaken manually in MRD for 2 min and then serially diluted using MRD followed by pour plate technique using Tryptone Bile X-Glucuronide (TBX) agar plates. Plates were incubated

at 44°C for 24 h, and presumptive colonies were counted on the basis of three replicate observations.

5.2.3 Impact of ozone treatment on L. innocua and L. seeligeri inoculated onto spinach leaves

Two strains of *Listeria* (*L. innocua* and *L. seeligeri*) were obtained from a culture collection maintained by Geneius Laboratories Ltd. Cultures were stored at 4°C on ALOA agar plates. Spinach leaves were then aseptically cut into discs measuring 1.13 cm^2 using a sterile cork borer. A suspension of *Listeria* sp. (10^7–10^8 CFU/mL MRD) was applied directly to the leaf disc in 300 µL aliquots and the inoculated leaves were maintained at 7°C to mimic produce storage conditions for 2 h to allow attachment of *Listeria* sp. to the leaf surface. Inoculated leaves were either exposed to 1 ppm ozone or charcoal filtered 'clean air' for 10 min at room temperature and survival rate enumerated (see below). For determining the survival and growth of *Listeria* sp. during storage, a proportion of the treated and untreated inoculated leaves were maintained at 7°C for a further 9 days. The number of colonies remaining (control and ozone exposed) on day 0 and day 9 was determined by vigorously shaking the leaf disc in MRD manually for 2 min after 1 h incubation at room temperature and then serially diluted in MRD followed by standard spread technique on ALOA agar plates. Plates were incubated at 30°C for 48 h, and colonies were counted.

5.2.4 Impact of higher/increased ozone concentrations on two strains of E. coli and Listeria inoculated onto spinach leaves

This experiment aimed to use the highest ozone exposure levels (10 ppm for 2 min) that did not cause produce damage to try and achieve higher reductions in pathogenic bacteria on the surface of baby spinach leaves. Two strains of *E. coli* (*E. coli* O157:K88a and *E. coli* O25:H4) and *Listeria* (*L. innocua* and *L. seeligeri*) were inoculated onto spinach leaves as described in Sections 5.2.2 and 5.2.3, respectively. Inoculated leaves were either treated with 10 ppm ozone or charcoal filtered 'clean air' for 2 min. The number of *E. coli* and *Listeria* sp. remaining (control and ozone exposed) was determined as described above (Sections 5.2.2 and 5.2.3).

To determine the impact of highest ozone exposure levels on the survival and growth of *E. coli* (*E. coli* O157:K88a and *E. coli* O25:H4) and *Listeria* (*L. innocua* and *L.*

seeligeri) during storage, the inoculated leaves were treated as described in Section 5.2.4. After the treatment, inoculated and control leaves were maintained at 7°C for 9 days. The number of colonies (control and ozone exposed) on day 9 was determined as mentioned in Section 5.2.4.

5.2.5 Age effects on ozone resistance of E. coli in vitro

To determine whether colony age affected ozone resistance, a colony of *E. coli* O157:K88a obtained from a culture collection maintained by Geneius Laboratories Ltd. was sub-cultured onto NA plates and incubated at 37°C for 7 days. A single colony was isolated on the 1st, 3rd, 5th and 7th day of the incubation and transferred to MRD. A standardized concentration of 10^4 cells per mL (100 µL) of each cell age was spread onto sterile NA plates, and these plates were then exposed to either 10 ppm ozone or charcoal filtered 'clean air' for 2 min. Colony count was determined after incubating NA plates at 37°C for 24 h.

5.2.6 Statistical analysis

Data were analysed using SPSS (IBM SPSS Statistics 19 64Bit) and graphs were produced using Microsoft Office Excel 2010 and SigmaPlot 12.5. Data distribution was tested using a Normality test and significant differences between mean values were verified using LSD ($P < 0.05$) following one-way ANOVA.

5.2.7 Log reduction

Microbial log reduction was calculated as follows:

$$\text{Log reduction} = \log_{10}(A) - \log_{10}(B) \text{ or Log reduction} = \log_{10}(A \div B)$$

Where A is the number of viable microorganism before treatment and B is the number of viable microorganism after treatment.

5.3 Results

5.3.1 Effect of ozone exposure on E. coli and Listeria sp. in vitro

Colony numbers (CFU) of *E. coli* K12 and *L. innocua in vitro* were significantly reduced ($P < 0.05$) by all ozone treatments (Fig. 5.1), even at the lowest levels of exposure (1 ppm for 10 min). Less than 1-log reduction was achieved when exposed to 1 ppm for 10 min but more than 1-log reduction was achieved when both the strains of food pathogens were treated with ozone concentrations of 10 and 50 ppm. This implies that ozone concentrations of 10 and 50 ppm reduced counts significantly more compared to 1 ppm ozone. However, there was no significant difference in colony counts between 10 and 50 ppm ozone treatment in both strains of food pathogens.

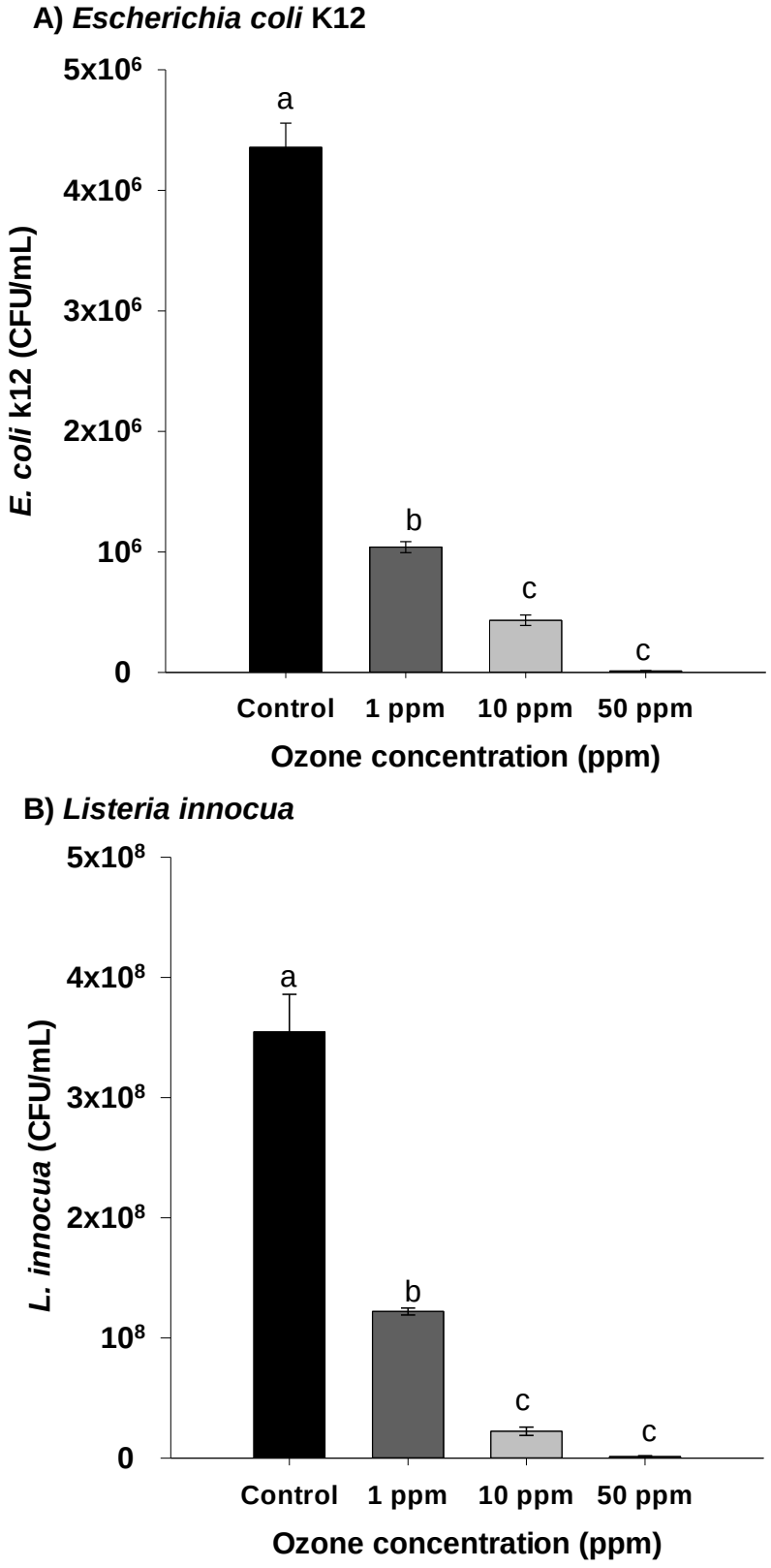

Figure 5. 1: Impacts of ozone treatment on A) *E. coli* K12 and B) *L. innocua* (CFU/mL) grown on agar plates. The treatment chamber was ventilated with 1, 10 or 50 ppm ozone for 10 min. Controls were exposed to 'clean air'. Values represent the mean (±Standard Error) of measurements made on three independent plates per treatment. Bars with different letters are statistically significantly different ($P < 0.05$).

5.3.2 Effect of ozone exposure (1 ppm for 10 min) on different strains of E. coli inoculated onto spinach leaf surfaces

Colony numbers (CFU) of six strains of *E. coli* i.e. *E. coli* O157:K88a, *E. coli* O25:H4, *E. coli* O128:K67, *E. coli* K12, *E. coli* O55:K59 and *E. coli* O104:H12 were significantly reduced ($P < 0.05$) by exposure to ozone (Table 5.2, .Fig. 5.2 and 5.3). No *E. coli* colonies were isolated from non-inoculated spinach leaves.

Table 5. 2: log reduction achieved by ozone treatment on six strains of *E. coli* inoculated onto spinach leaf surfaces

Different strains of *E. coli*	**Log reduction**
E. coli O157:K88a	**1.3**
E. coli O25:H4	**0.5**
E. coli O128:K67	**1**
E. coli K12	**0.7**
E. coli O55:K59	**1**
E. coli O104:H12	**1**

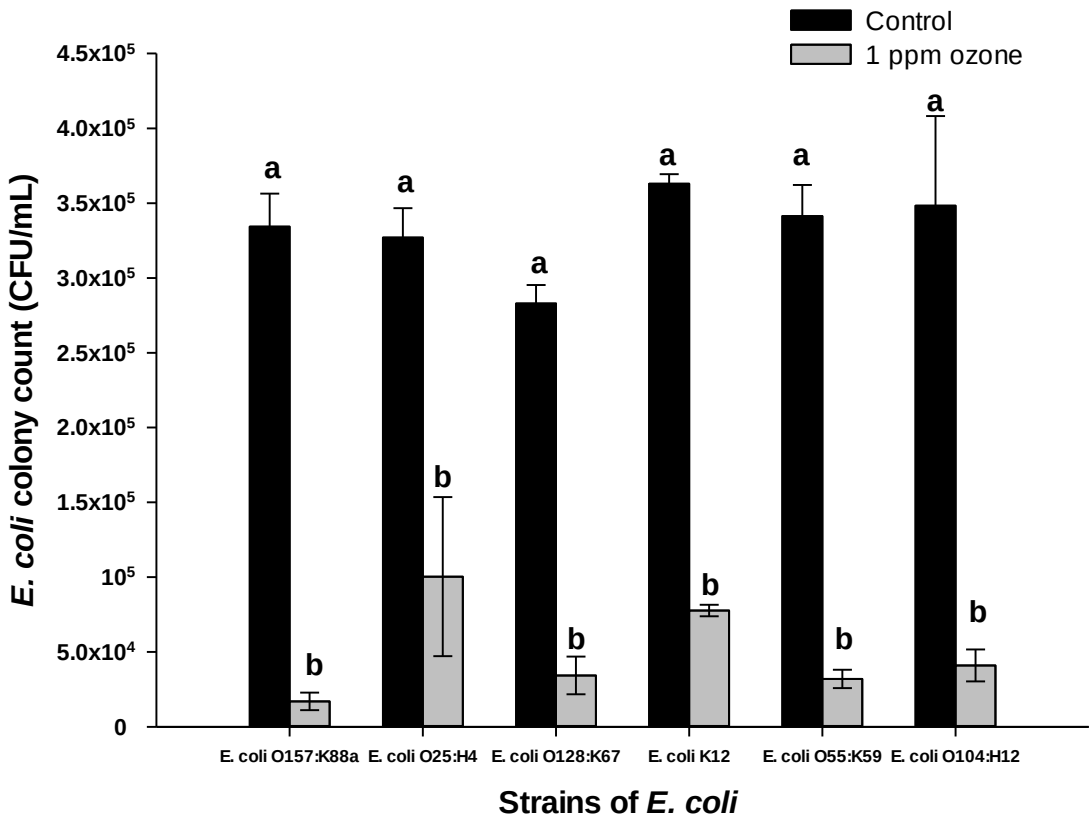

Figure 5. 2: Impacts of ozone-enrichment on six strains of E. coli inoculated onto the surface of spinach leaves. Leaves were either treated with 1 ppm ozone concentration (grey bar) or untreated (black bar) for 10 min. Values represent means (±Standard Error) of measurements made on three independent spinach leaves per treatment. Bars with different letters are significantly different ($P < 0.05$).

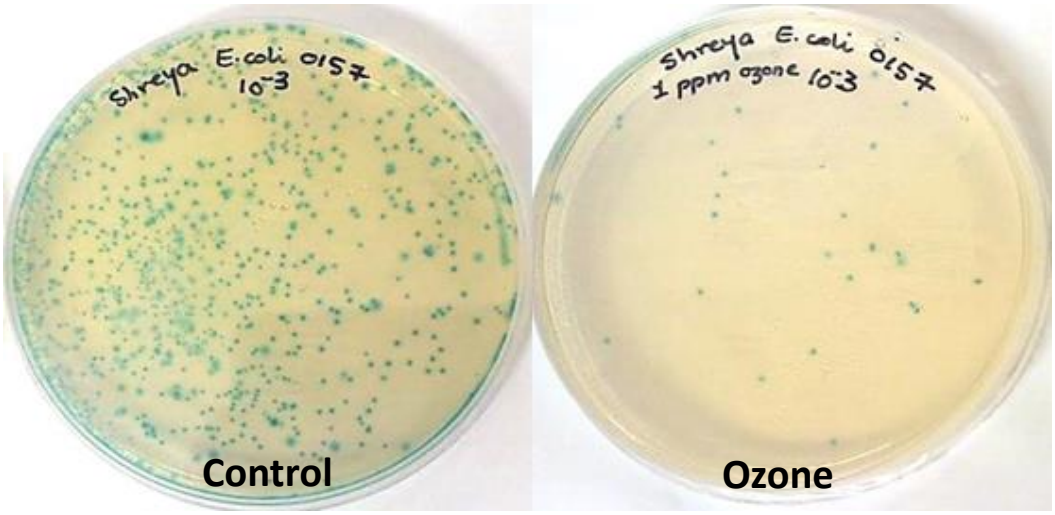

Figure 5. 3: Colonies of *E. coli* O157:K88a on TBX agar recovered from leaves after being exposed to either 'clean' air (control) or 1 ppm ozone concentration for 10 min

5.3.3 Impact of ozone treatment on L. innocua and L. seeligeri inoculated onto spinach leaves

Colony numbers (CFU) of *L. innocua* and *L. seeligeri* obtained directly from ozone exposed leaves i.e. day 0 were significantly reduced ($P < 0.05$) compared with non-ozone exposed controls (Table 5.3, Fig. 5.4). Viable counts of *Listeria* did reduce over continued storage time (9 days) in both control and ozone exposed treatments, but *Listeria* counts were significantly lower in exposed leaves compared with control after the 9 days (Fig. 5.4). No *Listeria* colonies were isolated from non-inoculated spinach leaves.

Table 5. 3: log reduction achieved by ozone treatment on two strains of *Listeria* spp. inoculated onto spinach leaf surfaces

***Listeria* spp.**	**Log reduction (Day 0)**	**Log reduction (Day 9)**
L. innocua	**0.7**	**0.7**
L. seeligeri	**0.4**	**0.8**

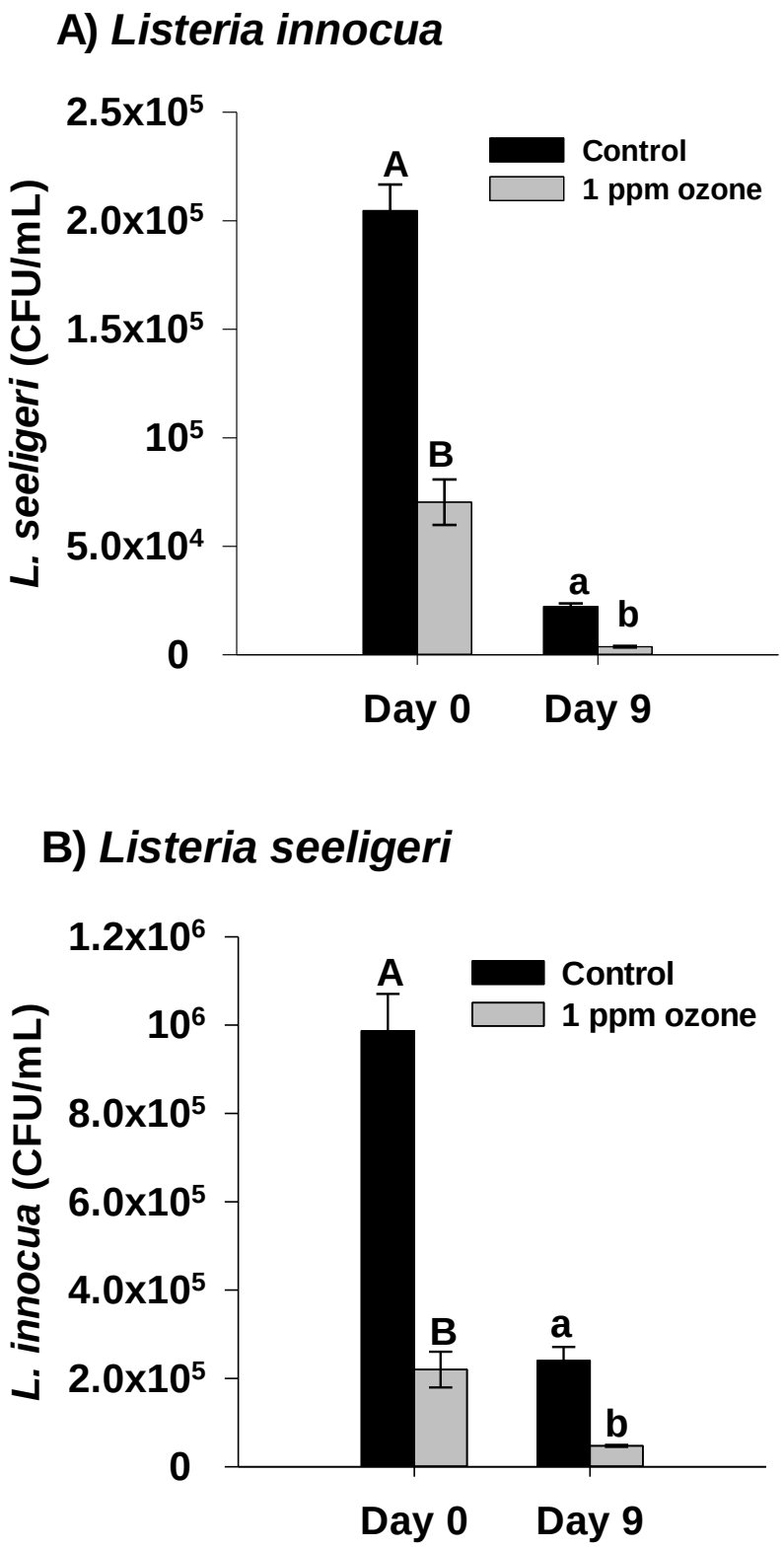

Figure 5. 4: Impacts of ozone-enrichment on *L. innocua* and *L. seeligeri* inoculated onto the surface of spinach leaves. Leaves were either treated with 1 ppm ozone concentration (grey bar) or untreated (black bar) for 10 min. Colonies were enumerated either directly after the treatments i.e. day 0 or after 9 days storage. Values represent means (±Standard Error) of measurements made on three independent spinach leaves per treatment. Bars with different letters are significantly different ($P < 0.05$).

5.3.4 Effect of higher ozone treatment on E. coli and Listeria sp. inoculated onto spinach leaf surface

Results of spinach inoculated with two strains of *E. coli* (*E. coli* O157:K88a and *E. coli* O25:H4) and *Listeria* (*L. innocua* and *L. seeligeri*) treated with 10 ppm of ozone for 10 min are shown in Fig. 5.5. For *E. coli* O157:K88a and *E. coli* O25:H4, ozone treatment significantly ($P < 0.05$) reduced counts by 1-$\log_{10}$ compared with the untreated control (Table 5.4 & Fig. 5.5A). Ozone had less than 1-log effect on *L. innocua* and *L. seeligeri* on day 0 (Table 5.4 & Fig. 5.5B). In addition, the results obtained from this treatment i.e. 10 ppm for 2 min were not significantly effective in reducing bacterial viable counts in comparison to previous ozone treatment i.e. 1 ppm for 10 min.

To investigate the after effects of the ozone treatment on pathogen growth, inoculated spinach leaves were stored at 7°C for 9 days. Fig. 5.6 shows that population of both *E. coli* (*E. coli* O157:K88a and *E. coli* O25:H4) and *Listeria* spp. (*L. innocua* and *L. seeligeri*) after 9 day storage did not regrow, because a significant reduction in number of colonies was observed as compared with the untreated control. However, the effect of higher ozone treatment on pathogen recovery did not show significant difference in count as compared with treatment with lower ozone concentration.

Table 5. 4: log reduction achieved by higher ozone treatment on two strains of *E. coli* and *Listeria* spp. inoculated onto spinach leaf surfaces

Pathogens	Log reduction (Day 0)	Log reduction (Day 9)
E. coli O157:K88a	**1.7**	**1.2**
E. coli O25:H4	**1.4**	**0.7**
L. innocua	**0.8**	**0.9**
L. seeligeri	**0.7**	**0.7**

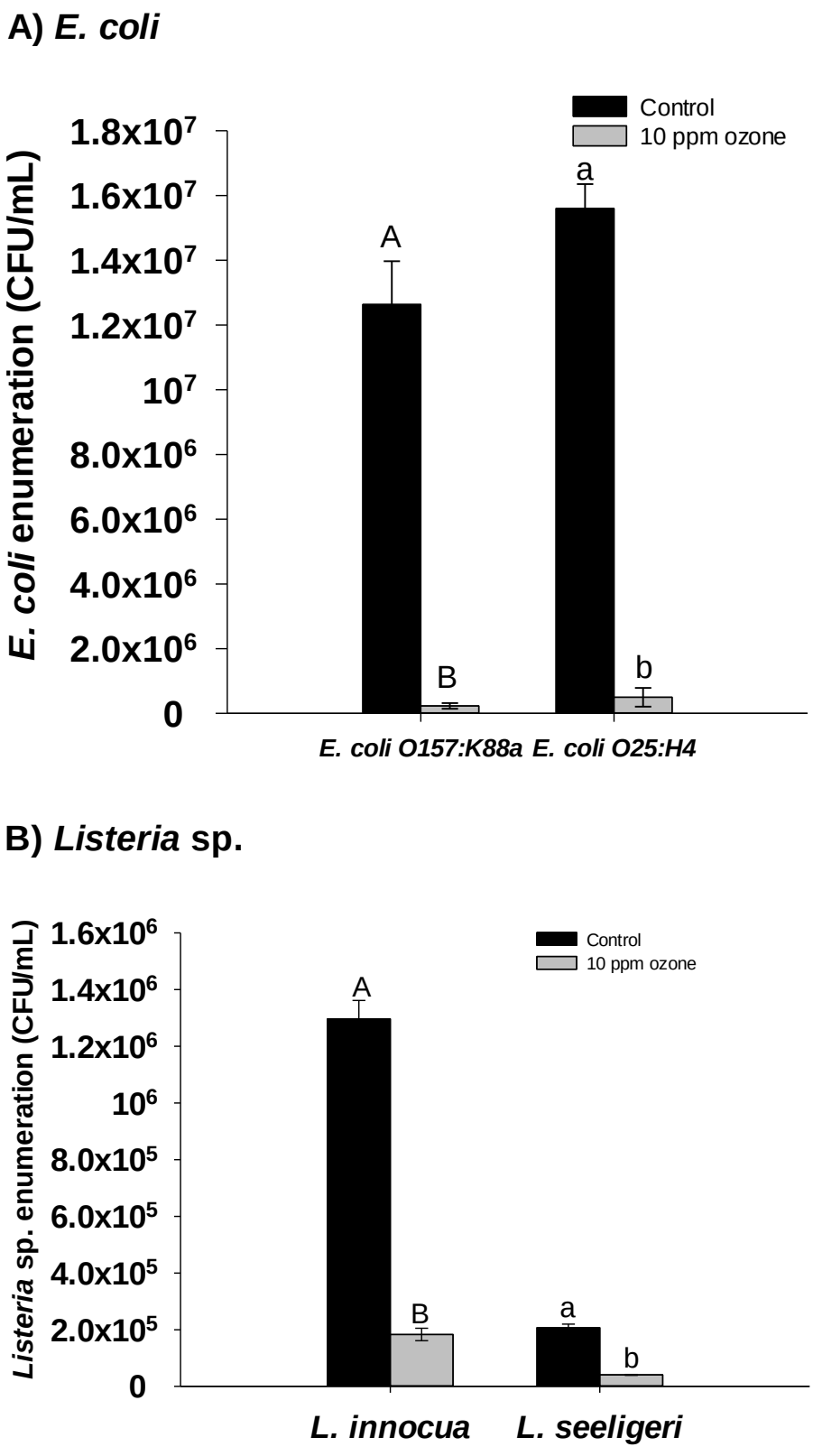

Figure 5. 5: Impacts of increased levels of ozone exposure on two strains of *E. coli* and *Listeria* inoculated onto the surface of spinach leaves. Leaves were either treated with 10 ppm ozone (grey bar) or untreated (black bar) for 2 min. Values represent means (±Standard Error) of measurements made on three independent spinach leaves per treatment. Bars with different letters are significantly different ($P < 0.05$).

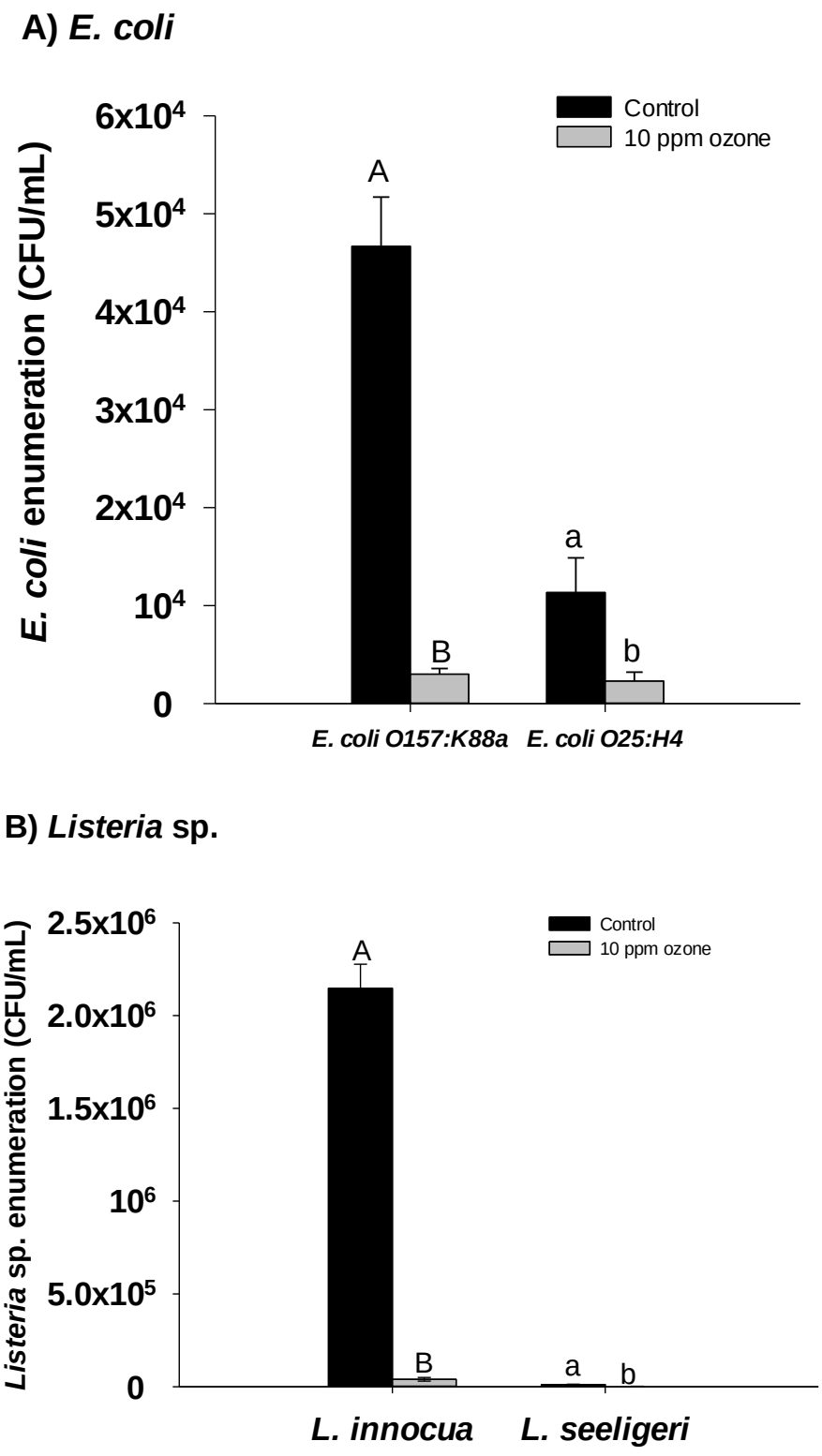

Figure 5. 6: Impacts of ozone-enrichment on two strains of *E. coli* and *Listeria* inoculated onto the surface of spinach leaves. Leaves were either treated with 10 ppm ozone concentration (grey bar) or untreated (black bar) for 2 min. Colonies were enumerated after 9 days storage. Values represent means (±Standard Error) of measurements made on three independent spinach leaves per treatment. Bars with different letters are significantly different ($P < 0.05$).

5.3.5 Effect of age on ozone resistance of E. coli O157:k88a in vitro

E. coli cells obtained from increasing age colonies were exposed to ozone (*in vitro*) and results demonstrated a clear increase in ozone resistance of *E. coli* O157:K88a with increasing colony age. For example, survival of *E. coli* O157:K88a was observed to be greater (approximately 15%) after 5 days of growth compared with day 1 time point. This increased level of survival was also maintained at day 7 (Fig. 5.7) suggesting that cells in older bacterial colonies are more ozone resistant than cells from younger colonies.

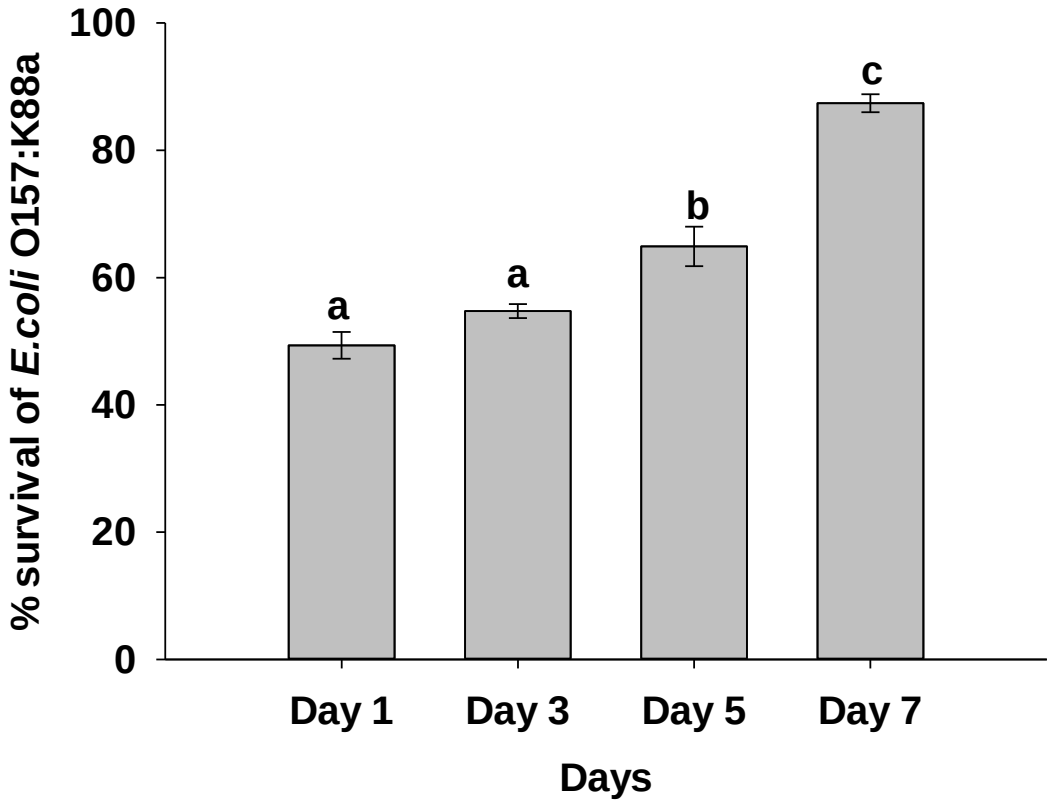

Figure 5. 7: Survival of cells obtained from different colony ages of *E. coli* O157:K88a exposed to 10 ppm ozone for 2 min. After ozone exposure, the culture plates were maintained at 37°C for 7 days. Values represent means (±Standard Error) of measurements made on three independent culture plates per treatment. Bars with different letters are significantly different ($P < 0.05$).

5.4 Discussion

5.4.1 Effect of ozone treatment on E. coli and L. innocua in vitro

The antimicrobial effects of gaseous ozone on *E. coli* K12 and *L. innocua in vitro* are presented in Fig 5.1. The data obtained show that the treatment resulted in significant reduction in *E. coli* K12 and *L. innocua*. Similar results were observed by Alwi (2014), when *E. coli* O157, *L. monocytogenes* and *S. Typhimurium* were treated *in vitro* with 0.1, 0.3, 0.5 and 1.0 ppm ozone concentration for exposure times of 0.5, 3, 6 and 24 h, respectively.

Interestingly, the agar based *in vitro* assay on both pathogens showed that the effectiveness of gaseous ozone increased with increasing ozone concentration from 1 to 10 ppm, but that the effectiveness of ozone exposure did not significantly increase above this level. This may be due to live bacterial cells being physically protected by other cells on the surface of the agar plates; thus, this interferes with the oxidation action of ozone treatment (Alwi 2014). Alternatively, some cells may have an intrinsic resistance to ozone exposure perhaps due to their age and exposure to stress. Fan and colleagues (2007) reported that the maximum inactivation of *L. innocua* cells was observed in less than 2 h, and inactivation reached a plateau after 4 h when treated with gaseous ozone *in vitro*.

5.4.2 Effect of ozone exposure on different E. coli strains inoculated onto spinach leaf surfaces

The results indicate that 1 ppm ozone concentration for 1 min significantly reduced *E. coli* O157:K88a survival. The treatment was also effective on *E. coli* O25:H4, *E. coli* O128:K67, *E. coli* K12, *E. coli* O55:K59 and *E. coli* O104:H12, confirming that *E. coli* species are sensitive to ozone. In the past, gaseous ozone treatment at 1 ppm for 5 min showed 3–5 $\log_{10}$ reduction of *E. coli* O157:H7 on spinach after 24 h of storage (Klockow 2009). An experiment, in which ozone was introduced during vacuum-cooling exposure to 10 ppm for up to 3 days, showed 1.4 $\log_{10}$ reduction of *E. coli* O157:H7 on spinach (Karaca 2014). Gaseous ozone treatment has also proven to be effective in reducing *E. coli* on a range of products including lettuce (Singh et al. 2002), parsley (Karaca 2014), mushrooms (Yuk et al. 2007), blueberries (Bialka and Demirci

2007) and dried figs (Akbas and Ozdemir 2008). Singh et al. (2002) reported that the bactericidal effect of ozone against *E. coli* O157:H7 increased with exposure time and ozone concentration. For example, they observed 0.79–1.79 $\log_{10}$ CFU/g reduction on *E. coli* O157:H7 population on lettuce when exposed to ozone for 15 min. However, ozone treatment for 5 or 10 min did not decrease the *E. coli* O157:H7 population.

5.4.3 Impact of ozone treatment on L. innocua and L. seeligeri onto spinach leaves

In this study, *L. innocua* and *L. seeligeri* were used as surrogate for *L. monocytogenes* as they are useful indicators of contamination and have demonstrated behaviour similar to *L. monocytogenes* on fresh produce (Scifò et al. 2009). Results from spinach artificially contaminated with *L. innocua* and *L. seeligeri* treated with 1 ppm ozone for an exposure time of 10 min showed 0.4–0.8 $\log_{10}$ reduction in colony count compared with the untreated control. Karaca and his colleague (2014) reported that *L. innocua* reduced by 1.14 $\log_{10}$ CFU/g on flat-leaved parsley when treated with high ozone concentration of 950 ppm for 20 min. Similar results have been shown by previous research on mushrooms, alfalfa sprouts, alfalfa seeds and lettuce (Yuk et al. 2007). The growth of *L. innocua* and *L. seeligeri* on spinach remained significantly supressed after 9 days of storage. This may be due to the interactions between the natural background microflora of spinach and *L. innocua* which can affect its growth and survival (O'Beirne 1998). O'Berine and his colleague (1998) reported that lactic acid bacteria and mixed population of natural microflora isolated from shredded lettuce reduced *L. innocua* growth in model media. Rodgers and colleagues (2004) demonstrated complete inactivation of *L. monocytogenes* on lettuce during 9 days storage when treated with 3 ppm ozone for 3 min.

5.4.4 Impact of high ozone treatment on E. coli and Listeria sp. inoculated onto spinach leaf

Higher ozone concentration for shorter exposure time was studied to explore the possibility of time-saving treatment that may fit into the produce processing unit after the harvest. Increasing ozone exposure levels, i.e. 10 ppm for 2 min on *E. coli* (*E. coli* O157:K88a and *E. coli* O25:H4) and *Listeria* spp. (*L. innocua* and *L. seeligeri*) onto spinach, resulted in 1.2–1.7 log and 0.7–0.9 log reduction, respectively. Awli and colleagues (2014) achieved a reduction of 2.89 and 3.06 $\log_{10}$ for *E. coli O157* and *L.*

monocytogenes, respectively, on bell pepper when exposed to 9 ppm ozone for 6 h. Their work met the standards for an antimicrobial agent by attaining a minimum of 2 $\log_{10}$ reduction (Alwi 2014). Similar reductions were observed from application of 5 ppm ozone for 3 min on whole tomato (Bermúdez-Aguirre and Barbosa-Cánovas 2013). When results from this work (on leafy produce) are compared with other hardy produce, it appears that ozone treatment was less successful. This is most probably due to the delicate nature of leafy produce which limits the use of increased ozone concentration and exposure time. In addition, the results obtained from this treatment, i.e. 10 ppm for 2 min, were not significantly more effective in reducing bacterial viable counts in comparison with previous ozone treatment used in this study, i.e. 1 ppm for 10 min (Section 5.3.2 and 5.3.3).

Ozone inactivates bacterial cells by the progressive oxidation of important cellular constituents (Karaca 2014) and suggestions for the principal target of ozonation include the bacterial cell surface. Bacterial cell death as a result of exposure to ozone has been attributed to the rupture of the cell membrane and the disintegration of the cell wall (Karaca 2014; Alwi 2014; Fan et al. 2007). *E. coli* may be particularly sensitive to ozone treatment because it has a thin peptidoglycan lamella that is covered by an outer membrane made of polysaccharides and lipoproteins (Zuma et al. 2009). However, some studies claim that Gram-negative bacteria are more resistant to ozone treatment as compared with Gram-positive bacteria (Vaz-Velho 2006). Results from this study show that ozone treatment was effective in controlling both *E. coli* and *Listeria* spp. though *Listeria* spp. were more resistant. These results are in line with Yuk and colleagues (2007) who showed that *E. coli* O157:H7 to be more sensitive than *L. monocytogenes*.

5.4.5 Impact of high ozone treatment on E. coli strains and Listeria spp. inoculated on spinach after 9-day storage:

Impact of high ozone treatment i.e. 10 ppm for 2 min on *E. coli* (*E. coli* O157:K88a and *E. coli* O25:H4) and *Listeria* sp. (*L. innocua* and *L. seeligeri*) onto spinach after 9-day storage did not show any regrowth. Survival of bacteria after 9-day storage could be due to its ability to consequently develop responses to modify themselves and adapt to survive in harsh environment as they are constantly exposed to fluctuations in their growth conditions (Marles-Wright and Lewis 2007).

5.4.6 Effect of age on ozone resistance of E. coli in vitro:

The data show that survival of *E. coli* O157:K88a *in vitro* after ozone treatment was affected by colony age with older colonies (5–7 days old) exhibits greater ozone resistance than cells from younger colonies (3 days old). This is possibly because older *E. coli* colonies might to be in their long-term stationary phase (fifth phase of bacterial growth cycle which survives on the nutrient released by the dead population of bacteria). These older colonies can survive external stress unlike the younger colonies (probably in first or second phase of bacterial growth cycle) and can remain viable for months or even years once they enter long-term stationary phase (Navarro Llorens et al. 2010). This stationary phase is dominated by the accumulation of the sigma factor RpoS (Hengge-Aronis 2002). The entire cellular physiology of *E. coli* is influenced by RpoS which directly or indirectly affects the expression of 10% of the *E. coli* genes. These genes are involved in morphological variations within the cell and responsible for increasing resistance during numerous stress conditions, e.g. oxidative stress, osmotic stress and heat shock (Navarro Llorens et al. 2010). This result works in line with data from Chapter 3 & 4 discussing the potential reasons for ozone resistance in aged bacteria. *E. coli* being Gram-negative may express the same genes with some variation as aged *Pseudomonas* sp. exhibit the same mechanisms against ozone resistance. However, this is just a hypothesis and in future, it may be confirmed using transcriptome approaches.

5.5 Conclusion

Exposure to 1 ppm and 10 ppm ozone treatment for 10 and 2 min, respectively, significantly reduced *E. coli* and *Listeria* spp. populations on spinach leaves. In addition, the pathogens did not re-grow after treatment, i.e. over a 9-day storage period. Although ozone treatment on *E. coli* and *Listeria* spp. onto spinach, resulted in 1.2–1.7 log and 0.7–0.9 log reduction, respectively, there is still commercial potential as ozone is easy to produce on site and apply at levels which do not damage sensitive leafy produce. The findings from this study show that some bacteria in populations are resistant to ozone treatment and increasing colony age of *E. coli* was shown to be linked to enhanced ozone resistance. Further work is needed to better understand the mechanisms responsible for pathogen resistance.

Chapter 6 General Discussion

6.1 Introduction

Fresh produce has gained increasing popularity as a food source due to its accepted importance as a source of vitamins, fibre and nutrients for humans (Olaimat and Holley 2012). Fresh leafy produce typically has a limited shelf-life due to microbial spoilage, receives minimum processing and is generally consumed raw (Naito and Takahara 2006). Food spoilage is a severe problem for the food industry as it renders products undesirable for human consumption and is associated with economic loss (Saranraj 2012). In addition, there are increasing concerns about the contamination of fresh leafy produce with human pathogens which can occur either at pre-harvest and/or post-harvest processes (Gil et al. 2015). To ensure the safety of the product, the fresh produce industry has conventionally used chlorine as one of the effective disinfectant (Gil et al. 2009). However, there are major concerns about its effectiveness on the fresh produce, environment and health threats linked with the formation of carcenogenic halogenated by-product; therefore, there is an industry need to replace chlorine in the sanitizing process (Ölmez and Kretzschmar 2009). Many companies are now using water washes only which again leaves 'Ready-to-Eat' produce susceptible to bacterial pathogen contamination. The main reason and motivation behind the work reported in this thesis was the development of a novel ozone gas based on method to treat leafy produce, to ensure product safety, and to maintain its physical integrity. The key advantage of using ozone is that it is very powerful oxidising agent which does not leave behind any toxic residue as it decomposes in to oxygen (Mahapatra et al. 2005). This interest is accompanied by a US-FDA approval of ozone for the safe use in food processing industry, and there is no labeling requirement for the ozone-treated products (Horvitz and Cantalejo 2014). Though gaseous ozone has been used to reduce micorbial loads on a variety of fresh produce, this investigation has been one of the few to evaluate the technology for the study of less hardy leaf surfaces. Here, application of ozone was studied on five economically high-value leafy produce types: spinach, watercress, rocket, corainder and lettuce, to broaden knowledge that could potentially benefit the fresh produce industry. To accomplish this, the concentration and exposure duration of gaseous ozone was initially optimized that would inactivate bacterial growth without physically damaging the produce. This allowed an insight into the impact of ozone gas on key spoilage bacteria present on leaf surface. Further, confocal

microscopy was performed to study the growth and location of bacteria present on the leaf surface. This revealed that majority of the bacteria on the leaf surface were killed by ozone treatment but a minority (approximately 1−10%) survived the treatment. Subsequent studies on aged colonies and cold-stressed cells demonstrated that these treatments increased bacterial ozone resistance, and gene expression studies using recently-developed RNA-Seq methodology was used to attempt to gain further understanding of the potential reasons for bacterial ozone resistance. The study also sought to determine whether gaseous ozone treatment could effectively inactivate bacterial food pathogens present on leaf surfaces.The research was able to answer the following questions.

6.2 Is there an impact of gaseous ozone on key post-harvest microbes without causing visual damage on leafy produce?

Ozone levels that significantly reduced microbial load without causing visual damage to leafy produce were determined. It was observed that different produce types had varying ozone resistance, for example, rocket and coriander could tolerate a higher ozone level (10 ppm for 10 min), whereas spinach, watercress and lettuce were more sensitive (1 ppm for 10 min). This may be related to the difference in the physiology of the produce, e.g. stomatal conductance (Jin-Gab Kim 1998; Alexopoulos et al. 2013; Karaca 2014) These exposure levels significantly reduced key post-harvest microbes *in vitro*; however, the equivalent ozone exposure resulted in no microbial load when a packet of targeted produce was treated *per se*. This indicated the importance of ozone access to leaf surfaces. Therefore, to achieve better ozone access, a modified ozone fumigation system was developed to treat leafy produce at higher ozone concentrations for shorter durations. This arrangement could be commercially simulated using a conveyor belt system or during the industry standard vacuum cooling process where maximum air (and hence ozone) exposure of produce would occur in an industrial setting. The vacuum cooler is also an enclosed treatment process indicating that ozone could be safely introduced at this stage with minimal risk of worker exposure to high ozone levels. Using the modified fumigation system, the vast majority of the bacteria were killed when ozone treated at 10 ppm for 2 min and 15 ppm for 30 s. However, 1−10% of the surface population survived and ozone concentrations higher than 20 ppm visually damaged leafy produce. Klockow and colleagues (2009) observed microbial

reduction (3–5 $\log_{10}$ CFU/leaf) on spinach leaves when treated with higher ozone concentration but treated leaves showed discolouration after 24-h storage period. This is typically observed in leafy produce industry while treating with high concentrations of other sanitizers (Klockow 2009).

6.3 What are the potential reasons for bacterial survival on leaf surfaces after ozone treatment?

Confocal scanning microscopy in combination with LIVE/DEAD BacLight staining was used to investigate potential reasons for bacterial survival on leaf surfaces after ozone treatment. It demonstrated that bacterial cells, which were able to survive ozone exposure, occurred both in micro-colonies and as individuals on the leaf surface. This suggested that bacterial ozone resistance was likely due to a number of factors e.g. physical protection in small colonies and inherent resistance of individual cells. A subpopulation of cells in a micro-colony surviving ozone treatment may be physiologically older and thus more resistant than younger cells (Sharma and Beuchat 2004). Survival of individual cells to ozone treatment could be explained due to 'cross protection' where developed resistance is caused from previous exposure to the stress which results into physiological changes in bacterial cell to enhance survival (Capozzi et al. 2009). This is commonly observed in food processing unit among spoilage bacteria as well as foodborne pathogens (Davidson 2002). Subsequent results reported in this thesis confirmed that increasing colony age and prior exposure to cold-stress of a typical leaf surface bacterium (*Pseudomonas* sp. isolated from coriander in the initial stages of this work) enhanced ozone resistance *in vitro.* Most disinfectants known in the fresh produce industry have been in use for approximately a century and concerns have been raised about the development of resistance to these compounds (Davidson 2002). However, there is lack of adequate data addressing a solution to this problem and understanding the mechanisms of ozone resistance in aged colonies and stressed cells of *Pseudomonas* sp. may lead to methods that can overcome resistance. Therefore, it was decided to conduct a detailed comparison of gene expression in aged colonies (10-day-old) and cold-stressed *Pseudomonas* cells compared with a control population (4-day-old) using RNA-Seq technology.

6.4 What are the possible mechanisms by which bacteria are able to resist ozone treatment?

Transcriptome analysis using RNA-Sequencing was studied to understand the differences in gene expression of aged colonies or cold-stressed *Pseudomonas* cells compared with control cells. As expected, significant changes in the expression of genes related to stress resistance compared with controls was observed. In particular, it was observed that in aged colonies, approximately 90% of the changes in gene expression mapped to one gene (a non-coding RNA that is part of RNase P). This gene interacts with cellular mRNA transcripts to control bacterial growth in response to environmental stress conditions.

Four biological processes were induced in cold stressed bacteria: 'Inorganic ion transport and metabolism', 'Energy production and conversion', 'Amino acid transport and metabolism' and 'Coenzyme transport and metabolism'. 'Amino acid transport and metabolism' and 'Energy production and conversion' have been previously reported in cold-stressed *Pseudomonas putida* (Fonseca et al. 2011b, 2013). For instance, amino acid permeases, a well-characterized part of amino acid transport systems which is crucial for cold-adaptation were up-regulated in cold-stressed cells (Moreno and Rojo 2014). Similarly, enzymes such as phosphoenolpyruvate carboxykinase (ATP) and phosphoenolpyruvate carboxylase, which are part of energy production and conversion required for surviving environmental stress, were also over-represented (Reva et al. 2006). Phosphoenolpyruvate carboxykinase (ATP) and phosphoenolpyruvate carboxylase, which are part of energy production and conversion, were also observed in aged colonies suggesting that inhibition of these enzymes in *Pseudomonas* sp. makes them less/non-resistant to stress. 'Cell cycle control, cell division, chromosome partitioning', 'Translational, ribosomal structure and biogenesis', 'Replication, recombination and repair' and 'Cell wall/membrane/envelope biogenesis' were under-represented in cold-stressed bacteria. For example, lipid metabolism in the outer membrane of bacteria plays a vital role in responding to environmental stress (Reva et al. 2006). It was detected that the expression of lipid-A acyl-CoA transferases was down-regulated in cold stressed bacteria suggesting that this aids in the adaptation process that facilitates the growth of *Pseudomonas* bacteria at low temperature. However, the role of these processes needs to be evaluated further to determine their contribution to bacterial resistance.

‘Energy production and conversion’, ‘Carbohydrate transport & metabolism’, ‘cell cycle control, cell division’ and ‘post-translational modification’ were over-expressed in aged colonies. Genes such as ATPases involved in cell division and chromosome partitioning were up-regulated in aged colonies. These genes are responsible for reducing cellular growth and preventing cell division resulting into dormant state to aid survival in stressed conditions (Waite et al. 2006). ‘Cell motility’, ‘General function prediction only’ and ‘Intracellular trafficking, secretion, and vesicular transport’ were under-represented in aged bacteria. ‘Cell motility’ was also under-represented in cold-stressed cells. For instance, genes involved in flagella and type IV, which are responsible for cell motility, were down-regulated in aged colonies. It has been demonstrated in the past that flagellar motility in *P. aeruginosa* is only required in the initial phase of biofilm formation and not in mature cells which are capable of surviving environmental stress (Beloin and Ghigo 2005). This indicates that aged colonies behave similarly to those in biofilm capable of coping with stress/applied disinfectant.

Many of the genes showing differential expression were involved in energy production, transport, motility or cell wall/membrane integrity. Several changes appeared directed towards neutralizing problems created by low temperature or aging, such as increased stability of RNA/DNA structures, changes in protein folding and reduced growth rate. In total, this novel information may lead to new anti-microbial treatments that will probably hinge upon a better understanding of stress-induced physiological responses. For example, in the near future, fresh produce will be treated with appropriate disinfectant with strategies directed to inhibit cold stressed cells before it has been subjected to refrigeration and/or addition of a growth substrate to the water wash to activate bacteria and make them more susceptible to treatments.

6.5 Is ozone treatment able to inactivate *E. coli* and *Listeria* on spinach?

In addition to reducing produce spoilage, it was important to establish the effect of ozone treatment on foodborne pathogens because all leafy produce types have the potential to harbour pathogens responsible for lethal food-borne outbreaks. In this study, the food pathogens examined were six strains of *E. coli*, *L. innocua* and *L. seeligeri*. Exposure to 1 ppm and 10 ppm ozone treatment for 10 and 2 min, respectively, significantly reduced *E. coli* and *Listeria* sp. populations on spinach. At the same time, the treatments reduced the levels of pathogens even after 9-days storage compared with

untreated controls. However, the ozone treatment on *Listeria* spp. did not achieve more than 1-log reduction. This suggests that a proportion of these pathogenic bacteria survived ozone treatment and colony age of the pathogen was speculated to be the potential reason for enhanced ozone resistance. *In vitro* studies using *E. coli* demonstrated a clear increase in ozone resistance with increasing colony age.

6.6 Comments on safety recommendations for handling gaseous ozone in a commercial context

When considering ozone technology, there are numerous concerns that must be taken into account to ensure safe application of ozone gas in an industrial context. (Horvitz and Cantalejo 2014). Exposure to this sanitizer above certain concentrations can lead to acute symptoms in humans. Severe irritation is caused to the upper and lower respiratory tract resulting into symptoms such as coughing, headaches, nausea, burning sensation in eyes and dizziness when exposed to low ozone concentration such as 1 ppm (Guzel-Seydim et al. 2004; Hems 2005). At higher concentrations, it can lead to lung congestion, haemorrhage and pulmonary edema, eventually resulting into diminished breathing (Perry and Yousef 2011; Hems 2005). Therefore, it is important to follow recommended ozone exposure levels established by government institutes such as Food and Drug Administration (FDA), Occupational Safety and Health Administration (OSHA), National Institute of Occupational Safety and Health (NIOSH) and Environmental Protection Agency (EPA) (Goncalves 2009b).

Application of ozone in fresh produce industry involves generation of the gas on site, and hence, it is important to maintain the off gas in a closed system until it is destroyed to avoid any inadvertent gas exposure (Perry and Yousef 2011). Generation of excess ozone should be degassed and converted into oxygen before releasing it in the atmosphere. Ambient ozone levels should be monitored in the working area and destruction systems, and respirators are necessary for the safety of the workers in the food processing unit. At high concentration, ozone is corrosive, and hence, surfaces exposed to ozone should consist only of compatible materials such as stainless steel and Perspex plastic (Ölmez and Kretzschmar 2009). Therefore, the idea previously mooted of using ozone gas exposure in enclosed vacuum cooler systems would appear a useful solution.

6.7 Conclusions and future perspectives

The data reported in this study showed that ozone treatment can be used to reduce microbial spoilage and food pathogens on leafy produce. The optimization of ozone processing for a particular leafy produce must be assessed. Only a well-balanced impact between safety and quality will result into favourable outcomes for majority of the products. Therefore, studies on the impact of ozone treatment on specific produce type and range of micro-organisms are required to achieve microbiological safe products with high-quality features. Such integrated methodologies are vital before introducing ozone treatments into commercial trials.

The ozone concentrations optimized to treat leafy produce in this research did not cause any visual damage; however, browning appearance and russet spotting was observed on all targeted produce above optimized levels. Colour is the primary judging criteria but further research is required on the physiological changes and sensory acceptability of ozone treated leafy produce (Rico et al. 2007). It is vital to maintain the flavor, texture and nutrition along with the safety of produce (Klockow 2009). Sensory evaluation of the treated produce can be obtained from different device such as gas chromatographs, texturometers, image analysis software or colourimeters (Rico et al. 2007). Chemical composition of fresh leafy produce can be affected by ozone due to its strong oxidizing activity (Karaca 2014). Nutritional content of the produce can be assessed by measuring the variations in antioxidant capacity caused by ascorbic acid, Vitamin C or polyphenols (Rico et al. 2007; Ölmez and Akbas 2009). The effects of ozone treatment on several colour pigments in many products have been previously studied. For example, no significant difference in vitamin C, organic acid or total phenol content was observed in ozone treated tomato fruit (Tzortzakis et al. 2007).

Although combinations of treatments are commonly practiced to treat leafy produce, studies that combine ozone with other approaches to improve the quality and/or safety are rare. Therefore, studies that combine ozone with other systems (such as chlorine) are required, as they could provide useful alternatives to improve the health and safety of leafy produce.

The transcriptome study in this thesis represents the first RNA-Seq based gene expression analysis in response to cold-stress and colony age in *Pseudomonas* species. The overlap among DEGs and regulated pathways after different treatments (age and

cold-stress) suggest a comprehensive co-ordination in response to different stressors. The differences in DEGs and regulated pathways in the response to different types of stress indicate the fine-tuning of gene regulation during different stresses. Further detailed analysis of the functions of DEGs and pathways, as well as their links will improve understanding of the molecular mechanisms involved in stress response potentially leading to methods which could make bacteria less resistant/non-resistant to applied disinfectants.

In summary, this thesis has demonstrated that gaseous ozone treatment shows promise as a commercially-viable tool to reduce microbial loads and food pathogen contamination of leafy produce and ozone technology is worth exploring on a pilot-scale in an industrial setting. Further research to enhance the efficacy of ozone (and other) treatments by developing commercially applicable methods that alter the susceptibility of food-borne microbes to treatment offers huge potential for the fresh produce industry.

Appendix A: Microbial identification from Geneius database

Microbial ID: Geneius 2011

Name of Client: University
Geneius Sample Reference: N101998_2001
Company Sample Reference:
Type of Sample: Salads DAY0 (Start of Life)
Date of Sample Receipt: 18OCT11
Number of Samples: 4
Date of Report: 20OCT11
Results from MicroSeq:

Specimen	% Match	Sequence Entry	Library
Coriander	99.21	Pseudomonas putida	AB_BacterialFullGeneLib_2.0
N101998	98.77	Pseudomonas flavescens	AB_BacterialFullGeneLib_2.0
	98.48	Pseudomonas fulva	AB_BacterialFullGeneLib_2.0
	98.28	Pseudomonas asplenii	AB_BacterialFullGeneLib_2.0
	98.11	Pseudomonas fuscovaginae	AB_BacterialFullGeneLib_2.0
coriander	99.88	Bacillus subtilis subtilis ATCC=6051	AB_BacterialFullGeneLib_2.0
N101998	99.79	Bacillus amyloliquefaciens	AB_BacterialFullGeneLib_2.0
	99.7	Bacillus subtilis spizizenii ATCC=6633	AB_BacterialFullGeneLib_2.0
	99.66	Bacillus mojavensis	AB_BacterialFullGeneLib_2.0
	99.29	Bacillus atrophaeus	AB_BacterialFullGeneLib_2.0
Org spinach	99.43	Pseudomonas fragi	AB_BacterialFullGeneLib_2.0
N101999	99.01	Pseudomonas taetrolens	AB_BacterialFullGeneLib_2.0
	98.9	Pseudomonas lundensis	AB_BacterialFullGeneLib_2.0
	98.45	Pseudomonas fluorescens ATCC=13525	AB_BacterialFullGeneLib_2.0
	98.42	Pseudomonas aurantiaca	AB_BacterialFullGeneLib_2.0
Org spinach	99.41	Pseudomonas fragi	AB_BacterialFullGeneLib_2.0
N101999	98.79	Pseudomonas taetrolens	AB_BacterialFullGeneLib_2.0
	98.74	Pseudomonas fluorescens C (bt) ATCC=17572	AB_BacterialFullGeneLib_2.0
	98.69	Pseudomonas lundensis	AB_BacterialFullGeneLib_2.0
	98.45	Pseudomonas mucidolens	AB_BacterialFullGeneLib_2.0
Rocket	98.28	Pseudomonas lundensis	AB_BacterialFullGeneLib_2.0
Wcress/spin	98.13	Pseudomonas corrugate	AB_BacterialFullGeneLib_2.0
N102000	98.12	Pseudomonas viridiflava	AB_BacterialFullGeneLib_2.0
	97.96	Pseudomonas taetrolens	AB_BacterialFullGeneLib_2.0
	97.89	Pseudomonas fluorescens ATCC=13525	AB_BacterialFullGeneLib_2.0
Rocket	99.97	Aeromonas bestiarum	AB_BacterialFullGeneLib_2.0
Wcress/spin	99.97	Aeromonas salmonicida	AB_BacterialFullGeneLib_2.0

N102000	99.97	Haemophilus piscium	AB_BacterialFullGeneLib_2.0
	99.31	Aeromonas sobria	AB_BacterialFullGeneLib_2.0
	99.11	Aeromonas eucrenophila	AB_BacterialFullGeneLib_2.0
Rocket	99.77	Pseudomonas synxantha	AB_BacterialFullGeneLib_2.0
Wcress/spin	99.77	Pseudomonas mucidolens	AB_BacterialFullGeneLib_2.0
N102000	99.63	Pseudomonas fluorescens ATCC=13525	AB_BacterialFullGeneLib_2.0
	99.54	Pseudomonas fluorescens C (bt) ATCC=17572	AB_BacterialFullGeneLib_2.0
	99.53	Pseudomonas marginalis	AB_BacterialFullGeneLib_2.0
Italian style salad	99.61	Rahnella aquatilis	AB_BacterialFullGeneLib_2.0
N102001	98	Yersinia enterocolitica	AB_BacterialFullGeneLib_2.0
	97.91	Yersinia rohdei	AB_BacterialFullGeneLib_2.0
	97.76	Ewingella Americana	AB_BacterialFullGeneLib_2.0
	97.73	Yersinia intermedia	AB_BacterialFullGeneLib_2.0
Italian style salad	97.65	Exiguobacterium acetylicum	AB_BacterialFullGeneLib_2.0
N102001	92.88	Kurthia gibsonii	AB_BacterialFullGeneLib_2.0
	92.8	Sporosarcina ureae	AB_BacterialFullGeneLib_2.0
	92.72	Kurthia zopfii	AB_BacterialFullGeneLib_2.0
	92.46	Bacillus pumilus	AB_BacterialFullGeneLib_2.0
Italian style salad	99.87	Aeromonas bestiarum	AB_BacterialFullGeneLib_2.0
N102001	99.87	Aeromonas salmonicida	AB_BacterialFullGeneLib_2.0
	99.87	Haemophilus piscium	AB_BacterialFullGeneLib_2.0
	99.51	Aeromonas sobria	AB_BacterialFullGeneLib_2.0
	99.39	Aeromonas eucrenophila	AB_BacterialFullGeneLib_2.0

Microbial ID: Geneius 2011

Name of Client: University
Geneius Sample Reference:N1098_2001
Company Sample Reference:
Type of Sample: salads DAY0
Date of Sample Receipt:18OCT11
Number of Samples: 4
Date of Report: 16NOV11
Results from MicroSeq:

Specimen	% Match	Sequence Entry	Library
N101999	92	Penicillium olsonii	AB_FungalLib_2.0
org spinach	90.87	Penicillium brevicompactum	AB_FungalLib_2.0
	86.26	Bullera dendrophila	AB_FungalLib_2.0

	85.93	Filobasidiella neoformans	AB_FungalLib_2.0
	85.16	Cryptococcus aerius	AB_FungalLib_2.0
N101999	99.35	Alternaria alternate	AB_FungalLib_2.0
org spinach	96.4	Alternaria tenuis	AB_FungalLib_2.0
	83.12	Trichosporon pullulans	AB_FungalLib_2.0
	81.73	Mrakia frigida	AB_FungalLib_2.0
N101998	97.99	Alternaria alternate	AB_FungalLib_2.0
coriander	96.86	Alternaria brassicae	AB_FungalLib_2.0
	95.58	Eupenicillium ochrosalmoneum	AB_FungalLib_2.0
	95.5	Eupenicillium baarnense	AB_FungalLib_2.0
	95.22	Penicillium roqueforti CBS=167.91	AB_FungalLib_2.0
N101998	99.66	Phaeosphaeria avenaria f. sp. avenaria	AB_FungalLib_2.0
coriander	99.66	Phaeosphaeria avenaria f. sp. Triticea	AB_FungalLib_2.0
	96.97	Septoria cyclaminis	AB_FungalLib_2.0
	96.24	Phoma terrestris	AB_FungalLib_2.0
	96.24	Pyrenochaeta lycopersici	AB_FungalLib_2.0
N102000	98.75	Cryptococcus macerans	AB_FungalLib_2.0
rocket/wcress/spinach	97.18	Cystofilobasidium bisporidii	AB_FungalLib_2.0
	96.25	Cystofilobasidium capitatum	AB_FungalLib_2.0
	82.83	Trichosporon pullulans	AB_FungalLib_2.0
	81.93	Mrakia frigida	AB_FungalLib_2.0
N102000	100	Debaryomyces hansenii	AB_FungalLib_2.0
rocket/wcress/spinach	98.22	Wingea robertsii	AB_FungalLib_2.0
	97.87	Debaryomyces udenii	AB_FungalLib_2.0
	95.74	Candida multigemmis	AB_FungalLib_2.0
	94.17	Candida krissii	AB_FungalLib_2.0
N102001	99.66	Cladosporium cladosporioides	AB_FungalLib_2.0
italian salad	99.66	Cladosporium herbarum	AB_FungalLib_2.0
	99.66	Mycosphaerella aronici	AB_FungalLib_2.0
	89.09	Scirrhia acicula	AB_FungalLib_2.0
	88.4	Gloeodes pomigena	AB_FungalLib_2.0
N102001	99.37	Cryptococcus ater	AB_FungalLib_2.0
italian salad	95.64	Filobasidium uniguttulatum	AB_FungalLib_2.0
	93.52	Cryptococcus terreus	AB_FungalLib_2.0
	93.46	Filobasidium capsuligenum	AB_FungalLib_2.0
	93.21	Cryptococcus aerius	AB_FungalLib_2.0
N102001	99.71	Debaryomyces hansenii	AB_FungalLib_2.0
italian salad	96.35	Debaryomyces udenii	AB_FungalLib_2.0
	83.91	Scirrhia acicula	AB_FungalLib_2.0
	81.93	Mrakia frigida	AB_FungalLib_2.0

Appendix B: Bioanalyzer results

Assay Class: Prokaryote Total RNA Nano
Data Path: C:\...rokaryote Total RNA Nano_DE72905416_2014-02-28_11-22-38.xad

Created: 2/28/2014 11:22:38 AM
Modified: 2/28/2014 11:46:31 AM

Electropherogram Summary Continued ...

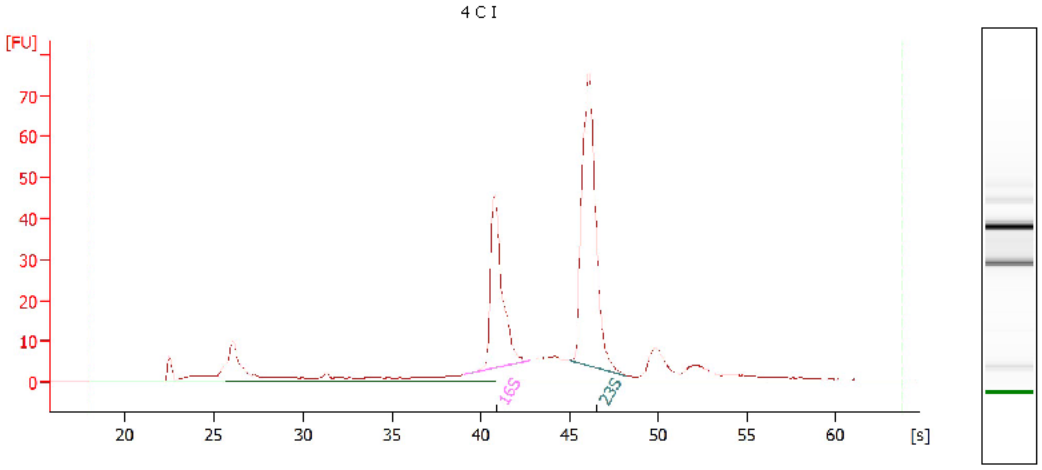

Overall Results for sample 4 : 4 C I

RNA Area:	422.2	rRNA Ratio [23s / 16s]:	1.8
RNA Concentration:	327 ng/µl	RNA Integrity Number (RIN):	9.7 (B.02.08)

Fragment table for sample 4 : 4 C I

Name	Start Time [s]	End Time [s]	Area	% of total Area
16S	39.04	42.74	77.1	18.3
23S	45.00	48.23	139.7	33.1

Assay Class: Prokaryote Total RNA Nano
Data Path: C:\...rokaryote Total RNA Nano_DE72905416_2014-02-28_11-22-38.xad

Created: 2/28/2014 11:22:38 AM
Modified: 2/28/2014 11:46:31 AM

Electropherogram Summary Continued ...

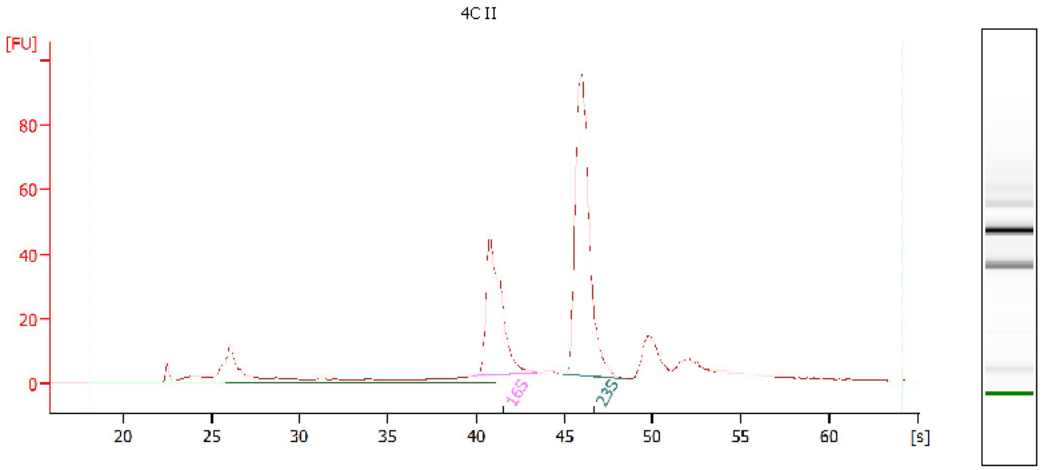

Overall Results for sample 5 : 4C II

RNA Area:	523.3	rRNA Ratio [23s / 16s]:	1.8
RNA Concentration:	405 ng/µl	RNA Integrity Number (RIN):	9.6 (B.02.08)

Fragment table for sample 5 : 4C II

Name	Start Time [s]	End Time [s]	Area	% of total Area
16S	39.79	43.47	105.4	20.1
23S	44.95	48.44	187.5	35.8

Assay Class: Prokaryote Total RNA Nano
Data Path: C:\...rokaryote Total RNA Nano_DE72905416_2014-02-28_11-22-38.xad

Created: 2/28/2014 11:22:38 AM
Modified: 2/28/2014 11:46:31 AM

Electropherogram Summary Continued ...

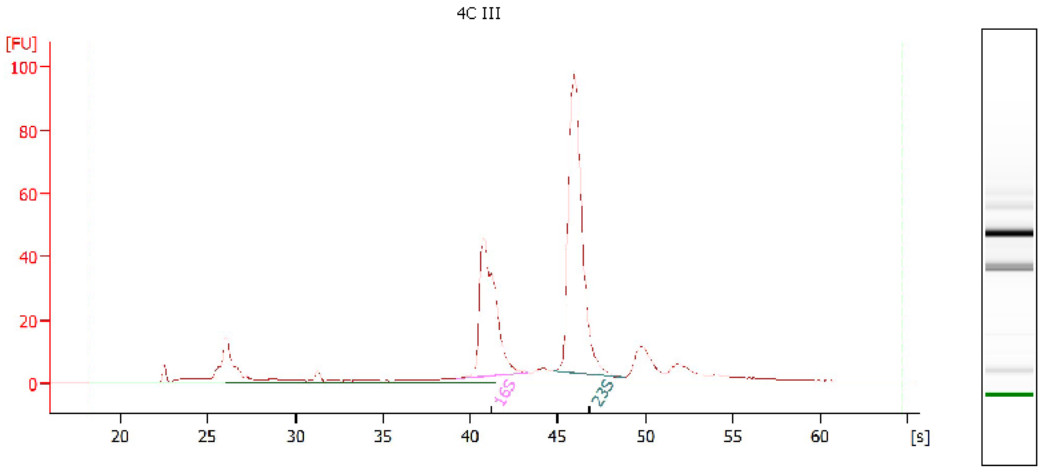

Overall Results for sample 6 : 4C III

RNA Area:	513.0	rRNA Ratio [23s / 16s]:	1.7
RNA Concentration:	397 ng/µl	RNA Integrity Number (RIN):	9.7 (B.02.08)

Fragment table for sample 6 : 4C III

Name	Start Time [s]	End Time [s]	Area	% of total Area
16S	39.19	43.31	110.6	21.6
23S	44.77	48.84	189.2	36.9

Assay Class: Prokaryote Total RNA Nano
Data Path: C:\...rokaryote Total RNA Nano_DE72905416_2014-02-28_11-22-38.xad

Created: 2/28/2014 11:22:38 AM
Modified: 2/28/2014 11:46:31 AM

Electropherogram Summary Continued ...

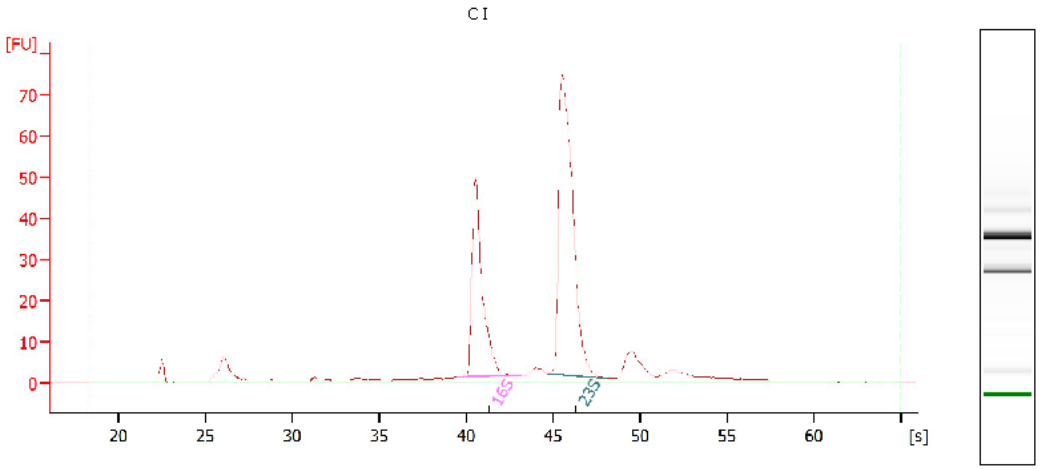

Overall Results for sample 7 : C I

RNA Area:	353.6	rRNA Ratio [23s / 16s]:	1.8
RNA Concentration:	274 ng/µl	RNA Integrity Number (RIN):	10 (B.02.08)

Fragment table for sample 7 : C I

Name	Start Time [s]	End Time [s]	Area	% of total Area
16S	39.49	43.12	82.4	23.3
23S	44.67	48.06	147.6	41.7

Assay Class: Prokaryote Total RNA Nano
Data Path: C:\...rokaryote Total RNA Nano_DE72905416_2014-02-28_11-22-38.xad

Created: 2/28/2014 11:22:38 AM
Modified: 2/28/2014 11:46:31 AM

Electropherogram Summary Continued ...

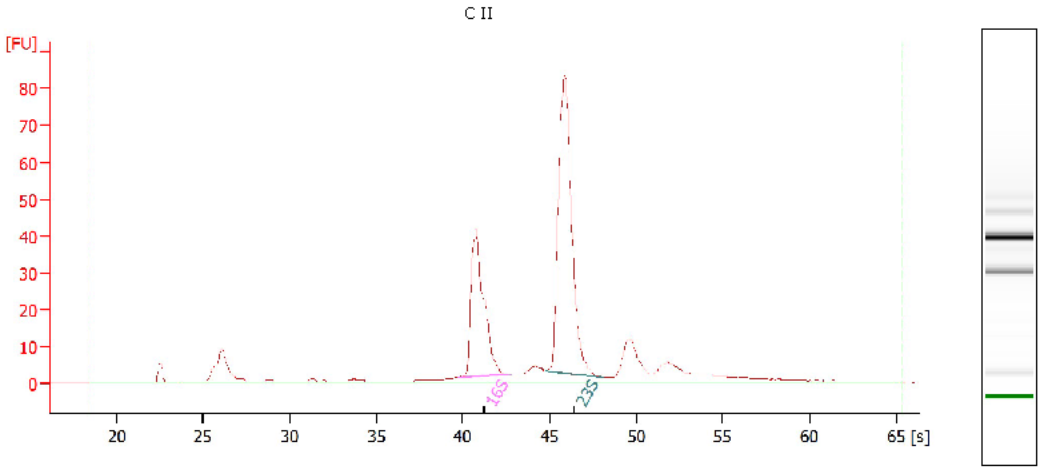

Overall Results for sample 8 : C II

RNA Area:	407.0	rRNA Ratio [23s / 16s]:	1.9
RNA Concentration:	315 ng/µl	RNA Integrity Number (RIN):	9.8 (B.02.08)

Fragment table for sample 8 : C II

Name	Start Time [s]	End Time [s]	Area	% of total Area
16S	39.69	42.82	82.6	20.3
23S	44.72	48.13	156.4	38.4

Assay Class: Prokaryote Total RNA Nano
Data Path: C:\...rokaryote Total RNA Nano_DE72905416_2014-02-28_11-22-38.xad

Created: 2/28/2014 11:22:38 AM
Modified: 2/28/2014 11:46:31 AM

Electropherogram Summary Continued ...

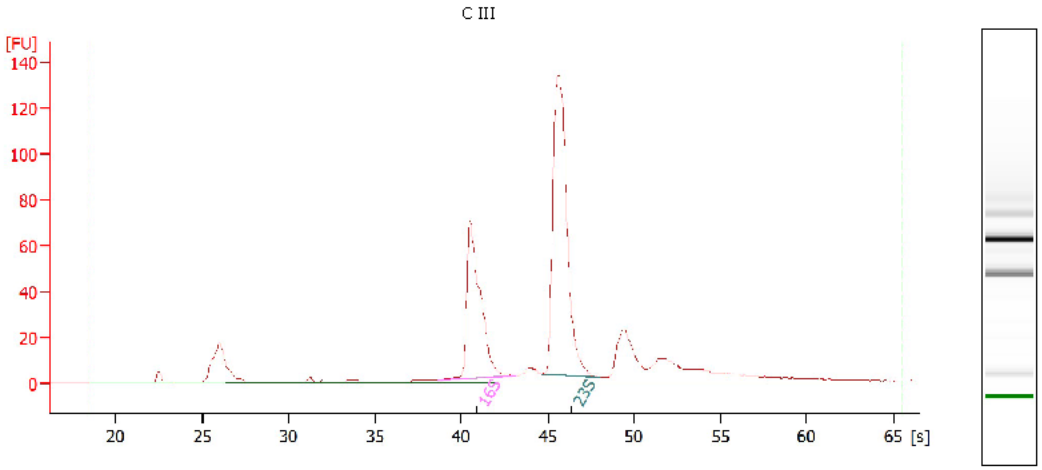

Overall Results for sample 9 : C III

RNA Area:	704.0	rRNA Ratio [23s / 16s]:	1.8
RNA Concentration:	545 ng/µl	RNA Integrity Number (RIN):	10 (B.02.08)

Fragment table for sample 9 : C III

Name	Start Time [s]	End Time [s]	Area	% of total Area
16S	38.64	43.15	152.0	21.6
23S	44.67	48.04	269.7	38.3

Assay Class: Prokaryote Total RNA Nano
Data Path: C:\...rokaryote Total RNA Nano_DE72905416_2014-02-28_11-22-38.xad

Created: 2/28/2014 11:22:38 AM
Modified: 2/28/2014 11:46:31 AM

Electropherogram Summary Continued ...

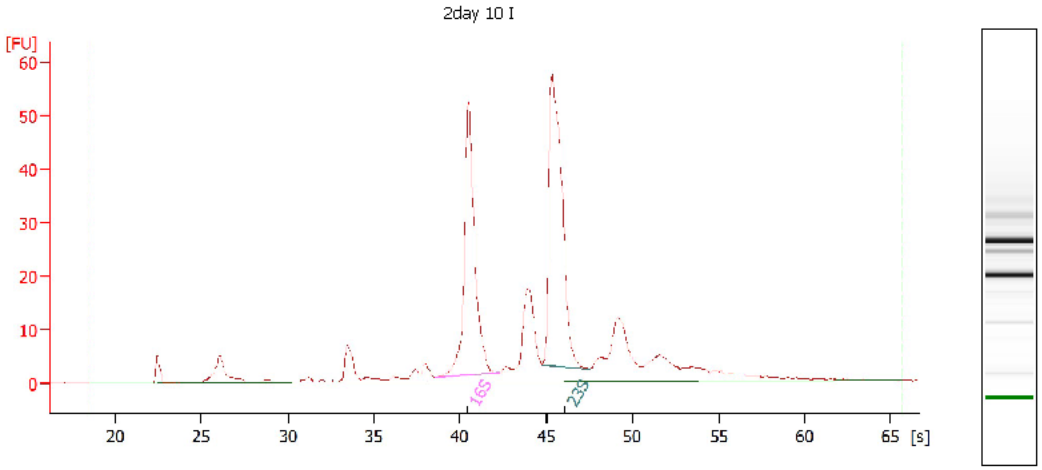

Overall Results for sample 10 : 2day 10 I

RNA Area:	380.9	rRNA Ratio [23s / 16s]:	1.2
RNA Concentration:	295 ng/µl	RNA Integrity Number (RIN):	9.5 (B.02.08)

Fragment table for sample 10 : 2day 10 I

Name	Start Time [s]	End Time [s]	Area	% of total Area
16S	38.58	42.29	88.8	23.3
23S	44.76	47.52	104.6	27.5

Assay Class: Prokaryote Total RNA Nano
Data Path: C:\...rokaryote Total RNA Nano_DE72905416_2014-02-28_11-22-38.xad

Created: 2/28/2014 11:22:38 AM
Modified: 2/28/2014 11:46:31 AM

Electropherogram Summary Continued ...

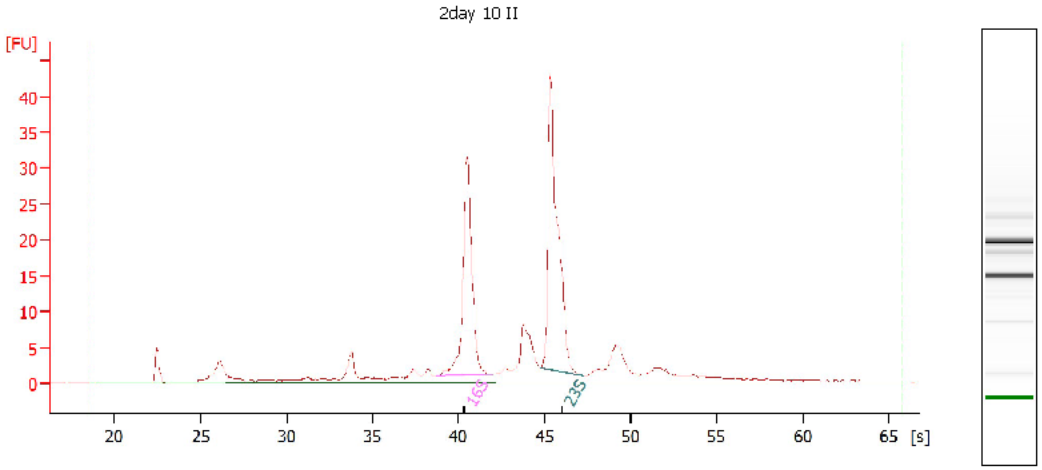

Overall Results for sample 11 : 2day 10 II

RNA Area:	206.2	rRNA Ratio [23s / 16s]:	1.2
RNA Concentration:	160 ng/µl	RNA Integrity Number (RIN):	9.3 (B.02.08)

Fragment table for sample 11 : 2day 10 II

Name	Start Time [s]	End Time [s]	Area	% of total Area
16S	38.71	42.00	46.9	22.7
23S	44.76	47.24	56.8	27.5

Assay Class: Prokaryote Total RNA Nano
Data Path: C:\...rokaryote Total RNA Nano_DE72905416_2014-02-28_11-22-38.xad

Created: 2/28/2014 11:22:38 AM
Modified: 2/28/2014 11:46:31 AM

Electropherogram Summary Continued ...

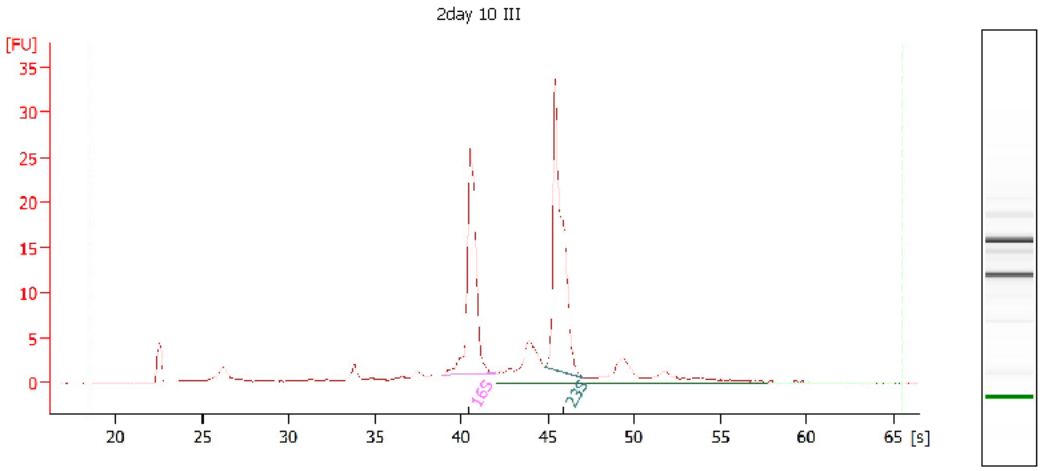

Overall Results for sample 12 : 2day 10 III

RNA Area:	151.0	rRNA Ratio [23s / 16s]:	1.2
RNA Concentration:	117 ng/µl	RNA Integrity Number (RIN):	9.5 (B.02.08)

Fragment table for sample 12 : 2day 10 III

Name	Start Time [s]	End Time [s]	Area	% of total Area
16S	38.78	41.96	37.1	24.6
23S	44.81	47.09	44.7	29.6

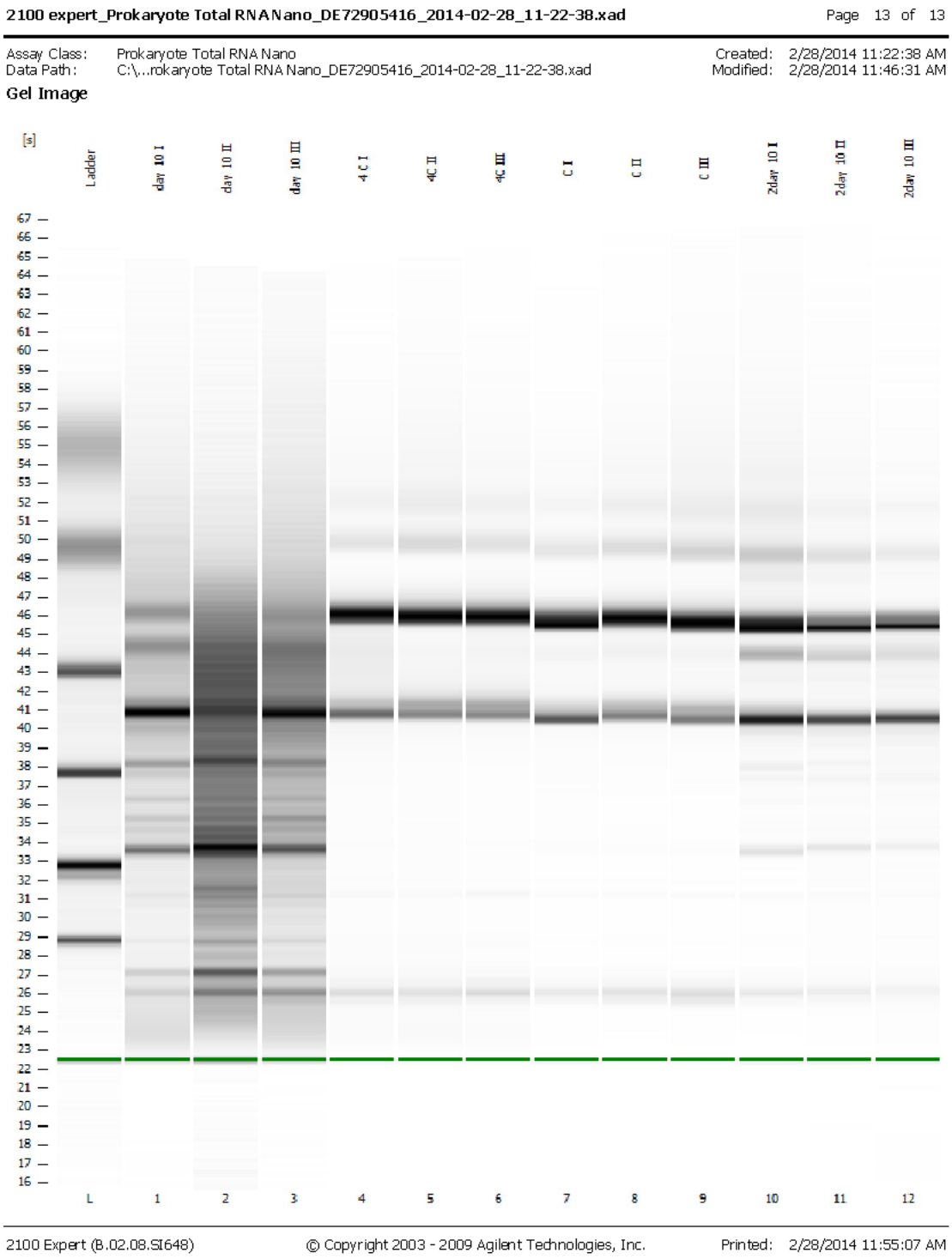

Appendix C: List of up- and down-regulated DEGs in cold-stressed *Pseudomonas* sp. compared to control

ID	regFC	Product_name	COG_category
PMI32_01763	24.619604	Glycine/D-amino acid oxidases (deaminating)	[E] Amino acid transport and metabolism
PMI32_00477	18.100357	coenzyme PQQ biosynthesis protein B	[R] General function prediction only
PMI32_01765	17.518479	Glutamine synthetase	[E] Amino acid transport and metabolism
PMI32_04694	15.842329	hypothetical protein	

PMI32_00487	14.627673	Histidine kinase-, DNA gyrase B-, and HSP90-like ATPase./Histidine kinase./HAMP domain.	
PMI32_00491	14.292767	ABC transporter, ATP-binding subunit, PQQ-dependent alcohol dehydrogenase system	[V] Defense mechanisms
PMI32_00485	13.941343	Uncharacterized low-complexity proteins	[S] Function unknown
PMI32_00426	13.466628	Agmatinase	[E] Amino acid transport and metabolism
PMI32_01766	11.840226	Predicted glutamine amidotransferases	[R] General function prediction only
PMI32_04286	11.265311	PAS domain S-box/diguanylate cyclase (GGDEF) domain	
PMI32_02731	10.934933	NADH dehydrogenase, FAD-containing subunit	[C] Energy production and conversion
PMI32_01768	10.556622	ABC-type spermidine/putrescine transport system, permease component I	[E] Amino acid transport and metabolism
PMI32_04620	9.9556846	2-keto-3-deoxy-6-phosphogluconate aldolase	[G] Carbohydrate transport and metabolism
PMI32_00492	9.6516307	alcohol ABC transporter, permease protein	[V] Defense mechanisms
PMI32_00476	9.3253129	coenzyme PQQ biosynthesis protein C	[H] Coenzyme transport and metabolism
PMI32_00480	9.1275863	Zn-dependent hydrolases, including glyoxylases	[R] General function prediction only
PMI32_01767	9.0289558	spermidine/putrescine ABC transporter ATP-binding subunit	[E] Amino acid transport and metabolism
PMI32_00489	8.8220995	ABC transporter, substrate binding protein, PQQ-dependent alcohol dehydrogenase system	[E] Amino acid transport and metabolism
PMI32_00243	8.5968833	ABC-type proline/glycine betaine transport systems, permease component	[E] Amino acid transport and metabolism
PMI32_04260	8.4480936	amine acid ABC transporter, permease protein, 3-TM region, His/Glu/Gln/Arg/opine family	[E] Amino acid transport and metabolism
PMI32_00483	8.2232903	Cytochrome c, mono- and diheme variants	
PMI32_01545	8.1658018	Predicted membrane protein	[S] Function unknown
PMI32_04619	8.1440448	2-keto-3-deoxy-galactonokinase	[G] Carbohydrate transport and metabolism
PMI32_00490	8.0700367	PQQ-dependent catabolism-associated beta-propeller protein	[S] Function unknown
PMI32_01544	7.7162165	transporter, SSS family	[R] General function prediction only
PMI32_01670	7.1336064	coenzyme PQQ biosynthesis probable peptidase PqqF	[O] Posttranslational modification, protein turnover, chaperones
PMI32_00242	6.9656091	Periplasmic glycine betaine/choline-binding (lipo)protein of an ABC-type transport system (osmoprotectant binding protein)	[M] Cell wall/membrane/envelope biogenesis
PMI32_02328	6.9580742	Transcriptional regulator	[K] Transcription
PMI32_01672	6.6718864	Monoamine oxidase	[E] Amino acid transport and metabolism
PMI32_00482	6.652121	ABC-type amino acid transport/signal transduction systems, periplasmic component/domain	[E] Amino acid transport and metabolism, [T] Signal transduction mechanisms
PMI32_00484	6.4309629	PQQ-dependent dehydrogenase, methanol/ethanol family	[G] Carbohydrate transport and metabolism
PMI32_05603	6.3580636	Predicted signal-transduction protein containing cAMP-binding and CBS domains	[T] Signal transduction mechanisms
PMI32_01557	6.331477	Putative glycerate kinase	[G] Carbohydrate transport and metabolism
PMI32_02719	6.3167925	benzoate 1,2-dioxygenase, large subunit	[P] Inorganic ion transport and metabolism, [R] General function prediction only
PMI32_02847	6.1692337	Protein of unknown function (DUF1282).	
PMI32_03397	6.1408488	hypothetical protein	
PMI32_02082	6.0709829	glycine dehydrogenase (decarboxylating)	[E] Amino acid transport and metabolism
PMI32_04457	5.7182195	Aspartate/tyrosine/aromatic aminotransferase	[E] Amino acid transport and metabolism
PMI32_04261	5.5415528	amine acid ABC transporter, permease protein, 3-TM region, His/Glu/Gln/Arg/opine family	[E] Amino acid transport and metabolism
PMI32_00496	5.5332089	Uncharacterized conserved protein	[S] Function unknown
PMI32_02052	5.4216783	succinate CoA transferases	[C] Energy production and conversion
PMI32_00478	5.3757579	NAD-dependent aldehyde dehydrogenases	[C] Energy production and conversion
PMI32_02078	5.3376671	Predicted membrane protein/domain	[S] Function unknown

PMI32_05549	5.2998715	hypothetical protein	
PMI32_00481	5.2578633	Sulphur oxidation protein SoxZ.	
PMI32_04612	5.0988953	Pirin-related protein	[R] General function prediction only
PMI32_00493	5.0904068	PQQ-dependent catabolism-associated CXXCW motif protein	[P] Inorganic ion transport and metabolism
PMI32_02504	5.0473225	hypothetical protein	
PMI32_00087	4.9907131	methylmalonic acid semialdehyde dehydrogenase	[C] Energy production and conversion
PMI32_04259	4.8220892	ABC-type amino acid transport/signal transduction systems, periplasmic component/domain	[T] Signal transduction mechanisms, [E] Amino acid transport and metabolism
PMI32_05961	4.7398074	Ethanolamine ammonia-lyase, large subunit	[E] Amino acid transport and metabolism
PMI32_04287	4.7298173	diguanylate cyclase (GGDEF) domain	
PMI32_04668	4.6972576	N-acyl-D-glucosamine 2-epimerase	[G] Carbohydrate transport and metabolism
PMI32_04672	4.6790735	ABC-type sugar transport systems, ATPase components	[G] Carbohydrate transport and metabolism
PMI32_05031	4.5530965	hypothetical protein	
PMI32_01769	4.5254453	ABC-type spermidine/putrescine transport system, permease component II	[E] Amino acid transport and metabolism
PMI32_05363	4.4974307	Lysine efflux permease	[R] General function prediction only
PMI32_03396	4.4539494	Arabinose efflux permease	[G] Carbohydrate transport and metabolism
PMI32_01770	4.4309449	Spermidine/putrescine-binding periplasmic protein	[E] Amino acid transport and metabolism
PMI32_05289	4.4194792	hypothetical protein	[R] General function prediction only
PMI32_05362	4.4046253	Uncharacterized protein conserved in bacteria	[S] Function unknown
PMI32_05962	4.3967158	Ethanolamine ammonia-lyase, small subunit	[E] Amino acid transport and metabolism
PMI32_03758	4.393239	RND family efflux transporter, MFP subunit	[M] Cell wall/membrane/envelope biogenesis
PMI32_05604	4.3867715	DNA polymerase III, alpha subunit (gram-positive type)	
PMI32_00654	4.3633412	uroporphyrinogen decarboxylase	[H] Coenzyme transport and metabolism
PMI32_02083	4.1782851	glycine cleavage system H protein	[E] Amino acid transport and metabolism
PMI32_04621	4.1725752	L-alanine-DL-glutamate epimerase and related enzymes of enolase superfamily	[R] General function prediction only, [M] Cell wall/membrane/envelope biogenesis
PMI32_01391	4.1354409	Enoyl-CoA hydratase/carnithine racemase	
PMI32_01497	4.1284452	Carbohydrate-selective porin	[M] Cell wall/membrane/envelope biogenesis
PMI32_01129	4.1032529	Uncharacterized conserved protein	[S] Function unknown
PMI32_02209	4.0948659	Universal stress protein UspA and related nucleotide-binding proteins	[T] Signal transduction mechanisms
PMI32_05897	4.074134	Choline dehydrogenase and related flavoproteins	[E] Amino acid transport and metabolism
PMI32_03335	4.0051234	thiopurine S-methyltransferase, Se/Te detoxification family	
PMI32_03331	3.9380399	Glutathione peroxidase	[O] Posttranslational modification, protein turnover, chaperones
PMI32_05551	3.9320282	acetate--CoA ligase	[I] Lipid transport and metabolism
PMI32_02053	3.8966849	NAD/NADP transhydrogenase beta subunit	[C] Energy production and conversion
PMI32_00999	3.8864735	ABC transporter periplasmic binding protein, urea carboxylase region	[P] Inorganic ion transport and metabolism
PMI32_01143	3.8828065	Glutamine synthetase	[E] Amino acid transport and metabolism
PMI32_00244	3.8794171	glycine betaine/L-proline transport ATP binding subunit	[E] Amino acid transport and metabolism
PMI32_01578	3.8667974	heme ABC exporter, ATP-binding protein CcmA	[O] Posttranslational modification, protein turnover, chaperones
PMI32_05315	3.8411261	Agmatinase	[E] Amino acid transport and metabolism
PMI32_04288	3.8369286	Cytochrome c peroxidase	[P] Inorganic ion transport and metabolism
PMI32_04671	3.6778441	ABC-type sugar transport system, permease component	[G] Carbohydrate transport and metabolism

PMI32_00797	3.6734723	hypothetical protein	
PMI32_02607	3.6658109	hypothetical protein	
PMI32_00241	3.6598064	ABC-type proline/glycine betaine transport systems, permease component	[E] Amino acid transport and metabolism
PMI32_05941	3.6594652	cobalamin biosynthesis protein CobW	[R] General function prediction only
PMI32_03104	3.6152644	Uncharacterized protein conserved in bacteria	[S] Function unknown
PMI32_04669	3.608215	ABC-type sugar transport system, periplasmic component	[G] Carbohydrate transport and metabolism
PMI32_01941	3.590752	16S rRNA (guanine(527)-N(7))-methyltransferase GidB	[M] Cell wall/membrane/envelope biogenesis
PMI32_01036	3.5658376	Arabinose efflux permease	[G] Carbohydrate transport and metabolism
PMI32_05275	3.5625604	Methylase involved in ubiquinone/menaquinone biosynthesis	
PMI32_05560	3.5528064	Uncharacterized protein conserved in bacteria	[S] Function unknown
PMI32_02033	3.5435686	Predicted aminopeptidase	[R] General function prediction only
PMI32_03960	3.5158466	Sterol desaturase	
PMI32_00486	3.4911332	Response regulator containing a CheY-like receiver domain and an HTH DNA-binding domain	[K] Transcription, [T] Signal transduction mechanisms
PMI32_01764	3.4892455	NAD-dependent aldehyde dehydrogenases	[C] Energy production and conversion
PMI32_00782	3.4006485	nucleotide sugar dehydrogenase	[M] Cell wall/membrane/envelope biogenesis
PMI32_01474	3.3717198	Ketosteroid isomerase-related protein	[R] General function prediction only
PMI32_02054	3.3636608	NAD/NADP transhydrogenase alpha subunit	
PMI32_01942	3.3529096	glucose-inhibited division protein A	[D] Cell cycle control, cell division, chromosome partitioning
PMI32_00479	3.3364765	PQQ-dependent dehydrogenase, methanol/ethanol family	[G] Carbohydrate transport and metabolism
PMI32_05361	3.3352848	transcriptional regulator, ArgP family	[K] Transcription
PMI32_02611	3.3337643	hypothetical protein	
PMI32_00182	3.2923992	transcription termination factor Rho	[K] Transcription
PMI32_04754	3.2633028	Riboflavin synthase beta-chain	[H] Coenzyme transport and metabolism
PMI32_04053	3.2261034	DNA polymerase III, epsilon subunit and related 3'-5' exonucleases	[L] Replication, recombination and repair
PMI32_05368	3.1899392	ABC-type branched-chain amino acid transport system, permease component	[E] Amino acid transport and metabolism
PMI32_02084	3.1848897	Transcriptional regulator of aromatic amino acids metabolism	[K] Transcription, [E] Amino acid transport and metabolism
PMI32_01191	3.1734064	dihydroxy-acid dehydratase	[E] Amino acid transport and metabolism, [G] Carbohydrate transport and metabolism
PMI32_02081	3.1708487	L-serine dehydratase, iron-sulfur-dependent, single chain form	[E] Amino acid transport and metabolism
PMI32_04540	3.167805	isocitrate lyase	[C] Energy production and conversion
PMI32_01967	3.150432	Coproporphyrinogen III oxidase	[H] Coenzyme transport and metabolism
PMI32_04800	3.1155396	Response regulator containing CheY-like receiver, AAA-type ATPase, and DNA-binding domains	[T] Signal transduction mechanisms
PMI32_01275	3.1055362	hypothetical protein	
PMI32_03419	3.0987224	Mg chelatase-related protein	[O] Posttranslational modification, protein turnover, chaperones
PMI32_02696	3.0687539	Uncharacterized protein conserved in bacteria	[S] Function unknown
PMI32_04393	3.0497671	Predicted Na+-dependent transporter	[R] General function prediction only
PMI32_00146	3.0495658	8-amino-7-oxononanoate synthase	[H] Coenzyme transport and metabolism
PMI32_05707	3.0404022	Delta-aminolevulinic acid dehydratase	[H] Coenzyme transport and metabolism
PMI32_00017	3.0402181	transketolase, bacterial and yeast	[G] Carbohydrate transport and metabolism
PMI32_04622	3.0334962	D-galactonate transporter	[G] Carbohydrate transport and metabolism
PMI32_05559	3.0329519	Tripartite tricarboxylate transporter TctB family.	

PMI32_00153	3.0303576	Type II secretory pathway, ATPase PulE/Tfp pilus assembly pathway, ATPase PilB	[N] Cell motility, [U] Intracellular trafficking, secretion, and vesicular transport
PMI32_04263	3.0210831	Signal transduction histidine kinase regulating C4-dicarboxylate transport system	[T] Signal transduction mechanisms
PMI32_04249	3.0176156	Anaerobic dehydrogenases, typically selenocysteine-containing	[C] Energy production and conversion
PMI32_05896	3.0113591	Metal-dependent hydrolase	[R] General function prediction only
PMI32_02505	2.9923224	Aerobic-type carbon monoxide dehydrogenase, large subunit CoxL/CutL homologs	[C] Energy production and conversion
PMI32_03944	2.9852448	Protein of unknown function (DUF3509).	
PMI32_01010	2.9803195	hypothetical protein	
PMI32_05550	2.9785554	Protein of unknown function (DUF2790).	
PMI32_05367	2.9741307	Branched-chain amino acid ABC-type transport system, permease components	[E] Amino acid transport and metabolism
PMI32_01445	2.9725384	hypothetical protein	
PMI32_01484	2.9703202	Leucyl aminopeptidase	[E] Amino acid transport and metabolism
PMI32_00777	2.9699769	parallel beta-helix repeat (two copies)	
PMI32_03803	2.9574882	Protein of unknown function (DUF2946).	
PMI32_01151	2.9457561	ABC-type spermidine/putrescine transport system, permease component I	[E] Amino acid transport and metabolism
PMI32_01483	2.9446296	DNA polymerase III, chi subunit	[L] Replication, recombination and repair
PMI32_00745	2.939895	serine transporter	[E] Amino acid transport and metabolism
PMI32_01392	2.919557	Acyl-CoA dehydrogenases	[I] Lipid transport and metabolism
PMI32_03124	2.9154814	Predicted membrane-associated, metal-dependent hydrolase	[R] General function prediction only
PMI32_02635	2.9094161	Cytochrome bd-type quinol oxidase, subunit 1	[C] Energy production and conversion
PMI32_03178	2.8904873	putative methyltransferase, YaeB/AF_0241 family	[S] Function unknown
PMI32_00474	2.8884992	coenzyme PQQ biosynthesis enzyme PqqE	[R] General function prediction only
PMI32_01972	2.8782833	putative choline sulfate-utilization transcription factor	[K] Transcription
PMI32_00086	2.8745187	NAD binding domain of 6-phosphogluconate dehydrogenase.	
PMI32_00271	2.8489227	translation initiation factor IF-2	[J] Translation, ribosomal structure and biogenesis
PMI32_01987	2.8358662	Small integral membrane protein	[S] Function unknown
PMI32_03002	2.8177779	single-stranded-DNA-specific exonuclease RecJ	[L] Replication, recombination and repair
PMI32_03415	2.8171268	Uncharacterized protein conserved in bacteria	[S] Function unknown
PMI32_00286	2.811312	Predicted periplasmic protein	
PMI32_01235	2.7888883	TonB family C-terminal domain	[M] Cell wall/membrane/envelope biogenesis
PMI32_01928	2.7884317	Transcriptional regulators of sugar metabolism	[K] Transcription, [G] Carbohydrate transport and metabolism
PMI32_01817	2.7838694	Cytochrome c, mono- and diheme variants	[C] Energy production and conversion
PMI32_04252	2.7763731	ABC-type spermidine/putrescine transport systems, ATPase components	[E] Amino acid transport and metabolism
PMI32_04798	2.7724857	hypothetical protein	
PMI32_04860	2.7574791	choline ABC transporter, periplasmic binding protein	[E] Amino acid transport and metabolism
PMI32_00495	2.7302951	PAS domain S-box	[T] Signal transduction mechanisms
PMI32_03628	2.7229507	Ribosomal protein L23	[J] Translation, ribosomal structure and biogenesis
PMI32_04726	2.715886	PAS domain S-box	[N] Cell motility, [T] Signal transduction mechanisms
PMI32_03216	2.7154588	hypothetical protein	
PMI32_03184	2.711452	K+ transporter	[P] Inorganic ion transport and metabolism
PMI32_03959	2.7037783	Gluconolactonase	
PMI32_01106	2.6990652	Stringent starvation protein B	[R] General function prediction only

PMI32_00780	2.6921642	Multidrug resistance efflux pump	
PMI32_01133	2.6921324	outer membrane porin, OprD family.	
PMI32_00375	2.6808377	NAD binding domain of 6-phosphogluconate dehydrogenase.	
PMI32_02485	2.6771977	hypothetical protein	
PMI32_02098	2.675839	RNA polymerase sigma factor, sigma-70 family	[K] Transcription
PMI32_01031	2.6668263	gamma-glutamyltranspeptidase	[E] Amino acid transport and metabolism
PMI32_05959	2.6587212	NAD-dependent aldehyde dehydrogenases	[C] Energy production and conversion
PMI32_05329	2.655899	Small-conductance mechanosensitive channel	[M] Cell wall/membrane/envelope biogenesis
PMI32_04673	2.6398527	Carbohydrate-selective porin	[M] Cell wall/membrane/envelope biogenesis
PMI32_00452	2.6396255	serine transporter	[E] Amino acid transport and metabolism
PMI32_03459	2.6352242	Phosphomannomutase	[G] Carbohydrate transport and metabolism
PMI32_00775	2.6284833	Alginate lyase.	
PMI32_05966	2.6272224	Inorganic pyrophosphatase	[C] Energy production and conversion
PMI32_05553	2.6197332	amine acid ABC transporter, permease protein, 3-TM region, His/Glu/Gln/Arg/opine family	[E] Amino acid transport and metabolism
PMI32_00872	2.6124808	2-isopropylmalate synthase, yeast type	[E] Amino acid transport and metabolism
PMI32_04285	2.6100212	Response regulator containing a CheY-like receiver domain and an HD-GYP domain	[T] Signal transduction mechanisms, [K] Transcription
PMI32_01671	2.5977995	Predicted amidohydrolase	[R] General function prediction only
PMI32_01927	2.5891735	glucosamine--fructose-6-phosphate aminotransferase (isomerizing)	[M] Cell wall/membrane/envelope biogenesis
PMI32_05598	2.5786941	Putative homoserine kinase type II (protein kinase fold)	[R] General function prediction only
PMI32_01475	2.5762948	Predicted endonuclease containing a URI domain	[L] Replication, recombination and repair
PMI32_00605	2.5726787	delta-1-pyrroline-5-carboxylate dehydrogenase (PutA C-terminal domain)	[C] Energy production and conversion
PMI32_04243	2.5721976	dihydroorotase, homodimeric type	[F] Nucleotide transport and metabolism
PMI32_04561	2.568869	ABC-type sugar transport systems, ATPase components	[G] Carbohydrate transport and metabolism
PMI32_01463	2.5615671	Transcriptional regulators	[K] Transcription
PMI32_04654	2.5611341	ABC-type multidrug transport system, ATPase component	[V] Defense mechanisms
PMI32_05921	2.5590333	hypothetical protein	
PMI32_04278	2.5581941	Predicted dithiol-disulfide isomerase involved in polyketide biosynthesis	[Q] Secondary metabolites biosynthesis, transport and catabolism
PMI32_04884	2.5541686	transketolase, bacterial and yeast	[G] Carbohydrate transport and metabolism
PMI32_00534	2.5486471	amine acid ABC transporter, permease protein, 3-TM region, His/Glu/Gln/Arg/opine family	[E] Amino acid transport and metabolism
PMI32_05558	2.5459572	Uncharacterized protein conserved in bacteria	[S] Function unknown
PMI32_00189	2.5391661	Exopolyphosphatase	[P] Inorganic ion transport and metabolism, [F] Nucleotide transport and metabolism
PMI32_05833	2.5301234	Transcriptional regulator	[K] Transcription
PMI32_03756	2.5249691	Predicted membrane protein	[S] Function unknown
PMI32_00989	2.5243282	hypothetical protein	
PMI32_02700	2.5171589	Isocitrate dehydrogenase kinase/phosphatase	[T] Signal transduction mechanisms
PMI32_04241	2.495274	argininosuccinate synthase	[E] Amino acid transport and metabolism
PMI32_04760	2.4912508	arginine/ornithine succinyltransferase, alpha subunit	[E] Amino acid transport and metabolism
PMI32_03868	2.4906594	Cytosine deaminase and related metal-dependent hydrolases	[R] General function prediction only, [F] Nucleotide transport and metabolism
PMI32_03759	2.4886519	Response regulators consisting of a CheY-like receiver domain and a winged-helix DNA-binding domain	[T] Signal transduction mechanisms, [K] Transcription
PMI32_05018	2.4852801	cob(II)yrinic acid a,c-diamide reductase	[C] Energy production and conversion

PMI32_05009	2.474738	DnaA regulatory inactivator Hda	
PMI32_03265	2.4743669	RND family efflux transporter, MFP subunit	[M] Cell wall/membrane/envelope biogenesis
PMI32_02249	2.4714102	hypothetical protein	
PMI32_04110	2.4673294	Predicted soluble lytic transglycosylase fused to an ABC-type amino acid-binding protein	[M] Cell wall/membrane/envelope biogenesis
PMI32_05680	2.4672545	thiamine-phosphate pyrophosphorylase	[H] Coenzyme transport and metabolism
PMI32_02042	2.4665034	Transcriptional regulator	[K] Transcription
PMI32_03033	2.4505841	Transcriptional regulator	[K] Transcription
PMI32_05898	2.438901	Transcriptional regulator	[K] Transcription
PMI32_03975	2.4371888	ribonuclease, Rne/Rng family	[J] Translation, ribosomal structure and biogenesis
PMI32_05007	2.4321825	Uncharacterized protein conserved in bacteria	[S] Function unknown
PMI32_04407	2.4273172	choline/carnitine/betaine transport	[M] Cell wall/membrane/envelope biogenesis
PMI32_04811	2.4268478	Uncharacterized protein involved in outer membrane biogenesis	
PMI32_04904	2.4259558	Monoamine oxidase	[E] Amino acid transport and metabolism
PMI32_00577	2.4241269	hypothetical protein	
PMI32_05594	2.4224238	Uncharacterized conserved protein	[S] Function unknown
PMI32_00088	2.4162566	Transcriptional regulator	[K] Transcription
PMI32_00669	2.4097078	primosomal protein N'	[L] Replication, recombination and repair
PMI32_04653	2.3934071	ABC-type polysaccharide/polyol phosphate export systems, permease component	[M] Cell wall/membrane/envelope biogenesis, [G] Carbohydrate transport and metabolism
PMI32_01705	2.3917978	spermidine/putrescine ABC transporter ATP-binding subunit	[E] Amino acid transport and metabolism
PMI32_03654	2.3805343	excinuclease ABC, A subunit	[L] Replication, recombination and repair
PMI32_00776	2.3800871	hypothetical protein	
PMI32_00166	2.376612	Uncharacterized protein conserved in bacteria	[S] Function unknown
PMI32_05783	2.3692104	nicotinate phosphoribosyltransferase	[H] Coenzyme transport and metabolism
PMI32_04036	2.3668329	hypothetical protein	
PMI32_04861	2.3657755	choline ABC transporter, permease protein	[E] Amino acid transport and metabolism
PMI32_05116	2.3654165	acetoacetyl-CoA synthase	[I] Lipid transport and metabolism
PMI32_00331	2.361112	flagellar biosynthetic protein FliR	[U] Intracellular trafficking, secretion, and vesicular transport, [N] Cell motility
PMI32_00389	2.3579401	adenylate kinases	[F] Nucleotide transport and metabolism
PMI32_03996	2.34885	Molybdenum cofactor biosynthesis enzyme	[H] Coenzyme transport and metabolism
PMI32_04054	2.3461336	Uncharacterized conserved protein	[S] Function unknown
PMI32_04876	2.3440209	Predicted metal-dependent hydrolase	[R] General function prediction only
PMI32_05950	2.339851	Gamma-aminobutyrate permease and related permeases	[E] Amino acid transport and metabolism
PMI32_00181	2.3380133	UbiD family decarboxylases	[H] Coenzyme transport and metabolism
PMI32_00472	2.3351111	PAS domain S-box	[T] Signal transduction mechanisms
PMI32_01561	2.3343041	sulfate/thiosulfate-binding protein	[P] Inorganic ion transport and metabolism
PMI32_00498	2.3156361	Signal transduction histidine kinase, nitrogen specific	[T] Signal transduction mechanisms
PMI32_01999	2.3074502	DNA polymerase I	[L] Replication, recombination and repair
PMI32_05906	2.3035464	DNA recombination-dependent growth factor C	[L] Replication, recombination and repair
PMI32_02710	2.3017212	Uncharacterized protein conserved in bacteria	[S] Function unknown
PMI32_03186	2.2986069	Uncharacterized conserved protein	[S] Function unknown
PMI32_05631	2.2877331	Predicted glutamine amidotransferase	[R] General function prediction only
PMI32_02604	2.2836741	FKBP-type peptidyl-prolyl cis-trans isomerases 1	[O] Posttranslational modification, protein turnover, chaperones

PMI32_01255	2.2810653	glycogen debranching enzyme GlgX	[G] Carbohydrate transport and metabolism
PMI32_05369	2.2773633	ABC-type branched-chain amino acid transport systems, ATPase component	[E] Amino acid transport and metabolism
PMI32_03345	2.2762783	C-terminal peptidase (prc)	[M] Cell wall/membrane/envelope biogenesis
PMI32_03316	2.2723755	transporter, monovalent cation:proton antiporter-2 (CPA2) family	[P] Inorganic ion transport and metabolism
PMI32_05449	2.2715477	Na+/H+ antiporter NhaA	[P] Inorganic ion transport and metabolism
PMI32_03028	2.2623652	ABC-type spermidine/putrescine transport system, permease component II	[E] Amino acid transport and metabolism
PMI32_05565	2.2514241	Uncharacterized conserved protein	[S] Function unknown
PMI32_02187	2.2503533	glycogen/starch/alpha-glucan phosphorylases	[G] Carbohydrate transport and metabolism
PMI32_05646	2.2426879	Putative effector of murein hydrolase LrgA	
PMI32_01839	2.2400733	phosphoserine phosphatase/homoserine phosphotransferase bifunctional protein	[E] Amino acid transport and metabolism
PMI32_00322	2.235141	Serine phosphatase RsbU, regulator of sigma subunit	[K] Transcription, [T] Signal transduction mechanisms
PMI32_01071	2.2309014	malate:quinone-oxidoreductase	[R] General function prediction only
PMI32_00604	2.2275849	sodium/proline symporter	[R] General function prediction only, [E] Amino acid transport and metabolism
PMI32_04042	2.2242999	hydro-lyases, Fe-S type, tartrate/fumarate subfamily, alpha region/hydro-lyases, Fe-S type, tartrate/fumarate subfamily, beta region	[C] Energy production and conversion
PMI32_00272	2.223499	transcription termination factor NusA/transcription termination factor NusA, C-terminal duplication	[K] Transcription
PMI32_01476	2.2172787	Glutathione S-transferase	[O] Posttranslational modification, protein turnover, chaperones
PMI32_04439	2.2111453	Glycerophosphoryl diester phosphodiesterase	[C] Energy production and conversion
PMI32_00501	2.2034311	Predicted rRNA methylase (SpoU class)	[J] Translation, ribosomal structure and biogenesis
PMI32_02055	2.1962776	NAD/NADP transhydrogenase alpha subunit	[C] Energy production and conversion
PMI32_03547	2.1895059	Transcriptional regulator	[K] Transcription
PMI32_00234	2.1846953	ABC-type dipeptide/oligopeptide/nickel transport systems, permease components	[P] Inorganic ion transport and metabolism, [E] Amino acid transport and metabolism
PMI32_04300	2.1832485	Transcriptional accessory protein	[K] Transcription
PMI32_02124	2.1809037	hypothetical protein	
PMI32_02491	2.1802248	Ribonuclease HI	[L] Replication, recombination and repair
PMI32_05571	2.1792708	Putative Zn-dependent protease, contains TPR repeats	[R] General function prediction only
PMI32_04028	2.17921	Exonuclease I	[L] Replication, recombination and repair
PMI32_01978	2.177955	Na/Pi-cotransporter	[P] Inorganic ion transport and metabolism
PMI32_01639	2.1688608	phosphate acetyltransferase	[C] Energy production and conversion
PMI32_01698	2.1688551	Organic solvent tolerance protein OstA	[M] Cell wall/membrane/envelope biogenesis
PMI32_03027	2.1682324	NAD-dependent aldehyde dehydrogenases	[C] Energy production and conversion
PMI32_00879	2.1674941	GMP synthase (glutamine-hydrolyzing), C-terminal domain or B subunit/GMP synthase (glutamine-hydrolyzing), N-terminal domain or A subunit	[F] Nucleotide transport and metabolism
PMI32_05347	2.1642316	Spermidine/putrescine-binding periplasmic protein	[E] Amino acid transport and metabolism
PMI32_02681	2.1565103	Septum formation initiator	[D] Cell cycle control, cell division, chromosome partitioning
PMI32_01012	2.1558983	hypothetical protein	
PMI32_01558	2.1376623	pyruvate kinase	[G] Carbohydrate transport and metabolism
PMI32_04901	2.134595	Superfamily II DNA and RNA helicases	[L] Replication, recombination and repair, [J] Translation, ribosomal structure and biogenesis, [K] Transcription
PMI32_05118	2.1345242	H+/gluconate symporter and related permeases	[G] Carbohydrate transport and metabolism, [E] Amino acid transport and metabolism
PMI32_04497	2.1340022	citrate synthase I (hexameric type)	[C] Energy production and conversion

PMI32_04041	2.1259717	diguanylate cyclase (GGDEF) domain	[T] Signal transduction mechanisms
PMI32_05873	2.1257263	Outer membrane protein	[U] Intracellular trafficking, secretion, and vesicular transport, [M] Cell wall/membrane/envelope biogenesis
PMI32_01645	2.1238139	thioredoxin-disulfide reductase	[O] Posttranslational modification, protein turnover, chaperones
PMI32_02615	2.1235434	ATP-binding cassette protein, ChvD family	[R] General function prediction only
PMI32_04879	2.12345	fructose-bisphosphate aldolase, class II, Calvin cycle subtype	[G] Carbohydrate transport and metabolism
PMI32_04572	2.1222959	Outer membrane protein	[M] Cell wall/membrane/envelope biogenesis
PMI32_05300	2.122024	Arabinose efflux permease	[G] Carbohydrate transport and metabolism
PMI32_01849	2.1212171	xanthine dehydrogenase, small subunit	[F] Nucleotide transport and metabolism
PMI32_02283	2.1202851	L-asparaginases, type II	[J] Translation, ribosomal structure and biogenesis, [E] Amino acid transport and metabolism
PMI32_05632	2.1175036	Protein of unknown function (DUF2937).	
PMI32_02438	2.1090436	Phosphoglycerate dehydrogenase and related dehydrogenases	[H] Coenzyme transport and metabolism, [E] Amino acid transport and metabolism
PMI32_05508	2.1054683	Protein related to penicillin acylase	[R] General function prediction only
PMI32_05726	2.1025778	3-oxoacyl-[acyl-carrier-protein] synthase III	[I] Lipid transport and metabolism
PMI32_00555	2.1023947	outer membrane porin, OprD family.	
PMI32_05624	2.1004461	Glycine/serine hydroxymethyltransferase	[E] Amino acid transport and metabolism
PMI32_03850	2.0994703	acetyl-CoA acetyltransferases	[I] Lipid transport and metabolism
PMI32_01166	2.0991034	Uncharacterized protein conserved in bacteria	[S] Function unknown
PMI32_05703	2.0910552	hypothetical protein	
PMI32_04688	2.085764	Acyl-CoA synthetases (AMP-forming)/AMP-acid ligases II	[Q] Secondary metabolites biosynthesis, transport and catabolism, [I] Lipid transport and metabolism
PMI32_00147	2.082149	biotin synthase	[H] Coenzyme transport and metabolism
PMI32_04262	2.0771568	ABC-type polar amino acid transport system, ATPase component	[E] Amino acid transport and metabolism
PMI32_04433	2.0749362	Arabinose efflux permease	
PMI32_03722	2.0740915	hypothetical protein	
PMI32_01980	2.0705456	Protein of unknown function (DUF2914).	
PMI32_00953	2.0677716	Beta-propeller domains of methanol dehydrogenase type	[R] General function prediction only
PMI32_00574	2.0646323	Transcriptional regulator	[K] Transcription
PMI32_00947	2.0577465	Beta-lactamase class C and other penicillin binding proteins	[V] Defense mechanisms
PMI32_05050	2.0537167	Predicted permeases	[R] General function prediction only
PMI32_04905	2.0534285	adenosylmethionine-8-amino-7-oxononanoate transaminase	[H] Coenzyme transport and metabolism
PMI32_01480	2.0523872	Predicted SAM-dependent methyltransferase	[R] General function prediction only
PMI32_05288	2.052108	hypothetical protein	
PMI32_02196	2.0488116	Response regulators consisting of a CheY-like receiver domain and a winged-helix DNA-binding domain	[T] Signal transduction mechanisms, [K] Transcription
PMI32_00694	2.0478697	ABC-type amino acid transport/signal transduction systems, periplasmic component/domain	[E] Amino acid transport and metabolism, [T] Signal transduction mechanisms
PMI32_02219	2.0473611	Predicted membrane protein	
PMI32_01418	2.0463167	AraC-type DNA-binding domain-containing proteins	[K] Transcription
PMI32_01273	2.0432383	Transcriptional regulator	[K] Transcription
PMI32_05893	2.0411039	trehalose synthase	[G] Carbohydrate transport and metabolism
PMI32_02341	2.0350222	drug resistance transporter, EmrB/QacA subfamily	
PMI32_01257	2.0345015	malto-oligosyltrehalose synthase	[G] Carbohydrate transport and metabolism

PMI32_00843	2.0295198	tRNA-guanine transglycosylase, queuosine-34-forming	[J] Translation, ribosomal structure and biogenesis
PMI32_01365	2.0275853	Site-specific recombinase XerD	[L] Replication, recombination and repair
PMI32_01236	2.0249964	glutathione synthetase, prokaryotic	[J] Translation, ribosomal structure and biogenesis, [H] Coenzyme transport and metabolism
PMI32_01885	2.0249823	Transcriptional regulators	[K] Transcription
PMI32_00792	2.0249119	cytochrome o ubiquinol oxidase, subunit I	[C] Energy production and conversion
PMI32_03780	2.0202652	Predicted permease	[R] General function prediction only
PMI32_01085	2.0199135	Lactate dehydrogenase and related dehydrogenases	[R] General function prediction only, [C] Energy production and conversion, [H] Coenzyme transport and metabolism
PMI32_05785	2.0186677	NAD-dependent aldehyde dehydrogenases	[C] Energy production and conversion
PMI32_02863	2.014433	flagellar basal-body rod protein FlgB	[N] Cell motility
PMI32_01940	2.0128564	ATPases involved in chromosome partitioning	[D] Cell cycle control, cell division, chromosome partitioning
PMI32_04281	2.0123241	Transcriptional regulator	[K] Transcription
PMI32_05592	2.0115664	Phosphoglycerate dehydrogenase and related dehydrogenases	[E] Amino acid transport and metabolism, [H] Coenzyme transport and metabolism
PMI32_04872	2.0108501	hypothetical membrane protein, TIGR01666	[S] Function unknown
PMI32_01193	2.0098518	Predicted SAM-dependent methyltransferases	[R] General function prediction only
PMI32_01599	2.0093921	cell shape determining protein, MreB/Mrl family	[D] Cell cycle control, cell division, chromosome partitioning
PMI32_05016	2.0072873	cob(I)alamin adenosyltransferase	[H] Coenzyme transport and metabolism
PMI32_05370	2.0050871	ABC-type branched-chain amino acid transport systems, ATPase component	[E] Amino acid transport and metabolism
PMI32_03938	2.0020503	Lysophospholipase	[I] Lipid transport and metabolism
PMI32_05469	1.99463	Uncharacterized protein conserved in bacteria	[S] Function unknown
PMI32_00184	1.9928602	Transcriptional regulators	[K] Transcription
PMI32_04723	1.9920907	Glutamine synthetase	[E] Amino acid transport and metabolism
PMI32_03559	1.9909545	Uncharacterized protein conserved in bacteria	[S] Function unknown
PMI32_01020	1.9796891	Short chain fatty acids transporter	[I] Lipid transport and metabolism
PMI32_02093	1.9795224	Methyl-accepting chemotaxis protein	[T] Signal transduction mechanisms, [N] Cell motility
PMI32_04903	1.9791292	Cytochrome B561	[C] Energy production and conversion
PMI32_05681	1.9784464	Hydroxymethylpyrimidine/phosphomethylpyrimidine kinase	[H] Coenzyme transport and metabolism
PMI32_01697	1.9755249	Parvulin-like peptidyl-prolyl isomerase	
PMI32_02185	1.9743723	GTP-binding protein TypA/BipA	[T] Signal transduction mechanisms
PMI32_02781	1.9694044	aspartyl-tRNA synthetase, bacterial type	[J] Translation, ribosomal structure and biogenesis
PMI32_01550	1.9680431	Surface lipoprotein	[M] Cell wall/membrane/envelope biogenesis
PMI32_03221	1.9662951	ATPase involved in DNA repair	[L] Replication, recombination and repair
PMI32_00869	1.96457	Aspartate/tyrosine/aromatic aminotransferase	[E] Amino acid transport and metabolism
PMI32_01725	1.962112	TIGR00701 family protein	[S] Function unknown
PMI32_05667	1.9620476	DNA polymerase III, delta subunit	[L] Replication, recombination and repair
PMI32_03697	1.9613699	glyceraldehyde-3-phosphate dehydrogenase, type I	[G] Carbohydrate transport and metabolism
PMI32_03801	1.960471	Uncharacterized iron-regulated membrane protein	[S] Function unknown
PMI32_05933	1.9580939	Fructose-2,6-bisphosphatase	[G] Carbohydrate transport and metabolism
PMI32_04780	1.9548298	acetolactate synthase, large subunit, biosynthetic type	[E] Amino acid transport and metabolism, [H] Coenzyme transport and metabolism
PMI32_03617	1.9506112	ribosomal protein L7/L12	[J] Translation, ribosomal structure and biogenesis
PMI32_00821	1.9445077	hypothetical protein	

PMI32_03190	1.9430841	hypothetical protein	
PMI32_02688	1.9382529	5'/3'-nucleotidase SurE	[R] General function prediction only
PMI32_04560	1.9344309	ABC-type sugar transport systems, ATPase components	[G] Carbohydrate transport and metabolism
PMI32_05423	1.93078	hydrolase, peptidase M42 family	[G] Carbohydrate transport and metabolism
PMI32_01911	1.9285622	Phosphatidylserine/phosphatidylglycerophosphate/cardiolipin synthases and related enzymes	[I] Lipid transport and metabolism
PMI32_03515	1.9274762	Bacterial nucleoid DNA-binding protein	[L] Replication, recombination and repair
PMI32_01245	1.9268232	malonate decarboxylase, alpha subunit	
PMI32_02461	1.9258976	oxygen-independent coproporphyrinogen III oxidase	[H] Coenzyme transport and metabolism
PMI32_00220	1.9223468	Transcription elongation factor	[K] Transcription
PMI32_01009	1.922266	hypothetical protein	
PMI32_00264	1.9146491	hypothetical protein	
PMI32_05744	1.9130143	ribosome small subunit-dependent GTPase A	[R] General function prediction only
PMI32_01208	1.911781	Predicted Zn-dependent peptidases	[R] General function prediction only
PMI32_03319	1.9116901	Predicted membrane protein	[S] Function unknown
PMI32_02486	1.9107651	Transcriptional regulator	[K] Transcription
PMI32_02492	1.9098845	Methyltransferase domain.	
PMI32_02645	1.906395	Transcriptional regulator	[K] Transcription
PMI32_03619	1.9045783	DNA-directed RNA polymerase, beta subunit	
PMI32_03828	1.8998763	diguanylate cyclase (GGDEF) domain	[T] Signal transduction mechanisms
PMI32_05668	1.8993418	Rare lipoprotein B	[M] Cell wall/membrane/envelope biogenesis
PMI32_02922	1.8981453	protein CrcB	[D] Cell cycle control, cell division, chromosome partitioning
PMI32_02418	1.8953174	transcription-repair coupling factor (mfd)	[L] Replication, recombination and repair, [K] Transcription
PMI32_01966	1.8950016	NADPH:quinone reductase and related Zn-dependent oxidoreductases	[C] Energy production and conversion, [R] General function prediction only
PMI32_03757	1.8949833	The (Largely Gram-negative Bacterial) Hydrophobe/Amphiphile Efflux-1 (HAE1) Family	[V] Defense mechanisms
PMI32_02184	1.8947818	thiazole biosynthesis/tRNA modification protein ThiI	[H] Coenzyme transport and metabolism
PMI32_01301	1.894367	transporter, SSS family	[R] General function prediction only
PMI32_04687	1.8906292	Lysophospholipase	[I] Lipid transport and metabolism
PMI32_01482	1.8858482	hypothetical protein	
PMI32_02614	1.8857684	Glutamate dehydrogenase/leucine dehydrogenase	[E] Amino acid transport and metabolism
PMI32_03192	1.8817842	AmpG-related permease	
PMI32_01150	1.8811739	spermidine/putrescine ABC transporter ATP-binding subunit	[E] Amino acid transport and metabolism
PMI32_04443	1.8809889	Mg2+ and Co2+ transporters	[P] Inorganic ion transport and metabolism
PMI32_01638	1.8807282	1-acyl-sn-glycerol-3-phosphate acyltransferase	[I] Lipid transport and metabolism
PMI32_01803	1.8748405	Predicted esterase of the alpha-beta hydrolase superfamily	[R] General function prediction only
PMI32_05554	1.8691801	ABC-type arginine/histidine transport system, permease component	[E] Amino acid transport and metabolism
PMI32_00465	1.8686241	Transcriptional regulator	[K] Transcription
PMI32_03191	1.8677894	prolyl-tRNA synthetase, family II	[J] Translation, ribosomal structure and biogenesis
PMI32_02798	1.8658859	Protein of unknown function (DUF721).	
PMI32_03388	1.8576704	intracellular septation protein A	[D] Cell cycle control, cell division, chromosome partitioning
PMI32_04674	1.8574434	Uncharacterized enzymes related to aldose 1-epimerase	[G] Carbohydrate transport and metabolism
PMI32_04667	1.8569969	hypothetical protein	

PMI32_01103	1.8549381	Cytochrome b subunit of the bc complex	[C] Energy production and conversion
PMI32_05669	1.8545891	leucyl-tRNA synthetase, eubacterial and mitochondrial family	[J] Translation, ribosomal structure and biogenesis
PMI32_03966	1.8523596	tetraacyldisaccharide 4'-kinase	[M] Cell wall/membrane/envelope biogenesis
PMI32_01170	1.8511542	Predicted integral membrane protein	[S] Function unknown
PMI32_00844	1.8450925	preprotein translocase, YajC subunit	[U] Intracellular trafficking, secretion, and vesicular transport
PMI32_04759	1.8416105	arginine N-succinyltransferase	[E] Amino acid transport and metabolism
PMI32_00580	1.8412107	ATP-dependent DNA helicase, RecQ family	
PMI32_04562	1.8391902	Transcriptional activator of acetoin/glycerol metabolism	[K] Transcription, [Q] Secondary metabolites biosynthesis, transport and catabolism
PMI32_05109	1.8354672	dTDP-4-dehydrorhamnose reductase	[M] Cell wall/membrane/envelope biogenesis
PMI32_01110	1.8316596	Putative lipoprotein	[R] General function prediction only
PMI32_05101	1.8300969	Thioredoxin	[O] Posttranslational modification, protein turnover, chaperones
PMI32_02058	1.8274324	Predicted acyl-CoA transferases/carnitine dehydratase	[C] Energy production and conversion
PMI32_03352	1.8197705	FKBP-type peptidyl-prolyl cis-trans isomerases 1	[O] Posttranslational modification, protein turnover, chaperones
PMI32_02680	1.8178282	phosphopyruvate hydratase	[G] Carbohydrate transport and metabolism
PMI32_03176	1.812289	Transcriptional regulator	[K] Transcription
PMI32_00917	1.8116651	hypothetical protein	
PMI32_03904	1.8095141	Spermidine synthase	[E] Amino acid transport and metabolism
PMI32_05629	1.8086112	Protease II	[E] Amino acid transport and metabolism
PMI32_00249	1.808206	Sulfite reductase, alpha subunit (flavoprotein)	[P] Inorganic ion transport and metabolism
PMI32_00845	1.8062965	protein-export membrane protein, SecD/SecF family	[U] Intracellular trafficking, secretion, and vesicular transport
PMI32_04301	1.803216	uncharacterized domain 1	[Q] Secondary metabolites biosynthesis, transport and catabolism
PMI32_02132	1.8030056	thiamine biosynthesis protein ThiC	[H] Coenzyme transport and metabolism
PMI32_05618	1.8011953	formaldehyde dehydrogenase, glutathione-independent	[R] General function prediction only, [E] Amino acid transport and metabolism
PMI32_01011	1.7974104	hypothetical protein	
PMI32_01597	1.7945562	aspartyl/glutamyl-tRNA(Asn/Gln) amidotransferase, A subunit	[J] Translation, ribosomal structure and biogenesis
PMI32_04858	1.7945558	Transcriptional regulator containing an amidase domain and an AraC-type DNA-binding HTH domain	[K] Transcription
PMI32_05745	1.7941988	Oligoribonuclease (3'->5' exoribonuclease)	[A] RNA processing and modification
PMI32_02676	1.7870047	acetyl-CoA carboxylase, carboxyl transferase, alpha subunit	[I] Lipid transport and metabolism
PMI32_01102	1.7822417	ubiquinol-cytochrome c reductase, iron-sulfur subunit	[C] Energy production and conversion
PMI32_01146	1.7796502	Glutamine synthetase	[E] Amino acid transport and metabolism
PMI32_02543	1.7771521	Protein of unknown function (DUF3094).	
PMI32_05278	1.773437	Signal transduction histidine kinase	[T] Signal transduction mechanisms
PMI32_04112	1.7717165	Acyl-CoA dehydrogenases	[I] Lipid transport and metabolism
PMI32_04085	1.7713551	DNA gyrase, A subunit	[L] Replication, recombination and repair
PMI32_00695	1.7687559	Membrane glycosyltransferase	[M] Cell wall/membrane/envelope biogenesis
PMI32_01207	1.767469	Predicted Zn-dependent peptidases	[R] General function prediction only
PMI32_03197	1.7646003	hypothetical protein	
PMI32_05964	1.7640842	Uncharacterized membrane-associated protein	[S] Function unknown
PMI32_02077	1.7632839	quinolinate synthetase complex, A subunit	[H] Coenzyme transport and metabolism
PMI32_05429	1.7628765	Phosphoglycerol transferase and related proteins, alkaline phosphatase superfamily	[M] Cell wall/membrane/envelope biogenesis
PMI32_01953	1.7624481	glycyl-tRNA synthetase, tetrameric type, beta subunit	[J] Translation, ribosomal structure and biogenesis

PMI32_02410	1.7602786	lipoprotein releasing system, ATP-binding protein	[V] Defense mechanisms
PMI32_04845	1.7564014	Zn-dependent dipeptidase, microsomal dipeptidase homolog	[E] Amino acid transport and metabolism
PMI32_00231	1.7526048	ABC-type dipeptide transport system, periplasmic component	[E] Amino acid transport and metabolism
PMI32_01847	1.7511174	chromosome segregation protein SMC, common bacterial type	[D] Cell cycle control, cell division, chromosome partitioning
PMI32_00896	1.7507363	NTP pyrophosphohydrolases including oxidative damage repair enzymes	[R] General function prediction only, [L] Replication, recombination and repair
PMI32_05940	1.7486646	cobaltochelatase, CobN subunit	[H] Coenzyme transport and metabolism
PMI32_02188	1.7440766	Predicted membrane protein	[S] Function unknown
PMI32_01549	1.7399131	hypothetical protein	
PMI32_03533	1.7378495	Uncharacterized enzymes related to aldose 1-epimerase	[G] Carbohydrate transport and metabolism
PMI32_03910	1.7375606	Pseudouridylate synthases, 23S RNA-specific	[J] Translation, ribosomal structure and biogenesis
PMI32_00263	1.7336854	nicotinate-nucleotide pyrophosphorylase	[H] Coenzyme transport and metabolism
PMI32_05322	1.7314186	Uncharacterized protein conserved in bacteria	[S] Function unknown
PMI32_02617	1.7303369	Glycine/serine hydroxymethyltransferase	[E] Amino acid transport and metabolism
PMI32_01600	1.7290428	rod shape-determining protein MreC	[M] Cell wall/membrane/envelope biogenesis
PMI32_01581	1.7287825	Predicted periplasmic/secreted protein	[S] Function unknown
PMI32_02139	1.7235771	DNA topoisomerase IV, B subunit, proteobacterial	[L] Replication, recombination and repair
PMI32_02636	1.7225384	Arabinose efflux permease	[G] Carbohydrate transport and metabolism
PMI32_01481	1.7223335	valyl-tRNA synthetase	[J] Translation, ribosomal structure and biogenesis
PMI32_03653	1.7219599	Bacterioferritin	[P] Inorganic ion transport and metabolism
PMI32_03445	1.713474	Predicted Fe-S-cluster oxidoreductase	
PMI32_05686	1.7109437	Protein of unknown function (DUF2788).	
PMI32_04799	1.7102619	PAS domain S-box	[E] Amino acid transport and metabolism, [R] General function prediction only
PMI32_00505	1.7075045	2,3-bisphosphoglycerate-independent phosphoglycerate mutase	[G] Carbohydrate transport and metabolism
PMI32_01632	1.7031446	histidinol dehydrogenase	[E] Amino acid transport and metabolism
PMI32_05091	1.702954	Phosphatidylglycerophosphatase A and related proteins	[I] Lipid transport and metabolism
PMI32_01105	1.7025138	Glutathione S-transferase	[O] Posttranslational modification, protein turnover, chaperones
PMI32_04257	1.7021397	Transcriptional regulators of sugar metabolism	[G] Carbohydrate transport and metabolism, [K] Transcription
PMI32_03404	1.6964731	flagellar basal-body rod protein FlgG, Gram-negative bacteria	[N] Cell motility
PMI32_01813	1.6918049	Protein of unknown function (DUF1260).	
PMI32_00245	1.6909469	Diaminopimelate decarboxylase	[E] Amino acid transport and metabolism
PMI32_01485	1.6820645	Predicted permeases	[R] General function prediction only
PMI32_01848	1.6820034	Transcriptional regulators	[K] Transcription
PMI32_01707	1.6815607	ABC-type spermidine/putrescine transport system, permease component I	[E] Amino acid transport and metabolism
PMI32_04517	1.6794465	Predicted redox protein, regulator of disulfide bond formation	[O] Posttranslational modification, protein turnover, chaperones
PMI32_02825	1.6695693	beta-hydroxyacyl-[acyl carrier protein] dehydratase FabA	[I] Lipid transport and metabolism
PMI32_05842	1.6693242	diguanylate cyclase (GGDEF) domain	
PMI32_03837	1.6662515	arginine decarboxylase, biosynthetic	[E] Amino acid transport and metabolism
PMI32_00696	1.6635082	Periplasmic glucans biosynthesis protein	[P] Inorganic ion transport and metabolism
PMI32_01044	1.66324	Flp pilus assembly protein TadD, contains TPR repeats	[U] Intracellular trafficking, secretion, and vesicular transport
PMI32_00165	1.6606781	Xaa-Pro aminopeptidase	[E] Amino acid transport and metabolism

PMI32_03457	1.6601341	phosphopantothenoylcysteine decarboxylase/phosphopantothenate--cysteine ligase, prokaryotic	[H] Coenzyme transport and metabolism
PMI32_00586	1.6591962	phosphoenolpyruvate carboxykinase (ATP)	[C] Energy production and conversion
PMI32_00037	1.6577901	phenylalanyl-tRNA synthetase, beta subunit, non-spirochete bacterial	[J] Translation, ribosomal structure and biogenesis
PMI32_00870	1.6577095	Predicted amidohydrolase	[R] General function prediction only
PMI32_03616	1.656518	Ribosomal protein L10	[J] Translation, ribosomal structure and biogenesis
PMI32_01013	1.6547083	ribosomal-protein-alanine acetyltransferase	[R] General function prediction only
PMI32_02405	1.6506797	7-cyano-7-deazaguanine reductase	[S] Function unknown
PMI32_04079	1.646975	ribosomal protein S1	[J] Translation, ribosomal structure and biogenesis
PMI32_00506	1.6427109	Membrane-bound metallopeptidase	[D] Cell cycle control, cell division, chromosome partitioning
PMI32_04014	1.6415932	Rad3-related DNA helicases	[K] Transcription, [L] Replication, recombination and repair
PMI32_05579	1.6278028	phosphoribosylaminoimidazole-succinocarboxamide synthase	[F] Nucleotide transport and metabolism
PMI32_02832	1.6169064	cysteine synthase B	[E] Amino acid transport and metabolism
PMI32_01635	1.6119172	dinuclear metal center protein, YbgI/SA1388 family	[S] Function unknown
PMI32_04543	1.610156	NADH (or F420H2) dehydrogenase, subunit C	[C] Energy production and conversion
PMI32_04804	1.6082984	3-methyl-2-oxobutanoate hydroxymethyltransferase	[H] Coenzyme transport and metabolism
PMI32_02592	1.6080474	isoleucyl-tRNA synthetase	[J] Translation, ribosomal structure and biogenesis
PMI32_03823	1.6069328	acetyl-CoA carboxylase, biotin carboxylase subunit	[I] Lipid transport and metabolism
PMI32_03782	1.6032354	DnaJ-class molecular chaperone with C-terminal Zn finger domain	[O] Posttranslational modification, protein turnover, chaperones
PMI32_04750	1.6026461	aspartate kinase, monofunctional class	[E] Amino acid transport and metabolism
PMI32_04026	1.6021672	formyltetrahydrofolate deformylase	[F] Nucleotide transport and metabolism
PMI32_04807	1.6018818	Glucose-6-phosphate isomerase	[G] Carbohydrate transport and metabolism
PMI32_01494	1.6003595	phosphoribosylformylglycinamidine synthase, single chain form	[F] Nucleotide transport and metabolism
PMI32_00473	1.6003158	Alcohol dehydrogenase, class IV	[C] Energy production and conversion
PMI32_05644	1.5997903	Aspartyl/asparaginyl beta-hydroxylase and related dioxygenases	[O] Posttranslational modification, protein turnover, chaperones
PMI32_01641	1.598884	Glutathione peroxidase	[O] Posttranslational modification, protein turnover, chaperones
PMI32_04883	1.5979938	erythrose-4-phosphate dehydrogenase	[G] Carbohydrate transport and metabolism
PMI32_02690	1.5973564	Membrane proteins related to metalloendopeptidases	[M] Cell wall/membrane/envelope biogenesis
PMI32_04778	1.5916347	ketol-acid reductoisomerase	[E] Amino acid transport and metabolism, [H] Coenzyme transport and metabolism
PMI32_05249	1.5898046	PAS domain S-box/diguanylate cyclase (GGDEF) domain	
PMI32_04701	1.5809494	PAS domain S-box	
PMI32_04867	1.5807393	Predicted Zn-dependent proteases and their inactivated homologs	[R] General function prediction only
PMI32_00656	1.5807083	Glutamate synthase domain 2	[E] Amino acid transport and metabolism
PMI32_05290	1.567769	conserved hypothetical protein	[S] Function unknown
PMI32_04716	1.5676935	Chemotaxis signal transduction protein	[T] Signal transduction mechanisms, [N] Cell motility
PMI32_02671	1.5640084	beta-hydroxyacyl-[acyl carrier protein] dehydratase FabZ	[I] Lipid transport and metabolism
PMI32_05359	1.5638795	hypothetical protein	
PMI32_00048	1.5596997	Inosine-uridine nucleoside N-ribohydrolase	[F] Nucleotide transport and metabolism
PMI32_01876	1.5572721	phosphoenolpyruvate synthase	[G] Carbohydrate transport and metabolism
PMI32_00207	1.5544589	Regulator of sigma D	[K] Transcription

PMI32_01968	1.5511559	shikimate 5-dehydrogenase	[E] Amino acid transport and metabolism
PMI32_05577	1.5462686	Uncharacterized lipoprotein	[M] Cell wall/membrane/envelope biogenesis
PMI32_01046	1.5361931	peptide chain release factor 1	[J] Translation, ribosomal structure and biogenesis
PMI32_02428	1.5355339	DNA topoisomerase I, bacterial	[L] Replication, recombination and repair
PMI32_00502	1.5352698	protein-export chaperone SecB	[U] Intracellular trafficking, secretion, and vesicular transport
PMI32_01095	1.5173489	tryptophanyl-tRNA synthetase	[J] Translation, ribosomal structure and biogenesis
PMI32_01202	1.5071774	Transcriptional regulator	
PMI32_02130	1.4999939	type I secretion outer membrane protein, TolC family	[M] Cell wall/membrane/envelope biogenesis, [U] Intracellular trafficking, secretion, and vesicular transport
PMI32_05663	1.4939628	lipoate synthase	[H] Coenzyme transport and metabolism
PMI32_04715	1.468255	Methylase of chemotaxis methyl-accepting proteins	[N] Cell motility, [T] Signal transduction mechanisms
PMI32_04256	-1.4896978	glycerol kinase	[C] Energy production and conversion
PMI32_00532	-1.5003085	ABC-type amino acid transport/signal transduction systems, periplasmic component/domain	[E] Amino acid transport and metabolism, [T] Signal transduction mechanisms
PMI32_05774	-1.502847	replicative DNA helicase	[L] Replication, recombination and repair
PMI32_04083	-1.522235	chorismate mutase domain of proteobacterial P-protein, clade 2	[E] Amino acid transport and metabolism
PMI32_04081	-1.5268401	3-phosphoshikimate 1-carboxyvinyltransferase	[E] Amino acid transport and metabolism
PMI32_04870	-1.5295038	Superfamily II DNA and RNA helicases	[L] Replication, recombination and repair, [K] Transcription, [J] Translation, ribosomal structure and biogenesis
PMI32_00617	-1.5381329	1-acyl-sn-glycerol-3-phosphate acyltransferase	[I] Lipid transport and metabolism
PMI32_02859	-1.5384012	ribonucleoside-diphosphate reductase, alpha subunit	[F] Nucleotide transport and metabolism
PMI32_01081	-1.5421967	Zn-dependent protease with chaperone function	[O] Posttranslational modification, protein turnover, chaperones
PMI32_03035	-1.5429061	Methyl-accepting chemotaxis protein	[N] Cell motility, [T] Signal transduction mechanisms
PMI32_03338	-1.5434451	ABC-type Fe3+ transport system, periplasmic component	[P] Inorganic ion transport and metabolism
PMI32_03648	-1.5488256	30S ribosomal protein S11	[J] Translation, ribosomal structure and biogenesis
PMI32_01710	-1.5559674	ribulose-phosphate 3-epimerase	[G] Carbohydrate transport and metabolism
PMI32_03530	-1.5575495	phosphate binding protein	[P] Inorganic ion transport and metabolism
PMI32_02029	-1.559162	Zn-dependent oligopeptidases	[E] Amino acid transport and metabolism
PMI32_02313	-1.5626121	amidophosphoribosyltransferase	[F] Nucleotide transport and metabolism
PMI32_05254	-1.5659006	sulfate ABC transporter, ATP-binding protein	[P] Inorganic ion transport and metabolism
PMI32_05971	-1.5713423	Large extracellular alpha-helical protein	[R] General function prediction only
PMI32_05768	-1.5761596	ribonuclease R	[K] Transcription
PMI32_01572	-1.5795488	periplasmic protein thiol:disulfide oxidoreductases, DsbE subfamily	[O] Posttranslational modification, protein turnover, chaperones, [C] Energy production and conversion
PMI32_02070	-1.5843232	TolA protein	
PMI32_00698	-1.5853004	proline iminopeptidase, Neisseria-type subfamily	[R] General function prediction only
PMI32_02920	-1.5885136	uroporphyrin-III C-methyltransferase	[H] Coenzyme transport and metabolism
PMI32_04902	-1.5890172	Uncharacterized conserved protein	[S] Function unknown
PMI32_02207	-1.5930569	Universal stress protein UspA and related nucleotide-binding proteins	[T] Signal transduction mechanisms
PMI32_04521	-1.5940425	Predicted metal-dependent hydrolase with the TIM-barrel fold	[R] General function prediction only
PMI32_00161	-1.597773	ABC-type Fe3+ transport system, periplasmic component	[P] Inorganic ion transport and metabolism
PMI32_02458	-1.5990581	copper-(or silver)-translocating P-type ATPase/heavy metal-(Cd/Co/Hg/Pb/Zn)-	[P] Inorganic ion transport and metabolism

		translocating P-type ATPase	
PMI32_02332	-1.6024953	Predicted thioesterase	[R] General function prediction only
PMI32_04899	-1.6038843	5,10-methylenetetrahydrofolate reductase, prokaryotic form	[E] Amino acid transport and metabolism
PMI32_00877	-1.6075261	hypothetical protein	
PMI32_03981	-1.6120009	Predicted metal-binding, possibly nucleic acid-binding protein	[R] General function prediction only
PMI32_02683	-1.6125905	Transcriptional regulator	[K] Transcription
PMI32_05782	-1.6152152	NAD+ synthetase	[H] Coenzyme transport and metabolism
PMI32_03167	-1.6158154	competence/damage-inducible protein CinA C-terminal domain	[R] General function prediction only
PMI32_05506	-1.6177759	HNH endonuclease.	
PMI32_05787	-1.6181047	ABC-type branched-chain amino acid transport systems, periplasmic component	[E] Amino acid transport and metabolism
PMI32_00661	-1.6193077	Tfp pilus assembly protein PilP	[N] Cell motility, [U] Intracellular trafficking, secretion, and vesicular transport
PMI32_04822	-1.6226635	catalase/peroxidase HPI	[P] Inorganic ion transport and metabolism
PMI32_00045	-1.6283964	Peptidase inhibitor I78 family.	
PMI32_03640	-1.6284642	Ribosomal protein S8	[J] Translation, ribosomal structure and biogenesis
PMI32_03391	-1.6304934	Uncharacterized conserved protein	[S] Function unknown
PMI32_03540	-1.6326261	amino acid carrier protein	[E] Amino acid transport and metabolism
PMI32_02930	-1.6334928	ABC-type uncharacterized transport system, duplicated ATPase component	[R] General function prediction only
PMI32_05821	-1.643109	Dinucleotide-utilizing enzymes involved in molybdopterin and thiamine biosynthesis family 1	[H] Coenzyme transport and metabolism
PMI32_00338	-1.6509504	ATPases involved in chromosome partitioning	[D] Cell cycle control, cell division, chromosome partitioning
PMI32_01627	-1.652011	ABC-type transport system involved in resistance to organic solvents, auxiliary component	[Q] Secondary metabolites biosynthesis, transport and catabolism
PMI32_05244	-1.6558262	Pyruvate/2-oxoglutarate dehydrogenase complex, dihydrolipoamide acyltransferase (E2) component, and related enzymes	[C] Energy production and conversion
PMI32_02849	-1.6571431	Predicted acyl-CoA transferases/carnitine dehydratase	[C] Energy production and conversion
PMI32_03348	-1.6589187	hypothetical protein	
PMI32_00128	-1.6629849	malate:quinone-oxidoreductase	[R] General function prediction only
PMI32_01148	-1.6641363	Spermidine/putrescine-binding periplasmic protein	[E] Amino acid transport and metabolism
PMI32_01709	-1.6659882	Alcohol dehydrogenase, class IV	[C] Energy production and conversion
PMI32_03957	-1.6669808	Excinuclease ATPase subunit	[L] Replication, recombination and repair
PMI32_03641	-1.6679452	ribosomal protein L6, bacterial type	[J] Translation, ribosomal structure and biogenesis
PMI32_05490	-1.6691244	Arabinose efflux permease	[G] Carbohydrate transport and metabolism
PMI32_03040	-1.6719938	Chemotaxis response regulator containing a CheY-like receiver domain and a methylesterase domain	[T] Signal transduction mechanisms, [N] Cell motility
PMI32_04038	-1.6734328	pyruvate kinase	[G] Carbohydrate transport and metabolism
PMI32_01934	-1.6757993	ATP synthase, F1 delta subunit	[C] Energy production and conversion
PMI32_05600	-1.6763655	Glycine cleavage system regulatory protein	[E] Amino acid transport and metabolism
PMI32_01459	-1.6846485	ABC-type amino acid transport/signal transduction systems, periplasmic component/domain	[T] Signal transduction mechanisms, [E] Amino acid transport and metabolism
PMI32_04458	-1.6877351	gluconate transporter	[G] Carbohydrate transport and metabolism, [E] Amino acid transport and metabolism
PMI32_00163	-1.6935139	hypothetical protein	
PMI32_05414	-1.6980744	Predicted signal-transduction protein containing cAMP-binding and CBS domains	
PMI32_01634	-1.6989577	Trypsin-like serine proteases, typically	[O] Posttranslational modification, protein

		periplasmic, contain C-terminal PDZ domain	turnover, chaperones
PMI32_04410	-1.7024976	ABC-type amino acid transport/signal transduction systems, periplasmic component/domain	[T] Signal transduction mechanisms, [E] Amino acid transport and metabolism
PMI32_02839	-1.7025883	hypothetical protein	
PMI32_03039	-1.7080547	Chemotaxis protein histidine kinase and related kinases	
PMI32_02478	-1.7099898	Uncharacterized membrane protein (homolog of Drosophila rhomboid)	[R] General function prediction only
PMI32_05954	-1.7131307	Predicted nucleoside-diphosphate-sugar epimerases	[G] Carbohydrate transport and metabolism, [M] Cell wall/membrane/envelope biogenesis
PMI32_01896	-1.7149086	Protein of unknown function (DUF3301).	
PMI32_05956	-1.7157936	polyprenyl P-hydroxybenzoate and phenylacrylic acid decarboxylases	[H] Coenzyme transport and metabolism
PMI32_03054	-1.7180918	DNA repair protein RecN	[L] Replication, recombination and repair
PMI32_03856	-1.7181966	copper-(or silver)-translocating P-type ATPase	[P] Inorganic ion transport and metabolism
PMI32_01571	-1.7193928	Uncharacterized protein involved in biosynthesis of c-type cytochromes	[O] Posttranslational modification, protein turnover, chaperones
PMI32_00205	-1.7197067	hypothetical protein	
PMI32_01178	-1.721834	Cd(II)/Pb(II)-responsive transcriptional regulator	[K] Transcription
PMI32_01167	-1.7220984	Uncharacterized protein conserved in bacteria	[S] Function unknown
PMI32_01262	-1.7238021	NTP pyrophosphohydrolases containing a Zn-finger, probably nucleic-acid-binding	[L] Replication, recombination and repair
PMI32_04470	-1.7279011	Xaa-Pro aminopeptidase	[E] Amino acid transport and metabolism
PMI32_02608	-1.7287189	hypothetical protein	
PMI32_02203	-1.7288525	Universal stress protein UspA and related nucleotide-binding proteins	[T] Signal transduction mechanisms
PMI32_05683	-1.7295889	Acyl-CoA dehydrogenases	[I] Lipid transport and metabolism
PMI32_01194	-1.7301247	uncharacterized domain HDIG	[T] Signal transduction mechanisms
PMI32_04818	-1.7318776	dephospho-CoA kinase	[H] Coenzyme transport and metabolism
PMI32_02733	-1.7324535	Predicted transcriptional regulators	[K] Transcription
PMI32_03036	-1.7361847	Chemotaxis signal transduction protein	[T] Signal transduction mechanisms, [N] Cell motility
PMI32_00922	-1.7375147	Acyl CoA:acetate/3-ketoacid CoA transferase, beta subunit	[I] Lipid transport and metabolism
PMI32_01015	-1.7378877	Carbonic anhydrase	[P] Inorganic ion transport and metabolism
PMI32_02590	-1.7438583	FKBP-type peptidyl-prolyl cis-trans isomerases 2	[O] Posttranslational modification, protein turnover, chaperones
PMI32_02012	-1.7444214	protoheme IX farnesyltransferase	[O] Posttranslational modification, protein turnover, chaperones
PMI32_00854	-1.748681	iron-sulfur cluster assembly protein IscA	[S] Function unknown
PMI32_01002	-1.7500979	hypothetical protein	
PMI32_02326	-1.7554048	3-isopropylmalate dehydratase, small subunit	[E] Amino acid transport and metabolism
PMI32_05920	-1.7587836	Predicted membrane protein	[S] Function unknown
PMI32_01616	-1.7607488	PTS IIA-like nitrogen-regulatory protein PtsN	[T] Signal transduction mechanisms, [G] Carbohydrate transport and metabolism
PMI32_01982	-1.7616149	ABC-type transport system involved in resistance to organic solvents, ATPase component	[Q] Secondary metabolites biosynthesis, transport and catabolism
PMI32_01183	-1.7633174	putative 2-aminoethylphosphonate ABC transporter, periplasmic 2-aminoethylphosphonate-binding protein	[P] Inorganic ion transport and metabolism
PMI32_04254	-1.7643288	ybaK/ebsC protein	[S] Function unknown
PMI32_01680	-1.7697529	PAS domain S-box/diguanylate cyclase (GGDEF) domain	
PMI32_01173	-1.7697826	phosphoenolpyruvate-protein phosphotransferase	[T] Signal transduction mechanisms
PMI32_01873	-1.7735257	Mg2+ and Co2+ transporters	[P] Inorganic ion transport and metabolism
PMI32_01690	-1.7751552	Uncharacterized conserved protein	[S] Function unknown

PMI32_03264	-1.7752174	Peroxiredoxin	[O] Posttranslational modification, protein turnover, chaperones
PMI32_01070	-1.775655	hypothetical protein	
PMI32_02595	-1.7758999	ribosomal protein S20	[J] Translation, ribosomal structure and biogenesis
PMI32_03060	-1.7760738	SsrA-binding protein	[O] Posttranslational modification, protein turnover, chaperones
PMI32_00035	-1.7801803	Predicted transcriptional regulators	[K] Transcription
PMI32_00697	-1.7806945	D-tyrosyl-tRNA(Tyr) deacylase	[J] Translation, ribosomal structure and biogenesis
PMI32_01225	-1.7819551	pyrroline-5-carboxylate reductase	[E] Amino acid transport and metabolism
PMI32_03769	-1.7820713	hypothetical protein	
PMI32_01929	-1.7869257	UDP-N-acetylglucosamine diphosphorylase/glucosamine-1-phosphate N-acetyltransferase	[M] Cell wall/membrane/envelope biogenesis
PMI32_01112	-1.7881804	Bacterial RNase P class A	
PMI32_01107	-1.7961762	Predicted periplasmic or secreted lipoprotein	[R] General function prediction only
PMI32_04007	-1.7976292	Purine-cytosine permease and related proteins	[F] Nucleotide transport and metabolism
PMI32_05111	-1.800219	Predicted amino acid aldolase or racemase	[E] Amino acid transport and metabolism
PMI32_04248	-1.8016342	monothiol glutaredoxin, Grx4 family	[O] Posttranslational modification, protein turnover, chaperones
PMI32_01440	-1.8055061	Glucose/sorbosone dehydrogenases	[G] Carbohydrate transport and metabolism
PMI32_02797	-1.8059305	preprotein translocase, SecA subunit	[U] Intracellular trafficking, secretion, and vesicular transport
PMI32_01935	-1.8148339	ATP synthase, F0 subunit b	[C] Energy production and conversion
PMI32_05325	-1.8175693	hypothetical protein	
PMI32_02451	-1.8221845	cytochrome c oxidase, cbb3-type, subunit II	[C] Energy production and conversion
PMI32_02323	-1.8222102	aspartate-semialdehyde dehydrogenase, gamma-proteobacterial	[E] Amino acid transport and metabolism
PMI32_01795	-1.8269022	Dehydrogenases with different specificities (related to short-chain alcohol dehydrogenases)	[R] General function prediction only, [I] Lipid transport and metabolism, [Q] Secondary metabolites biosynthesis, transport and catabolism
PMI32_02929	-1.8296627	translation initiation factor IF-1	[J] Translation, ribosomal structure and biogenesis
PMI32_00847	-1.8335117	Predicted outer membrane lipoprotein	[S] Function unknown
PMI32_02004	-1.8358904	ABC-type Mn/Zn transport systems, ATPase component	[P] Inorganic ion transport and metabolism
PMI32_03979	-1.8368068	signal peptide peptidase SppA, 36K type	[O] Posttranslational modification, protein turnover, chaperones, [U] Intracellular trafficking, secretion, and vesicular transport
PMI32_01180	-1.84071	aminoethylphosphonate catabolism associated LysR family transcriptional regulator	[K] Transcription
PMI32_01649	-1.8407884	FolB domain	[H] Coenzyme transport and metabolism
PMI32_04863	-1.8411748	choline/carnitine/betaine transport	[M] Cell wall/membrane/envelope biogenesis
PMI32_03198	-1.8421473	ABC-type histidine transport system, ATPase component	[E] Amino acid transport and metabolism
PMI32_03402	-1.8436415	Transcriptional regulator of aromatic amino acids metabolism	[K] Transcription, [E] Amino acid transport and metabolism
PMI32_00848	-1.8448949	Archaeal fructose-1,6-bisphosphatase and related enzymes of inositol monophosphatase family	[G] Carbohydrate transport and metabolism
PMI32_03564	-1.847795	Uncharacterized protein conserved in bacteria	[S] Function unknown
PMI32_01983	-1.8484985	ABC-type transport system involved in resistance to organic solvents, periplasmic component	[Q] Secondary metabolites biosynthesis, transport and catabolism
PMI32_04490	-1.8506065	hypothetical protein	
PMI32_02684	-1.8524301	S-(hydroxymethyl)glutathione dehydrogenase/class III alcohol dehydrogenase	[C] Energy production and conversion
PMI32_02030	-1.8532641	Carbonic anhydrases/acetyltransferases, isoleucine patch superfamily	[R] General function prediction only
PMI32_01699	-1.8542494	Predicted phosphotransferase related to Ser/Thr protein kinases	[R] General function prediction only

PMI32_03384	-1.8586035	P pilus assembly/Cpx signaling pathway, periplasmic inhibitor/zinc-resistance associated protein	[P] Inorganic ion transport and metabolism, [T] Signal transduction mechanisms, [U] Intracellular trafficking, secretion, and vesicular transport, [N] Cell motility
PMI32_04046	-1.8591978	acyl-CoA thioesterase II	[I] Lipid transport and metabolism
PMI32_04628	-1.8641068	Electron transfer flavoprotein, alpha subunit	[C] Energy production and conversion
PMI32_04868	-1.8681809	Predicted Zn-dependent proteases and their inactivated homologs	[R] General function prediction only
PMI32_01067	-1.8694202	Hypoxanthine-guanine phosphoribosyltransferase	[F] Nucleotide transport and metabolism
PMI32_00785	-1.8725761	Predicted ATPase related to phosphate starvation-inducible protein PhoH	[T] Signal transduction mechanisms
PMI32_05773	-1.8732518	ribosomal protein L9	[J] Translation, ribosomal structure and biogenesis
PMI32_04422	-1.8740511	Cation/multidrug efflux pump	[V] Defense mechanisms
PMI32_05252	-1.8755912	sulfate ABC transporter, permease protein CysT	[O] Posttranslational modification, protein turnover, chaperones
PMI32_00151	-1.8782423	Transcriptional regulators	[K] Transcription
PMI32_02424	-1.880237	SOS regulatory protein LexA	[T] Signal transduction mechanisms, [K] Transcription
PMI32_01089	-1.8802916	Protein of unknown function (DUF1329).	
PMI32_02828	-1.8808056	Uncharacterized protein conserved in bacteria	[S] Function unknown
PMI32_04438	-1.8849221	Protein of unknown function (DUF2025).	
PMI32_05310	-1.8886449	type I secretion outer membrane protein, TolC family	[U] Intracellular trafficking, secretion, and vesicular transport, [M] Cell wall/membrane/envelope biogenesis
PMI32_02858	-1.8913259	Response regulators consisting of a CheY-like receiver domain and a winged-helix DNA-binding domain	[K] Transcription, [T] Signal transduction mechanisms
PMI32_03464	-1.8940528	orotate phosphoribosyltransferase	[F] Nucleotide transport and metabolism
PMI32_05948	-1.8966376	Transglycosylase.	[M] Cell wall/membrane/envelope biogenesis
PMI32_01088	-1.8975523	Protein of unknown function (DUF1302).	
PMI32_01912	-1.899245	Cyclopropane fatty acid synthase and related methyltransferases	[M] Cell wall/membrane/envelope biogenesis
PMI32_01221	-1.9019366	hypothetical protein	
PMI32_01931	-1.9047081	ATP synthase, F1 beta subunit	[C] Energy production and conversion
PMI32_03042	-1.9051492	Dihydropteroate synthase and related enzymes	
PMI32_02005	-1.9051954	ABC-type Mn2+/Zn2+ transport systems, permease components	[P] Inorganic ion transport and metabolism
PMI32_02915	-1.9056263	sulfur relay protein TusC/DsrF	[P] Inorganic ion transport and metabolism
PMI32_04624	-1.9062418	Zn-dependent alcohol dehydrogenases	[R] General function prediction only
PMI32_01874	-1.9063549	RraA family	[H] Coenzyme transport and metabolism
PMI32_02447	-1.9091209	cytochrome c oxidase, cbb3-type, subunit II	[C] Energy production and conversion
PMI32_05259	-1.9098186	ATP-dependent protease La	[O] Posttranslational modification, protein turnover, chaperones
PMI32_03812	-1.912299	precorrin-2 C20-methyltransferase	[H] Coenzyme transport and metabolism
PMI32_05689	-1.9166258	hypothetical protein	
PMI32_02715	-1.9168112	muconate and chloromuconate cycloisomerases	[M] Cell wall/membrane/envelope biogenesis, [R] General function prediction only
PMI32_01872	-1.9177199	hypothetical protein	
PMI32_00276	-1.9219392	triosephosphate isomerase	[G] Carbohydrate transport and metabolism
PMI32_04660	-1.922825	Predicted metal-dependent hydrolases related to alanyl-tRNA synthetase HxxxH domain	[R] General function prediction only
PMI32_04836	-1.9231662	Flavodoxin reductases (ferredoxin-NADPH reductases) family 1	[C] Energy production and conversion
PMI32_04472	-1.9249118	Putative threonine efflux protein	[E] Amino acid transport and metabolism
PMI32_04084	-1.9282795	phosphoserine aminotransferase	[E] Amino acid transport and metabolism, [H] Coenzyme transport and metabolism
PMI32_02609	-1.9284794	Predicted ATP-dependent protease	[O] Posttranslational modification, protein

			turnover, chaperones
PMI32_04316	-1.9288021	heavy metal sensor kinase	[T] Signal transduction mechanisms
PMI32_05239	-1.9320165	Predicted permeases	[R] General function prediction only
PMI32_03935	-1.9341555	Amidases related to nicotinamidase	[Q] Secondary metabolites biosynthesis, transport and catabolism
PMI32_00990	-1.9364205	diguanylate cyclase (GGDEF) domain	[T] Signal transduction mechanisms
PMI32_05753	-1.9377135	N-acetylmuramoyl-L-alanine amidase	[M] Cell wall/membrane/envelope biogenesis
PMI32_05074	-1.938075	Membrane protein TerC, possibly involved in tellurium resistance	[P] Inorganic ion transport and metabolism
PMI32_00964	-1.9381014	Alcohol dehydrogenase, class IV	[C] Energy production and conversion
PMI32_01583	-1.940299	Response regulator consisting of a CheY-like receiver domain and a Fis-type HTH domain	[T] Signal transduction mechanisms, [K] Transcription
PMI32_05770	-1.9419931	ribosomal protein S6	[J] Translation, ribosomal structure and biogenesis
PMI32_01229	-1.9504155	Predicted membrane protein	[S] Function unknown
PMI32_01930	-1.9512986	ATP synthase, F1 epsilon subunit (delta in mitochondria)	[C] Energy production and conversion
PMI32_01492	-1.9548977	pyridoxine 5'-phosphate synthase	[H] Coenzyme transport and metabolism
PMI32_05586	-1.956558	Cyanate permease	[P] Inorganic ion transport and metabolism
PMI32_02445	-1.9577507	Predicted hydrolase of the alpha/beta-hydrolase fold	[R] General function prediction only
PMI32_02155	-1.959674	Uncharacterized conserved protein	[S] Function unknown
PMI32_01820	-1.9651685	3-hydroxyacyl-CoA dehydrogenase	[I] Lipid transport and metabolism
PMI32_02309	-1.9672546	tRNA_Undet_???	
PMI32_01114	-1.9675133	S-adenosyl-methyltransferase MraW	[M] Cell wall/membrane/envelope biogenesis
PMI32_04896	-1.9694463	Acyl-CoA hydrolase	[I] Lipid transport and metabolism
PMI32_03752	-1.9719214	Transcriptional regulators	[K] Transcription
PMI32_02225	-1.9733789	Glutathione S-transferase	[O] Posttranslational modification, protein turnover, chaperones
PMI32_01548	-1.9775989	hypothetical protein	
PMI32_05879	-1.9780173	Outer membrane receptor proteins, mostly Fe transport	[P] Inorganic ion transport and metabolism
PMI32_01612	-1.9799252	Superoxide dismutase	[P] Inorganic ion transport and metabolism
PMI32_03046	-1.9821633	hypothetical protein	
PMI32_05674	-1.9822198	metalloprotein, YbeY/UPF0054 family	[R] General function prediction only
PMI32_00687	-1.9847519	twin arginine-targeting protein translocase, TatA/E family	[U] Intracellular trafficking, secretion, and vesicular transport
PMI32_04749	-1.9853901	carbon storage regulator (csrA)	[T] Signal transduction mechanisms
PMI32_01717	-1.9856665	cAMP-binding proteins - catabolite gene activator and regulatory subunit of cAMP-dependent protein kinases	[T] Signal transduction mechanisms
PMI32_05408	-1.9877817	hypothetical protein	
PMI32_04491	-1.9940199	hypothetical protein	
PMI32_05242	-1.9982803	Pyruvate/2-oxoglutarate dehydrogenase complex, dehydrogenase (E1) component, eukaryotic type, alpha subunit	[C] Energy production and conversion
PMI32_02017	-2.0084663	Heme/copper-type cytochrome/quinol oxidase, subunit 3	[C] Energy production and conversion
PMI32_05243	-2.012787	Pyruvate/2-oxoglutarate dehydrogenase complex, dehydrogenase (E1) component, eukaryotic type, beta subunit	[C] Energy production and conversion
PMI32_03549	-2.0145473	Acetyltransferases, including N-acetylases of ribosomal proteins	[J] Translation, ribosomal structure and biogenesis
PMI32_05648	-2.0161315	Uncharacterized protein, similar to the N-terminal domain of Lon protease	[R] General function prediction only
PMI32_00494	-2.021096	Response regulator containing a CheY-like receiver domain and an HTH DNA-binding domain	[K] Transcription, [T] Signal transduction mechanisms
PMI32_04676	-2.0233555	glucose-6-phosphate 1-dehydrogenase	[G] Carbohydrate transport and metabolism

PMI32_02761	-2.0289619	Multisubunit Na+/H+ antiporter, MnhF subunit	[P] Inorganic ion transport and metabolism
PMI32_01807	-2.0307407	Phage terminase, small subunit	
PMI32_00595	-2.0307807	methionine-S-sulfoxide reductase	[O] Posttranslational modification, protein turnover, chaperones
PMI32_05261	-2.0329055	ATP-dependent Clp protease, proteolytic subunit ClpP	[O] Posttranslational modification, protein turnover, chaperones, [U] Intracellular trafficking, secretion, and vesicular transport
PMI32_02334	-2.033192	Transcriptional regulator	[K] Transcription
PMI32_03880	-2.0339982	methylmalonic acid semialdehyde dehydrogenase	[C] Energy production and conversion
PMI32_05276	-2.0357958	hypothetical protein	
PMI32_01936	-2.0377369	ATP synthase, F0 subunit c	[C] Energy production and conversion
PMI32_01812	-2.0426212	hypothetical protein	
PMI32_01815	-2.0465858	Uncharacterized protein conserved in bacteria	[S] Function unknown
PMI32_02829	-2.0509383	MazG family protein	
PMI32_03390	-2.0570062	Sua5/YciO/YrdC/YwlC family protein	[J] Translation, ribosomal structure and biogenesis
PMI32_05970	-2.0601277	Predicted secreted protein	[S] Function unknown
PMI32_02452	-2.0634147	Cbb3-type cytochrome oxidase, subunit 3	[O] Posttranslational modification, protein turnover, chaperones
PMI32_00701	-2.0652599	N-formylglutamate amidohydrolase	[E] Amino acid transport and metabolism
PMI32_03951	-2.0669265	Spermidine/putrescine-binding periplasmic protein	[E] Amino acid transport and metabolism
PMI32_03956	-2.0711355	PAS domain S-box	
PMI32_05754	-2.0750416	DNA mismatch repair protein MutL	[L] Replication, recombination and repair
PMI32_03855	-2.0766325	Cu(I)-responsive transcriptional regulator	[K] Transcription
PMI32_02031	-2.0820203	Predicted phosphatases	[R] General function prediction only
PMI32_04664	-2.0823396	tRNA_Undet_???	
PMI32_01092	-2.0872862	Outer membrane protein and related peptidoglycan-associated (lipo)proteins	[M] Cell wall/membrane/envelope biogenesis
PMI32_02020	-2.0897633	cytochrome c oxidase, subunit I	[C] Energy production and conversion
PMI32_05266	-2.0922486	tRNA_Undet_???	
PMI32_03127	-2.0927196	Acetyltransferases	
PMI32_00946	-2.0968716	hypothetical protein	
PMI32_05718	-2.0992944	Response regulator containing CheY-like receiver, AAA-type ATPase, and DNA-binding domains	[T] Signal transduction mechanisms
PMI32_01136	-2.1002918	FMN reductase, SsuE family	[R] General function prediction only
PMI32_01970	-2.1009401	choline ABC transporter, periplasmic binding protein	[E] Amino acid transport and metabolism
PMI32_02453	-2.1069999	cytochrome c oxidase, cbb3-type, subunit III	[C] Energy production and conversion
PMI32_04791	-2.1085611	ABC-type Fe3+-siderophore transport system, permease component	[P] Inorganic ion transport and metabolism
PMI32_03326	-2.1098182	HD-GYP domain	[T] Signal transduction mechanisms
PMI32_05643	-2.1103502	cysteine synthase A	[E] Amino acid transport and metabolism
PMI32_02265	-2.1119285	Signal transduction histidine kinase	[T] Signal transduction mechanisms
PMI32_05831	-2.1148868	Cation/multidrug efflux pump	[V] Defense mechanisms
PMI32_03516	-2.1271685	NAD(P)H-nitrite reductase	
PMI32_03139	-2.1299454	hypothetical protein	
PMI32_01782	-2.1371908	Cystathionine beta-lyases/cystathionine gamma-synthases	[E] Amino acid transport and metabolism
PMI32_03509	-2.1389671	type VI secretion protein, EvpB/VC_A0108 family	[S] Function unknown
PMI32_02193	-2.1391223	hypothetical protein	
PMI32_02647	-2.1411294	Sugar phosphate permease	[G] Carbohydrate transport and metabolism

PMI32_04720	-2.142836	Flagellar biosynthesis/type III secretory pathway chaperone	[N] Cell motility, [U] Intracellular trafficking, secretion, and vesicular transport, [O] Posttranslational modification, protein turnover, chaperones
PMI32_05206	-2.1449337	isocitrate dehydrogenase, NADP-dependent, prokaryotic type	[C] Energy production and conversion
PMI32_02599	-2.1511617	ribosomal protein L27	[J] Translation, ribosomal structure and biogenesis
PMI32_03004	-2.1517915	Periplasmic glucans biosynthesis protein	[P] Inorganic ion transport and metabolism
PMI32_01689	-2.1590095	Uncharacterized conserved protein	[S] Function unknown
PMI32_01933	-2.1592008	proton translocating ATP synthase, F1 alpha subunit	[C] Energy production and conversion
PMI32_03334	-2.16145	Zn-dependent protease with chaperone function	[O] Posttranslational modification, protein turnover, chaperones
PMI32_04603	-2.1637515	Transcriptional regulator	[K] Transcription
PMI32_04841	-2.1639682	Electron transfer flavoprotein, alpha subunit	[C] Energy production and conversion
PMI32_02194	-2.1671175	Bacterial lipocalin	[M] Cell wall/membrane/envelope biogenesis
PMI32_05119	-2.1693156	Transcriptional regulator containing PAS, AAA-type ATPase, and DNA-binding domains	[K] Transcription, [T] Signal transduction mechanisms
PMI32_03342	-2.1704245	ABC-type spermidine/putrescine transport systems, ATPase components	[E] Amino acid transport and metabolism
PMI32_03413	-2.1711628	ammonium transporter	[P] Inorganic ion transport and metabolism
PMI32_05312	-2.1727399	type I secretion membrane fusion protein, HlyD family	[V] Defense mechanisms
PMI32_02041	-2.1739171	Uncharacterized conserved protein	[S] Function unknown
PMI32_03806	-2.1741261	Precorrin-6x reductase	[H] Coenzyme transport and metabolism
PMI32_02457	-2.1752029	Uncharacterized protein conserved in bacteria	[S] Function unknown
PMI32_03919	-2.1755229	Predicted membrane protein	[S] Function unknown
PMI32_03168	-2.1808631	protein RecA	[L] Replication, recombination and repair
PMI32_03123	-2.1816509	hypothetical protein	
PMI32_02475	-2.1826097	aminopeptidase N, Escherichia coli type	[E] Amino acid transport and metabolism
PMI32_04124	-2.1830391	Predicted carboxypeptidase	[E] Amino acid transport and metabolism
PMI32_03145	-2.1836262	Ferredoxin	[C] Energy production and conversion
PMI32_01838	-2.18539	phosophoadenylyl-sulfate reductase (thioredoxin)/thioredoxin-dependent adenylylsulfate APS reductase	[H] Coenzyme transport and metabolism, [E] Amino acid transport and metabolism
PMI32_00705	-2.1885696	glycine betaine/L-proline transport ATP binding subunit	
PMI32_00253	-2.1939735	PTS system, fructose-specific, IIB component/PTS system, fructose subfamily, IIC component	[G] Carbohydrate transport and metabolism
PMI32_04073	-2.1958047	Short-chain dehydrogenases of various substrate specificities	[R] General function prediction only
PMI32_05825	-2.1994285	hypothetical protein	
PMI32_05341	-2.2021224	hypothetical protein	
PMI32_01869	-2.2066923	Outer membrane protein and related peptidoglycan-associated (lipo)proteins	[M] Cell wall/membrane/envelope biogenesis
PMI32_04855	-2.2115499	gamma-butyrobetaine hydroxylase	
PMI32_04061	-2.2228171	Adenosylmethionine-8-amino-7-oxononanoate aminotransferase	[H] Coenzyme transport and metabolism
PMI32_05241	-2.2238137	Transcriptional regulators	[K] Transcription
PMI32_02796	-2.2256981	glutamate N-acetyltransferase/amino-acid acetyltransferase	[E] Amino acid transport and metabolism
PMI32_05406	-2.2273004	DNA-directed DNA polymerase III (polc)	[L] Replication, recombination and repair
PMI32_03845	-2.2342569	hypothetical protein	
PMI32_03749	-2.236887	Sugar phosphate permease	[G] Carbohydrate transport and metabolism
PMI32_05781	-2.2462615	Azurin	[C] Energy production and conversion
PMI32_00738	-2.2698174	Uncharacterized conserved protein	[S] Function unknown

PMI32_00918	-2.2733271	hypothetical protein	
PMI32_05255	-2.2764601	Predicted membrane protein	[S] Function unknown
PMI32_04045	-2.28639	haloacid dehalogenase superfamily, subfamily IA, variant 3 with third motif having DD or ED/haloacid dehalogenase superfamily, subfamily IA, variant 1 with third motif having Dx(3-4)D or Dx(3-4)E	[R] General function prediction only
PMI32_05251	-2.2903549	sulfate/thiosulfate-binding protein	[P] Inorganic ion transport and metabolism
PMI32_02601	-2.2943271	Geranylgeranyl pyrophosphate synthase	[H] Coenzyme transport and metabolism
PMI32_03062	-2.2993691	L-lactate transport	[C] Energy production and conversion
PMI32_02912	-2.2994767	hypothetical protein	
PMI32_00040	-2.3009835	ribosomal protein L35	[J] Translation, ribosomal structure and biogenesis
PMI32_00194	-2.3060065	Uncharacterized protein involved in an early stage of isoprenoid biosynthesis	[Q] Secondary metabolites biosynthesis, transport and catabolism
PMI32_04524	-2.3073997	Esterase/lipase	[I] Lipid transport and metabolism
PMI32_01615	-2.3163327	Predicted P-loop-containing kinase	[R] General function prediction only
PMI32_00094	-2.3165362	exodeoxyribonuclease V, beta subunit	[L] Replication, recombination and repair
PMI32_01991	-2.3250736	Predicted signal transduction protein containing sensor and EAL domains	[T] Signal transduction mechanisms
PMI32_01819	-2.327875	acetyl-CoA acetyltransferases	[I] Lipid transport and metabolism
PMI32_02449	-2.3323924	cytochrome c oxidase, cbb3-type, subunit III	[C] Energy production and conversion
PMI32_05650	-2.3343944	Uncharacterized membrane-associated protein	[S] Function unknown
PMI32_04552	-2.3364966	proton-translocating NADH-quinone oxidoreductase, chain M	[C] Energy production and conversion
PMI32_05343	-2.338401	AraC-type DNA-binding domain-containing proteins	[K] Transcription
PMI32_05690	-2.3401824	cation diffusion facilitator family transporter	[P] Inorganic ion transport and metabolism
PMI32_03902	-2.3407538	Uncharacterized protein conserved in bacteria	[S] Function unknown
PMI32_03705	-2.3465664	tRNA_Undet_???	
PMI32_01681	-2.3487855	RNA polymerase sigma factor, sigma-70 family	[K] Transcription
PMI32_01073	-2.3519823	hypothetical protein	
PMI32_04567	-2.3600746	drug resistance transporter, EmrB/QacA subfamily	
PMI32_05481	-2.3601774	Membrane protease subunits, stomatin/prohibitin homologs	
PMI32_01691	-2.3634421	Putative Ser protein kinase	[T] Signal transduction mechanisms
PMI32_00576	-2.3657923	oxidoreductase alpha (molybdopterin) subunit	[C] Energy production and conversion
PMI32_04334	-2.3770835	hypothetical protein	
PMI32_01068	-2.3803657	hypothetical protein	
PMI32_05527	-2.3851142	hypothetical protein	
PMI32_03203	-2.3852898	DNA ligase, ATP-dependent, PP_1105 family	[L] Replication, recombination and repair
PMI32_02764	-2.3883991	Multisubunit Na+/H+ antiporter, MnhC subunit	[P] Inorganic ion transport and metabolism
PMI32_03401	-2.3892774	phenylalanine-4-hydroxylase, monomeric form	[E] Amino acid transport and metabolism
PMI32_05751	-2.3945275	yjeF C-terminal region, hydroxyethylthiazole kinase-related/yjeF N-terminal region	[G] Carbohydrate transport and metabolism
PMI32_02062	-2.3974491	23S rRNA. Bacterial LSU	
PMI32_02928	-2.3985263	Putative arginyl-tRNA:protein arginylyltransferase	[O] Posttranslational modification, protein turnover, chaperones
PMI32_01128	-2.3997137	UDP-3-0-acyl N-acetylglucosamine deacetylase	[M] Cell wall/membrane/envelope biogenesis
PMI32_02059	-2.4048071	16S rRNA. Bacterial SSU	
PMI32_05060	-2.4079794	Beta-lactamase class C and other penicillin binding proteins	[V] Defense mechanisms
PMI32_05969	-2.4105113	Uncharacterized protein conserved in bacteria	[S] Function unknown

PMI32_02206	-2.4192027	Predicted membrane protein	[S] Function unknown
PMI32_04423	-2.4195137	RND family efflux transporter, MFP subunit	[M] Cell wall/membrane/envelope biogenesis
PMI32_04455	-2.424997	Uncharacterized protein conserved in bacteria	[S] Function unknown
PMI32_01062	-2.4279258	Predicted NAD/FAD-dependent oxidoreductase	[R] General function prediction only
PMI32_01452	-2.428175	Transcriptional regulator containing GAF, AAA-type ATPase, and DNA binding domains	[T] Signal transduction mechanisms, [K] Transcription
PMI32_01816	-2.4289459	Transglutaminase-like enzymes, putative cysteine proteases	[E] Amino acid transport and metabolism
PMI32_04008	-2.4336426	Sugar kinases, ribokinase family	[G] Carbohydrate transport and metabolism
PMI32_00278	-2.4347543	dihydropteroate synthase	
PMI32_01042	-2.4434998	4-diphosphocytidyl-2C-methyl-D-erythritol kinase	[I] Lipid transport and metabolism
PMI32_00381	-2.44655	Putative NADPH-quinone reductase (modulator of drug activity B)	[R] General function prediction only
PMI32_00150	-2.4503142	Predicted phosphatase	[R] General function prediction only
PMI32_04604	-2.4521137	3-hydroxyacyl-CoA dehydrogenase	[I] Lipid transport and metabolism
PMI32_00247	-2.4672391	Uncharacterized iron-regulated protein	[S] Function unknown
PMI32_03521	-2.4693917	phosphate regulon transcriptional regulatory protein PhoB	[K] Transcription, [T] Signal transduction mechanisms
PMI32_02697	-2.470856	hypothetical protein	
PMI32_00962	-2.4717397	Predicted transcriptional regulators	[K] Transcription
PMI32_03031	-2.4754758	Spermidine/putrescine-binding periplasmic protein	[E] Amino acid transport and metabolism
PMI32_01606	-2.4797893	Predicted Zn-dependent proteases and their inactivated homologs	[R] General function prediction only
PMI32_01140	-2.4845003	ABC-type nitrate/sulfonate/bicarbonate transport system, ATPase component	[P] Inorganic ion transport and metabolism
PMI32_04459	-2.484507	carbohydrate kinase, thermoresistant glucokinase family	[G] Carbohydrate transport and metabolism
PMI32_01642	-2.4858536	NADH:flavin oxidoreductases, Old Yellow Enzyme family	[C] Energy production and conversion
PMI32_03783	-2.4983878	hypothetical protein	
PMI32_02570	-2.5014592	tRNA_Undet_???	
PMI32_05717	-2.5117362	His Kinase A (phosphoacceptor) domain./Histidine kinase-, DNA gyrase B-, and HSP90-like ATPase./PAS fold.	
PMI32_03474	-2.5202698	hypothetical protein	
PMI32_04005	-2.5229451	Transcriptional regulators	[K] Transcription
PMI32_02837	-2.5237946	Lactate dehydrogenase and related dehydrogenases	[C] Energy production and conversion, [H] Coenzyme transport and metabolism, [R] General function prediction only
PMI32_03498	-2.5242712	type VI secretion ATPase, ClpV1 family	[O] Posttranslational modification, protein turnover, chaperones
PMI32_05752	-2.5320927	ATPase, YjeE family	[R] General function prediction only
PMI32_03517	-2.5435849	Rubredoxin	[C] Energy production and conversion
PMI32_05597	-2.5481329	Predicted rRNA methylase (SpoU class)	[J] Translation, ribosomal structure and biogenesis
PMI32_02789	-2.5492851	Small-conductance mechanosensitive channel	
PMI32_01806	-2.5494392	Acyl-CoA thioesterase	[I] Lipid transport and metabolism
PMI32_00548	-2.5532836	Dehydrogenases with different specificities (related to short-chain alcohol dehydrogenases)	[I] Lipid transport and metabolism, [R] General function prediction only, [Q] Secondary metabolites biosynthesis, transport and catabolism
PMI32_01064	-2.5593178	Ferrochelatase	[H] Coenzyme transport and metabolism
PMI32_05834	-2.5640292	Protein of unknown function (DUF548).	
PMI32_01139	-2.5644521	ABC-type nitrate/sulfonate/bicarbonate transport system, permease component	[P] Inorganic ion transport and metabolism
PMI32_00267	-2.5696089	ribosomal protein S15, bacterial/organelle	[J] Translation, ribosomal structure and biogenesis

PMI32_01174	-2.5731493	Uncharacterized conserved protein	[S] Function unknown
PMI32_00937	-2.5743426	Transcriptional regulator	[K] Transcription
PMI32_02310	-2.5758457	tRNA_Undet_???	
PMI32_01119	-2.5766639	phospho-N-acetylmuramoyl-pentapeptide-transferase	[M] Cell wall/membrane/envelope biogenesis
PMI32_05952	-2.5824188	Acyl dehydratase	[I] Lipid transport and metabolism
PMI32_04538	-2.5882432	Predicted acyltransferase	[R] General function prediction only
PMI32_03942	-2.5891628	Uncharacterized conserved protein, contains double-stranded beta-helix domain	[S] Function unknown
PMI32_00447	-2.5904081	hypothetical protein	
PMI32_02018	-2.5962843	Cytochrome oxidase assembly factor	[O] Posttranslational modification, protein turnover, chaperones
PMI32_05886	-2.5979346	Dehydrogenases with different specificities (related to short-chain alcohol dehydrogenases)	[Q] Secondary metabolites biosynthesis, transport and catabolism, [R] General function prediction only, [I] Lipid transport and metabolism
PMI32_05693	-2.5996764	Predicted permease	[R] General function prediction only
PMI32_01086	-2.6059009	Putative threonine efflux protein	[E] Amino acid transport and metabolism
PMI32_01098	-2.6086001	Acyl-CoA dehydrogenases	[I] Lipid transport and metabolism
PMI32_04502	-2.6132743	2-oxoglutarate dehydrogenase, E1 component	[C] Energy production and conversion
PMI32_04064	-2.6191023	High-affinity K+ transport system, ATPase chain B	
PMI32_02014	-2.629068	hypothetical protein	
PMI32_05086	-2.6318529	Uncharacterized protein conserved in bacteria	[S] Function unknown
PMI32_01127	-2.6399165	cell division protein FtsZ	[D] Cell cycle control, cell division, chromosome partitioning
PMI32_03555	-2.6430304	Biotin carboxylase	[I] Lipid transport and metabolism
PMI32_02624	-2.643336	Uncharacterized small protein	[S] Function unknown
PMI32_04019	-2.646317	Outer membrane protein and related peptidoglycan-associated (lipo)proteins	[M] Cell wall/membrane/envelope biogenesis
PMI32_00036	-2.6505669	integration host factor, alpha subunit	[L] Replication, recombination and repair
PMI32_00971	-2.6530275	Putative threonine efflux protein	[E] Amino acid transport and metabolism
PMI32_03144	-2.6596169	Protein related to penicillin acylase	[R] General function prediction only
PMI32_05911	-2.6659065	PAS domain S-box/diguanylate cyclase (GGDEF) domain	[T] Signal transduction mechanisms
PMI32_01854	-2.6744671	benzoate transporter	[Q] Secondary metabolites biosynthesis, transport and catabolism
PMI32_03102	-2.6975441	Acyl carrier protein phosphodiesterase	[I] Lipid transport and metabolism
PMI32_04568	-2.7018276	Multidrug resistance efflux pump	[V] Defense mechanisms
PMI32_03399	-2.7023848	Aspartate/tyrosine/aromatic aminotransferase	[E] Amino acid transport and metabolism
PMI32_01605	-2.7152985	Predicted amidohydrolase	[R] General function prediction only
PMI32_04936	-2.7183005	Predicted Fe-S protein	
PMI32_04898	-2.7255764	adenosylhomocysteinase	[H] Coenzyme transport and metabolism
PMI32_05723	-2.726222	Flagellin and related hook-associated proteins	
PMI32_04234	-2.7284721	electron transport complex, RnfABCDGE type, D subunit	[C] Energy production and conversion
PMI32_00802	-2.7421222	Lysine 2,3-aminomutase	[E] Amino acid transport and metabolism
PMI32_03890	-2.7437455	Transcriptional regulator	[K] Transcription
PMI32_04337	-2.7498126	RND family efflux transporter, MFP subunit	[M] Cell wall/membrane/envelope biogenesis
PMI32_00464	-2.7756679	dihydroorotate dehydrogenase (subfamily 1) family protein	[F] Nucleotide transport and metabolism
PMI32_01850	-2.7836867	xanthine dehydrogenase, molybdopterin binding subunit	[F] Nucleotide transport and metabolism
PMI32_03467	-2.7925705	Uncharacterized protein conserved in bacteria	[S] Function unknown
PMI32_04121	-2.7944946	SOS-response transcriptional repressors (RecA-mediated autopeptidases)	[K] Transcription, [T] Signal transduction mechanisms

PMI32_03400	-2.7952048	Pterin-4a-carbinolamine dehydratase	[H] Coenzyme transport and metabolism
PMI32_01116	-2.8069002	Cell division protein FtsI/penicillin-binding protein 2	[M] Cell wall/membrane/envelope biogenesis
PMI32_05320	-2.8073175	hypothetical protein	
PMI32_01101	-2.8162871	Ribosomal protein S9	[J] Translation, ribosomal structure and biogenesis
PMI32_01821	-2.8208477	GMP synthase - Glutamine amidotransferase domain	[F] Nucleotide transport and metabolism
PMI32_01121	-2.8339745	cell division protein FtsW	[D] Cell cycle control, cell division, chromosome partitioning
PMI32_03607	-2.8373368	hypothetical protein	
PMI32_02784	-2.8446311	DNA-binding ferritin-like protein (oxidative damage protectant)	[P] Inorganic ion transport and metabolism
PMI32_02215	-2.8462656	tRNA_Undet_???	
PMI32_00277	-2.8636989	phosphoglucosamine mutase	[G] Carbohydrate transport and metabolism
PMI32_02333	-2.870529	Esterase/lipase	[R] General function prediction only
PMI32_03182	-2.8706722	Acetyltransferases	
PMI32_02972	-2.8873589	Uncharacterized conserved protein	[S] Function unknown
PMI32_02476	-2.8875401	Protein of unknown function (DUF2797).	
PMI32_04505	-2.8958688	succinyl-CoA synthetase, beta subunit	[C] Energy production and conversion
PMI32_03943	-2.8993328	2,3-diketo-5-methylthio-1-phosphopentane phosphatase	[C] Energy production and conversion
PMI32_03608	-2.9025644	tRNA_Undet_???	
PMI32_01220	-2.9134565	non-canonical purine NTP pyrophosphatase, RdgB/HAM1 family	[F] Nucleotide transport and metabolism
PMI32_02208	-2.9175348	Sortase and related acyltransferases	
PMI32_04506	-2.9223654	succinyl-CoA synthetase, alpha subunit	[C] Energy production and conversion
PMI32_04336	-2.9288585	ABC-type antimicrobial peptide transport system, ATPase component	[V] Defense mechanisms
PMI32_01283	-2.9440601	Predicted enzyme of the cupin superfamily	[R] General function prediction only
PMI32_05570	-2.9461819	periplasmic serine protease, Do/DeqQ family	[O] Posttranslational modification, protein turnover, chaperones
PMI32_02938	-2.9481414	phospho-2-dehydro-3-deoxyheptonate aldolase	[E] Amino acid transport and metabolism
PMI32_00748	-2.9518394	Sigma 54 modulation protein / S30EA ribosomal protein.	
PMI32_03709	-2.9624283	hypothetical protein	
PMI32_02572	-2.9651241	tRNA_Undet_???	
PMI32_01851	-2.9836239	xanthine dehydrogenase accessory protein XdhC	[O] Posttranslational modification, protein turnover, chaperones
PMI32_01118	-2.9891165	UDP-N-acetylmuramoyl-tripeptide--D-alanyl-D-alanine ligase	[M] Cell wall/membrane/envelope biogenesis
PMI32_01100	-3.0020483	ribosomal protein L13, bacterial type	[J] Translation, ribosomal structure and biogenesis
PMI32_04339	-3.0044853	Lysine/ornithine N-monooxygenase	[Q] Secondary metabolites biosynthesis, transport and catabolism
PMI32_03356	-3.0137087	tRNA_Undet_???	
PMI32_03053	-3.0158526	Molecular chaperone GrpE (heat shock protein)	[O] Posttranslational modification, protein turnover, chaperones
PMI32_04504	-3.0177557	dihydrolipoamide dehydrogenase	[C] Energy production and conversion
PMI32_04569	-3.0213501	efflux transporter, outer membrane factor (OMF) lipoprotein, NodT family	[U] Intracellular trafficking, secretion, and vesicular transport, [M] Cell wall/membrane/envelope biogenesis
PMI32_04055	-3.021658	Uncharacterized protein conserved in bacteria	[S] Function unknown
PMI32_03193	-3.0302413	Predicted methylated DNA-protein cysteine methyltransferase	[L] Replication, recombination and repair
PMI32_00972	-3.0317713	PAS domain S-box/diguanylate cyclase (GGDEF) domain	[T] Signal transduction mechanisms
PMI32_01141	-3.0317825	molybdenum-pterin binding domain	[H] Coenzyme transport and metabolism
PMI32_00624	-3.0681899	Histidine ammonia-lyase	[E] Amino acid transport and metabolism

PMI32_05085	-3.0697213	2,4-diaminobutyrate 4-transaminases	[E] Amino acid transport and metabolism
PMI32_00387	-3.0724779	hypothetical protein	
PMI32_02425	-3.0790011	SOS-response cell division inhibitor, blocks FtsZ ring formation	[D] Cell cycle control, cell division, chromosome partitioning
PMI32_04475	-3.0929441	alkanesulfonate monooxygenase, FMNH(2)-dependent	[C] Energy production and conversion
PMI32_01125	-3.0966785	Cell division septal protein	[M] Cell wall/membrane/envelope biogenesis
PMI32_01132	-3.104508	taurine ABC transporter, periplasmic binding protein	[P] Inorganic ion transport and metabolism
PMI32_02982	-3.1069753	NADH:flavin oxidoreductases, Old Yellow Enzyme family	[C] Energy production and conversion
PMI32_04943	-3.1108027	Predicted SAM-dependent methyltransferase	[R] General function prediction only
PMI32_01852	-3.1215247	guanine deaminase	[R] General function prediction only, [F] Nucleotide transport and metabolism
PMI32_00463	-3.1233813	NADPH-dependent glutamate synthase beta chain and related oxidoreductases	[E] Amino acid transport and metabolism, [R] General function prediction only
PMI32_00148	-3.1445713	Predicted amidophosphoribosyltransferases	[R] General function prediction only
PMI32_01126	-3.1556201	cell division protein FtsA	[D] Cell cycle control, cell division, chromosome partitioning
PMI32_01303	-3.1664496	Acyl-CoA synthetases (AMP-forming)/AMP-acid ligases II	[Q] Secondary metabolites biosynthesis, transport and catabolism, [I] Lipid transport and metabolism
PMI32_00446	-3.1675216	hypothetical protein	
PMI32_05076	-3.167855	Transcriptional regulator	[K] Transcription
PMI32_01153	-3.1785782	HD domain.	
PMI32_02500	-3.1844393	Enoyl-[acyl-carrier-protein] reductase (NADH)	[I] Lipid transport and metabolism
PMI32_03577	-3.1848978	hypothetical protein	
PMI32_04227	-3.191841	Protein affecting phage T7 exclusion by the F plasmid	[R] General function prediction only
PMI32_01201	-3.2280611	NAD-dependent aldehyde dehydrogenases	[C] Energy production and conversion
PMI32_00894	-3.2310776	Uncharacterized protein conserved in bacteria	
PMI32_02790	-3.2340002	Uncharacterized protein conserved in bacteria	[S] Function unknown
PMI32_05354	-3.2390334	hypothetical protein	
PMI32_00893	-3.2435563	ATP-dependent protease La	[O] Posttranslational modification, protein turnover, chaperones
PMI32_03061	-3.2565095	Transcriptional regulators	[K] Transcription
PMI32_00771	-3.2683754	mannose-1-phosphate guanylyltransferase/mannose-6-phosphate isomerase	[M] Cell wall/membrane/envelope biogenesis
PMI32_03750	-3.2790296	Sugar kinases, ribokinase family	[G] Carbohydrate transport and metabolism
PMI32_04237	-3.2806623	endonuclease III	[L] Replication, recombination and repair
PMI32_00867	-3.2968404	hypothetical protein	
PMI32_03541	-3.318385	L-asparaginase/archaeal Glu-tRNAGln amidotransferase subunit D	[J] Translation, ribosomal structure and biogenesis, [E] Amino acid transport and metabolism
PMI32_05376	-3.3197903	Transcriptional regulator	[K] Transcription
PMI32_05771	-3.3268203	ribosomal protein S18	[J] Translation, ribosomal structure and biogenesis
PMI32_04451	-3.3581105	conserved hypothetical protein	[S] Function unknown
PMI32_04819	-3.3611707	Uncharacterized protein conserved in bacteria	[S] Function unknown
PMI32_05673	-3.3734676	Putative Mg2+ and Co2+ transporter CorC	[P] Inorganic ion transport and metabolism
PMI32_03473	-3.3747943	endoribonuclease L-PSP, putative	[J] Translation, ribosomal structure and biogenesis
PMI32_04414	-3.3756202	sulfur acquisition oxidoreductase, SfnB family	[I] Lipid transport and metabolism
PMI32_00955	-3.3774696	hypothetical protein	
PMI32_05479	-3.395094	Uncharacterized conserved protein	[S] Function unknown
PMI32_00466	-3.3955233	Uncharacterized protein, homolog of Cu	[R] General function prediction only

		resistance protein CopC	
PMI32_02216	-3.4056448	Integral membrane protein, interacts with FtsH	[R] General function prediction only
PMI32_02722	-3.4074949	Dehydrogenases with different specificities (related to short-chain alcohol dehydrogenases)	[R] General function prediction only, [Q] Secondary metabolites biosynthesis, transport and catabolism, [I] Lipid transport and metabolism
PMI32_04255	-3.4378044	MIP family channel proteins	[G] Carbohydrate transport and metabolism
PMI32_00519	-3.4629535	Fe-S cluster protector protein	[O] Posttranslational modification, protein turnover, chaperones, [C] Energy production and conversion
PMI32_03355	-3.4793489	tRNA_Undet_???	
PMI32_03948	-3.4921304	Conserved protein/domain typically associated with flavoprotein oxygenases, DIM6/NTAB family	[R] General function prediction only
PMI32_03125	-3.4988824	TonB-dependent siderophore receptor	[P] Inorganic ion transport and metabolism
PMI32_04503	-3.5028299	2-oxoglutarate dehydrogenase complex dihydrolipoamide succinyltransferase (E2 component)	[C] Energy production and conversion
PMI32_00254	-3.5189027	1-phosphofructokinase	[G] Carbohydrate transport and metabolism
PMI32_04067	-3.530135	ethanolamine permease	[E] Amino acid transport and metabolism
PMI32_01617	-3.5410125	ribosomal subunit interface protein	[J] Translation, ribosomal structure and biogenesis
PMI32_05219	-3.5452371	General secretion pathway protein M.	
PMI32_01422	-3.5859349	ABC-type sugar transport systems, ATPase components	[G] Carbohydrate transport and metabolism
PMI32_01589	-3.5972122	NAD-dependent aldehyde dehydrogenases	[C] Energy production and conversion
PMI32_04006	-3.5991672	ADP-ribosylglycohydrolase	[O] Posttranslational modification, protein turnover, chaperones
PMI32_01491	-3.6382407	DNA repair protein RecO	[L] Replication, recombination and repair
PMI32_02285	-3.6543629	Endonuclease I	[L] Replication, recombination and repair
PMI32_03733	-3.6564729	H-NS histone family.	
PMI32_01792	-3.6639434	Succinate dehydrogenase/fumarate reductase, flavoprotein subunit	[C] Energy production and conversion
PMI32_00804	-3.6642922	Taurine catabolism dioxygenase TauD, TfdA family.	
PMI32_02284	-3.6900973	Protein of unknown function (DUF1654).	
PMI32_04177	-3.6968067	Methyl-accepting chemotaxis protein	
PMI32_00520	-3.7098298	tRNA_Undet_???	
PMI32_03898	-3.721177	Transcriptional regulator	[K] Transcription
PMI32_04258	-3.7928155	Glycerol-3-phosphate dehydrogenase	[C] Energy production and conversion
PMI32_00674	-3.7956063	Uncharacterized protein conserved in bacteria	[S] Function unknown
PMI32_02610	-3.8000982	Protein of unknown function (DUF3015).	
PMI32_03065	-3.8205174	Uncharacterized conserved protein	[S] Function unknown
PMI32_05226	-3.8208863	Curli production assembly/transport component CsgF.	
PMI32_00940	-3.8264108	NADH:flavin oxidoreductases, Old Yellow Enzyme family	[C] Energy production and conversion
PMI32_04513	-3.8352177	uncharacterized domain 1	[Q] Secondary metabolites biosynthesis, transport and catabolism
PMI32_01137	-3.8500751	ABC transporter, substrate-binding protein, aliphatic sulfonates family	[P] Inorganic ion transport and metabolism
PMI32_03879	-3.9202534	Adenosylmethionine-8-amino-7-oxononanoate aminotransferase	[H] Coenzyme transport and metabolism
PMI32_04677	-3.9243509	6-phosphogluconolactonase	[G] Carbohydrate transport and metabolism
PMI32_02127	-3.932339	Membrane transporters of cations and cationic drugs	[P] Inorganic ion transport and metabolism
PMI32_01138	-3.9516508	alkanesulfonate monooxygenase, FMNH(2)-dependent	[C] Energy production and conversion
PMI32_02623	-3.9740715	Putative GTPases (G3E family)	[R] General function prediction only

PMI32_02181	-3.987655	penicillin-binding protein 2	[M] Cell wall/membrane/envelope biogenesis
PMI32_03416	-3.9895854	Prophage antirepressor	[K] Transcription
PMI32_01124	-4.0309062	D-alanine--D-alanine ligase	[M] Cell wall/membrane/envelope biogenesis
PMI32_01122	-4.0484888	undecaprenyldiphospho-muramoylpentapeptide beta-N-acetylglucosaminyltransferase	[M] Cell wall/membrane/envelope biogenesis
PMI32_03594	-4.0787508	hypothetical protein	
PMI32_01115	-4.1052813	cell division protein FtsL	[D] Cell cycle control, cell division, chromosome partitioning
PMI32_03508	-4.1068296	type VI secretion system lysozyme-related protein	[S] Function unknown
PMI32_02638	-4.1273185	hypothetical protein	
PMI32_04515	-4.1301012	Molecular chaperone, HSP90 family	[O] Posttranslational modification, protein turnover, chaperones
PMI32_04233	-4.1591597	electron transport complex, RnfABCDGE type, B subunit	
PMI32_03542	-4.160833	AraC-type DNA-binding domain-containing proteins	[K] Transcription
PMI32_01123	-4.1837075	UDP-N-acetylmuramate--alanine ligase	[M] Cell wall/membrane/envelope biogenesis
PMI32_03289	-4.1901044	non-ribosomal peptide synthase domain TIGR01720/amino acid adenylation domain	[Q] Secondary metabolites biosynthesis, transport and catabolism
PMI32_04017	-4.1983051	Predicted membrane protein	[S] Function unknown
PMI32_04522	-4.2551372	Amidases related to nicotinamidase	[Q] Secondary metabolites biosynthesis, transport and catabolism
PMI32_03554	-4.2931031	oxaloacetate decarboxylase alpha subunit	[C] Energy production and conversion
PMI32_01117	-4.2985464	UDP-N-acetylmuramyl-tripeptide synthetase	[M] Cell wall/membrane/envelope biogenesis
PMI32_03586	-4.4501871	Uncharacterized conserved protein	[S] Function unknown
PMI32_04678	-4.4602308	Entner-Doudoroff aldolase	[G] Carbohydrate transport and metabolism
PMI32_00673	-4.4905836	ATP-dependent protease HslVU, ATPase subunit	[O] Posttranslational modification, protein turnover, chaperones
PMI32_02477	-4.5048478	Uncharacterized protein conserved in bacteria	[S] Function unknown
PMI32_00208	-4.5217002	Disulfide bond formation protein DsbB	[O] Posttranslational modification, protein turnover, chaperones
PMI32_05380	-4.5283344	Predicted esterase of the alpha/beta hydrolase fold	[R] General function prediction only
PMI32_00385	-4.5809688	Outer membrane protein and related peptidoglycan-associated (lipo)proteins	[M] Cell wall/membrane/envelope biogenesis
PMI32_02272	-4.5931044	hypothetical protein	
PMI32_02213	-4.5964364	Universal stress protein UspA and related nucleotide-binding proteins	[T] Signal transduction mechanisms
PMI32_04348	-4.6201933	Pirin-related protein	[R] General function prediction only
PMI32_04226	-4.6867122	Co-chaperonin GroES (HSP10)	[O] Posttranslational modification, protein turnover, chaperones
PMI32_02717	-4.693933	catechol 1,2-dioxygenase, proteobacterial	[Q] Secondary metabolites biosynthesis, transport and catabolism
PMI32_00803	-4.7122276	branched-chain amino acid aminotransferase, group I	[E] Amino acid transport and metabolism, [H] Coenzyme transport and metabolism
PMI32_04225	-4.7297696	chaperonin GroL	[O] Posttranslational modification, protein turnover, chaperones
PMI32_01501	-4.8135535	Predicted transcriptional regulators	
PMI32_05452	-4.8462943	Uncharacterized protein conserved in bacteria	[S] Function unknown
PMI32_01120	-4.9839622	UDP-N-acetylmuramoylalanine--D-glutamate ligase	[M] Cell wall/membrane/envelope biogenesis
PMI32_00386	-5.0421406	hypothetical protein	
PMI32_00204	-5.0480876	TIGR02444 family protein	[S] Function unknown
PMI32_04325	-5.0586464	non-ribosomal peptide synthase domain TIGR01720/amino acid adenylation domain	[Q] Secondary metabolites biosynthesis, transport and catabolism
PMI32_00093	-5.1051981	exodeoxyribonuclease V, alpha subunit	[L] Replication, recombination and repair
PMI32_03291	-5.1614629	Acetyltransferases, including N-acetylases of ribosomal proteins	[J] Translation, ribosomal structure and biogenesis
PMI32_03051	-5.1840091	chaperone protein DnaJ	[O] Posttranslational modification, protein

			turnover, chaperones
PMI32_02415	-5.2714069	Membrane-associated lipoprotein involved in thiamine biosynthesis	[H] Coenzyme transport and metabolism
PMI32_03066	-5.4116125	FAD/FMN-containing dehydrogenases	[C] Energy production and conversion
PMI32_01669	-5.4310683	coenzyme PQQ biosynthesis protein B	[R] General function prediction only
PMI32_05910	-5.493499	Pyrroloquinoline quinone (Coenzyme PQQ) biosynthesis protein C	[H] Coenzyme transport and metabolism
PMI32_04238	-5.5252716	hypothetical protein	
PMI32_01420	-5.7054105	ABC-type sugar transport systems, permease components	[G] Carbohydrate transport and metabolism
PMI32_01424	-5.854918	D-xylulose kinase	[G] Carbohydrate transport and metabolism
PMI32_03050	-6.0216434	dihydrodipicolinate reductase	[E] Amino acid transport and metabolism
PMI32_02079	-6.2134368	Cold shock proteins	[K] Transcription
PMI32_01500	-6.2549188	Siderophore-interacting protein	[P] Inorganic ion transport and metabolism
PMI32_00672	-6.4254137	ATP-dependent protease HslVU, peptidase subunit	[O] Posttranslational modification, protein turnover, chaperones
PMI32_01421	-6.4725374	ABC-type sugar transport system, permease component	[G] Carbohydrate transport and metabolism
PMI32_01135	-6.5364556	Peroxiredoxin	[O] Posttranslational modification, protein turnover, chaperones
PMI32_05377	-6.5516044	TonB family C-terminal domain	[M] Cell wall/membrane/envelope biogenesis
PMI32_03052	-6.9712763	chaperone protein DnaK	[O] Posttranslational modification, protein turnover, chaperones
PMI32_00892	-6.9880088	Predicted secreted protein	[S] Function unknown
PMI32_01773	-7.0665199	Uncharacterized conserved protein	[S] Function unknown
PMI32_03729	-7.8030125	Peroxiredoxin	[O] Posttranslational modification, protein turnover, chaperones
PMI32_02716	-8.6359663	muconolactone delta-isomerase	[Q] Secondary metabolites biosynthesis, transport and catabolism
PMI32_01791	-9.2093828	Ferredoxin	[C] Energy production and conversion
PMI32_03117	-9.8043169	hypothetical protein	
PMI32_03032	-9.9563689	NAD-dependent aldehyde dehydrogenases	[C] Energy production and conversion
PMI32_05381	-10.98232	Response regulator containing CheY-like receiver, AAA-type ATPase, and DNA-binding domains	
PMI32_01419	-17.333727	ABC-type sugar transport system, periplasmic component	[G] Carbohydrate transport and metabolism
PMI32_02330	-107.25691	Molecular chaperone (small heat shock protein)	[O] Posttranslational modification, protein turnover, chaperones

Appendix D: List of up- and down-regulated DEGs in aged *Pseudomonas* sp. compared to control

Locus_ID	**regFC**	**Product_name**	**COG_category**
PMI32_02062	27.907922	23S rRNA. Bacterial LSU	
PMI32_02059	20.342892	16S rRNA. Bacterial SSU	
PMI32_01179	17.198652	copper-(or silver)-translocating P-type ATPase	[P] Inorganic ion transport and metabolism
PMI32_04093	16.265493	Tellurite resistance protein and related permeases	[P] Inorganic ion transport and metabolism
PMI32_02731	13.77936	NADH dehydrogenase, FAD-containing subunit	[C] Energy production and conversion
PMI32_04612	10.061276	Pirin-related protein	[R] General function prediction only
PMI32_03547	9.2127863	Transcriptional regulator	[K] Transcription
PMI32_02043	9.1580457	tryptophan synthase, beta subunit	[E] Amino acid transport and metabolism
PMI32_04280	8.8563037	5-methyltetrahydropteroyltriglutamate--	[E] Amino acid transport and metabolism

		homocysteine S-methyltransferase	
PMI32_01112	8.8193041	Bacterial RNase P class A	
PMI32_05766	8.6779882	tRNA_Undet_???	
PMI32_02064	8.4919696	5S rRNA. Bacterial TSU	
PMI32_00577	7.9619867	hypothetical protein	
PMI32_03727	7.570732	Plasmid replication region DNA-binding N-term.	
PMI32_00791	7.5288292	cytochrome o ubiquinol oxidase subunit II	[C] Energy production and conversion
PMI32_03724	7.4079771	hypothetical protein	
PMI32_00948	7.285079	hypothetical protein	
PMI32_05220	6.8022439	hypothetical protein	
PMI32_02082	6.6675371	glycine dehydrogenase (decarboxylating)	[E] Amino acid transport and metabolism
PMI32_03751	6.1274228	Xylose isomerase-like TIM barrel.	[G] Carbohydrate transport and metabolism
PMI32_00812	6.0534828	methionine-R-sulfoxide reductase	[O] Posttranslational modification, protein turnover, chaperones
PMI32_00707	5.9409274	ABC-type proline/glycine betaine transport systems, periplasmic components	[E] Amino acid transport and metabolism
PMI32_05027	5.9240873	Nitrate/nitrite transporter	[P] Inorganic ion transport and metabolism
PMI32_00680	5.897649	poly(hydroxyalkanoate) granule-associated protein	
PMI32_05602	5.6729277	Response regulator containing CheY-like receiver, AAA-type ATPase, and DNA-binding domains	
PMI32_01180	5.630369	aminoethylphosphonate catabolism associated LysR family transcriptional regulator	[K] Transcription
PMI32_04773	5.6175906	L-aminopeptidase/D-esterase	[Q] Secondary metabolites biosynthesis, transport and catabolism, [E] Amino acid transport and metabolism
PMI32_05307	5.5492443	hypothetical protein	
PMI32_04221	5.5035165	Methylase involved in ubiquinone/menaquinone biosynthesis	[H] Coenzyme transport and metabolism
PMI32_01524	5.4865669	Transcriptional regulator containing an amidase domain and an AraC-type DNA-binding HTH domain	[K] Transcription
PMI32_01500	5.439816	Siderophore-interacting protein	[P] Inorganic ion transport and metabolism
PMI32_04491	5.3824328	hypothetical protein	
PMI32_02083	5.2607948	glycine cleavage system H protein	[E] Amino acid transport and metabolism
PMI32_04416	5.0519793	FMN-dependent oxidoreductase, nitrilotriacetate monooxygenase family	[C] Energy production and conversion
PMI32_03748	5.0320024	Lactate dehydrogenase and related dehydrogenases	[R] General function prediction only, [H] Coenzyme transport and metabolism, [C] Energy production and conversion
PMI32_05026	4.9935959	Transcriptional regulators	[K] Transcription
PMI32_00708	4.9362393	Purine-cytosine permease and related proteins	[F] Nucleotide transport and metabolism
PMI32_05670	4.9338929	hypothetical protein	
PMI32_03716	4.9253041	O-6-methylguanine DNA methyltransferase	[F] Nucleotide transport and metabolism
PMI32_01423	4.8721903	Mannitol-1-phosphate/altronate dehydrogenases	[G] Carbohydrate transport and metabolism
PMI32_00480	4.841757	Zn-dependent hydrolases, including glyoxylases	[R] General function prediction only
PMI32_04620	4.8089723	2-keto-3-deoxy-6-phosphogluconate aldolase	[G] Carbohydrate transport and metabolism
PMI32_01304	4.7219988	PAS domain S-box	
PMI32_00795	4.6312619	protoheme IX farnesyltransferase	[O] Posttranslational modification, protein turnover, chaperones
PMI32_05475	4.6005409	Transcriptional regulators	[K] Transcription
PMI32_01453	4.589184	Hemoglobin-like flavoprotein	[C] Energy production and conversion
PMI32_02460	4.5721255	Uncharacterized conserved protein	[S] Function unknown

PMI32_03218	4.5671535	hypothetical protein	
PMI32_00178	4.5035363	glycerol-3-phosphate transporter	[G] Carbohydrate transport and metabolism
PMI32_04496	4.4831202	ABC-type metal ion transport system, periplasmic component/surface adhesin	[P] Inorganic ion transport and metabolism
PMI32_05357	4.4436246	drug resistance transporter, EmrB/QacA subfamily	[G] Carbohydrate transport and metabolism
PMI32_04061	4.3805683	Adenosylmethionine-8-amino-7-oxononanoate aminotransferase	[H] Coenzyme transport and metabolism
PMI32_03728	4.3782136	Site-specific recombinase XerD	[L] Replication, recombination and repair
PMI32_01272	4.3710837	RND family efflux transporter, MFP subunit	[M] Cell wall/membrane/envelope biogenesis
PMI32_02488	4.3518338	Arginine/lysine/ornithine decarboxylases	[E] Amino acid transport and metabolism
PMI32_00709	4.3469552	urocanate hydratase	[E] Amino acid transport and metabolism
PMI32_01819	4.2457671	acetyl-CoA acetyltransferases	[I] Lipid transport and metabolism
PMI32_02078	4.2123345	Predicted membrane protein/domain	[S] Function unknown
PMI32_02444	4.1891579	PAS domain S-box	[N] Cell motility, [T] Signal transduction mechanisms
PMI32_05023	4.1629599	nicotinate-nucleotide--dimethylbenzimidazole phosphoribosyltransferase	[H] Coenzyme transport and metabolism
PMI32_02465	4.1432766	Acyl-CoA dehydrogenases	[I] Lipid transport and metabolism
PMI32_00239	4.1295393	hypothetical protein	
PMI32_01820	4.1071638	3-hydroxyacyl-CoA dehydrogenase	[I] Lipid transport and metabolism
PMI32_03447	4.0327073	Uncharacterized conserved small protein	[S] Function unknown
PMI32_04451	4.0080396	conserved hypothetical protein	[S] Function unknown
PMI32_03901	4.0018742	Uncharacterized conserved small protein	[S] Function unknown
PMI32_03630	3.9434395	ribosomal protein S19, bacterial/organelle	[J] Translation, ribosomal structure and biogenesis
PMI32_03856	3.9290002	copper-(or silver)-translocating P-type ATPase	[P] Inorganic ion transport and metabolism
PMI32_04752	3.9208413	Threonine aldolase	[E] Amino acid transport and metabolism
PMI32_05029	3.913338	Glutathione peroxidase	[O] Posttranslational modification, protein turnover, chaperones
PMI32_05080	3.9121134	Thiol-disulfide isomerase and thioredoxins	[O] Posttranslational modification, protein turnover, chaperones, [C] Energy production and conversion
PMI32_04129	3.8969657	RNA polymerase sigma factor, sigma-70 family	[K] Transcription
PMI32_04279	3.8523797	Predicted hydrolases or acyltransferases (alpha/beta hydrolase superfamily)	[R] General function prediction only
PMI32_00793	3.8118102	cytochrome o ubiquinol oxidase, subunit III	[C] Energy production and conversion
PMI32_00327	3.8097699	flagellar motor switch protein FliN	[N] Cell motility, [U] Intracellular trafficking, secretion, and vesicular transport
PMI32_02272	3.7906826	hypothetical protein	
PMI32_02038	3.7698892	luciferase family oxidoreductase, group 1	[C] Energy production and conversion
PMI32_03760	3.7478669	Signal transduction histidine kinase	[T] Signal transduction mechanisms
PMI32_04601	3.7110836	Uncharacterized protein conserved in bacteria	[S] Function unknown
PMI32_03958	3.7066251	Protein of unknown function (DUF465).	
PMI32_00243	3.7021001	ABC-type proline/glycine betaine transport systems, permease component	[E] Amino acid transport and metabolism
PMI32_02181	3.687089	penicillin-binding protein 2	[M] Cell wall/membrane/envelope biogenesis
PMI32_02077	3.6764582	quinolinate synthetase complex, A subunit	[H] Coenzyme transport and metabolism
PMI32_01249	3.6489206	malonate decarboxylase, gamma subunit	
PMI32_05452	3.6433341	Uncharacterized protein conserved in bacteria	[S] Function unknown
PMI32_00792	3.6405187	cytochrome o ubiquinol oxidase, subunit I	[C] Energy production and conversion
PMI32_02806	3.6375685	Dehydrogenases with different specificities (related to short-chain alcohol dehydrogenases)	[I] Lipid transport and metabolism, [R] General function prediction only, [Q] Secondary metabolites biosynthesis, transport and catabolism

PMI32_04532	3.6341558	Monomeric isocitrate dehydrogenase	
PMI32_00656	3.5755863	Glutamate synthase domain 2	[E] Amino acid transport and metabolism
PMI32_03873	3.5566868	Uncharacterized ABC-type transport system, permease component	[R] General function prediction only
PMI32_00575	3.5383256	formate dehydrogenase family accessory protein FdhD	[C] Energy production and conversion
PMI32_01228	3.5348316	Cell wall-associated hydrolases (invasion-associated proteins)	[M] Cell wall/membrane/envelope biogenesis
PMI32_03182	3.5196159	Acetyltransferases	
PMI32_02036	3.5030144	Protein of unknown function (DUF1161).	
PMI32_01422	3.4974415	ABC-type sugar transport systems, ATPase components	[G] Carbohydrate transport and metabolism
PMI32_05346	3.4888484	ABC-type spermidine/putrescine transport system, permease component I	[E] Amino acid transport and metabolism
PMI32_00879	3.4714986	GMP synthase (glutamine-hydrolyzing), C-terminal domain or B subunit/GMP synthase (glutamine-hydrolyzing), N-terminal domain or A subunit	[F] Nucleotide transport and metabolism
PMI32_00171	3.4432344	hypothetical protein	
PMI32_02276	3.4405733	Ribokinase	[G] Carbohydrate transport and metabolism
PMI32_00706	3.424886	ABC-type proline/glycine betaine transport system, permease component	[E] Amino acid transport and metabolism
PMI32_05481	3.4122102	Membrane protease subunits, stomatin/prohibitin homologs	
PMI32_05832	3.3996496	RND family efflux transporter, MFP subunit	[M] Cell wall/membrane/envelope biogenesis
PMI32_05255	3.3531795	Predicted membrane protein	[S] Function unknown
PMI32_01271	3.3376374	The (Largely Gram-negative Bacterial) Hydrophobe/Amphiphile Efflux-1 (HAE1) Family	[V] Defense mechanisms
PMI32_03791	3.3315489	Urease accessory protein UreH	[O] Posttranslational modification, protein turnover, chaperones
PMI32_00788	3.3298705	Molybdopterin converting factor, large subunit	[H] Coenzyme transport and metabolism
PMI32_05586	3.3073062	Cyanate permease	[P] Inorganic ion transport and metabolism
PMI32_03848	3.2997279	Acyl dehydratase	[I] Lipid transport and metabolism
PMI32_05977	3.2935324	5-methyltetrahydrofolate--homocysteine methyltransferase	[E] Amino acid transport and metabolism
PMI32_00704	3.2740741	histidine ammonia-lyase	[E] Amino acid transport and metabolism
PMI32_00608	3.2457802	Uncharacterized protein conserved in bacteria	[S] Function unknown
PMI32_05247	3.239532	PAS domain S-box/diguanylate cyclase (GGDEF) domain	[T] Signal transduction mechanisms
PMI32_03859	3.2381195	drug resistance transporter, Bcr/CflA subfamily	[G] Carbohydrate transport and metabolism
PMI32_05229	3.2340178	FAD/FMN-containing dehydrogenases	
PMI32_02342	3.2127789	excinuclease ABC, B subunit	[L] Replication, recombination and repair
PMI32_01282	3.1949254	Glycine/D-amino acid oxidases (deaminating)	[E] Amino acid transport and metabolism
PMI32_04865	3.1943645	glycine betaine aldehyde dehydrogenase	[C] Energy production and conversion
PMI32_00614	3.1918796	Thioredoxin domain-containing protein	
PMI32_00163	3.1799648	hypothetical protein	
PMI32_00878	3.1754687	inosine-5'-monophosphate dehydrogenase	[F] Nucleotide transport and metabolism
PMI32_05062	3.174793	glucarate dehydratase	[M] Cell wall/membrane/envelope biogenesis, [R] General function prediction only
PMI32_05244	3.1728507	Pyruvate/2-oxoglutarate dehydrogenase complex, dihydrolipoamide acyltransferase (E2) component, and related enzymes	[C] Energy production and conversion
PMI32_00703	3.1715265	histidine ammonia-lyase	[E] Amino acid transport and metabolism
PMI32_00477	3.1711977	coenzyme PQQ biosynthesis protein B	[R] General function prediction only
PMI32_04281	3.163213	Transcriptional regulator	[K] Transcription
PMI32_04073	3.1510552	Short-chain dehydrogenases of various substrate specificities	[R] General function prediction only

PMI32_05992	3.1435437	ABC-type proline/glycine betaine transport systems, periplasmic components	[E] Amino acid transport and metabolism
PMI32_05838	3.1289645	hypothetical protein	
PMI32_00847	3.0994687	Predicted outer membrane lipoprotein	[S] Function unknown
PMI32_02306	3.0961684	RNA polymerase sigma factor, sigma-70 family	[K] Transcription
PMI32_04258	3.0850387	Glycerol-3-phosphate dehydrogenase	[C] Energy production and conversion
PMI32_03567	3.0732745	hypothetical protein	
PMI32_03235	3.0655815	Uncharacterized conserved protein	[S] Function unknown
PMI32_04234	3.0518776	electron transport complex, RnfABCDGE type, D subunit	[C] Energy production and conversion
PMI32_05708	3.050983	2-polyprenyl-6-methoxyphenol hydroxylase and related FAD-dependent oxidoreductases	[C] Energy production and conversion, [H] Coenzyme transport and metabolism
PMI32_01837	3.0417257	Cytosine/uracil/thiamine/allantoin permeases	[F] Nucleotide transport and metabolism, [H] Coenzyme transport and metabolism
PMI32_02204	3.028967	Threonine dehydrogenase and related Zn-dependent dehydrogenases	[R] General function prediction only, [E] Amino acid transport and metabolism
PMI32_03046	3.0142936	hypothetical protein	
PMI32_03348	3.0014552	hypothetical protein	
PMI32_04290	2.996447	His Kinase A (phosphoacceptor) domain./Histidine kinase-, DNA gyrase B-, and HSP90-like ATPase./Response regulator receiver domain.	
PMI32_01927	2.9950473	glucosamine--fructose-6-phosphate aminotransferase (isomerizing)	[M] Cell wall/membrane/envelope biogenesis
PMI32_03747	2.9918645	Aspartate/tyrosine/aromatic aminotransferase	[E] Amino acid transport and metabolism
PMI32_01701	2.9843324	DnaJ-domain-containing proteins 1	[O] Posttranslational modification, protein turnover, chaperones
PMI32_01152	2.9830252	ABC-type spermidine/putrescine transport system, permease component II	[E] Amino acid transport and metabolism
PMI32_05647	2.969881	Putative effector of murein hydrolase	[M] Cell wall/membrane/envelope biogenesis
PMI32_05239	2.962163	Predicted permeases	[R] General function prediction only
PMI32_02205	2.9569738	hypothetical protein	
PMI32_02334	2.9568071	Transcriptional regulator	[K] Transcription
PMI32_02977	2.9522343	aminoethylphosphonate catabolism associated LysR family transcriptional regulator	[K] Transcription
PMI32_01157	2.9520587	Lysophospholipase	[I] Lipid transport and metabolism
PMI32_03849	2.9044623	Dehydrogenases with different specificities (related to short-chain alcohol dehydrogenases)	[R] General function prediction only, [I] Lipid transport and metabolism, [Q] Secondary metabolites biosynthesis, transport and catabolism
PMI32_01256	2.8963501	Protein of unknown function (DUF2934).	
PMI32_02051	2.8948505	Uncharacterized conserved small protein	[S] Function unknown
PMI32_04449	2.8897151	Predicted RNA polymerase sigma factor containing a TPR repeat domain	[K] Transcription
PMI32_00147	2.8886037	biotin synthase	[H] Coenzyme transport and metabolism
PMI32_04072	2.8730255	beta-ketoacyl-acyl-carrier-protein synthase II	[I] Lipid transport and metabolism, [Q] Secondary metabolites biosynthesis, transport and catabolism
PMI32_01301	2.8569123	transporter, SSS family	[R] General function prediction only
PMI32_00794	2.855187	cytochrome o ubiquinol oxidase subunit IV	[C] Energy production and conversion
PMI32_00799	2.8409622	Putative translation initiation inhibitor, yjgF family	[J] Translation, ribosomal structure and biogenesis
PMI32_05069	2.837939	hypothetical protein	
PMI32_03335	2.831809	thiopurine S-methyltransferase, Se/Te detoxification family	
PMI32_02436	2.8164204	ABC transporter, permease/ATP-binding protein	[V] Defense mechanisms
PMI32_03549	2.81185	Acetyltransferases, including N-acetylases of ribosomal proteins	[J] Translation, ribosomal structure and biogenesis
PMI32_01684	2.8105806	putative glycoprotease GCP	[O] Posttranslational modification, protein

			turnover, chaperones
PMI32_02664	2.8016892	undecaprenyl diphosphate synthase	[I] Lipid transport and metabolism
PMI32_03189	2.79702	Nucleotidyltransferase/DNA polymerase involved in DNA repair	[L] Replication, recombination and repair
PMI32_05245	2.795289	dihydrolipoamide dehydrogenase	[C] Energy production and conversion
PMI32_00180	2.7917003	2-polyprenylphenol hydroxylase and related flavodoxin oxidoreductases	[H] Coenzyme transport and metabolism, [C] Energy production and conversion
PMI32_05591	2.7819059	Uncharacterized protein conserved in bacteria	[S] Function unknown
PMI32_02696	2.7746279	Uncharacterized protein conserved in bacteria	[S] Function unknown
PMI32_05398	2.771779	Protein of unknown function (DUF3182).	
PMI32_04934	2.7690582	cation diffusion facilitator family transporter	[P] Inorganic ion transport and metabolism
PMI32_02573	2.7686948	ATP-dependent chaperone ClpB	[O] Posttranslational modification, protein turnover, chaperones
PMI32_01397	2.7615813	acetyl-CoA acetyltransferases	[I] Lipid transport and metabolism
PMI32_00810	2.7536299	His Kinase A (phosphoacceptor) domain./Histidine kinase-, DNA gyrase B-, and HSP90-like ATPase./HAMP domain.	
PMI32_04054	2.7533729	Uncharacterized conserved protein	[S] Function unknown
PMI32_03900	2.7422699	Transcriptional regulator	[K] Transcription
PMI32_01654	2.7360277	hypothetical protein	
PMI32_01611	2.7354497	hypothetical protein	
PMI32_05019	2.7315162	cobalamin biosynthesis protein CobD	[H] Coenzyme transport and metabolism
PMI32_02004	2.7281112	ABC-type Mn/Zn transport systems, ATPase component	[P] Inorganic ion transport and metabolism
PMI32_03844	2.7149424	hypothetical protein	
PMI32_03298	2.7106956	Enoyl-CoA hydratase/carnithine racemase	[I] Lipid transport and metabolism
PMI32_03469	2.7021399	TIGR00255 family protein	[S] Function unknown
PMI32_03925	2.6875012	Putative threonine efflux protein	[E] Amino acid transport and metabolism
PMI32_03637	2.6840465	ribosomal protein L24, bacterial/organelle	[J] Translation, ribosomal structure and biogenesis
PMI32_03546	2.6697304	Transcriptional regulators containing a DNA-binding HTH domain and an aminotransferase domain (MocR family) and their eukaryotic orthologs	[K] Transcription, [E] Amino acid transport and metabolism
PMI32_03101	2.6676099	Predicted dienelactone hydrolase	[R] General function prediction only
PMI32_02695	2.6620891	MIP family channel proteins	[G] Carbohydrate transport and metabolism
PMI32_03445	2.6520732	Predicted Fe-S-cluster oxidoreductase	
PMI32_04608	2.6510363	Hydrolases of the alpha/beta superfamily	[R] General function prediction only
PMI32_01774	2.6478994	hypothetical protein	
PMI32_03449	2.6386639	Phosphatidylserine/phosphatidylglycerophosphate/cardiolipin synthases and related enzymes	[I] Lipid transport and metabolism
PMI32_00445	2.6354711	Signal transduction histidine kinase	[T] Signal transduction mechanisms
PMI32_04694	2.6213909	hypothetical protein	
PMI32_04866	2.6191188	choline dehydrogenase	[E] Amino acid transport and metabolism
PMI32_05243	2.6183063	Pyruvate/2-oxoglutarate dehydrogenase complex, dehydrogenase (E1) component, eukaryotic type, beta subunit	[C] Energy production and conversion
PMI32_04055	2.6153139	Uncharacterized protein conserved in bacteria	[S] Function unknown
PMI32_01277	2.6115617	phosphoglucomutase, alpha-D-glucose phosphate-specific	[G] Carbohydrate transport and metabolism
PMI32_00149	2.60722	ModE molybdate transport repressor domain/molybdenum-pterin binding domain	[R] General function prediction only
PMI32_04042	2.5999305	hydro-lyases, Fe-S type, tartrate/fumarate subfamily, alpha region/hydro-lyases, Fe-S type, tartrate/fumarate subfamily, beta region	[C] Energy production and conversion
PMI32_02536	2.5891675	Protein of unknown function (DUF2790).	

PMI32_03808	2.5818793	precorrin-6y C5,15-methyltransferase (decarboxylating), CbiE subunit/precorrin-6Y C5,15-methyltransferase (decarboxylating), CbiT subunit	[H] Coenzyme transport and metabolism
PMI32_02080	2.5786446	glycine cleavage system T protein	[E] Amino acid transport and metabolism
PMI32_04914	2.578514	Transcriptional regulator	[K] Transcription
PMI32_02445	2.5762475	Predicted hydrolase of the alpha/beta-hydrolase fold	[R] General function prediction only
PMI32_01212	2.5726905	alternative sigma factor RpoH	[K] Transcription
PMI32_01961	2.5667425	methionyl-tRNA formyltransferase	[J] Translation, ribosomal structure and biogenesis
PMI32_04183	2.5666067	Integrase	
PMI32_05050	2.5649153	Predicted permeases	[R] General function prediction only
PMI32_04536	2.5546455	adenylosuccinate lyase	[F] Nucleotide transport and metabolism
PMI32_01174	2.543473	Uncharacterized conserved protein	[S] Function unknown
PMI32_00513	2.5400438	imidazole glycerol phosphate synthase, glutamine amidotransferase subunit	[E] Amino acid transport and metabolism
PMI32_05278	2.5233851	Signal transduction histidine kinase	[T] Signal transduction mechanisms
PMI32_05277	2.5169084	Response regulator containing CheY-like receiver, AAA-type ATPase, and DNA-binding domains	[T] Signal transduction mechanisms
PMI32_04687	2.5106573	Lysophospholipase	[I] Lipid transport and metabolism
PMI32_05932	2.5100934	Periplasmic serine proteases (ClpP class)	[O] Posttranslational modification, protein turnover, chaperones, [U] Intracellular trafficking, secretion, and vesicular transport
PMI32_02044	2.5080637	tryptophan synthase, alpha subunit	[E] Amino acid transport and metabolism
PMI32_03144	2.5079459	Protein related to penicillin acylase	[R] General function prediction only
PMI32_05526	2.5031888	Predicted Zn-dependent hydrolases of the beta-lactamase fold	[R] General function prediction only
PMI32_05897	2.4986577	Choline dehydrogenase and related flavoproteins	[E] Amino acid transport and metabolism
PMI32_05079	2.4917876	Protein-disulfide isomerase	[O] Posttranslational modification, protein turnover, chaperones
PMI32_02636	2.4913493	Arabinose efflux permease	[G] Carbohydrate transport and metabolism
PMI32_01606	2.4897668	Predicted Zn-dependent proteases and their inactivated homologs	[R] General function prediction only
PMI32_02842	2.4817424	arsenate reductase (glutaredoxin)	[P] Inorganic ion transport and metabolism
PMI32_05831	2.4657171	Cation/multidrug efflux pump	[V] Defense mechanisms
PMI32_03448	2.4458728	Transcriptional regulators containing a DNA-binding HTH domain and an aminotransferase domain (MocR family) and their eukaryotic orthologs	[K] Transcription, [E] Amino acid transport and metabolism
PMI32_04007	2.445368	Purine-cytosine permease and related proteins	[F] Nucleotide transport and metabolism
PMI32_01491	2.4446556	DNA repair protein RecO	[L] Replication, recombination and repair
PMI32_03432	2.4430046	Methyl-accepting chemotaxis protein	[T] Signal transduction mechanisms, [N] Cell motility
PMI32_02732	2.4403311	Glycine/D-amino acid oxidases (deaminating)	[E] Amino acid transport and metabolism
PMI32_01273	2.4403282	Transcriptional regulator	[K] Transcription
PMI32_01808	2.4389041	Methyl-accepting chemotaxis protein	[T] Signal transduction mechanisms, [N] Cell motility
PMI32_03184	2.4361486	K+ transporter	[P] Inorganic ion transport and metabolism
PMI32_04744	2.4127201	Mg2+ transporter (mgtE)	[P] Inorganic ion transport and metabolism
PMI32_00786	2.4125944	molybdenum cofactor biosynthesis protein MoaC	[H] Coenzyme transport and metabolism
PMI32_03055	2.4043646	Fe2+/Zn2+ uptake regulation proteins	[P] Inorganic ion transport and metabolism
PMI32_02273	2.4030556	NAD-dependent protein deacetylases, SIR2 family	[K] Transcription
PMI32_04911	2.4015238	ABC-type proline/glycine betaine transport systems, periplasmic components	[E] Amino acid transport and metabolism

PMI32_00974	2.3983464	Predicted outer membrane protein	[S] Function unknown
PMI32_05081	2.3954559	Thiol:disulfide interchange protein	[O] Posttranslational modification, protein turnover, chaperones, [C] Energy production and conversion
PMI32_03393	2.3875888	pseudouridine synthase	[J] Translation, ribosomal structure and biogenesis
PMI32_03806	2.3735729	Precorrin-6x reductase	[H] Coenzyme transport and metabolism
PMI32_03047	2.3734016	transcription elongation factor GreA	[K] Transcription
PMI32_05550	2.3689039	Protein of unknown function (DUF2790).	
PMI32_04541	2.3651409	NADH:ubiquinone oxidoreductase subunit 3 (chain A)	[C] Energy production and conversion
PMI32_03803	2.3585319	Protein of unknown function (DUF2946).	
PMI32_03317	2.3568648	Ammonia permease	[P] Inorganic ion transport and metabolism
PMI32_05273	2.351675	ABC-type transport system, involved in lipoprotein release, permease component	[M] Cell wall/membrane/envelope biogenesis
PMI32_02430	2.3511071	fatty oxidation complex, beta subunit FadA	[I] Lipid transport and metabolism
PMI32_05690	2.3501821	cation diffusion facilitator family transporter	[P] Inorganic ion transport and metabolism
PMI32_05707	2.3446055	Delta-aminolevulinic acid dehydratase	[H] Coenzyme transport and metabolism
PMI32_04466	2.3445246	Short-chain alcohol dehydrogenase of unknown specificity	[R] General function prediction only
PMI32_04220	2.3407495	Lipopolysaccharide kinase (Kdo/WaaP) family.	
PMI32_00726	2.3401872	TonB-dependent siderophore receptor	[P] Inorganic ion transport and metabolism
PMI32_05686	2.339246	Protein of unknown function (DUF2788).	
PMI32_04086	2.3375889	S-methyl-5-thioribose-1-phosphate isomerase	[J] Translation, ribosomal structure and biogenesis
PMI32_04348	2.3368703	Pirin-related protein	[R] General function prediction only
PMI32_00921	2.3334675	Acyl CoA:acetate/3-ketoacid CoA transferase, alpha subunit	[I] Lipid transport and metabolism
PMI32_00129	2.3304887	dihydroxy-acid dehydratase	[G] Carbohydrate transport and metabolism, [E] Amino acid transport and metabolism
PMI32_03349	2.3293369	hypothetical protein	
PMI32_00207	2.327399	Regulator of sigma D	[K] Transcription
PMI32_03938	2.3248321	Lysophospholipase	[I] Lipid transport and metabolism
PMI32_03782	2.3243914	DnaJ-class molecular chaperone with C-terminal Zn finger domain	[O] Posttranslational modification, protein turnover, chaperones
PMI32_04322	2.3210209	non-ribosomal peptide synthase domain TIGR01720/amino acid adenylation domain	[Q] Secondary metabolites biosynthesis, transport and catabolism
PMI32_04223	2.3169106	Response regulators consisting of a CheY-like receiver domain and a winged-helix DNA-binding domain	[K] Transcription, [T] Signal transduction mechanisms
PMI32_05117	2.306826	3-hydroxybutyrate dehydrogenase	[Q] Secondary metabolites biosynthesis, transport and catabolism, [I] Lipid transport and metabolism, [R] General function prediction only
PMI32_03722	2.3040739	hypothetical protein	
PMI32_04667	2.2962322	hypothetical protein	
PMI32_02479	2.2931016	Calcineurin-like phosphoesterase.	
PMI32_04525	2.2871805	Transcriptional regulator	[K] Transcription
PMI32_01605	2.280251	Predicted amidohydrolase	[R] General function prediction only
PMI32_00654	2.2761149	uroporphyrinogen decarboxylase	[H] Coenzyme transport and metabolism
PMI32_03116	2.2747617	Response regulator containing CheY-like receiver, AAA-type ATPase, and DNA-binding domains	[T] Signal transduction mechanisms
PMI32_00226	2.2730964	tyrosine recombinase XerC	[L] Replication, recombination and repair
PMI32_00738	2.2688602	Uncharacterized conserved protein	[S] Function unknown
PMI32_01857	2.2665972	PAS domain S-box/diguanylate cyclase (GGDEF) domain	

PMI32_05921	2.2642811	hypothetical protein	
PMI32_04864	2.2626985	transcriptional repressor BetI	[K] Transcription
PMI32_05680	2.2612761	thiamine-phosphate pyrophosphorylase	[H] Coenzyme transport and metabolism
PMI32_05209	2.2561661	ATP-dependent Clp protease ATP-binding subunit clpA	[O] Posttranslational modification, protein turnover, chaperones
PMI32_01659	2.2521158	Dehydrogenases with different specificities (related to short-chain alcohol dehydrogenases)	[Q] Secondary metabolites biosynthesis, transport and catabolism, [R] General function prediction only, [I] Lipid transport and metabolism
PMI32_05111	2.2485594	Predicted amino acid aldolase or racemase	[E] Amino acid transport and metabolism
PMI32_01763	2.2445473	Glycine/D-amino acid oxidases (deaminating)	[E] Amino acid transport and metabolism
PMI32_00621	2.2363875	Acyl-coenzyme A synthetases/AMP-(fatty) acid ligases	[I] Lipid transport and metabolism
PMI32_04092	2.2280519	1-acyl-sn-glycerol-3-phosphate acyltransferase	[I] Lipid transport and metabolism
PMI32_03996	2.2261615	Molybdenum cofactor biosynthesis enzyme	[H] Coenzyme transport and metabolism
PMI32_03453	2.2258151	ribosomal protein L33, bacterial type	[J] Translation, ribosomal structure and biogenesis
PMI32_00146	2.2231939	8-amino-7-oxononanoate synthase	[H] Coenzyme transport and metabolism
PMI32_04008	2.2230133	Sugar kinases, ribokinase family	[G] Carbohydrate transport and metabolism
PMI32_05689	2.2205097	hypothetical protein	
PMI32_03812	2.2157577	precorrin-2 C20-methyltransferase	[H] Coenzyme transport and metabolism
PMI32_02820	2.2154861	hypothetical protein	
PMI32_02438	2.2130613	Phosphoglycerate dehydrogenase and related dehydrogenases	[H] Coenzyme transport and metabolism, [E] Amino acid transport and metabolism
PMI32_03389	2.2052392	Predicted metal-dependent phosphoesterases (PHP family)	[R] General function prediction only
PMI32_02203	2.1980429	Universal stress protein UspA and related nucleotide-binding proteins	[T] Signal transduction mechanisms
PMI32_02505	2.1844809	Aerobic-type carbon monoxide dehydrogenase, large subunit CoxL/CutL homologs	[C] Energy production and conversion
PMI32_03294	2.1818941	Protein of unknown function (DUF1446).	
PMI32_02311	2.1796775	Dehydrogenases with different specificities (related to short-chain alcohol dehydrogenases)	[Q] Secondary metabolites biosynthesis, transport and catabolism, [R] General function prediction only, [I] Lipid transport and metabolism
PMI32_01253	2.179497	malonate transporter, MadM subunit	
PMI32_03396	2.1776279	Arabinose efflux permease	[G] Carbohydrate transport and metabolism
PMI32_04666	2.1728057	tRNA_Undet_???	
PMI32_03314	2.1657553	hypothetical protein	
PMI32_01464	2.1622893	cyanate transporter	[P] Inorganic ion transport and metabolism
PMI32_00452	2.1570136	serine transporter	[E] Amino acid transport and metabolism
PMI32_05205	2.1530011	isocitrate dehydrogenase, NADP-dependent, monomeric type	[C] Energy production and conversion
PMI32_05695	2.1467211	Transcriptional regulator	[K] Transcription
PMI32_00877	2.1458357	hypothetical protein	
PMI32_01966	2.1437853	NADPH:quinone reductase and related Zn-dependent oxidoreductases	[C] Energy production and conversion, [R] General function prediction only
PMI32_01769	2.141244	ABC-type spermidine/putrescine transport system, permease component II	[E] Amino acid transport and metabolism
PMI32_00971	2.1357578	Putative threonine efflux protein	[E] Amino acid transport and metabolism
PMI32_01226	2.1343573	pyridoxal phosphate enzyme, YggS family	[R] General function prediction only
PMI32_01294	2.1328234	Rad3-related DNA helicases	[K] Transcription, [L] Replication, recombination and repair
PMI32_05343	2.1294297	AraC-type DNA-binding domain-containing proteins	[K] Transcription
PMI32_03636	2.1282896	ribosomal protein L14, bacterial/organelle	[J] Translation, ribosomal structure and biogenesis
PMI32_01038	2.1245136	peptidyl-tRNA hydrolase	[J] Translation, ribosomal structure and biogenesis

PMI32_04804	2.1226206	3-methyl-2-oxobutanoate hydroxymethyltransferase	[H] Coenzyme transport and metabolism
PMI32_02913	2.1207882	Predicted membrane protein	[S] Function unknown
PMI32_00639	2.1173043	Transcriptional regulator	[K] Transcription
PMI32_02655	2.117052	Predicted metalloprotease	[R] General function prediction only
PMI32_01497	2.1080218	Carbohydrate-selective porin	[M] Cell wall/membrane/envelope biogenesis
PMI32_00712	2.1050751	formiminoglutamate deiminase	[R] General function prediction only, [F] Nucleotide transport and metabolism
PMI32_05652	2.094731	gamma-glutamyl phosphate reductase	[E] Amino acid transport and metabolism
PMI32_02816	2.0907296	Predicted hydrolases or acyltransferases (alpha/beta hydrolase superfamily)	[R] General function prediction only
PMI32_00273	2.0843912	Uncharacterized protein conserved in bacteria	[S] Function unknown
PMI32_05358	2.082969	hypothetical protein	
PMI32_00181	2.0818024	UbiD family decarboxylases	[H] Coenzyme transport and metabolism
PMI32_02635	2.0813845	Cytochrome bd-type quinol oxidase, subunit 1	[C] Energy production and conversion
PMI32_02760	2.079643	monovalent cation/proton antiporter, MnhG/PhaG subunit	[P] Inorganic ion transport and metabolism
PMI32_03820	2.0779459	putative TIM-barrel protein, nifR3 family	[J] Translation, ribosomal structure and biogenesis
PMI32_02431	2.0751024	fatty oxidation complex, alpha subunit FadB	[I] Lipid transport and metabolism
PMI32_00900	2.0711862	phosphoribosylglycinamide formyltransferase 2	[F] Nucleotide transport and metabolism
PMI32_05617	2.064713	Protein of unknown function VcgC/VcgE (DUF2780).	
PMI32_04068	2.0631606	Protein of unknown function (DUF2897).	
PMI32_01633	2.0628137	histidinol-phosphate aminotransferase	[E] Amino acid transport and metabolism
PMI32_03119	2.0614383	Na+/H+ antiporter	[P] Inorganic ion transport and metabolism
PMI32_03923	2.0522793	putative urate catabolism protein	[G] Carbohydrate transport and metabolism
PMI32_01138	2.0500809	alkanesulfonate monooxygenase, FMNH(2)-dependent	[C] Energy production and conversion
PMI32_00361	2.0462477	Predicted amidohydrolase	
PMI32_03384	2.0415929	P pilus assembly/Cpx signaling pathway, periplasmic inhibitor/zinc-resistance associated protein	[P] Inorganic ion transport and metabolism, [T] Signal transduction mechanisms, [U] Intracellular trafficking, secretion, and vesicular transport, [N] Cell motility
PMI32_02518	2.0395304	O-6-methylguanine DNA methyltransferase	[F] Nucleotide transport and metabolism
PMI32_01608	2.0391623	Predicted Zn-dependent proteases and their inactivated homologs	[R] General function prediction only
PMI32_03289	2.034198	non-ribosomal peptide synthase domain TIGR01720/amino acid adenylation domain	[Q] Secondary metabolites biosynthesis, transport and catabolism
PMI32_04881	2.030022	hypothetical protein	
PMI32_03434	2.0227669	putative efflux protein, MATE family	[V] Defense mechanisms
PMI32_03027	2.0224576	NAD-dependent aldehyde dehydrogenases	[C] Energy production and conversion
PMI32_00655	2.020503	glutamate synthase small subunit family protein, proteobacterial	[R] General function prediction only, [E] Amino acid transport and metabolism
PMI32_02093	2.0148455	Methyl-accepting chemotaxis protein	[T] Signal transduction mechanisms, [N] Cell motility
PMI32_04450	2.0109333	Uncharacterized protein conserved in bacteria	[S] Function unknown
PMI32_03644	2.0095289	ribosomal protein L30, bacterial/organelle	[J] Translation, ribosomal structure and biogenesis
PMI32_04674	2.0053287	Uncharacterized enzymes related to aldose 1-epimerase	[G] Carbohydrate transport and metabolism
PMI32_01421	2.0024692	ABC-type sugar transport system, permease component	[G] Carbohydrate transport and metabolism
PMI32_02223	2.0018582	Response regulators consisting of a CheY-like receiver domain and a winged-helix DNA-binding domain	[T] Signal transduction mechanisms, [K] Transcription
PMI32_05208	1.9988469	Uncharacterized conserved protein	[S] Function unknown
PMI32_03699	1.9956446	glucokinase, proteobacterial type	[G] Carbohydrate transport and metabolism

PMI32_01603	1.9914241	ribonuclease, Rne/Rng family	[J] Translation, ribosomal structure and biogenesis
PMI32_05624	1.9858284	Glycine/serine hydroxymethyltransferase	[E] Amino acid transport and metabolism
PMI32_01098	1.9844408	Acyl-CoA dehydrogenases	[I] Lipid transport and metabolism
PMI32_00705	1.9821632	glycine betaine/L-proline transport ATP binding subunit	
PMI32_05447	1.9821277	Uncharacterized FAD-dependent dehydrogenases	[R] General function prediction only
PMI32_00387	1.9796752	hypothetical protein	
PMI32_02439	1.9737228	putative efflux protein, MATE family	[V] Defense mechanisms
PMI32_01533	1.9699644	Predicted hydrolases or acyltransferases (alpha/beta hydrolase superfamily)	[R] General function prediction only
PMI32_05479	1.9692949	Uncharacterized conserved protein	[S] Function unknown
PMI32_05983	1.966485	Probable cobalt transporter subunit (CbtB).	
PMI32_02418	1.9645516	transcription-repair coupling factor (mfd)	[L] Replication, recombination and repair, [K] Transcription
PMI32_00842	1.964319	S-adenosylmethionine:tRNA ribosyltransferase-isomerase	[J] Translation, ribosomal structure and biogenesis
PMI32_00918	1.9640609	hypothetical protein	
PMI32_04128	1.9587152	Catalase	
PMI32_04457	1.9579585	Aspartate/tyrosine/aromatic aminotransferase	[E] Amino acid transport and metabolism
PMI32_01213	1.9531447	monofunctional biosynthetic peptidoglycan transglycosylase	
PMI32_04882	1.9522817	3-phosphoglycerate kinase	[G] Carbohydrate transport and metabolism
PMI32_05880	1.9512171	Nitrate/nitrite transporter	[P] Inorganic ion transport and metabolism
PMI32_03402	1.9511271	Transcriptional regulator of aromatic amino acids metabolism	[K] Transcription, [E] Amino acid transport and metabolism
PMI32_00375	1.9499039	NAD binding domain of 6-phosphogluconate dehydrogenase.	
PMI32_03228	1.9495323	MoxR-like ATPases	[R] General function prediction only
PMI32_02593	1.9423407	riboflavin kinase/FMN adenylyltransferase	[H] Coenzyme transport and metabolism
PMI32_02666	1.9414964	1-deoxy-D-xylulose 5-phosphate reductoisomerase	[I] Lipid transport and metabolism
PMI32_03801	1.9408055	Uncharacterized iron-regulated membrane protein	[S] Function unknown
PMI32_01432	1.9342136	Protein of unknown function (DUF1652).	
PMI32_00920	1.9323417	benzoate transport	[G] Carbohydrate transport and metabolism
PMI32_00927	1.9282469	3-carboxy-cis,cis-muconate cycloisomerase	[F] Nucleotide transport and metabolism
PMI32_01804	1.921673	hypothetical protein	
PMI32_02617	1.9156361	Glycine/serine hydroxymethyltransferase	[E] Amino acid transport and metabolism
PMI32_01239	1.9142915	Chemotaxis signal transduction protein	[N] Cell motility, [T] Signal transduction mechanisms
PMI32_00249	1.9139065	Sulfite reductase, alpha subunit (flavoprotein)	[P] Inorganic ion transport and metabolism
PMI32_03628	1.9108281	Ribosomal protein L23	[J] Translation, ribosomal structure and biogenesis
PMI32_01434	1.9101018	threonine ammonia-lyase, biosynthetic, long form	[E] Amino acid transport and metabolism
PMI32_05338	1.9094904	ABC-type multidrug transport system, ATPase and permease components	[V] Defense mechanisms
PMI32_03467	1.9075046	Uncharacterized protein conserved in bacteria	[S] Function unknown
PMI32_01237	1.9073209	Response regulators consisting of a CheY-like receiver domain and a winged-helix DNA-binding domain	
PMI32_01060	1.9016882	Uncharacterized conserved protein	[S] Function unknown
PMI32_02798	1.9008189	Protein of unknown function (DUF721).	
PMI32_04879	1.8998016	fructose-bisphosphate aldolase, class II, Calvin cycle subtype	[G] Carbohydrate transport and metabolism
PMI32_03378	1.8989174	Predicted HD phosphohydrolase	[R] General function prediction only

PMI32_02599	1.8974392	ribosomal protein L27	[J] Translation, ribosomal structure and biogenesis
PMI32_00257	1.8939773	hydrolase, TatD family	[L] Replication, recombination and repair
PMI32_03295	1.8908243	Dehydrogenases with different specificities (related to short-chain alcohol dehydrogenases)	[Q] Secondary metabolites biosynthesis, transport and catabolism, [R] General function prediction only, [I] Lipid transport and metabolism
PMI32_03411	1.8878144	hypothetical protein	
PMI32_01874	1.8870805	RraA family	[H] Coenzyme transport and metabolism
PMI32_01011	1.8856615	hypothetical protein	
PMI32_00926	1.8841844	metabolite-proton symporter	[G] Carbohydrate transport and metabolism
PMI32_02312	1.8818155	O-succinylhomoserine sulfhydrylase	[E] Amino acid transport and metabolism
PMI32_05097	1.8796725	riboflavin biosynthesis protein RibD	[H] Coenzyme transport and metabolism
PMI32_05978	1.8750633	Fatty acid cis/trans isomerase (CTI).	
PMI32_01835	1.8720179	Transcriptional regulator	[K] Transcription
PMI32_03517	1.8715644	Rubredoxin	[C] Energy production and conversion
PMI32_05400	1.8685484	Predicted integral membrane protein	[S] Function unknown
PMI32_02843	1.8664989	NAD(P)H:quinone oxidoreductase, type IV	[R] General function prediction only
PMI32_05653	1.8655183	nicotinate (nicotinamide) nucleotide adenylyltransferase	[H] Coenzyme transport and metabolism
PMI32_05886	1.8651198	Dehydrogenases with different specificities (related to short-chain alcohol dehydrogenases)	[Q] Secondary metabolites biosynthesis, transport and catabolism, [R] General function prediction only, [I] Lipid transport and metabolism
PMI32_01139	1.8649456	ABC-type nitrate/sulfonate/bicarbonate transport system, permease component	[P] Inorganic ion transport and metabolism
PMI32_02625	1.8607977	Carbon starvation protein, predicted membrane protein	[T] Signal transduction mechanisms
PMI32_01856	1.8592518	D-alanyl-D-alanine carboxypeptidase, serine-type, PBP4 family	[M] Cell wall/membrane/envelope biogenesis
PMI32_04053	1.8588315	DNA polymerase III, epsilon subunit and related 3'-5' exonucleases	[L] Replication, recombination and repair
PMI32_04085	1.8587018	DNA gyrase, A subunit	[L] Replication, recombination and repair
PMI32_05114	1.8577693	PAS domain S-box	
PMI32_00342	1.8533886	Chemotaxis protein histidine kinase and related kinases	[N] Cell motility, [T] Signal transduction mechanisms
PMI32_00195	1.8528144	Uncharacterized protein conserved in bacteria	[S] Function unknown
PMI32_03629	1.8514209	ribosomal protein L2, bacterial/organellar	[J] Translation, ribosomal structure and biogenesis
PMI32_02614	1.8505533	Glutamate dehydrogenase/leucine dehydrogenase	[E] Amino acid transport and metabolism
PMI32_02333	1.8495021	Esterase/lipase	[R] General function prediction only
PMI32_01071	1.8417351	malate:quinone-oxidoreductase	[R] General function prediction only
PMI32_03458	1.839055	deoxyuridine 5'-triphosphate nucleotidohydrolase (dut)	[F] Nucleotide transport and metabolism
PMI32_00036	1.838612	integration host factor, alpha subunit	[L] Replication, recombination and repair
PMI32_03919	1.8373471	Predicted membrane protein	[S] Function unknown
PMI32_04538	1.8367465	Predicted acyltransferase	[R] General function prediction only
PMI32_05599	1.8342739	rarD protein	[R] General function prediction only
PMI32_05409	1.8311612	SOS regulatory protein LexA	[K] Transcription, [T] Signal transduction mechanisms
PMI32_03049	1.8303344	carbamoyl-phosphate synthase, small subunit	[E] Amino acid transport and metabolism, [F] Nucleotide transport and metabolism
PMI32_03465	1.829935	exodeoxyribonuclease III (xth)	[L] Replication, recombination and repair
PMI32_01635	1.8288888	dinuclear metal center protein, YbgI/SA1388 family	[S] Function unknown
PMI32_01409	1.8287765	Response regulator containing CheY-like receiver, AAA-type ATPase, and DNA-binding domains	

PMI32_01596	1.8282174	aspartyl/glutamyl-tRNA(Asn/Gln) amidotransferase, B subunit	[J] Translation, ribosomal structure and biogenesis
PMI32_03464	1.8275213	orotate phosphoribosyltransferase	[F] Nucleotide transport and metabolism
PMI32_04421	1.8237847	Methyltransferase domain.	
PMI32_03768	1.8172175	Predicted metal-binding protein	[R] General function prediction only
PMI32_04013	1.809493	hypothetical protein	
PMI32_01494	1.8066037	phosphoribosylformylglycinamidine synthase, single chain form	[F] Nucleotide transport and metabolism
PMI32_01002	1.8065982	hypothetical protein	
PMI32_05692	1.8039891	ATP-dependent helicase HrpB	[L] Replication, recombination and repair
PMI32_05994	1.8015943	hypothetical protein	
PMI32_05405	1.8001888	Lhr-like helicases	[R] General function prediction only
PMI32_01575	1.7970446	heme exporter protein CcmD	[U] Intracellular trafficking, secretion, and vesicular transport
PMI32_03460	1.7959352	acetylglutamate kinase	[E] Amino acid transport and metabolism
PMI32_03250	1.7958247	Protein of unknown function (DUF3313).	
PMI32_01189	1.7956755	Predicted Na+/dicarboxylate symporter	[R] General function prediction only
PMI32_04089	1.7783438	haloacid dehalogenase superfamily, subfamily IA, variant 3 with third motif having DD or ED/haloacid dehalogenase superfamily, subfamily IA, variant 1 with third motif having Dx(3-4)D or Dx(3-4)E	[R] General function prediction only
PMI32_02155	1.7773489	Uncharacterized conserved protein	[S] Function unknown
PMI32_03115	1.7759732	hypothetical protein	
PMI32_01263	1.775175	Predicted permeases	[R] General function prediction only
PMI32_02492	1.7736551	Methyltransferase domain.	
PMI32_03930	1.7723818	GTP cyclohydrolase I	[H] Coenzyme transport and metabolism
PMI32_03653	1.7714946	Bacterioferritin	[P] Inorganic ion transport and metabolism
PMI32_00461	1.7713931	Cytosine/uracil/thiamine/allantoin permeases	[F] Nucleotide transport and metabolism, [H] Coenzyme transport and metabolism
PMI32_05929	1.7711889	Sulfite reductase, beta subunit (hemoprotein)	[P] Inorganic ion transport and metabolism
PMI32_02799	1.767218	Predicted ATPase	[R] General function prediction only
PMI32_01509	1.7666117	acetyl-CoA acetyltransferases	[I] Lipid transport and metabolism
PMI32_04904	1.7646375	Monoamine oxidase	[E] Amino acid transport and metabolism
PMI32_02616	1.7609482	PAS domain S-box/diguanylate cyclase (GGDEF) domain	
PMI32_03061	1.7601919	Transcriptional regulators	[K] Transcription
PMI32_04099	1.7595859	Na+/proline symporter	[R] General function prediction only, [E] Amino acid transport and metabolism
PMI32_00854	1.7538603	iron-sulfur cluster assembly protein IscA	[S] Function unknown
PMI32_04544	1.7532531	NADH-quinone oxidoreductase, E subunit	[C] Energy production and conversion
PMI32_01229	1.7487332	Predicted membrane protein	[S] Function unknown
PMI32_03490	1.7469717	Serine/threonine protein phosphatase	[T] Signal transduction mechanisms
PMI32_01978	1.7398332	Na/Pi-cotransporter	[P] Inorganic ion transport and metabolism
PMI32_02831	1.7362846	23S rRNA (uracil-5-)-methyltransferase RumA	[J] Translation, ribosomal structure and biogenesis
PMI32_05930	1.7355352	Uncharacterized protein conserved in bacteria	[S] Function unknown
PMI32_04800	1.7354222	Response regulator containing CheY-like receiver, AAA-type ATPase, and DNA-binding domains	[T] Signal transduction mechanisms
PMI32_03174	1.7339173	Response regulator containing a CheY-like receiver domain and an HTH DNA-binding domain	[T] Signal transduction mechanisms, [K] Transcription
PMI32_01480	1.7307079	Predicted SAM-dependent methyltransferase	[R] General function prediction only

PMI32_00168	1.7300924	Uncharacterized protein conserved in bacteria	[S] Function unknown
PMI32_05821	1.7273985	Dinucleotide-utilizing enzymes involved in molybdopterin and thiamine biosynthesis family 1	[H] Coenzyme transport and metabolism
PMI32_05751	1.7269705	yjeF C-terminal region, hydroxyethylthiazole kinase-related/yjeF N-terminal region	[G] Carbohydrate transport and metabolism
PMI32_01630	1.726586	UDP-N-acetylglucosamine 1-carboxyvinyltransferase	[M] Cell wall/membrane/envelope biogenesis
PMI32_00037	1.7234599	phenylalanyl-tRNA synthetase, beta subunit, non-spirochete bacterial	[J] Translation, ribosomal structure and biogenesis
PMI32_00904	1.7224797	signal recognition particle protein	[U] Intracellular trafficking, secretion, and vesicular transport
PMI32_03051	1.7146522	chaperone protein DnaJ	[O] Posttranslational modification, protein turnover, chaperones
PMI32_01147	1.7133725	Adenosylmethionine-8-amino-7-oxononanoate aminotransferase	[H] Coenzyme transport and metabolism
PMI32_05569	1.7126637	Negative regulator of sigma E activity	[T] Signal transduction mechanisms
PMI32_01443	1.7110647	ATPase components of ABC transporters with duplicated ATPase domains	[R] General function prediction only
PMI32_02053	1.7100227	NAD/NADP transhydrogenase beta subunit	[C] Energy production and conversion
PMI32_01591	1.7092006	galactarate dehydratase	[G] Carbohydrate transport and metabolism
PMI32_02007	1.7076356	ABC-type metal ion transport system, ATPase component	[P] Inorganic ion transport and metabolism
PMI32_00912	1.7040247	Protein-disulfide isomerase	[O] Posttranslational modification, protein turnover, chaperones
PMI32_01041	1.7036009	tRNA_Undet_???	
PMI32_03634	1.6963404	ribosomal protein L29	[J] Translation, ribosomal structure and biogenesis
PMI32_05842	1.6907714	diguanylate cyclase (GGDEF) domain	
PMI32_03939	1.6883529	chorismate synthase	[E] Amino acid transport and metabolism
PMI32_04082	1.6854399	histidinol-phosphate aminotransferase	[E] Amino acid transport and metabolism
PMI32_05262	1.6815911	trigger factor	[O] Posttranslational modification, protein turnover, chaperones
PMI32_05648	1.678545	Uncharacterized protein, similar to the N-terminal domain of Lon protease	[R] General function prediction only
PMI32_02794	1.6713699	mutator mutT protein	[H] Coenzyme transport and metabolism
PMI32_01629	1.6694783	Predicted transcriptional regulator, BolA superfamily	[K] Transcription
PMI32_02194	1.6661897	Bacterial lipocalin	[M] Cell wall/membrane/envelope biogenesis
PMI32_05756	1.6650085	RNA chaperone Hfq	[R] General function prediction only
PMI32_00336	1.6562668	flagellar biosynthetic protein FlhF	[N] Cell motility
PMI32_05083	1.6553151	Signal transduction histidine kinase	[T] Signal transduction mechanisms
PMI32_01641	1.6494583	Glutathione peroxidase	[O] Posttranslational modification, protein turnover, chaperones
PMI32_05397	1.6420534	Transcriptional regulator containing an amidase domain and an AraC-type DNA-binding HTH domain	[K] Transcription
PMI32_02480	1.6387252	Predicted sugar kinase	[G] Carbohydrate transport and metabolism
PMI32_01045	1.6369709	glutamyl-tRNA reductase	[H] Coenzyme transport and metabolism
PMI32_05267	1.6359928	5,10-methylene-tetrahydrofolate dehydrogenase/Methenyl tetrahydrofolate cyclohydrolase	[H] Coenzyme transport and metabolism
PMI32_04422	1.635907	Cation/multidrug efflux pump	[V] Defense mechanisms
PMI32_03385	1.6303978	Response regulators consisting of a CheY-like receiver domain and a winged-helix DNA-binding domain	[K] Transcription, [T] Signal transduction mechanisms
PMI32_01217	1.6297603	tRNA (guanine-N(7)-)-methyltransferase	[R] General function prediction only
PMI32_05834	1.6280285	Protein of unknown function (DUF548).	
PMI32_05108	1.6258925	Nucleoside-diphosphate-sugar epimerases	[G] Carbohydrate transport and metabolism, [M] Cell wall/membrane/envelope biogenesis
PMI32_04012	1.6249313	Beta-lactamase class C and other penicillin binding proteins	[V] Defense mechanisms

PMI32_02316	1.6047399	folylpolyglutamate synthase/dihydrofolate synthase	[H] Coenzyme transport and metabolism
PMI32_01962	1.6010885	peptide deformylase	[J] Translation, ribosomal structure and biogenesis
PMI32_05779	1.5997699	hypothetical protein	
PMI32_02184	1.5968856	thiazole biosynthesis/tRNA modification protein ThiI	[H] Coenzyme transport and metabolism
PMI32_01216	1.5946295	Uncharacterized enzyme of thiazole biosynthesis	[H] Coenzyme transport and metabolism
PMI32_02065	1.5912157	Holliday junction DNA helicase, RuvA subunit	[L] Replication, recombination and repair
PMI32_00596	1.5856698	Protein involved in catabolism of external DNA	[R] General function prediction only
PMI32_01102	1.5850898	ubiquinol-cytochrome c reductase, iron-sulfur subunit	[C] Energy production and conversion
PMI32_01203	1.5783329	Rhodanese-related sulfurtransferase	[P] Inorganic ion transport and metabolism
PMI32_00515	1.5782542	Nitrate/nitrite transporter	[P] Inorganic ion transport and metabolism
PMI32_02598	1.5718375	Obg family GTPase CgtA	[R] General function prediction only
PMI32_03627	1.5677478	50S ribosomal protein L4, bacterial/organelle	[J] Translation, ribosomal structure and biogenesis
PMI32_00683	1.5615149	Uncharacterized protein conserved in bacteria	[S] Function unknown
PMI32_02667	1.5589802	RIP metalloprotease RseP	
PMI32_03191	1.5536741	prolyl-tRNA synthetase, family II	[J] Translation, ribosomal structure and biogenesis
PMI32_03056	1.5202128	Small protein A (tmRNA-binding)	[J] Translation, ribosomal structure and biogenesis
PMI32_01487	1.5152724	GTP-binding protein LepA	[M] Cell wall/membrane/envelope biogenesis
PMI32_01303	1.5127099	Acyl-CoA synthetases (AMP-forming)/AMP-acid ligases II	[Q] Secondary metabolites biosynthesis, transport and catabolism, [I] Lipid transport and metabolism
PMI32_03613	1.4879385	transcription termination/antitermination factor NusG	[K] Transcription
PMI32_01931	-1.5069139	ATP synthase, F1 beta subunit	[C] Energy production and conversion
PMI32_05768	-1.5091419	ribonuclease R	[K] Transcription
PMI32_02601	-1.5102392	Geranylgeranyl pyrophosphate synthase	[H] Coenzyme transport and metabolism
PMI32_00684	-1.517037	2-polyprenylphenol 6-hydroxylase	[R] General function prediction only
PMI32_00660	-1.5172301	type IV pilus secretin (or competence protein) PilQ	[U] Intracellular trafficking, secretion, and vesicular transport
PMI32_04761	-1.5198945	acetylornithine and succinylornithine transaminases/succinylornithine transaminase family	[E] Amino acid transport and metabolism
PMI32_04410	-1.5289177	ABC-type amino acid transport/signal transduction systems, periplasmic component/domain	[T] Signal transduction mechanisms, [E] Amino acid transport and metabolism
PMI32_00190	-1.5314143	polyphosphate kinase 1	[P] Inorganic ion transport and metabolism
PMI32_02790	-1.5361432	Uncharacterized protein conserved in bacteria	[S] Function unknown
PMI32_02433	-1.5505507	Universal stress protein UspA and related nucleotide-binding proteins	[T] Signal transduction mechanisms
PMI32_05758	-1.5630459	HflK protein	[O] Posttranslational modification, protein turnover, chaperones
PMI32_00040	-1.5655695	ribosomal protein L35	[J] Translation, ribosomal structure and biogenesis
PMI32_02534	-1.5660264	aconitate hydratase 2	[C] Energy production and conversion
PMI32_03329	-1.5739075	Signal transduction histidine kinase	
PMI32_05956	-1.6004835	polyprenyl P-hydroxybenzoate and phenylacrylic acid decarboxylases	[H] Coenzyme transport and metabolism
PMI32_05777	-1.6049747	Uncharacterized conserved protein	[S] Function unknown
PMI32_03554	-1.6110706	oxaloacetate decarboxylase alpha subunit	[C] Energy production and conversion
PMI32_05825	-1.6157844	hypothetical protein	
PMI32_03985	-1.6164093	3-oxoacyl-(acyl-carrier-protein) reductase	[R] General function prediction only, [Q] Secondary metabolites biosynthesis, transport and catabolism, [I] Lipid transport and

			metabolism
PMI32_01103	-1.6170996	Cytochrome b subunit of the bc complex	[C] Energy production and conversion
PMI32_02101	-1.6188944	Pyruvate/2-oxoglutarate dehydrogenase complex, dihydrolipoamide acyltransferase (E2) component, and related enzymes	
PMI32_05290	-1.6224746	conserved hypothetical protein	[S] Function unknown
PMI32_01934	-1.6265898	ATP synthase, F1 delta subunit	[C] Energy production and conversion
PMI32_05948	-1.6266182	Transglycosylase.	[M] Cell wall/membrane/envelope biogenesis
PMI32_01939	-1.6293545	ParB-like partition proteins	[K] Transcription
PMI32_03381	-1.6316583	potassium uptake protein, TrkH family	[P] Inorganic ion transport and metabolism
PMI32_04564	-1.6364979	glutaminyl-tRNA synthetase	[J] Translation, ribosomal structure and biogenesis
PMI32_01618	-1.6384455	RNA polymerase sigma-54 factor	[K] Transcription
PMI32_05672	-1.6451239	apolipoprotein N-acyltransferase	[M] Cell wall/membrane/envelope biogenesis
PMI32_02789	-1.6459078	Small-conductance mechanosensitive channel	
PMI32_03957	-1.6487686	Excinuclease ATPase subunit	[L] Replication, recombination and repair
PMI32_01877	-1.6491995	Uncharacterized protein conserved in bacteria	[S] Function unknown
PMI32_04470	-1.6542572	Xaa-Pro aminopeptidase	[E] Amino acid transport and metabolism
PMI32_03391	-1.6565499	Uncharacterized conserved protein	[S] Function unknown
PMI32_03624	-1.6580564	translation elongation factor TU	[J] Translation, ribosomal structure and biogenesis
PMI32_04088	-1.6614472	ubiquinone biosynthesis O-methyltransferase	[H] Coenzyme transport and metabolism
PMI32_05684	-1.6687866	AMP nucleosidase	[F] Nucleotide transport and metabolism
PMI32_04888	-1.6704779	Protein of unknown function (DUF1090).	
PMI32_03992	-1.6710155	Tfp pilus assembly protein PilZ	[U] Intracellular trafficking, secretion, and vesicular transport, [N] Cell motility
PMI32_03802	-1.6786389	TonB-dependent copper receptor	[P] Inorganic ion transport and metabolism
PMI32_04216	-1.6815241	Predicted periplasmic lipoprotein	[R] General function prediction only
PMI32_01811	-1.6817038	spermidine synthase	[E] Amino acid transport and metabolism
PMI32_01015	-1.6856702	Carbonic anhydrase	[P] Inorganic ion transport and metabolism
PMI32_04895	-1.6885153	Formate/nitrite family of transporters	[P] Inorganic ion transport and metabolism
PMI32_01893	-1.692282	Kef-type K+ transport systems, membrane components	[P] Inorganic ion transport and metabolism
PMI32_01211	-1.694042	Cell division protein	[D] Cell cycle control, cell division, chromosome partitioning
PMI32_02029	-1.6952526	Zn-dependent oligopeptidases	[E] Amino acid transport and metabolism
PMI32_01462	-1.710265	ABC-type polar amino acid transport system, ATPase component	[E] Amino acid transport and metabolism
PMI32_03209	-1.7110654	Transcriptional regulators	[K] Transcription
PMI32_00689	-1.7214232	Twin arginine targeting (Tat) protein translocase TatC	[U] Intracellular trafficking, secretion, and vesicular transport
PMI32_00170	-1.7245768	5,10-methenyltetrahydrofolate synthetase	[H] Coenzyme transport and metabolism
PMI32_00219	-1.7248615	Adenylate cyclase	[F] Nucleotide transport and metabolism
PMI32_01717	-1.7252769	cAMP-binding proteins - catabolite gene activator and regulatory subunit of cAMP-dependent protein kinases	[T] Signal transduction mechanisms
PMI32_01233	-1.7259633	RNAse H-fold protein YqgF	[L] Replication, recombination and repair
PMI32_01933	-1.7296001	proton translocating ATP synthase, F1 alpha subunit	[C] Energy production and conversion
PMI32_04778	-1.7325249	ketol-acid reductoisomerase	[E] Amino acid transport and metabolism, [H] Coenzyme transport and metabolism
PMI32_03956	-1.7331733	PAS domain S-box	
PMI32_01521	-1.7389355	lysine-arginine-ornithine-binding periplasmic protein	[T] Signal transduction mechanisms, [E] Amino acid transport and metabolism
PMI32_04244	-1.7399299	ribonuclease T	[L] Replication, recombination and repair

PMI32_01105	-1.7405536	Glutathione S-transferase	[O] Posttranslational modification, protein turnover, chaperones
PMI32_00275	-1.7414052	tRNA_Undet_???	
PMI32_02132	-1.7420071	thiamine biosynthesis protein ThiC	[H] Coenzyme transport and metabolism
PMI32_03050	-1.7420408	dihydrodipicolinate reductase	[E] Amino acid transport and metabolism
PMI32_04763	-1.7424317	Transcriptional regulator containing an amidase domain and an AraC-type DNA-binding HTH domain	[K] Transcription
PMI32_03470	-1.7464331	guanylate kinase	[F] Nucleotide transport and metabolism
PMI32_01059	-1.7486813	Predicted transcriptional regulators	[K] Transcription
PMI32_01947	-1.7490391	DNA polymerase III, beta subunit	[L] Replication, recombination and repair
PMI32_02475	-1.7525129	aminopeptidase N, Escherichia coli type	[E] Amino acid transport and metabolism
PMI32_01615	-1.7553182	Predicted P-loop-containing kinase	[R] General function prediction only
PMI32_00494	-1.7588094	Response regulator containing a CheY-like receiver domain and an HTH DNA-binding domain	[K] Transcription, [T] Signal transduction mechanisms
PMI32_03763	-1.7619989	hypothetical protein	
PMI32_00506	-1.763685	Membrane-bound metallopeptidase	[D] Cell cycle control, cell division, chromosome partitioning
PMI32_01870	-1.7643392	RNA polymerase sigma factor, sigma-70 family	[K] Transcription
PMI32_04749	-1.7811961	carbon storage regulator (csrA)	[T] Signal transduction mechanisms
PMI32_05874	-1.7818781	hypothetical protein	
PMI32_03042	-1.7866271	Dihydropteroate synthase and related enzymes	
PMI32_02918	-1.7877682	Anthranilate phosphoribosyltransferase	[E] Amino acid transport and metabolism
PMI32_01149	-1.7879872	Spermidine/putrescine-binding periplasmic protein	[E] Amino acid transport and metabolism
PMI32_00613	-1.7903239	Uncharacterized conserved protein	[S] Function unknown
PMI32_02543	-1.7951397	Protein of unknown function (DUF3094).	
PMI32_01696	-1.7987885	4-hydroxythreonine-4-phosphate dehydrogenase	[H] Coenzyme transport and metabolism
PMI32_01550	-1.7990829	Surface lipoprotein	[M] Cell wall/membrane/envelope biogenesis
PMI32_05911	-1.7992721	PAS domain S-box/diguanylate cyclase (GGDEF) domain	[T] Signal transduction mechanisms
PMI32_03168	-1.7993826	protein RecA	[L] Replication, recombination and repair
PMI32_01412	-1.8005961	Methylase of chemotaxis methyl-accepting proteins	[T] Signal transduction mechanisms, [N] Cell motility
PMI32_01571	-1.8041366	Uncharacterized protein involved in biosynthesis of c-type cytochromes	[O] Posttranslational modification, protein turnover, chaperones
PMI32_01854	-1.8150961	benzoate transporter	[Q] Secondary metabolites biosynthesis, transport and catabolism
PMI32_04516	-1.8224483	Pirin-related protein	[R] General function prediction only
PMI32_03206	-1.8247618	Uncharacterized protein related to plant photosystem II stability/assembly factor	[R] General function prediction only
PMI32_05764	-1.8253807	ABC-type Fe3+ transport system, periplasmic component	[P] Inorganic ion transport and metabolism
PMI32_01688	-1.8270792	tRNA nucleotidyltransferase/poly(A) polymerase	[J] Translation, ribosomal structure and biogenesis
PMI32_01699	-1.8288785	Predicted phosphotransferase related to Ser/Thr protein kinases	[R] General function prediction only
PMI32_01945	-1.832783	ribonuclease P protein component, eubacterial	[J] Translation, ribosomal structure and biogenesis
PMI32_04818	-1.8404967	dephospho-CoA kinase	[H] Coenzyme transport and metabolism
PMI32_00473	-1.8436066	Alcohol dehydrogenase, class IV	[C] Energy production and conversion
PMI32_01669	-1.8449839	coenzyme PQQ biosynthesis protein B	[R] General function prediction only
PMI32_01970	-1.8452336	choline ABC transporter, periplasmic binding protein	[E] Amino acid transport and metabolism
PMI32_00697	-1.8455073	D-tyrosyl-tRNA(Tyr) deacylase	[J] Translation, ribosomal structure and biogenesis

PMI32_03062	-1.8455705	L-lactate transport	[C] Energy production and conversion
PMI32_01649	-1.8467217	FolB domain	[H] Coenzyme transport and metabolism
PMI32_04098	-1.8580192	Transcriptional regulator	
PMI32_01694	-1.8598982	Uncharacterized protein affecting Mg2+/Co2+ transport	[P] Inorganic ion transport and metabolism
PMI32_02138	-1.8613864	Predicted esterase	[R] General function prediction only
PMI32_03842	-1.8649562	Predicted pyrophosphatase	[R] General function prediction only
PMI32_03903	-1.8670215	3-deoxy-7-phosphoheptulonate synthase, class II	[E] Amino acid transport and metabolism
PMI32_02068	-1.8697224	TolQ protein	[U] Intracellular trafficking, secretion, and vesicular transport
PMI32_00914	-1.8699074	threonine synthase	[E] Amino acid transport and metabolism
PMI32_03943	-1.8720793	2,3-diketo-5-methylthio-1-phosphopentane phosphatase	[C] Energy production and conversion
PMI32_05910	-1.8735014	Pyrroloquinoline quinone (Coenzyme PQQ) biosynthesis protein C	[H] Coenzyme transport and metabolism
PMI32_02613	-1.8766115	Transcription elongation factor	[K] Transcription
PMI32_03539	-1.8788383	aspartate ammonia-lyase	[E] Amino acid transport and metabolism
PMI32_05673	-1.8803593	Putative Mg2+ and Co2+ transporter CorC	[P] Inorganic ion transport and metabolism
PMI32_00675	-1.8812057	poly(R)-hydroxyalkanoic acid synthase, class II	[I] Lipid transport and metabolism
PMI32_04628	-1.884037	Electron transfer flavoprotein, alpha subunit	[C] Energy production and conversion
PMI32_01981	-1.8847114	conserved hypothetical integral membrane protein	[Q] Secondary metabolites biosynthesis, transport and catabolism
PMI32_05674	-1.8873253	metalloprotein, YbeY/UPF0054 family	[R] General function prediction only
PMI32_05370	-1.8913446	ABC-type branched-chain amino acid transport systems, ATPase component	[E] Amino acid transport and metabolism
PMI32_01708	-1.8928492	ABC-type spermidine/putrescine transport system, permease component II	[E] Amino acid transport and metabolism
PMI32_04900	-1.8945245	ABC-type amino acid transport/signal transduction systems, periplasmic component/domain	[T] Signal transduction mechanisms, [E] Amino acid transport and metabolism
PMI32_00893	-1.8947891	ATP-dependent protease La	[O] Posttranslational modification, protein turnover, chaperones
PMI32_00901	-1.8979393	metabolite-proton symporter	
PMI32_05626	-1.9015005	Threonine aldolase	[E] Amino acid transport and metabolism
PMI32_01508	-1.9090183	3-oxoacid CoA-transferase, B subunit	[I] Lipid transport and metabolism
PMI32_01963	-1.9148028	LysM domain.	
PMI32_00465	-1.915489	Transcriptional regulator	[K] Transcription
PMI32_00742	-1.9179143	Uncharacterized protein conserved in bacteria	[S] Function unknown
PMI32_01930	-1.9181225	ATP synthase, F1 epsilon subunit (delta in mitochondria)	[C] Energy production and conversion
PMI32_03322	-1.9192667	deoxyguanosinetriphosphate triphosphohydrolase, putative	[F] Nucleotide transport and metabolism
PMI32_04005	-1.9193583	Transcriptional regulators	[K] Transcription
PMI32_00872	-1.920224	2-isopropylmalate synthase, yeast type	[E] Amino acid transport and metabolism
PMI32_05252	-1.9270639	sulfate ABC transporter, permease protein CysT	[O] Posttranslational modification, protein turnover, chaperones
PMI32_01607	-1.933559	Uncharacterized protein conserved in bacteria	[S] Function unknown
PMI32_05750	-1.9336949	iron-sulfur cluster binding protein, putative	[C] Energy production and conversion
PMI32_03934	-1.9346889	hypothetical protein	
PMI32_02928	-1.9363778	Putative arginyl-tRNA:protein arginylyltransferase	[O] Posttranslational modification, protein turnover, chaperones
PMI32_00687	-1.9445896	twin arginine-targeting protein translocase, TatA/E family	[U] Intracellular trafficking, secretion, and vesicular transport
PMI32_01259	-1.9456567	malto-oligosyltrehalose trehalohydrolase	[G] Carbohydrate transport and metabolism
PMI32_02715	-1.9477016	muconate and chloromuconate cycloisomerases	[M] Cell wall/membrane/envelope biogenesis, [R] General function prediction only

PMI32_01148	-1.9512515	Spermidine/putrescine-binding periplasmic protein	[E] Amino acid transport and metabolism
PMI32_05827	-1.954356	glycerol-3-phosphate O-acyltransferase	[I] Lipid transport and metabolism
PMI32_00236	-1.9616435	oligopeptide/dipeptide ABC transporter, ATP-binding protein, C-terminal domain	[P] Inorganic ion transport and metabolism, [E] Amino acid transport and metabolism
PMI32_02668	-1.9623529	outer membrane protein assembly complex, YaeT protein	[M] Cell wall/membrane/envelope biogenesis
PMI32_03413	-1.9656971	ammonium transporter	[P] Inorganic ion transport and metabolism
PMI32_01935	-1.9728405	ATP synthase, F0 subunit b	[C] Energy production and conversion
PMI32_02071	-1.9746151	tol-pal system beta propeller repeat protein TolB	[U] Intracellular trafficking, secretion, and vesicular transport
PMI32_05933	-1.9747365	Fructose-2,6-bisphosphatase	[G] Carbohydrate transport and metabolism
PMI32_00907	-1.9785923	tRNA (guanine-N1)-methyltransferase	[J] Translation, ribosomal structure and biogenesis
PMI32_01680	-1.993713	PAS domain S-box/diguanylate cyclase (GGDEF) domain	
PMI32_02072	-1.995228	peptidoglycan-associated lipoprotein	[M] Cell wall/membrane/envelope biogenesis
PMI32_04842	-1.9952635	Fe-S oxidoreductase	[C] Energy production and conversion
PMI32_00937	-2.0017322	Transcriptional regulator	[K] Transcription
PMI32_04870	-2.0047396	Superfamily II DNA and RNA helicases	[L] Replication, recombination and repair, [K] Transcription, [J] Translation, ribosomal structure and biogenesis
PMI32_02022	-2.0077549	hypothetical protein	
PMI32_02914	-2.0081287	sulfur relay protein TusD/DsrE	[P] Inorganic ion transport and metabolism
PMI32_01671	-2.0093099	Predicted amidohydrolase	[R] General function prediction only
PMI32_01650	-2.0152233	GTP cyclohydrolase I	[H] Coenzyme transport and metabolism
PMI32_03825	-2.0188843	3-dehydroquinate dehydratase, type II	[E] Amino acid transport and metabolism
PMI32_01976	-2.0194023	citrate transporter, CitMHS family	[C] Energy production and conversion
PMI32_03981	-2.0204633	Predicted metal-binding, possibly nucleic acid-binding protein	[R] General function prediction only
PMI32_05639	-2.0236488	MoxR-like ATPases	[R] General function prediction only
PMI32_03380	-2.0241526	AraC-type DNA-binding domain-containing proteins	[K] Transcription
PMI32_05074	-2.0242673	Membrane protein TerC, possibly involved in tellurium resistance	[P] Inorganic ion transport and metabolism
PMI32_00894	-2.0248886	Uncharacterized protein conserved in bacteria	
PMI32_03319	-2.0289487	Predicted membrane protein	[S] Function unknown
PMI32_01334	-2.0324487	Thymidylate kinase	[F] Nucleotide transport and metabolism
PMI32_05088	-2.0356049	hypothetical protein	
PMI32_01076	-2.0372715	Glycerol-3-phosphate O-acyltransferase	
PMI32_01459	-2.0373815	ABC-type amino acid transport/signal transduction systems, periplasmic component/domain	[T] Signal transduction mechanisms, [E] Amino acid transport and metabolism
PMI32_01941	-2.0382028	16S rRNA (guanine(527)-N(7))-methyltransferase GidB	[M] Cell wall/membrane/envelope biogenesis
PMI32_01713	-2.038981	glutamine amidotransferase of anthranilate synthase or aminodeoxychorismate synthase	[H] Coenzyme transport and metabolism, [E] Amino acid transport and metabolism
PMI32_01714	-2.0391132	anthranilate phosphoribosyltransferase	[E] Amino acid transport and metabolism
PMI32_04896	-2.0396326	Acyl-CoA hydrolase	[I] Lipid transport and metabolism
PMI32_03244	-2.0398779	cytochrome c oxidase, cbb3-type, subunit I	[O] Posttranslational modification, protein turnover, chaperones
PMI32_00447	-2.0438348	hypothetical protein	
PMI32_00688	-2.0454139	twin arginine-targeting protein translocase TatB	[U] Intracellular trafficking, secretion, and vesicular transport
PMI32_03982	-2.0471269	ribosomal protein L32	[J] Translation, ribosomal structure and biogenesis
PMI32_05682	-2.0483426	Signal transduction histidine kinase	[T] Signal transduction mechanisms
PMI32_00694	-2.0501464	ABC-type amino acid transport/signal transduction systems, periplasmic	[E] Amino acid transport and metabolism, [T] Signal transduction mechanisms

		component/domain	
PMI32_03194	-2.050484	Protein of unknown function, DUF481.	
PMI32_01162	-2.0509663	hypothetical protein	
PMI32_04084	-2.053189	phosphoserine aminotransferase	[E] Amino acid transport and metabolism, [H] Coenzyme transport and metabolism
PMI32_01134	-2.0535094	outer membrane porin, OprD family.	
PMI32_04501	-2.0542761	succinate dehydrogenase and fumarate reductase iron-sulfur protein	[C] Energy production and conversion
PMI32_04669	-2.0557156	ABC-type sugar transport system, periplasmic component	[G] Carbohydrate transport and metabolism
PMI32_03523	-2.0559474	Hemolysins and related proteins containing CBS domains	[R] General function prediction only
PMI32_04019	-2.0566739	Outer membrane protein and related peptidoglycan-associated (lipo)proteins	[M] Cell wall/membrane/envelope biogenesis
PMI32_03232	-2.0579655	NAD-specific glutamate dehydrogenase	[E] Amino acid transport and metabolism
PMI32_02067	-2.0583284	tol-pal system-associated acyl-CoA thioesterase	[R] General function prediction only
PMI32_00561	-2.0671818	N-carbamoylputrescine amidase	[R] General function prediction only
PMI32_03510	-2.0681716	type VI secretion protein, VC_A0107 family	[S] Function unknown
PMI32_04307	-2.0686147	Predicted oxidoreductases (related to aryl-alcohol dehydrogenases)	[C] Energy production and conversion
PMI32_00594	-2.0706073	PAS domain S-box/diguanylate cyclase (GGDEF) domain	
PMI32_01936	-2.07102	ATP synthase, F0 subunit c	[C] Energy production and conversion
PMI32_05745	-2.0717503	Oligoribonuclease (3'->5' exoribonuclease)	[A] RNA processing and modification
PMI32_00205	-2.0724894	hypothetical protein	
PMI32_01964	-2.0755694	DNA protecting protein DprA	[U] Intracellular trafficking, secretion, and vesicular transport, [L] Replication, recombination and repair
PMI32_01170	-2.079162	Predicted integral membrane protein	[S] Function unknown
PMI32_04944	-2.0831904	Transcriptional regulators	
PMI32_01124	-2.0874302	D-alanine--D-alanine ligase	[M] Cell wall/membrane/envelope biogenesis
PMI32_00095	-2.0915914	exodeoxyribonuclease V, gamma subunit	[L] Replication, recombination and repair
PMI32_03823	-2.0938888	acetyl-CoA carboxylase, biotin carboxylase subunit	[I] Lipid transport and metabolism
PMI32_05923	-2.1019081	polyphosphate:AMP phosphotransferase	[S] Function unknown
PMI32_03440	-2.1048589	Predicted transcriptional regulators	
PMI32_00785	-2.1078905	Predicted ATPase related to phosphate starvation-inducible protein PhoH	[T] Signal transduction mechanisms
PMI32_01581	-2.1117246	Predicted periplasmic/secreted protein	[S] Function unknown
PMI32_04885	-2.120428	Methylase involved in ubiquinone/menaquinone biosynthesis	
PMI32_01093	-2.1213636	Uncharacterized protein conserved in bacteria	[S] Function unknown
PMI32_03207	-2.1213637	Predicted exporters of the RND superfamily	[R] General function prediction only
PMI32_02018	-2.12553	Cytochrome oxidase assembly factor	[O] Posttranslational modification, protein turnover, chaperones
PMI32_03526	-2.1268929	phosphate transport system regulatory protein PhoU	[P] Inorganic ion transport and metabolism
PMI32_03824	-2.1290445	acetyl-CoA carboxylase, biotin carboxyl carrier protein	[I] Lipid transport and metabolism
PMI32_05952	-2.1309504	Acyl dehydratase	[I] Lipid transport and metabolism
PMI32_04298	-2.1337533	Signal transduction histidine kinase	[T] Signal transduction mechanisms
PMI32_02590	-2.1388605	FKBP-type peptidyl-prolyl cis-trans isomerases 2	[O] Posttranslational modification, protein turnover, chaperones
PMI32_04225	-2.1441002	chaperonin GroL	[O] Posttranslational modification, protein turnover, chaperones
PMI32_01938	-2.1566083	F0F1-type ATP synthase, subunit I	[C] Energy production and conversion
PMI32_01998	-2.1578768	ribosome biogenesis GTP-binding protein YsxC/EngB	[R] General function prediction only

PMI32_02609	-2.1635722	Predicted ATP-dependent protease	[O] Posttranslational modification, protein turnover, chaperones
PMI32_01133	-2.1641871	outer membrane porin, OprD family.	
PMI32_02717	-2.1648872	catechol 1,2-dioxygenase, proteobacterial	[Q] Secondary metabolites biosynthesis, transport and catabolism
PMI32_00151	-2.1654352	Transcriptional regulators	[K] Transcription
PMI32_01720	-2.1672738	Ubiquinone biosynthesis protein COQ7	[H] Coenzyme transport and metabolism
PMI32_05575	-2.1691095	Glycine cleavage system regulatory protein	[E] Amino acid transport and metabolism
PMI32_00153	-2.1710044	Type II secretory pathway, ATPase PulE/Tfp pilus assembly pathway, ATPase PilB	[N] Cell motility, [U] Intracellular trafficking, secretion, and vesicular transport
PMI32_02024	-2.1724142	Carbonic anhydrase	[P] Inorganic ion transport and metabolism
PMI32_02801	-2.1773896	Glycosyltransferase	[M] Cell wall/membrane/envelope biogenesis
PMI32_05354	-2.1801739	hypothetical protein	
PMI32_02782	-2.1819414	putative regulatory protein, FmdB family	[S] Function unknown
PMI32_05030	-2.1861691	Long-chain fatty acid transport protein	[I] Lipid transport and metabolism
PMI32_02933	-2.1894996	ABC-type oligopeptide transport system, periplasmic component	[E] Amino acid transport and metabolism
PMI32_00531	-2.1925944	ABC-type histidine transport system, ATPase component	[E] Amino acid transport and metabolism
PMI32_05675	-2.1969033	Phosphate starvation-inducible protein PhoH, predicted ATPase	[T] Signal transduction mechanisms
PMI32_02442	-2.1970457	aconitate hydratase 1	[C] Energy production and conversion
PMI32_01707	-2.1993373	ABC-type spermidine/putrescine transport system, permease component I	[E] Amino acid transport and metabolism
PMI32_01691	-2.2008442	Putative Ser protein kinase	[T] Signal transduction mechanisms
PMI32_01721	-2.2009935	Diadenosine tetraphosphate (Ap4A) hydrolase and other HIT family hydrolases	[F] Nucleotide transport and metabolism, [R] General function prediction only, [G] Carbohydrate transport and metabolism
PMI32_03705	-2.2076923	tRNA_Undet_???	
PMI32_05781	-2.2116332	Azurin	[C] Energy production and conversion
PMI32_03326	-2.2125153	HD-GYP domain	[T] Signal transduction mechanisms
PMI32_03268	-2.217707	efflux transporter, outer membrane factor (OMF) lipoprotein, NodT family	[M] Cell wall/membrane/envelope biogenesis, [U] Intracellular trafficking, secretion, and vesicular transport
PMI32_04551	-2.2193609	proton-translocating NADH-quinone oxidoreductase, chain L	[P] Inorganic ion transport and metabolism, [C] Energy production and conversion
PMI32_01441	-2.2200417	hypothetical protein	
PMI32_04461	-2.2210157	Glutathione S-transferase	[O] Posttranslational modification, protein turnover, chaperones
PMI32_00211	-2.2283888	Uroporphyrinogen-III synthase	[H] Coenzyme transport and metabolism
PMI32_03942	-2.2343925	Uncharacterized conserved protein, contains double-stranded beta-helix domain	[S] Function unknown
PMI32_04680	-2.2413863	Selenocysteine lyase	[E] Amino acid transport and metabolism
PMI32_03300	-2.2418147	Inhibitor of the KinA pathway to sporulation, predicted exonuclease	[R] General function prediction only
PMI32_00179	-2.2450166	Uncharacterized protein involved in cation transport	[P] Inorganic ion transport and metabolism
PMI32_01617	-2.2524918	ribosomal subunit interface protein	[J] Translation, ribosomal structure and biogenesis
PMI32_01091	-2.2552197	Zn-dependent hydrolases, including glyoxylases	[R] General function prediction only
PMI32_03451	-2.2578949	NAD-dependent aldehyde dehydrogenases	[C] Energy production and conversion
PMI32_00456	-2.2607386	Predicted aminoglycoside phosphotransferase	[R] General function prediction only
PMI32_05506	-2.2628736	HNH endonuclease.	
PMI32_03117	-2.2669782	hypothetical protein	
PMI32_00317	-2.271152	succinyldiaminopimelate transaminase	[E] Amino acid transport and metabolism
PMI32_04658	-2.2731164	hypothetical protein	
PMI32_03890	-2.2773744	Transcriptional regulator	[K] Transcription

PMI32_05685	-2.2780427	pseudouridine synthase	[J] Translation, ribosomal structure and biogenesis
PMI32_01712	-2.2780432	anthranilate synthase component I, non-proteobacterial lineages	[E] Amino acid transport and metabolism, [H] Coenzyme transport and metabolism
PMI32_01937	-2.2789751	F0F1-type ATP synthase, subunit a	[C] Energy production and conversion
PMI32_01089	-2.2796103	Protein of unknown function (DUF1329).	
PMI32_00502	-2.2805496	protein-export chaperone SecB	[U] Intracellular trafficking, secretion, and vesicular transport
PMI32_01892	-2.281853	hypothetical protein	
PMI32_02700	-2.2854843	Isocitrate dehydrogenase kinase/phosphatase	[T] Signal transduction mechanisms
PMI32_03342	-2.28641	ABC-type spermidine/putrescine transport systems, ATPase components	[E] Amino acid transport and metabolism
PMI32_02544	-2.2894476	NADH dehydrogenase, FAD-containing subunit	[C] Energy production and conversion
PMI32_02496	-2.2914537	ABC-type oligopeptide transport system, periplasmic component	[E] Amino acid transport and metabolism
PMI32_00676	-2.3000238	poly(3-hydroxyalkanoate) depolymerase	[R] General function prediction only
PMI32_00094	-2.3060106	exodeoxyribonuclease V, beta subunit	[L] Replication, recombination and repair
PMI32_00533	-2.3066248	amine acid ABC transporter, permease protein, 3-TM region, His/Glu/Gln/Arg/opine family	[E] Amino acid transport and metabolism
PMI32_03474	-2.3090986	hypothetical protein	
PMI32_00962	-2.3106511	Predicted transcriptional regulators	[K] Transcription
PMI32_03594	-2.3141234	hypothetical protein	
PMI32_01666	-2.3217975	fumarylacetoacetase	[Q] Secondary metabolites biosynthesis, transport and catabolism
PMI32_00132	-2.323343	coenzyme PQQ biosynthesis enzyme PqqE	[R] General function prediction only
PMI32_03301	-2.3248381	Uncharacterized protein conserved in bacteria	[S] Function unknown
PMI32_01132	-2.3406763	taurine ABC transporter, periplasmic binding protein	[P] Inorganic ion transport and metabolism
PMI32_02538	-2.3448404	outer membrane porin, OprD family.	
PMI32_03951	-2.3456112	Spermidine/putrescine-binding periplasmic protein	[E] Amino acid transport and metabolism
PMI32_01549	-2.351492	hypothetical protein	
PMI32_01815	-2.3594695	Uncharacterized protein conserved in bacteria	[S] Function unknown
PMI32_03202	-2.3655643	ABC-type amino acid transport/signal transduction systems, periplasmic component/domain	[T] Signal transduction mechanisms, [E] Amino acid transport and metabolism
PMI32_03170	-2.3691578	TIGR00730 family protein	[R] General function prediction only
PMI32_05643	-2.3841566	cysteine synthase A	[E] Amino acid transport and metabolism
PMI32_04860	-2.3932505	choline ABC transporter, periplasmic binding protein	[E] Amino acid transport and metabolism
PMI32_02837	-2.3999318	Lactate dehydrogenase and related dehydrogenases	[C] Energy production and conversion, [H] Coenzyme transport and metabolism, [R] General function prediction only
PMI32_02718	-2.4072535	AraC-type DNA-binding domain-containing proteins	[K] Transcription
PMI32_03940	-2.4112979	Arabinose efflux permease	
PMI32_00186	-2.4130863	amine acid ABC transporter, permease protein, 3-TM region, His/Glu/Gln/Arg/opine family	[E] Amino acid transport and metabolism
PMI32_00763	-2.413359	Transcriptional regulator	[K] Transcription
PMI32_05829	-2.4158257	hypothetical protein	
PMI32_01044	-2.416498	Flp pilus assembly protein TadD, contains TPR repeats	[U] Intracellular trafficking, secretion, and vesicular transport
PMI32_04720	-2.4177825	Flagellar biosynthesis/type III secretory pathway chaperone	[N] Cell motility, [U] Intracellular trafficking, secretion, and vesicular transport, [O] Posttranslational modification, protein turnover, chaperones
PMI32_02686	-2.4185777	2-C-methyl-D-erythritol 2,4-cyclodiphosphate synthase	[I] Lipid transport and metabolism
PMI32_05525	-2.4217287	Transcriptional regulator	[K] Transcription

PMI32_02283	-2.4254642	L-asparaginases, type II	[J] Translation, ribosomal structure and biogenesis, [E] Amino acid transport and metabolism
PMI32_03473	-2.4265986	endoribonuclease L-PSP, putative	[J] Translation, ribosomal structure and biogenesis
PMI32_03004	-2.4323165	Periplasmic glucans biosynthesis protein	[P] Inorganic ion transport and metabolism
PMI32_03876	-2.4332804	Uncharacterized conserved protein	[S] Function unknown
PMI32_02435	-2.433314	Soluble lytic murein transglycosylase and related regulatory proteins (some contain LysM/invasin domains)	[M] Cell wall/membrane/envelope biogenesis
PMI32_02310	-2.4352057	tRNA_Undet_???	
PMI32_00949	-2.4435183	Uncharacterized conserved protein	
PMI32_04552	-2.4538001	proton-translocating NADH-quinone oxidoreductase, chain M	[C] Energy production and conversion
PMI32_03712	-2.454959	molybdate ABC transporter, permease protein	[P] Inorganic ion transport and metabolism
PMI32_01090	-2.4575787	ATP-dependent transcriptional regulator	[K] Transcription
PMI32_03343	-2.4580527	HAD-superfamily subfamily IB hydrolase, TIGR01490	[E] Amino acid transport and metabolism
PMI32_03192	-2.4581402	AmpG-related permease	
PMI32_04299	-2.4604837	Response regulators consisting of a CheY-like receiver domain and a winged-helix DNA-binding domain	[T] Signal transduction mechanisms, [K] Transcription
PMI32_04868	-2.4618639	Predicted Zn-dependent proteases and their inactivated homologs	[R] General function prediction only
PMI32_05310	-2.4872829	type I secretion outer membrane protein, TolC family	[U] Intracellular trafficking, secretion, and vesicular transport, [M] Cell wall/membrane/envelope biogenesis
PMI32_03199	-2.487929	Predicted deacylase	[R] General function prediction only
PMI32_05251	-2.4944884	sulfate/thiosulfate-binding protein	[P] Inorganic ion transport and metabolism
PMI32_04794	-2.4948936	sugar fermentation stimulation protein	[R] General function prediction only
PMI32_05206	-2.4963514	isocitrate dehydrogenase, NADP-dependent, prokaryotic type	[C] Energy production and conversion
PMI32_04259	-2.5017411	ABC-type amino acid transport/signal transduction systems, periplasmic component/domain	[T] Signal transduction mechanisms, [E] Amino acid transport and metabolism
PMI32_00624	-2.5026293	Histidine ammonia-lyase	[E] Amino acid transport and metabolism
PMI32_01719	-2.5048405	S-adenosylmethionine decarboxylase proenzyme, Escherichia coli form	[E] Amino acid transport and metabolism
PMI32_01584	-2.5050889	ABC-type uncharacterized transport system, permease and ATPase components	[R] General function prediction only
PMI32_00761	-2.513158	Lactate dehydrogenase and related dehydrogenases	[C] Energy production and conversion, [R] General function prediction only, [H] Coenzyme transport and metabolism
PMI32_01070	-2.5136948	hypothetical protein	
PMI32_05791	-2.5148056	ABC-type branched-chain amino acid transport systems, ATPase component	[E] Amino acid transport and metabolism
PMI32_00321	-2.5150535	Anti-anti-sigma regulatory factor (antagonist of anti-sigma factor)	[T] Signal transduction mechanisms
PMI32_02938	-2.5153789	phospho-2-dehydro-3-deoxyheptonate aldolase	[E] Amino acid transport and metabolism
PMI32_01985	-2.5217982	Uncharacterized membrane protein, required for spore maturation in B.subtilis.	[R] General function prediction only
PMI32_01727	-2.5237784	Iron-sulfur cluster assembly accessory protein	[S] Function unknown
PMI32_05373	-2.5237888	Response regulators consisting of a CheY-like receiver domain and a winged-helix DNA-binding domain	
PMI32_03338	-2.5240272	ABC-type Fe3+ transport system, periplasmic component	[P] Inorganic ion transport and metabolism
PMI32_05717	-2.5567252	His Kinase A (phosphoacceptor) domain./Histidine kinase-, DNA gyrase B-, and HSP90-like ATPase./PAS fold.	
PMI32_04815	-2.5590634	type IV-A pilus assembly ATPase PilB	[U] Intracellular trafficking, secretion, and vesicular transport, [N] Cell motility
PMI32_00640	-2.5593588	Arabinose efflux permease	[G] Carbohydrate transport and metabolism

PMI32_05610	-2.5745149	Glutathione S-transferase	[O] Posttranslational modification, protein turnover, chaperones
PMI32_02326	-2.5791638	3-isopropylmalate dehydratase, small subunit	[E] Amino acid transport and metabolism
PMI32_04503	-2.5798618	2-oxoglutarate dehydrogenase complex dihydrolipoamide succinyltransferase (E2 component)	[C] Energy production and conversion
PMI32_04548	-2.5870129	NADH-quinone oxidoreductase, chain I	[C] Energy production and conversion
PMI32_00378	-2.590419	Transcriptional regulator	[K] Transcription
PMI32_05315	-2.5931782	Agmatinase	[E] Amino acid transport and metabolism
PMI32_03962	-2.5964607	Uncharacterized protein conserved in bacteria	[S] Function unknown
PMI32_01440	-2.5995997	Glucose/sorbosone dehydrogenases	[G] Carbohydrate transport and metabolism
PMI32_00774	-2.599972	Predicted membrane protein involved in D-alanine export	[M] Cell wall/membrane/envelope biogenesis
PMI32_03327	-2.602462	GAF domain-containing protein	[T] Signal transduction mechanisms
PMI32_03935	-2.6058039	Amidases related to nicotinamidase	[Q] Secondary metabolites biosynthesis, transport and catabolism
PMI32_01050	-2.6172997	Lipid A 3-O-deacylase (PagL).	
PMI32_03003	-2.6278198	NADH:flavin oxidoreductases, Old Yellow Enzyme family	[C] Energy production and conversion
PMI32_04726	-2.6344315	PAS domain S-box	[N] Cell motility, [T] Signal transduction mechanisms
PMI32_01400	-2.6345938	AraC-type DNA-binding domain-containing proteins	[K] Transcription
PMI32_03481	-2.6352449	Predicted signal transduction protein	[T] Signal transduction mechanisms
PMI32_03528	-2.6403572	phosphate ABC transporter, permease protein PstA	[P] Inorganic ion transport and metabolism
PMI32_03480	-2.6466834	ATP-dependent DNA helicase RecG	[L] Replication, recombination and repair, [K] Transcription
PMI32_00039	-2.6477738	ribosomal protein L20	[J] Translation, ribosomal structure and biogenesis
PMI32_03804	-2.6618933	Uncharacterized protein conserved in bacteria	[S] Function unknown
PMI32_05620	-2.6629537	sarcosine oxidase, gamma subunit family, heterotetrameric form	[E] Amino acid transport and metabolism
PMI32_03544	-2.6729413	Spermidine/putrescine-binding periplasmic protein	[E] Amino acid transport and metabolism
PMI32_01709	-2.6847329	Alcohol dehydrogenase, class IV	[C] Energy production and conversion
PMI32_02220	-2.6847398	NAD-dependent aldehyde dehydrogenases	[C] Energy production and conversion
PMI32_00745	-2.6882295	serine transporter	[E] Amino acid transport and metabolism
PMI32_02495	-2.7080693	ABC-type oligopeptide transport system, periplasmic component	[E] Amino acid transport and metabolism
PMI32_00359	-2.7103553	hypothetical protein	
PMI32_03479	-2.71372	Transcriptional regulator	[K] Transcription
PMI32_02620	-2.7169329	Na+/H+-dicarboxylate symporters	[C] Energy production and conversion
PMI32_03555	-2.721492	Biotin carboxylase	[I] Lipid transport and metabolism
PMI32_00360	-2.7246937	AraC-type DNA-binding domain-containing proteins	[K] Transcription
PMI32_01872	-2.7294644	hypothetical protein	
PMI32_05638	-2.7498745	Uncharacterized protein conserved in bacteria	[S] Function unknown
PMI32_00217	-2.7575632	hypothetical protein	
PMI32_04114	-2.7610241	Predicted transcriptional regulators	[K] Transcription
PMI32_05333	-2.7821429	Acyl carrier protein phosphodiesterase	[I] Lipid transport and metabolism
PMI32_04347	-2.7826825	Transcriptional regulator	[K] Transcription
PMI32_01155	-2.7949396	Protein related to penicillin acylase	[R] General function prediction only
PMI32_02046	-2.8025491	hypothetical protein	
PMI32_04508	-2.8148449	Predicted membrane protein	[S] Function unknown
PMI32_01130	-2.8230599	acetylornithine deacetylase (ArgE)	[E] Amino acid transport and metabolism

PMI32_04760	-2.8266402	arginine/ornithine succinyltransferase, alpha subunit	[E] Amino acid transport and metabolism
PMI32_01792	-2.8468282	Succinate dehydrogenase/fumarate reductase, flavoprotein subunit	[C] Energy production and conversion
PMI32_02829	-2.8658763	MazG family protein	
PMI32_04113	-2.8681145	Transcriptional regulator	[K] Transcription
PMI32_03542	-2.8780091	AraC-type DNA-binding domain-containing proteins	[K] Transcription
PMI32_04018	-2.8852655	Outer membrane protein and related peptidoglycan-associated (lipo)proteins	[M] Cell wall/membrane/envelope biogenesis
PMI32_01284	-2.8866195	Spermidine/putrescine-binding periplasmic protein	[E] Amino acid transport and metabolism
PMI32_01665	-2.8871592	homogentisate 1,2-dioxygenase	[Q] Secondary metabolites biosynthesis, transport and catabolism
PMI32_03540	-2.8953492	amino acid carrier protein	[E] Amino acid transport and metabolism
PMI32_02788	-2.8955815	outer membrane porin, OprD family.	
PMI32_01166	-2.9025687	Uncharacterized protein conserved in bacteria	[S] Function unknown
PMI32_03729	-2.9039669	peroxiredoxin	[O] Posttranslational modification, protein turnover, chaperones
PMI32_03509	-2.9052064	type VI secretion protein, EvpB/VC_A0108 family	[S] Function unknown
PMI32_04861	-2.9098971	choline ABC transporter, permease protein	[E] Amino acid transport and metabolism
PMI32_05368	-2.9113661	ABC-type branched-chain amino acid transport system, permease component	[E] Amino acid transport and metabolism
PMI32_05954	-2.9162475	Predicted nucleoside-diphosphate-sugar epimerases	[G] Carbohydrate transport and metabolism, [M] Cell wall/membrane/envelope biogenesis
PMI32_02328	-2.9169989	Transcriptional regulator	[K] Transcription
PMI32_04810	-2.9348991	Predicted SAM-dependent methyltransferases	[R] General function prediction only
PMI32_05788	-2.9412734	Branched-chain amino acid ABC-type transport system, permease components	[E] Amino acid transport and metabolism
PMI32_03879	-2.9590234	Adenosylmethionine-8-amino-7-oxononanoate aminotransferase	[H] Coenzyme transport and metabolism
PMI32_00977	-2.9757797	Trans-aconitate methyltransferase	[R] General function prediction only
PMI32_04894	-2.9760619	NhaP-type Na+/H+ and K+/H+ antiporters	[P] Inorganic ion transport and metabolism
PMI32_05817	-2.9766943	transcriptional regulator, Spx/MgsR family	[P] Inorganic ion transport and metabolism
PMI32_00942	-2.9891848	Predicted transcriptional regulators	[K] Transcription
PMI32_03521	-3.0010066	phosphate regulon transcriptional regulatory protein PhoB	[K] Transcription, [T] Signal transduction mechanisms
PMI32_00589	-3.0177248	Uncharacterized protein conserved in archaea	[O] Posttranslational modification, protein turnover, chaperones
PMI32_01479	-3.0191237	Bacterial nucleoid DNA-binding protein	[L] Replication, recombination and repair
PMI32_02127	-3.0330109	Membrane transporters of cations and cationic drugs	[P] Inorganic ion transport and metabolism
PMI32_03821	-3.0346302	Protein of unknown function (DUF3426).	
PMI32_03841	-3.0442577	hypothetical protein	
PMI32_00736	-3.0457153	Signal transduction histidine kinase	[T] Signal transduction mechanisms
PMI32_01692	-3.0774443	Rhodanese-related sulfurtransferase	[P] Inorganic ion transport and metabolism
PMI32_01053	-3.0839385	Cyclopropane fatty acid synthase and related methyltransferases	[M] Cell wall/membrane/envelope biogenesis
PMI32_04037	-3.1036822	hypothetical protein	
PMI32_04257	-3.1054567	Transcriptional regulators of sugar metabolism	[G] Carbohydrate transport and metabolism, [K] Transcription
PMI32_03941	-3.1205373	methylthioribulose-1-phosphate dehydratase	[G] Carbohydrate transport and metabolism
PMI32_02586	-3.1452126	type IV pilus modification protein PilV	
PMI32_03986	-3.167773	acyl carrier protein	[Q] Secondary metabolites biosynthesis, transport and catabolism, [I] Lipid transport and metabolism
PMI32_03312	-3.1762934	Bacterial protein of unknown function (DUF903).	
PMI32_01891	-3.1924264	Uncharacterized protein conserved in bacteria	[S] Function unknown

PMI32_00519	-3.2198974	Fe-S cluster protector protein	[O] Posttranslational modification, protein turnover, chaperones, [C] Energy production and conversion
PMI32_04456	-3.2209426	Putative threonine efflux protein	[E] Amino acid transport and metabolism
PMI32_05519	-3.2218596	hypothetical protein	
PMI32_02146	-3.2219656	hypothetical protein	
PMI32_02236	-3.2241616	Dienelactone hydrolase and related enzymes	[Q] Secondary metabolites biosynthesis, transport and catabolism
PMI32_01449	-3.2247938	hypothetical protein	
PMI32_03524	-3.2261294	Membrane proteins related to metalloendopeptidases	
PMI32_05582	-3.2276804	Transcriptional regulator	[K] Transcription
PMI32_01672	-3.231429	Monoamine oxidase	[E] Amino acid transport and metabolism
PMI32_00615	-3.2327928	ATPases involved in chromosome partitioning	[D] Cell cycle control, cell division, chromosome partitioning
PMI32_03341	-3.2369826	ABC-type spermidine/putrescine transport system, permease component II	[E] Amino acid transport and metabolism
PMI32_04336	-3.2647607	ABC-type antimicrobial peptide transport system, ATPase component	[V] Defense mechanisms
PMI32_03713	-3.3187214	molybdenum ABC transporter, periplasmic molybdate-binding protein	[P] Inorganic ion transport and metabolism
PMI32_00777	-3.3190185	parallel beta-helix repeat (two copies)	
PMI32_04566	-3.3225181	UDP-2,3-diacylglucosamine hydrolase	[S] Function unknown
PMI32_01723	-3.3317277	Predicted membrane protein	[S] Function unknown
PMI32_00686	-3.3323566	phosphoribosyl-ATP pyrophosphohydrolase	[E] Amino acid transport and metabolism
PMI32_01616	-3.3436366	PTS IIA-like nitrogen-regulatory protein PtsN	[T] Signal transduction mechanisms, [G] Carbohydrate transport and metabolism
PMI32_03175	-3.3538807	Diacylglycerol kinase	[M] Cell wall/membrane/envelope biogenesis
PMI32_03756	-3.3750372	Predicted membrane protein	[S] Function unknown
PMI32_03224	-3.3879426	Uncharacterized protein conserved in bacteria	
PMI32_02702	-3.4083057	Predicted permeases	[R] General function prediction only
PMI32_05703	-3.4105307	hypothetical protein	
PMI32_02611	-3.415954	hypothetical protein	
PMI32_01710	-3.4274613	ribulose-phosphate 3-epimerase	[G] Carbohydrate transport and metabolism
PMI32_03789	-3.4334378	Sortase and related acyltransferases	[M] Cell wall/membrane/envelope biogenesis
PMI32_02037	-3.4465078	peroxiredoxin, OsmC subfamily	[O] Posttranslational modification, protein turnover, chaperones
PMI32_05086	-3.4530461	Uncharacterized protein conserved in bacteria	[S] Function unknown
PMI32_00677	-3.4539079	poly(R)-hydroxyalkanoic acid synthase, class II	[I] Lipid transport and metabolism
PMI32_02217	-3.4658912	Transcriptional regulators	[K] Transcription
PMI32_00386	-3.4718414	hypothetical protein	
PMI32_04245	-3.4896823	Peroxiredoxin	[O] Posttranslational modification, protein turnover, chaperones
PMI32_05076	-3.4951753	Transcriptional regulator	[K] Transcription
PMI32_04908	-3.5163156	Transcriptional regulator	[K] Transcription
PMI32_01715	-3.5186237	Indole-3-glycerol phosphate synthase	[E] Amino acid transport and metabolism
PMI32_00150	-3.543175	Predicted phosphatase	[R] General function prediction only
PMI32_04681	-3.5448817	Uncharacterized protein conserved in bacteria	[S] Function unknown
PMI32_02934	-3.5649498	Parvulin-like peptidyl-prolyl isomerase	
PMI32_01097	-3.5863838	Transcriptional regulator containing an amidase domain and an AraC-type DNA-binding HTH domain	[K] Transcription
PMI32_03264	-3.5877941	Peroxiredoxin	[O] Posttranslational modification, protein turnover, chaperones
PMI32_05693	-3.5936145	Predicted permease	[R] General function prediction only

PMI32_02582	-3.5994494	prepilin-type N-terminal cleavage/methylation domain	[N] Cell motility, [U] Intracellular trafficking, secretion, and vesicular transport
PMI32_01689	-3.6097074	Uncharacterized conserved protein	[S] Function unknown
PMI32_04522	-3.6485638	Amidases related to nicotinamidase	[Q] Secondary metabolites biosynthesis, transport and catabolism
PMI32_01614	-3.6610465	Phosphotransferase System HPr (HPr) Family	[G] Carbohydrate transport and metabolism
PMI32_03527	-3.6708515	phosphate ABC transporter, ATP-binding protein	[P] Inorganic ion transport and metabolism
PMI32_02425	-3.6780375	SOS-response cell division inhibitor, blocks FtsZ ring formation	[D] Cell cycle control, cell division, chromosome partitioning
PMI32_01656	-3.7132385	Flavodoxins	[C] Energy production and conversion
PMI32_01087	-3.7149408	Acyl-CoA synthetases (AMP-forming)/AMP-acid ligases II	[Q] Secondary metabolites biosynthesis, transport and catabolism, [I] Lipid transport and metabolism
PMI32_02424	-3.7209338	SOS regulatory protein LexA	[T] Signal transduction mechanisms, [K] Transcription
PMI32_00233	-3.7224212	ABC-type dipeptide transport system, periplasmic component	[E] Amino acid transport and metabolism
PMI32_02216	-3.7278135	Integral membrane protein, interacts with FtsH	[R] General function prediction only
PMI32_04902	-3.7378656	Uncharacterized conserved protein	[S] Function unknown
PMI32_00748	-3.7435729	Sigma 54 modulation protein / S30EA ribosomal protein.	
PMI32_02049	-3.7829337	conserverd hypothetical protein	
PMI32_03908	-3.8020048	hypothetical protein	
PMI32_00337	-3.8028199	hypothetical protein	
PMI32_04504	-3.8316411	dihydrolipoamide dehydrogenase	[C] Energy production and conversion
PMI32_00385	-3.8418711	Outer membrane protein and related peptidoglycan-associated (lipo)proteins	[M] Cell wall/membrane/envelope biogenesis
PMI32_03169	-3.8521236	Uncharacterized protein conserved in bacteria	[R] General function prediction only
PMI32_00771	-3.8570627	mannose-1-phosphate guanylyltransferase/mannose-6-phosphate isomerase	[M] Cell wall/membrane/envelope biogenesis
PMI32_04124	-3.8622035	Predicted carboxypeptidase	[E] Amino acid transport and metabolism
PMI32_02500	-3.9322754	Enoyl-[acyl-carrier-protein] reductase (NADH)	[I] Lipid transport and metabolism
PMI32_01349	-3.9446123	Spermidine/putrescine-binding periplasmic protein	[E] Amino acid transport and metabolism
PMI32_02041	-3.9557388	Uncharacterized conserved protein	[S] Function unknown
PMI32_05256	-3.9596092	cAMP-binding proteins - catabolite gene activator and regulatory subunit of cAMP-dependent protein kinases	[T] Signal transduction mechanisms
PMI32_04889	-3.9601386	Cytochrome c556	[C] Energy production and conversion
PMI32_01183	-4.0109467	putative 2-aminoethylphosphonate ABC transporter, periplasmic 2-aminoethylphosphonate-binding protein	[P] Inorganic ion transport and metabolism
PMI32_02412	-4.0253592	PilZ domain.	
PMI32_05316	-4.0651653	Ketosteroid isomerase homolog	[S] Function unknown
PMI32_04502	-4.1085804	2-oxoglutarate dehydrogenase, E1 component	[C] Energy production and conversion
PMI32_03127	-4.113236	Acetyltransferases	
PMI32_00261	-4.1370847	Negative regulator of beta-lactamase expression	
PMI32_02880	-4.1742867	NIPSNAP.	
PMI32_04102	-4.1767332	hypothetical protein	
PMI32_04817	-4.1948081	Type II secretory pathway, prepilin signal peptidase PulO and related peptidases	[O] Posttranslational modification, protein turnover, chaperones, [N] Cell motility, [U] Intracellular trafficking, secretion, and vesicular transport
PMI32_05380	-4.1977288	Predicted esterase of the alpha/beta hydrolase fold	[R] General function prediction only
PMI32_04771	-4.2012171	DNA-binding HTH domain-containing proteins	[K] Transcription

PMI32_04558	-4.2276004	ABC-type sugar transport system, permease component	[G] Carbohydrate transport and metabolism
PMI32_01869	-4.2668433	Outer membrane protein and related peptidoglycan-associated (lipo)proteins	[M] Cell wall/membrane/envelope biogenesis
PMI32_04786	-4.2953078	Uncharacterized low-complexity proteins	
PMI32_02016	-4.3123306	Protein of unknown function (DUF2909).	
PMI32_01055	-4.3170476	Predicted NAD/FAD-binding protein	[R] General function prediction only
PMI32_01351	-4.3298509	Uncharacterized paraquat-inducible protein A	
PMI32_01137	-4.3519969	ABC transporter, substrate-binding protein, aliphatic sulfonates family	[P] Inorganic ion transport and metabolism
PMI32_03340	-4.3528111	ABC-type uncharacterized transport system, permease component	[R] General function prediction only
PMI32_00208	-4.3744676	Disulfide bond formation protein DsbB	[O] Posttranslational modification, protein turnover, chaperones
PMI32_00944	-4.3822222	1-acyl-sn-glycerol-3-phosphate acyltransferase	[I] Lipid transport and metabolism
PMI32_04152	-4.3948147	integral membrane protein, TerC family	[P] Inorganic ion transport and metabolism
PMI32_01072	-4.436415	hypothetical protein	
PMI32_00532	-4.4631951	ABC-type amino acid transport/signal transduction systems, periplasmic component/domain	[E] Amino acid transport and metabolism, [T] Signal transduction mechanisms
PMI32_03557	-4.4739952	hypothetical protein	
PMI32_04837	-4.4848553	Phenylpropionate dioxygenase and related ring-hydroxylating dioxygenases, large terminal subunit	[R] General function prediction only, [P] Inorganic ion transport and metabolism
PMI32_00218	-4.5084184	TIGR02647 family protein	
PMI32_04506	-4.5112369	succinyl-CoA synthetase, alpha subunit	[C] Energy production and conversion
PMI32_01184	-4.5204032	FAD dependent oxidoreductase TIGR03364	[E] Amino acid transport and metabolism
PMI32_05527	-4.5242215	hypothetical protein	
PMI32_04459	-4.5650204	carbohydrate kinase, thermoresistant glucokinase family	[G] Carbohydrate transport and metabolism
PMI32_03535	-4.5743781	Predicted membrane protein	[S] Function unknown
PMI32_01992	-4.6738348	Negative regulator of beta-lactamase expression	[V] Defense mechanisms
PMI32_01145	-4.6763071	Predicted glutamine amidotransferases	
PMI32_04813	-4.6826508	Predicted periplasmic or secreted lipoprotein	
PMI32_03529	-4.740506	ABC-type uncharacterized transport system, permease component	[R] General function prediction only
PMI32_04505	-4.8366777	succinyl-CoA synthetase, beta subunit	[C] Energy production and conversion
PMI32_00376	-4.8573833	Predicted enzyme of the cupin superfamily	[R] General function prediction only
PMI32_03022	-4.8645642	Flp pilus assembly protein, secretin CpaC	[U] Intracellular trafficking, secretion, and vesicular transport
PMI32_05364	-4.9038373	Superoxide dismutase	[P] Inorganic ion transport and metabolism
PMI32_02183	-4.9379547	glutamine synthetase, type I	[E] Amino acid transport and metabolism
PMI32_02284	-4.9529671	Protein of unknown function (DUF1654).	
PMI32_00232	-4.9635222	outer membrane porin, OprD family.	
PMI32_03416	-5.0528091	Prophage antirepressor	[K] Transcription
PMI32_01782	-5.0797333	Cystathionine beta-lyases/cystathionine gamma-synthases	[E] Amino acid transport and metabolism
PMI32_01670	-5.0799424	coenzyme PQQ biosynthesis probable peptidase PqqF	[O] Posttranslational modification, protein turnover, chaperones
PMI32_02407	-5.1127172	heavy metal response regulator	[K] Transcription, [T] Signal transduction mechanisms
PMI32_02716	-5.1946965	muconolactone delta-isomerase	[Q] Secondary metabolites biosynthesis, transport and catabolism
PMI32_03869	-5.2316006	hypothetical protein	
PMI32_05377	-5.298621	TonB family C-terminal domain	[M] Cell wall/membrane/envelope biogenesis
PMI32_02610	-5.3306397	Protein of unknown function (DUF3015).	

PMI32_05376	-5.4307697	Transcriptional regulator	[K] Transcription
PMI32_01088	-5.4753012	Protein of unknown function (DUF1302).	
PMI32_04512	-5.5275987	hypothetical protein	
PMI32_05060	-5.5439255	Beta-lactamase class C and other penicillin binding proteins	[V] Defense mechanisms
PMI32_01531	-5.5765778	diguanylate cyclase (GGDEF) domain	[T] Signal transduction mechanisms
PMI32_00805	-5.6957255	P-aminobenzoate N-oxygenase AurF.	
PMI32_01136	-5.7292412	FMN reductase, SsuE family	[R] General function prediction only
PMI32_02998	-5.8213007	Protein of unknown function (DUF3509).	
PMI32_02784	-5.8402975	DNA-binding ferritin-like protein (oxidative damage protectant)	[P] Inorganic ion transport and metabolism
PMI32_00804	-5.9502136	Taurine catabolism dioxygenase TauD, TfdA family.	
PMI32_00917	-6.0534118	hypothetical protein	
PMI32_05972	-6.1226158	Uncharacterized protein conserved in bacteria	[S] Function unknown
PMI32_00528	-6.1262974	hypothetical protein	
PMI32_02579	-6.2047766	Signal transduction histidine kinase, nitrogen specific	[T] Signal transduction mechanisms
PMI32_05378	-6.2274958	Biopolymer transport proteins	[U] Intracellular trafficking, secretion, and vesicular transport
PMI32_03882	-6.2383183	Protein of unknown function (DUF3359).	
PMI32_04443	-6.2505423	Mg2+ and Co2+ transporters	[P] Inorganic ion transport and metabolism
PMI32_03652	-6.2759366	Catalase	[P] Inorganic ion transport and metabolism
PMI32_02827	-6.4276207	hypothetical protein	
PMI32_02115	-6.4292616	Uncharacterized proteins, LmbE homologs	[S] Function unknown
PMI32_00290	-6.7966946	ABC-type nitrate/sulfonate/bicarbonate transport systems, periplasmic components	[P] Inorganic ion transport and metabolism
PMI32_05363	-6.8974018	Lysine efflux permease	[R] General function prediction only
PMI32_05337	-6.9230441	Peptidyl-prolyl cis-trans isomerase (rotamase) - cyclophilin family	[O] Posttranslational modification, protein turnover, chaperones
PMI32_05428	-6.9765667	Protein of unknown function (DUF3309).	
PMI32_01281	-7.0631359	AraC-type DNA-binding domain-containing proteins	[K] Transcription
PMI32_05381	-7.0949749	Response regulator containing CheY-like receiver, AAA-type ATPase, and DNA-binding domains	
PMI32_01353	-7.2360009	Paraquat-inducible protein B	[R] General function prediction only
PMI32_00559	-7.2828751	hypothetical protein	
PMI32_04613	-7.32303	Transcriptional regulator containing an amidase domain and an AraC-type DNA-binding HTH domain	[K] Transcription
PMI32_03530	-7.6628352	phosphate binding protein	[P] Inorganic ion transport and metabolism
PMI32_01182	-7.6717037	putative 2-aminoethylphosphonate ABC transporter, permease protein	[P] Inorganic ion transport and metabolism
PMI32_03200	-8.0073267	amine acid ABC transporter, permease protein, 3-TM region, His/Glu/Gln/Arg/opine family	[E] Amino acid transport and metabolism
PMI32_01135	-8.0653641	Peroxiredoxin	[O] Posttranslational modification, protein turnover, chaperones
PMI32_02344	-8.6496722	hypothetical protein	
PMI32_05723	-8.65591	Flagellin and related hook-associated proteins	
PMI32_01283	-9.0260073	Predicted enzyme of the cupin superfamily	[R] General function prediction only
PMI32_05362	-9.3890555	Uncharacterized protein conserved in bacteria	[S] Function unknown
PMI32_00945	-9.6200344	Putative hemolysin	[R] General function prediction only
PMI32_05597	-9.9205378	Predicted rRNA methylase (SpoU class)	[J] Translation, ribosomal structure and biogenesis
PMI32_02048	-11.345931	conserverd hypothetical protein	

PMI32_03339	-12.291927	Uncharacterized proteins of the AP superfamily	
PMI32_00520	-12.425017	tRNA_Undet_???	
PMI32_02697	-13.630986	hypothetical protein	
PMI32_04575	-14.085355	ABC-type phosphate transport system, periplasmic component	[P] Inorganic ion transport and metabolism
PMI32_03398	-15.815545	hypothetical protein	
PMI32_01679	-19.782796	tRNA_Undet_???	
PMI32_04724	-20.537541	Histidine kinase-, DNA gyrase B-, and HSP90-like ATPase.	
PMI32_03377	-20.710087	Uncharacterized protein conserved in bacteria	[S] Function unknown
PMI32_04718	-22.916291	hypothetical protein	
PMI32_03272	-23.527009	AraC-type DNA-binding domain-containing proteins	[K] Transcription
PMI32_04775	-23.645215	Predicted membrane protein	[S] Function unknown
PMI32_02652	-24.078923	Transcriptional regulator	[K] Transcription
PMI32_01643	-24.362452	Glycosyltransferase	[M] Cell wall/membrane/envelope biogenesis
PMI32_05996	-24.634518	hypothetical protein	
PMI32_05719	-25.496256	hypothetical protein	
PMI32_00892	-25.93186	Predicted secreted protein	[S] Function unknown
PMI32_01747	-26.359148	Purine-cytosine permease and related proteins	[F] Nucleotide transport and metabolism
PMI32_01580	-26.507765	Uncharacterized homolog of the cytoplasmic domain of flagellar protein FhlB	[S] Function unknown
PMI32_03777	-26.757921	EamA-like transporter family.	
PMI32_02270	-31.580729	Uncharacterized protein conserved in bacteria	[S] Function unknown
PMI32_01054	-38.910963	Uncharacterized conserved protein	[S] Function unknown
PMI32_02406	-40.359993	Uncharacterized copper-binding protein	[P] Inorganic ion transport and metabolism
PMI32_03927	-40.633964	Transcriptional regulators	[K] Transcription
PMI32_02945	-48.588137	tRNA_Undet_???	
PMI32_03776	-57.221109	Predicted acetyltransferases and hydrolases with the alpha/beta hydrolase fold	[R] General function prediction only
PMI32_00678	-61.55709	Transcriptional regulator	[K] Transcription

Appendix E: Effect of Ozone Treatment on Inactivation of *Escherichia coli* and *Listeria* sp. on Spinach (This paper is published using data from Chapter 5)

Agriculture **2015**, *5*, 155-169; doi:10.3390/agriculture5020155

OPEN ACCESS

agriculture

ISSN 2077-0472

www.mdpi.com/journal/agriculture

Article

Effect of Ozone Treatment on Inactivation of *Escherichia coli* and *Listeria* sp. on Spinach

Shreya Wani, Jagpreet K. Maker, Joseph R. Thompson, Jeremy Barnes * and Ian Singleton *

School of Biology, Newcastle University, Newcastle upon Tyne, NE1 7RU, UK;
E-Mails: shrenrique@gmail.com (S.W.); jagmaker@gmail.com (J.K.M.);
j.thompson5@newcastle.ac.uk (J.R.T.)

* Authors to whom correspondence should be addressed; E-Mails: jerry.barnes@newcastle.ac.uk (J.B.); ian.singleton@ncl.ac.uk (I.S.); Tel.: +44-0-191-243-0871 (J.B.); +44-0-191-208-3043 (I.S.).

Academic Editor: Pascal Delaquis

Received: 15 February 2015 / Accepted: 17 March 2015 / Published: 26 March 2015

Abstract: The efficacy of "gaseous" ozone in reducing numbers and re-growth of food-borne pathogens, (*Escherichia coli* and *Listeria* spp.), on leafy salads was investigated using spinach. A preliminary *in vivo* study showed 1-log reduction in six strains of *E. coli* and two species of *Listeria* spp. on spinach exposed to 1 ppm ozone for 10 min. A range of ozone treatments were explored to deliver optimal bacterial inactivation while maintaining the visual appearance (color) of produce. Exposure to a higher ozone concentration for a shorter duration (10 ppm for 2 min) significantly reduced *E. coli* and *Listeria* spp. viable counts by 1-log and the pathogens did not re-grow following treatment (over a nine-day storage period). Impacts of 1 and 10 ppm ozone treatments were not significantly different. Approximately 10% of the pathogen population was resistant to ozone treatment. We hypothesized that cell age may be one of several factors responsible for variation in ozone resistance. *E. coli* cells from older colonies demonstrated higher ozone resistance in subsequent experiments. Overall, we speculate that gaseous ozone treatment constitutes the basis for an alternative customer-friendly method to reduce food pathogen contamination of leafy produce and is worth exploring on a pilot-scale in an industrial setting.

Keywords: gaseous ozone; *E. coli*; *Listeria* spp.

1. Introduction

In addition to reducing produce spoilage, an increased incidence in the outbreaks of microbial borne diseases associated with the consumption of raw leafy produce have added to the need to find alternative methods to reduce microbial loads [1]. All types of leafy produce have the potential to harbor pathogens, such as *Escherichia coli*, *Listeria monocytogenes*, *Shigella* spp., and *Salmonella* spp., which are ultimately responsible for the majority of foodborne outbreaks [2,3]. Contamination of fresh produce with pathogens can occur either pre-harvest and/or post-harvest. Pre-harvest sources of pathogens generally include organic fertilizers, irrigation water, and soil, whereas post-harvest sources mainly result from handling procedures including equipment, transport vehicles, and containers [4].

A recent investigation of retail leafy salads revealed contamination of a significant proportion with *E. coli* and *L. monocytogenes* [5]. *E. coli* is a Gram-negative, facultative anaerobic member of the *Enterobacteriaceae* family. It is commonly present in gastrointestinal tract of humans and animals including deer, cattle, and pigs [6]. Although most *E. coli* are harmless to humans, epidemiological research has documented that intake of leafy produce contaminated with *E. coli* O157:H7 and variants thereof, with a dose as low as 10 cells, can pose severe threat to human health [7]. *E. coli* that cause disease are categorized on the basis of pathogenic mechanisms, virulence, and clinical syndrome. For example, *E. coli* O157:H7 belongs to the enterohaemorrhagic (EHEC) group [8]. Infection with *E. coli* O157:H7 causes major outbreaks particularly associated with raw leafy produce [5]. Although leaf surfaces are not a suitable environment for *E. coli*, it can survive both harsh field and post-harvest storage conditions [5].

L. monocytogenes is a Gram-positive, facultative anaerobic, non-spore forming rod, which is capable of growing at low temperatures. This pathogen is widely present in soil, plant, and water surfaces [9]. It causes less than one percent of foodborne diseases, but it is responsible for causing listeriosis in human [10]. In healthy individuals, the main symptoms are fever and diarrhea, whereas in pregnant women, *L. monocytogenes* causes septicaemia, meningitis, abortion, or stillbirth [5,10]. *L. monocytogenes* is capable of growing at refrigeration temperatures and also surviving in food-processing sites [5].

Microbial contamination of fresh produce by pathogenic microbes not only poses significant risk to public health but also affects the industry financially by resulting in costly product recalls. For example, the recent Shiga toxin-producing *E. coli* O157 outbreak in watercress is estimated to have required the recall of 200,000 items in the United Kingdom [11]. Foodborne outbreaks are common in many countries. This could be due to the pathogens developing resistance to traditional sanitizing agents, thus posing a hazard to the safety of the food supply [12].

Ozone has been successfully used as a principal sanitizer for treating drinking and municipal waters for 100 years, but recently gained attention in the food and agriculture industry [13]. It is well known for its strong oxidizing capacity and has been recognized as a powerful antimicrobial agent, reacting with organic substances approximately 3000 times quicker than chlorine [14]. Ozone is capable of inactivating microorganisms including both Gram positive and Gram negative bacteria, bacterial spores, fungi, fungal spores, viruses, and protozoa [15]. In 1997, the United States Food and Drug Administration (US-FDA) in union with an expert panel granted ozone as GRAS (Generally Recognised as Safe) status [16], and in 2003, it received formal approval from the US-FDA as a "direct contact food sanitizing agent" [17]. One of the major advantages of ozone treatment is the fact the gas leaves no detectable

residues in/on treated products, as ozone rapidly decomposes into oxygen unlike other sanitizers used in the food processing industry [13].

Given the importance of controlling pathogen contamination of leafy fresh produce, the present study aimed to determine the antimicrobial effects of ozone for the control of different strains of *E. coli* and *Listeria* spp. and to observe the regrowth of these pathogenic bacteria on ozone-treated produce during storage of produce for nine days at 4 °C. Previous studies have shown the impact of ozone on pathogens [14,18,19] but have not investigated re-growth after treatment. We also wanted to use ozone levels that did not damage produce, *i.e.*, we investigated commercially-relevant ozone levels for produce treatment. Previous research has shown that not all pathogens are killed by ozone treatment [20] and another objective of this work was to establish why this may occur. Accordingly, we examined the effect of cell age on *E. coli* resistance to ozone. Spinach was artificially contaminated by inoculating with *E. coli* or *Listeria* spp. before ozone treatment. Six different strains of non-pathogenic *E. coli* were used as a representative model for *E. coli* O157:H7, as there have been no reports suggesting significant differences in growth pattern and survival strategy between non-pathogenic *E. coli* and pathogenic *E. coli* O157:H7 [21]. In addition, *L. innocua* and *L. seeligeri* were used as surrogates for *L. monocytogenes* because these offer safe non-pathogenic alternatives for experimental purposes whilst exhibiting similar growth characteristics and behavior on leafy produce as *L. monocytogenes* [20,22].

2. Results and Discussion

2.1. Effect of Ozone Exposure on E. coli and Listeria sp. in Vitro

Colony numbers (CFU) of *E. coli* K12 and *L. innocua in vitro* were significantly reduced ($p < 0.05$) by all ozone treatments (Figure 1), even at the lowest level used (1 ppm for 10 min). Less than 1-log reduction was achieved when colonies on agar were exposed to 1 ppm ozone for 10 min, but more than 1-log reduction was achieved when both the strains of food pathogens were treated with ozone concentrations of 10 and 50 ppm. Similar results were observed by Alwi [18], when *E. coli* O157, *L. monocytogenes*, and *Salmonella typhimurium* were treated *in vitro* with 0.1, 0.3, 0.5, and 1.0 ppm ozone concentration for exposure times of 0.5, 3, 6, and 24 h, respectively. They also observed increases in ozone concentration, and exposure time increased the antibacterial activity.

Interestingly, the agar based *in vitro* assay on both Gram-positive and Gram-negative pathogens showed no significant difference in colony counts between 10 ppm and 50 ppm ozone concentration treatment. This is possibly due to cells being physically protected by others on the surface of the agar plates, *i.e.*, when the cells are spread on agar some cells may not be present as individuals but as groups that provide physical protection; thus, this could reduce the effectiveness of ozone treatment [18]. Alternatively, some cells may have an intrinsic resistance to ozone exposure perhaps due to their age and exposure to stress (see below Section 2.6). Fan and colleagues [20] reported that the maximum inactivation of *L. innocua* cells was observed in less than 2 h and inactivation reached a plateau after 4 h when treated with gaseous ozone *in vitro*.

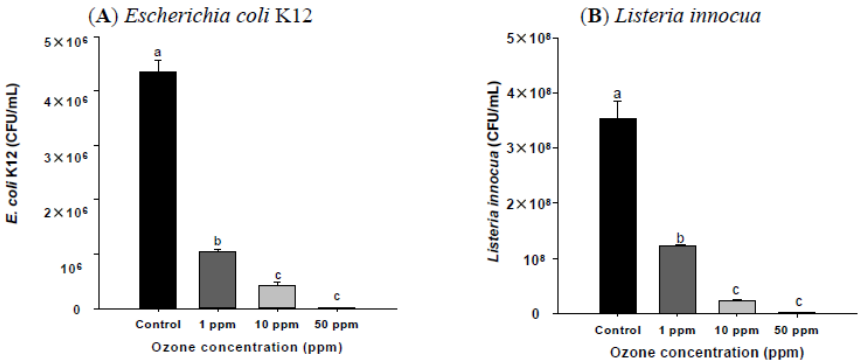

Figure 1. Impacts of ozone treatment on (**A**) *E. coli* K12 and (**B**) *L. innocua* (CFU/mL) grown on agar plates. The treatment chamber was ventilated with 1, 10, or 50 ppm ozone for 10 min. Controls were exposed to "clean air". Values represent the mean (± Standard Error) of measurements made on three independent plates per treatment. Bars with different letters are statistically significantly different ($p < 0.05$).

2.2. Optimization of the Concentration and Duration of Ozone Exposure Levels to Treat Spinach without Causing Visual Damage

The visual appearance and freshness of leafy produce has been the main judging criteria for quality distinction at purchase or consumption [23]. No visual ozone damage was observed when spinach was treated with 1 ppm gaseous ozone, but higher levels, e.g., 10 ppm for 10 min, caused significant visual blemishes and discoloration to spinach (Figure 2A). Similar results were previously observed on fresh produce like lettuce, spinach, and rocket leaves when treated with similar ozone concentrations [24]. Figure 2B illustrates ozone injury/visual damage on spinach when exposed to 10 ppm ozone concentration for 10 min. It is evident that the impact of ozone treatment on the quality of leafy produce is dependent on concentration; it may be beneficial up to a certain level to apply ozone, whereas after a critical level acceleration of browning responses will result in inferior quality.

No visual ozone damage was observed when spinach was exposed to higher concentrations such as 10, 15, and 20 ppm ozone for shorter durations (Table 1). Ozone treated produce visually looked as fresh and as attractive as untreated produce (control) after seven days of storage. Ozone injury/visible damage were observed on spinach when exposed to 25 ppm ozone concentration for all durations examined (30 s, 45 s, and 2 min).

Subsequent experiments examined the effect of varying ozone levels and exposure times on pathogens inoculated onto spinach surfaces.

Table 1. The maximum ozone exposure levels that can be applied on spinach without causing visible damage.

	Duration of the Exposure of Spinach			
Ozone concentration	10 ppm	15 ppm	20 ppm	25 ppm
Time	2 min	45 s	30 s	Damaged at 30 s, 45 s and 2 min

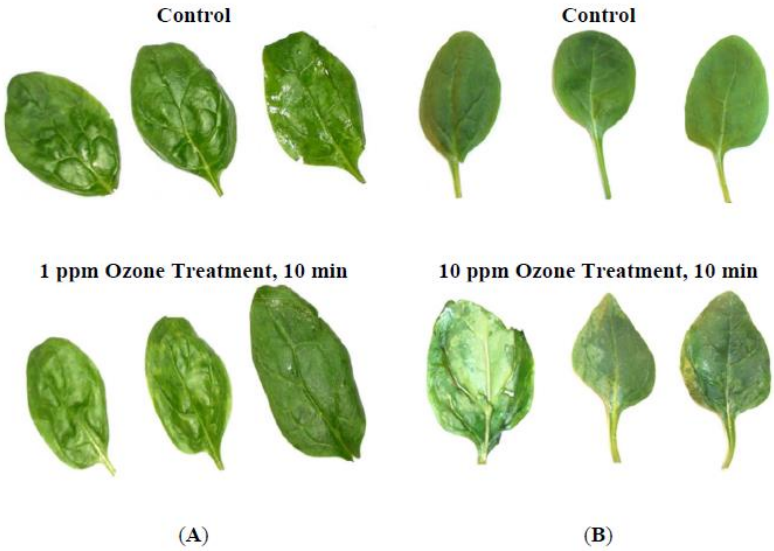

Figure 2. (**A**) Impact of ozone exposure levels on visual quality of spinach when treated at 1 ppm ozone concentration for 10 min and (**B**) Ozone injury/visual damage on spinach when exposed to 10 ppm ozone concentration for 10 min.

2.3. Effect of Ozone Exposure (1 ppm for 10 min) on Different Strains of E. coli Inoculated onto Spinach Leaf Surfaces

Colony numbers (CFU) of all six strains of *E. coli*, *i.e.*, *E. coli* O157:K88a, *E. coli* O25:H4, *E. coli* O128:K67, *E. coli* K12, *E. coli* O55:K59, and *E. coli* O104:H12 obtained from ozone exposed leaves were significantly reduced ($p < 0.05$) compared with non-ozone exposed controls (Figures 3 and 4). No *E. coli* colonies were isolated from non-inoculated spinach leaves. In the past, gaseous ozone treatment at 1 ppm for 5 min showed 3–5 $\log_{10}$ reduction of *E. coli* O157:H7 on spinach after 24 h of storage [25]. An experiment conducted in vacuum-cooling in combination with ozone gas (10 ppm for up to three days) showed 1.4 $\log_{10}$ reduction of *E. coli* O157:H7 on spinach [17]. Gaseous ozone treatment has also proved to be effective in reducing *E. coli* on many products like lettuce [14], parsley [17], mushrooms [19], blueberries [26], and dried figs [27]. Singh *et al.* [14] reported that the bactericidal effect of ozone against *E. coli* O157:H7 increased with exposure time and ozone concentration. For example, they observed 0.79–1.79 $\log_{10}$ CFU/g reduction of *E. coli* O157:H7 population on lettuce when exposed to ozone for 15 min. However, ozone treatment for 5 or 10 min did not decrease the *E. coli* O157:H7 population.

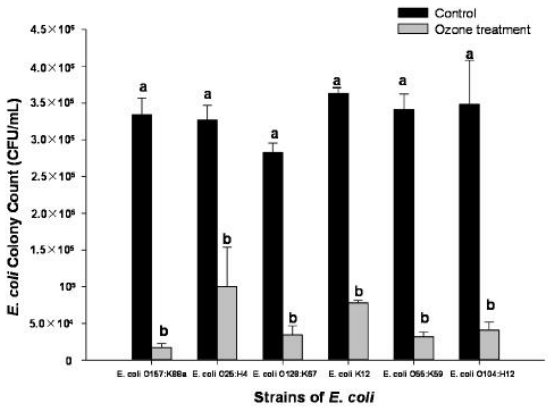

Figure 3. Impacts of ozone-enrichment on six strains of *E. coli* inoculated onto the surface of spinach leaves. Leaves were either treated with 1 ppm ozone concentration (grey bar) or untreated (black bar) for 10 min. Values represent means (±Standard Error) of measurements made on three independent spinach leaves per treatment. Bars with different letters are significantly different ($p < 0.05$).

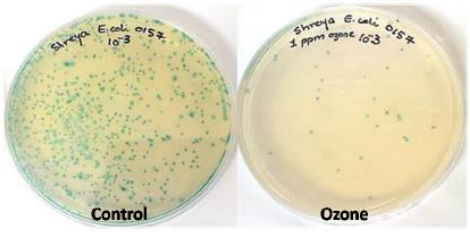

Figure 4. Colonies of *E. coli* O157:K88a on Tryptone Bile X-Glucuronide (TBX) agar recovered from leaves after being exposed to either "clean" air (control) or 1 ppm ozone concentration for 10 min.

2.4. Impact of Ozone Treatment on Listeria innocua and L. seeligeri Inoculated onto Spinach Leaves

In the present study, *L. innocua* and *L. seeligeri* were used as microbial surrogate of *L. monocytogenes*, as they are useful indicators of contamination and have also demonstrated behavior similar to *L. monocytogenes* on fresh produce [28]. Results from spinach artificially contaminated with *L. innocua* and *L. seeligeri* treated with 1 ppm ozone for an exposure time of 10 min showed a 1-log reduction in colony count compared with the untreated control (Figure 5). Karaca and his colleague [17] reported a reduction in *L. innocua* of 1.14 $\log_{10}$ CFU/g on flat-leaved parsley when treated with high ozone concentration of 950 ppm for 20 min. Similar results have been shown by previous research on mushrooms, alfalfa sprouts, alfalfa seeds, and lettuce [19]. The growth of *L. innocua* and *L. seeligeri* on spinach remained significantly reduced after Day 9 of storage (Figure 5). This may be due to the interactions between the natural background microflora of spinach and *L. innocua*, which can affect its growth and survival [22]. O'Berine and his colleague [22] reported that lactic acid bacteria and mixed population of natural microflora isolated from shredded lettuce reduced *L. innocua* growth in model

media. Rodgers and colleagues [19] demonstrated complete inactivation of *L. monocytogenes* on lettuce during nine days of storage when treated with 3 ppm ozone for 3 min.

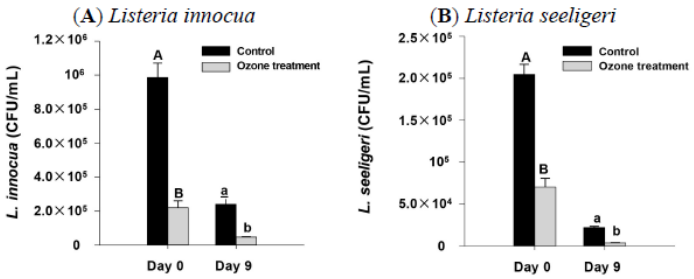

Figure 5. Impacts of ozone-enrichment on (**A**) *L. innocua* and (**B**) *L. seeligeri* inoculated onto the surface of spinach leaves. Leaves were either treated with 1 ppm ozone concentration (grey bar) or untreated (black bar) for 10 min. Colonies were enumerated either directly after the treatments, *i.e.*, Day 0 or after nine days of storage. Values represent means (±Standard Error) of measurements made on three independent spinach leaves per treatment. Bars with different letters are significantly different ($p < 0.05$).

2.5. Effect of Higher Ozone Treatment on E. coli and Listeria sp. Inoculated onto Spinach Leaf Surface

Results of spinach artificially contaminated with two strains of *E. coli* (*E. coli* O157:K88a and *E. coli* O25:H4) and *Listeria* (*L. innocua* and *L. seeligeri*) treated with 10 ppm of ozone concentration for 2 min are shown in Figure 6. For *E. coli* O157:K88a and *E. coli* O25:H4, ozone treatment significantly ($p < 0.05$) reduced counts by 1-log compared with the untreated control (Figure 6A). Ozone had less than 1-log effect on *L. innocua* and *L. seeligeri* (Figure 6B). Awli [18] achieved reduction of 2.89 and 3.06 $\log_{10}$ for *E. coli O157* and *L. monocytogenes*, respectively, on bell pepper when exposed to 9 ppm ozone for 6 h. Their work met the standards for an antimicrobial agent by attaining a minimum of 2 $\log_{10}$ reduction [18]. Similar reductions were observed from application of 5 ppm ozone for 3 min on whole tomato [29]. When results from this work (on leafy produce) are compared with other hardy produce, it appears that ozone treatment was less successful. This is most probably due to the delicate nature of leafy produce, which limits the use of increased ozone concentration and exposure time (results from Section 2.2). In addition, the results obtained from this treatment, *i.e.*, 10 ppm for 2 min were not significantly more effective in reducing bacterial viable counts in comparison to previous ozone treatment used in this study, *i.e.*, 1 ppm for 10 min (from Sections 2.3 and 2.4).

Ozone inactivates bacterial cells by the progressive oxidation of important cellular constituents [17], and suggestions for the principal target of ozonation include the bacterial cell surface. Bacterial cell death was observed as a consequence of a ruptured cell membrane and as a result of disintegration of cell wall to function as a barrier [17,18,20]. *E. coli*, a Gram-negative bacterium, is more susceptible to ozone treatment because it has a thin peptidoglycan lamella that is covered by an outer membrane made of polysaccharides and lipoproteins [30]. In contrast, some studies claimed that Gram-negative bacteria were more resistant to ozone treatment as compared with Gram-positive bacteria [31]. Results from this study show that ozone treatment was effective in both *E. coli* and *Listeria* spp. inactivation but

Listeria spp. were slightly more resistant. These results are in line with Yuk and colleagues [19], who showed that *E. coli* O157:H7 is more sensitive than *Listeria monocytogenes*.

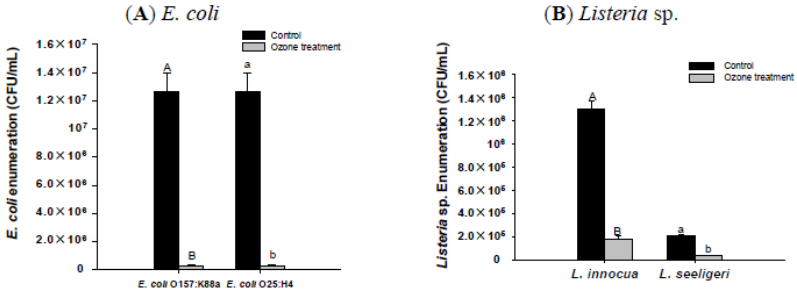

Figure 6. Impacts of increased levels of ozone exposure on two strains of (**A**) *E. coli* and (**B**) *Listeria* sp. inoculated onto the surface of spinach leaves. Leaves were either treated with 10 ppm ozone concentration (grey bar) or untreated (black bar) for 2 min. Values represent means (±Standard Error) of measurements made on three independent spinach leaves per treatment. Bars with different letters are significantly different ($p < 0.05$).

To investigate the after effects of the ozone treatment on pathogen growth, artificially contaminated spinach was stored at 7 °C for nine days. Figure 7 shows that populations of both *E. coli* (*E. coli* O157:K88a and *E. coli* O25:H4) and *Listeria* sp. (*L. innocua* and *L. seeligeri*) after nine days of storage did not regrow, as a significant reduction in number of colonies was observed in comparison with the untreated control. However, effect of higher ozone treatment on pathogen recovery did not show a significant difference in count as compared with treatment with lower ozone concentration.

2.6. Effect of Age on Ozone Resistance of E. coli O157:K88a in Vitro

Throughout the study, we observed that a certain proportion of cells survived ozone exposure and we were interested to make initial investigations into potential ozone resistance mechanisms. *E. coli* cells of increasing colony age were exposed to ozone (*in vitro*) and results demonstrated a clear increase in ozone resistance of *E. coli* O157:K88a with increasing colony age. For example, survival of *E. coli* O157:K88a was observed to be greater (approximately 15%) after five days of growth compared with the day 1 time point. Survival levels increased even further by Day 7 (Figure 8) suggesting that cells in older bacterial colonies are more ozone resistant than cells from younger colonies. This is possibly because the older *E. coli* cells may to be in their long-term stationary phase (fifth phase of bacterial growth cycle that survives on the nutrient released by the dead population of bacteria). These older cells can survive external stress unlike the younger cells (probably in first or second phase of bacterial growth cycle) and can remain viable for months or even years once they enter long-term stationary phase [32]. This stationary phase is dominated by the accumulation of the sigma factor RpoS [32]. The entire cellular physiology of *E. coli* is influenced by RpoS that directly or indirectly affects the expression of 10% of the *E. coli* genes. These genes are involved in morphological variations within the cell and responsible for increasing resistance during numerous stress conditions, e.g., oxidative stress, osmotic stress, heat shock, *etc.* [32].

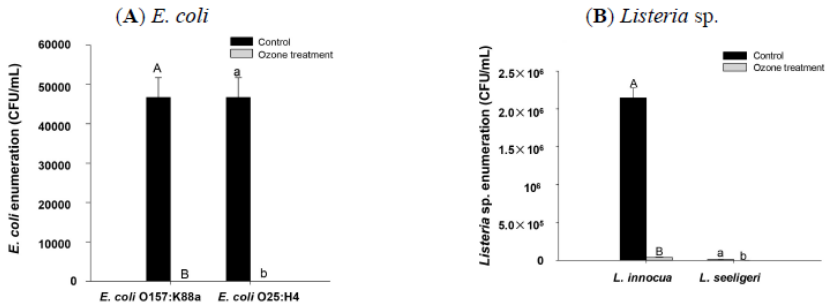

Figure 7. Impacts of ozone-enrichment on two strains of (**A**) *E. coli* and (**B**) *Listeria* sp. inoculated onto the surface of spinach leaves. Leaves were either treated with 10 ppm ozone concentration (grey bar) or untreated (black bar) for 2 min. Colonies were enumerated after nine days of storage. Values represent means (±Standard Error) of measurements made on three independent spinach leaves per treatment. Bars with different letters are significantly different ($p < 0.05$).

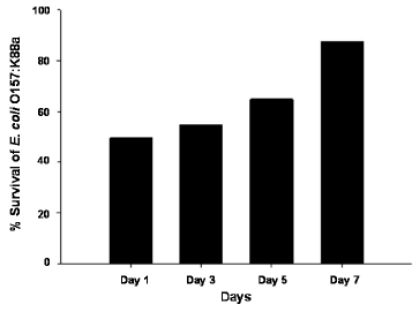

Figure 8. Survival of cells obtained from different colony ages of *E. coli* O157:K88a exposed to 10 ppm ozone concentration for 2 min. After ozone exposure, the culture plates were maintained at 37 °C for seven days.

3. Experimental Section

3.1. Ozone Fumigation System

A purpose designed ozone fumigation system (Figure 9) was housed in a fume hood and constructed of stainless steel (diameter 35 cm). An inlet pipe was used to add ozone generated by electric discharge from oxygen (model SGA01 Pacific Ozone Technology Inc., Brentwood, CA, USA), and the introduction of ozone was manually controlled via stainless steel needle valves/gap flow meters. Once the desired ozone concentration was achieved, Petri plates/produce to be exposed to ozone was placed at the bottom of the system and the fumigation system closed with the Pyrex cover (Figure 9). The ozone concentration in the system was recorded using a photometric analyzer (model 450, manufactured by Advanced Pollution Instrumentation Division, 9480 Carroll Park Drive, San Diego, CA, USA). The ozone monitor employed in these studies was serviced weekly and calibrated routinely against standards using a Dasibi 1008PC unit.

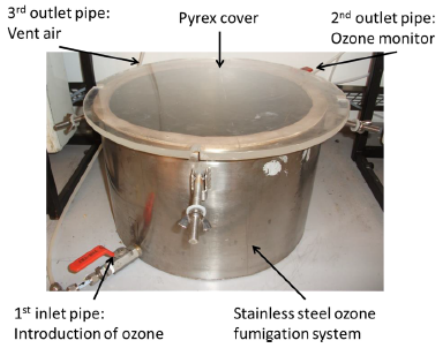

Figure 9. Ozone fumigation system.

3.2. Assessing the Impact of Ozone Treatment on Food Pathogens E. coli and L. innocua in Vitro

E. coli K12 and *L. innocua* were obtained from a culture collection maintained by Geneius Laboratories Ltd. (44 Colbourne Crescent, Nelson Park, Cramlington, UK). These cultures were sub-cultured by spread plating on Nutrient agar (NA) and Agar Listeria according to Ottaviani and Agosti (ALOA) agar plates, respectively. A single colony was isolated from each culture plate after incubation at 37 °C for 24 h and 30 °C for 48 h, respectively, and transferred to minimum recovery diluent (MRD). A standardized concentration of 10^4 cells per mL (100 µL) of each culture was spread onto sterile NA and ALOA agar plates, respectively. These plates were then either exposed to 1 ppm, 10 ppm, 50 ppm ozone concentration, or charcoal filtered "clean air" (controls) for 10 min at room temperature. After treatment, NA and ALOA agar plates were incubated at 37 °C for 24 h and 30 °C for 48 h, respectively. The number of colonies produced on control plates (non-ozone exposed) were compared with the numbers found on ozone-treated plates based on three replicate observations.

3.3. Optimization of Ozone Exposure Levels (Concentration and Duration) to Treat Leafy Salads without Causing Visual Damage to Produce

This experiment focused on optimizing the concentration and duration of ozone exposure to which fresh produce could be exposed without causing visible damage/deterioration. To determine the impact on visual quality of the produce, baby spinach was received from Vitacress Ltd. (Hampshire, UK) and then exposed to 1, 10, 25, 50 ppm ozone or "clean air" (controls) for varying periods of time (1–60 min). Following exposure to ozone, the produce was then packed in a sterile self-seal bag and maintained at 4 °C in dark conditions. Ozone injury was assessed visually by comparing ozone exposed produce with control (non-ozone exposed) produce every alternate day for seven days.

3.4. Ozone Resistance of Different Strains of E. coli: Inoculation of E. coli onto Spinach Leaves and Ozone Exposure Conditions

Six strains of *E. coli* (*E. coli* O157:K88a, *E. coli* O25:H4, *E. coli* O128:K67, *E. coli* K12, *E. coli* O55:K59, and *E. coli* O104:H12) were obtained from a culture collection maintained by Geneius Laboratories Ltd. (Nelson Park, Cramlington, UK). Cultures were stored at 4 °C on Luria-Bertani (LB)

agar plates, and activated in LB broth at 37 °C. Baby-leaf spinach was purchased from a local retailer and aseptically cut into discs measuring 1.13 cm^2 using a sterile cork borer. A suspension of *E. coli* (overnight culture, 10^8–10^9 CFU/mL LB broth) was applied directly to the leaf disc in 300 µL aliquots, and then the inoculated leaves were stored overnight at 7 °C to mimic produce storage conditions and to allow attachment of *E. coli* to the leaf surface. Inoculated leaves were either exposed to 1 ppm ozone or charcoal filtered "clean air" for 10 min at room temperature. To determine the number of *E. coli* remaining (control and ozone exposed), the leaf discs were vigorously shaken in MRD for 2 min and then serially diluted using MRD, followed by pour plate technique using Tryptone Bile X-Glucuronide (TBX) agar plates. Plates were incubated at 44 °C for 24 h, and presumptive colonies were counted on the basis of three replicate observations.

3.5. Impact of Ozone Treatment on L. innocua and L. seeligeri Inoculated onto Spinach Leaves

Two strains of *Listeria* (*L. innocua* and *L. seeligeri*) were obtained from a culture collection maintained by Geneius Laboratories Ltd. Cultures and stored at 4 °C on ALOA agar plates. Spinach leaves were then aseptically cut into discs measuring 1.13 cm^2 using a sterile cork borer. A suspension of *Listeria* sp. (10^7–10^8 CFU/mL MRD) was applied directly to the leaf disc in 300 µL aliquots, and the inoculated leaves were maintained at 7 °C to mimic produce storage conditions for 2 h to allow attachment of *Listeria* sp. to the leaf surface. Inoculated leaves were either exposed to 1 ppm ozone or charcoal filtered "clean air" for 10 min at room temperature and survival rate enumerated (see below). For determining the survival and growth of *Listeria* sp. during storage, a proportion of the treated and untreated inoculated leaves were maintained at 7 °C for a further nine days. The number of colonies remaining (control and ozone exposed) on Day 0 and Day 9 was determined by vigorously shaking the leaf disc in MRD for 2 min after 1 h incubation at room temperature, and then serially diluting in MRD followed by standard spread technique on ALOA agar plates. Plates were incubated at 30 °C for 48 h, and colonies were counted.

3.6. Modified Ozone Fumigation System—Delivery of High Ozone Concentrations for Short Time Durations (Seconds)

A modified ozone fumigation system was engineered to improve the application of ozone to produce surfaces, and to reduce the time required to build up the desired ozone concentrations needed for produce treatment. The aim was to develop a system allowing application of higher ozone concentrations for shorter durations to achieve better bacterial kill without damaging the produce. This system was developed after discussions/meetings with industrial partners who ideally wanted to be able to expose produce to ozone quickly during their harvest and processing procedures. The modified ozone exposure apparatus was housed in a fume hood and constructed from 20 cm^2 Perspex. Produce was placed on a steel mesh in a 2 cm deep tray within the box and produce was then exposed to ozone once the desired concentration was achieved (Figure 10). An inlet pipe was used to add ozone generated by electric discharge from oxygen, with the introduction of ozone controlled manually. The ozone concentration was recorded by a photometric analyzer (model 450, manufactured by Advanced Pollution Instrumentation Inc., San Diego, CA, USA). The ozone monitor employed in these studies was serviced routinely.

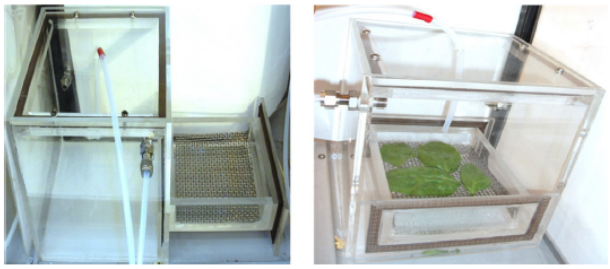

Figure 10. Modified ozone fumigation system.

3.7. Exploration of Higher Ozone Exposure Levels to Treat Spinach without Causing Visual Damage

This experiment aimed to determine the highest ozone concentration and exposure time that could be used on organic baby spinach without causing visible damage/deterioration to the produce. Produce was exposed to 10, 15, 20, 25 ppm ozone or "clean air" (controls) for varying periods of time ranging from 30 s to 2 min. Following exposure to ozone, produce was then packed in a sterile self-seal bag and maintained at 4 °C in the dark. Ozone injury was assessed visually by comparing ozone exposed produce with control (non-ozone exposed) produce every alternate day for seven days.

3.8. Impact of Higher/Increased Ozone Concentrations on Two Strains of E. coli and Listeria Inoculated onto Spinach Leaves

This experiment aimed to use the highest ozone exposure levels that did not cause produce damage (data obtained from Section 3.7—Result Section 2.2) to try and achieve higher reductions in pathogenic bacteria on the surface of baby spinach leaves. Two strains of *E. coli* (*E. coli* O157:K88a and *E. coli* O25:H4) and *Listeria* (*L. innocuous* and *L. seeligeri*) were inoculated onto spinach leaves as described in Sections 3.4 and 3.5, respectively. Inoculated leaves were either treated with 10 ppm ozone concentration or charcoal filtered "clean air" for 2 min. The number of *E. coli* and *Listeria* sp. remaining (control and ozone exposed) was determined as described above (Sections 3.4 and 3.5).

To determine the impact of highest ozone exposure levels on the survival and growth of *E. coli* (*E. coli* O157:K88a and *E. coli* O25:H4) and *Listeria* (*L. innocua* and *L. seeligeri*) during storage, the inoculated leaves were treated as mentioned in Section 3.5. After the treatment, inoculated and control leaves were maintained at 7 °C for nine days. The number of colonies remaining (control and ozone exposed) on day 9 was determined as mentioned in Section 3.5.

3.9. Age Effects on Ozone Resistance of E. coli in Vitro

To determine whether cell age affected the ozone resistance of the bacteria, a colony of *E. coli* O157:K88a obtained from a culture collection maintained by Geneius Laboratories Ltd. was sub-cultured onto NA plates and incubated at 37 °C for seven days. A single colony was isolated on the first, third, fifth, and seventh day of the incubation and transferred to MRD. A standardized concentration of 10^4 cells per mL (100 µL) of each cell age was spread onto sterile NA plates and these plates were then exposed to either 10 ppm ozone concentration or charcoal filtered "clean air" for 2 min. Colony count was determined after incubating NA plates at 37 °C for 24 h.

3.10. Statistical Analysis

Data were analyzed using SPSS (IBM SPSS Statistics 19 64Bit) and graphs were produced using Microsoft Office Excel 2010 and SigmaPlot 12.5. Normal data distribution was tested using a Normality test and significant differences between mean values were verified using LSD ($p < 0.05$) following one-way ANOVA.

4. Conclusions

Exposure to 1 ppm and 10 ppm gaseous ozone treatment for 10 and 2 min, respectively, significantly reduced *E. coli* and *Listeria* spp. populations on spinach. In addition, the pathogens did not re-grow after treatment, *i.e.*, over a nine-day storage period. Although ozone treatment only reduced bacterial loads by 1 log, there is still commercial potential as ozone is easy to produce on site and apply at levels which do not damage sensitive leafy produce. The findings from this study show that some bacteria in populations are resistant to ozone treatment and increasing cell (colony) age of *E. coli* was shown to be linked to enhanced ozone resistance. Further work is needed to better understand the exact mechanism of resistance, and this may lead to determining methods that can overcome resistance. Such applications could deliver immense potential benefits for commercial use and improving public health.

Acknowledgments

This study was supported by the ADHB/Horticultural Development Company (HDC) (FV 386) via the award of a PhD studentship to Shreya Wani. All *E. coli* and *Listeria* spp. strains were kindly provided by Geneius laboratories Ltd. (www.geneiuslabs.com). We thank Matthew Peake for technical help and Alan Craig for maintaining and calibrating the ozone fumigation.

Author Contributions

The work presented is a part of a PhD project funded by the UK-ADHB/HDC; the data were managed, designed, collected, and analyzed by Shreya Wani who took the lead on writing the manuscript. Ian Singleton and Jeremy Barnes supervised the work, assisted in experimental design and data interpretation, and won the grant award. Joseph Thompson was a summer intern and assisted with some experimental work in the laboratory. Jagpreet Maker was a post-graduate student who contributed to the editing and approval of the manuscript.

Conflicts of Interest

The authors declare no conflict of interest.

References

1. Burnett, S.L.; Beuchat, L.R. Human pathogens associated with raw produce and unpasteurized juices, and difficulties in decontamination. *J. Ind. Microbiol. Biotechnol* **2000**, *25*, 281–287.

2. Abadias, M.; Usall, J.; Anguera, M.; Solsona, C.; Vinas, I. Microbiological quality of fresh, minimally-processed fruit and vegetables, and sprouts from retail establishments. *Int. J. Food Microbiol.* **2008**, *123*, 121–129.
3. Velusamy, V.; Arshak, K.; Korostynska, O.; Oliwa, K.; Adley, C. An overview of foodborne pathogen detection: In the perspective of biosensors. *Biotechnol. Adv.* **2010**, *28*, 232–254.
4. Olaimat, A.N.; Holley, R.A. Factors influencing the microbial safety of fresh produce: A review. *Food Microbiol.* **2012**, *32*, 1–19.
5. Engels, C.; Weiss, A.; Carle, R.; Schmidt, H.; Schieber, A.; Ganzle, M.G. Effect of gallotannin treatment on attachment, growth and survival of *Escherichia coli* O157:H7 and *Listeria monocytogenes* on spinach and lettuce. *Eur. Food Res. Technol.* **2012**, *234*, 1081–1090.
6. Griffin, P.M.; Tauxe, R.V. The epidemiology of infections caused by *Escherichia coli* O157:H7, other enterohemorrhagic *E.coli*, and the associated Hemolytic Uremic Syndrome. *Epidemiol. Rev.* **1991**, *13*, 60–99.
7. Tomas-Callejas, A.; Lopez-Velasco, G.; Camacho, A.B.; Artes, F.; Artes-Hernandez, F.; Suslow, T.V. Survival and distribution of *Escherichia coli* on diverse fresh-cut baby leafy greens under preharvest through postharvest conditions. *Int. J. Food Microbiol.* **2011**, *151*, 216–222.
8. Coia, J.E. Clinical, microbiological and epidemiological aspects of *Escherichia coli* O157 infection. *FEMS Immunol. Med. Microbiol.* **1998**, *20*, 1–9.
9. Farber, J.M.; Peterkin, P.I. *Listeria monocytogenes*, a Food-Borne pathogen. *Microbiol. Rev.* **1991**, *55*, 476–511.
10. Notermans, S.; Todd, E.C.D. Surveillance of listeriosis and its causative pathogen, *Listeria monocytogenes*. *Food Control* **2011**, *22*, 1484–1490.
11. Launders, N.; Byrne, L.; Adams, N.; Glen, K.; Jenkins, C.; Tubin-Delic, D.; Locking, M.; Williams, C.; Morgan, D.; Outbreak Control Team. Outbreak of Shiga toxin-producing *E.coli* O157 associated with consumption of watercress, United Kingdom, August to September 2013. *Euro Surveill.* **2013**, *18*, doi:10.2807/1560-7917.ES2013.18.44.20624.
12. Bower, C.K.; Daeschel, M.A. Resistance responses of microorganisms in food environments. *Int. J. Food Microbiol.* **1999**, *50*, 33–44.
13. Mahapatra, A.K.; Muthukumarappan, K.; Julson, J.L. Applications of ozone, bacteriocins and irradiation in food processing: A review. *Crit. Rev. Food Sci. Nutr.* **2005**, *45*, 447–461.
14. Singh, N.; Singh, R.K.; Bhunia, A.K.; Stroshine, R.L. Efficacy of chlorine dioxide, ozone, and thyme essential oil or a sequential washing in killing *Escherichia coli* O157:H7 on lettuce and baby carrots. *LWT Food Sci. Technol.* **2002**, *35*, 720–729.
15. Goncalves, A.A. Ozone—An emerging technology for the seafood industry. *Braz. Arch. Biol. Technol.* **2009**, *52*, 1527–1539.
16. Tzortzakis, N.; Borland, A.; Singleton, I.; Barnes, J. Impact of atmospheric ozone-enrichment on quality-related attributes of tomato fruit. *Postharvest Biol. Technol.* **2007**, *45*, 317–325.
17. Karaca, H.; Velioglu, Y.S. Effects of ozone treatments on microbial quality and some chemical properties of lettuce, spinach, and parsley. *Postharvest Biol. Technol.* **2014**, *88*, 46–53.
18. Alwi, N.A.; Ali, A. Reduction of *Escherichia coli* O157, *Listeria monocytogenes* and *Salmonella enterica* sv. Typhimurium populations on fresh-cut bell pepper using gaseous ozone. *Food Control* **2014**, *46*, 304–311.

19. Yuk, H.G.; Yoo, M.Y.; Yoon, J.W.; Marshall, D.L.; Oh, D.H. Effect of combined ozone and organic acid treatment for control of *Escherichia coli* O157:H7 and Listeria monocytogenes on enoki mushroom. *Food Control* **2007**, *18*, 548–553.
20. Fan, L.; Song, J.; McRae, K.B.; Walker, B.A.; Sharpe, D. Gaseous ozone treatment inactivates *Listeria innocua in vitro*. *J. Appl. Microbiol*. **2007**, *103*, 2657–2663.
21. Gleeson, E.; O'Beirne, D. Effects of process severity on survival & growth of *Escherichia coli* & *Listeria innocua* on minimally processed vegetables. *Food Control* **2005**, *16*, 677–685.
22. O'Beirne, D.; Francis, A.G. Effects of the indigenous microflora of minimally processed lettuce on the survival and growth of *Listeria innocua*. *Int. J. Food Sci. Technol*. **1998**, *33*, 477–488.
23. Rico, D.; Martín-Diana, A.B.; Barat, J.M.; Barry-Ryan, C. Extending and measuring the quality of fresh-cut fruit and vegetables: A review. *Trends Food Sci. Technol*. **2007**, *18*, 373–386.
24. Alexopoulos, A.; Plessas, S.; Ceciu, S.; Lazar, V.; Mantzourani, I.; Voidarou, C.; Stavropouloua, E.; Bezirtzogloua, E. Evaluation of ozone efficacy on the reduction of microbial population of fresh cut lettuce (*Lactuca sativa*) and green bell pepper (*Capsicum annuum*). *Food Control* **2013**, *30*, 491–496.
25. Klockow, P.A.; Keener, K.M. Safety and quality assessment of packaged spinach treated with a novel ozone-generation system. *LWT Food Sci. Technol.* **2009**, *42*, 1047–1053.
26. Bialka, K.L.; Demirci, A. Decontamination of *Escherichia coli* O157:H7 and *Salmonella enterica* on blueberries using ozone and pulsed UV-light. *J. Food Sci*. **2007**, *72*, 391–396.
27. Akbas, M.Y.; Ozdemir, M. Application of gaseous ozone to control populations of *Escherichia coli*, *Bacillus cereus* and *Bacillus cereus* spores in dried figs. *Food Microbiol*. **2008**, *25*, 386–391.
28. Scifò, G.O.; Randazzo, C.L.; Restuccia, C.; Fava, G.; Caggia, C. *Listeria innocua* growth in fresh cut mixed leafy salads packaged in modified atmosphere. *Food Control* **2009**, *20*, 611–617.
29. Bermúdez-Aguirre, D.; Barbosa-Cánovas, G.V. Disinfection of selected vegetables under nonthermal treatments: Chlorine, acid citric, ultraviolet light and ozone. *Food Control* **2013**, *29*, 82–90.
30. Zuma, F.; Lin, J.; Jonnalagadda, S.B. Ozone-initiated disinfection kinetics of *Escherichia coli* in water. *J. Environ. Sci. Health A Tox. Hazard. Subst. Environ. Eng*. **2009**, *44*, 48–56.
31. Vaz-Velho, M.; Silva, M.; Pessoa, J.; Gibbs, P. Inactivation by ozone of *Listeria innocua* on salmon-trout during cold-smoke processing. *Food Control* **2006**, *17*, 609–619.
32. Navarro Llorens, J.M.; Tormo, A.; Martinez-Garcia, E. Stationary phase in gram-negative bacteria. *FEMS Microbiol. Rev*. **2010**, *34*, 476–495.

Appendix F: Investigation of Potential reasons for bacterial survival on 'ready-to-eat' leafy produce during exposure to gaseous ozone (This paper is published using data from Chapter 3)

Postharvest Biology and Technology 111 (2016) 185–190

Contents lists available at ScienceDirect

Postharvest Biology and Technology

journal homepage: www.elsevier.com/locate/postharvbio

Investigation of potential reasons for bacterial survival on 'ready-to-eat' leafy produce during exposure to gaseous ozone

Shreya Wani, Jeremy Barnes*, Ian Singleton*

School of Biology, Newcastle University, Newcastle upon Tyne NE1 7RU, United Kingdom

ARTICLE INFO

Article history:
Received 21 May 2015
Received in revised form 7 August 2015
Accepted 13 August 2015
Available online xxx

Keywords:
Fresh produce
Ozone resistance
Confocal microscopy
Pseudomonas sp.
Spoilage
ozone gas

ABSTRACT

Fresh leafy produce, such as lettuce and coriander, are subject to post harvest microbial contamination and decay. Because of increasing pesticide resistance and consumer pressures, alternative residue free treatments, such as ozone, are being actively explored and encouraged to reduce microbial loads and curb spoilage of crops in storage/transit. However, several researchers have reported that a component of the bacterial population on leaf surfaces is resistant to ozone treatment. To investigate the potential reasons for this bacterial survival, confocal microscopy was used to visualise microbes on leaf surfaces before and after ozone treatment. Direct observation (live/dead cell staining) of cells after ozone exposure showed that some cells were still alive; this included cells in small colonies as well as individual cells. We hypothesised that cell (colony) age and prior stress (cold) contributes to, or is responsible for, the ozone resistance observed. Interestingly, cells derived from older agar grown colonies (7 12 day old) and cold stressed cells of a *Pseudomonas* sp. (isolated from coriander) showed higher ozone resistance than that of control cells (4 day old colonies). These findings suggest that a range of factors are responsible for ozone resistance and further work to improve our understanding of the mechanisms of ozone resistance may lead to improved methods to reduce microbial spoilage of fresh produce.

1. Introduction

Over the past decade, there have been increasing concerns about food quality and microbial safety, especially with regard to leafy salads, herbs, seed and vegetables which may be minimally processed and are often consumed raw (Losio et al., 2015). It appears that microbial contamination can occur at any stage from production to consumer handling, and may arise from animal, environmental or human sources or by simple multiplication of surface biofilms to create slime and off odours (Olaimat and Holley, 2012). The microbial flora is assumed, often incorrectly, to be limited to the surface of the healthy produce, whereas the internal tissue remains sterile (Naito and Takahara, 2006). To prevent potential microbial spoilage, ozone has been suggested as an alternative sanitizer because of its strong oxidizing capacity (Goncalves, 2009). It has been used as a key disinfectant to treat municipal and drinking water since the late 19th century, but has lately gained attention in the agrifood sector. The use of ozone is already permitted in many Asian and European countries, and the gas holds generally recognised as safe (GRAS) status in USA and was approved by US-FDA as a 'direct contact food sanitizing agent' in 2001 (Palou et al., 2003). One of the major advantages of ozone treatment is that the gas spontaneously decomposes in to inert products unlike other sanitizers used in the food processing industry (Mahapatra et al., 2005). However, research shows that treatment with ozone does not completely inactivate bacteria on fresh produce (Wei et al., 2007; Srey et al., 2013; Wani et al., 2015). This could be due to a combination of physical protection of cells in micro-colonies and/or increased ozone resistance induced by parallel factors such as refrigeration (Finkel, 2006). Epiphytic bacteria i.e. bacteria present on plant surfaces are exposed to numerous environmental stresses in nature, such as nutrient stress, water stress, variable weather conditions, and exposure to UV radiation (Capozzi et al., 2009). However, bacteria are capable of adapting to, and growing, under stressful conditions (Beattie and Lindow, 1999) and initiating stress response mechanisms (Capozzi et al., 2009).

In this study, we used confocal scanning laser microscopy (CSLM) to differentiate between live and dead bacteria on the surface of a range of leafy salads and herbs (spinach, rocket, watercress, coriander and lettuce) in the presence and absence of ozone treatment. CSLM allows quick and direct assessment of microbial colonization on leaf surface by producing sharp, in-focus images from three-dimensional specimens (Ferrando and Spiess,

* Corresponding author.
E-mail addresses: shrenrique@gmail.com (S. Wani), jerry.barnes@ncl.ac.uk (J. Barnes), ian.singleton@ncl.ac.uk (I. Singleton).

http://dx.doi.org/10.1016/j.postharvbio.2015.08.007

2000). We also tested the hypothesis that prior exposure to stress (cold) and increasing cell age would enhance cell resistance to ozone exposure using a *Pseudomonas* species isolated from coriander. *Pseudomonas* sp. was used as a model in this work as species from this genera are known to be involved in the microbial proteolytic and pectinolytic activities that cause soft rot of fresh produce at storage temperatures as low as 0.2 °C (Saranraj et al., 2012).

2. Materials and methods

2.1. Bacterial staining and visualisation for cell viability assessment on leafy produce

Packets of 'ready-to-eat' organic baby spinach, Iceberg lettuce, wild rocket, coriander and watercress were purchased from a local retailer and stored at 4 °C until the use-by-date i.e., 'EOL' (end of life). The leaves were then aseptically cut into discs measuring 1.13 cm^2 using a sterile cork borer for visualization of cell viability and enumeration of natural flora bacteria. Cell viability stains (LIVE/DEAD® BacLight™ Viability Kit, Invitrogen/Molecular Probes, Eugene, Oregon, USA) were prepared separately as per the manufacturer's instructions. This protocol utilizes green-fluorescent SYTO®9 stain to label live bacterial cells green, whereas red-fluorescent propidium iodide stains dead cells red. The staining solutions were prepared in Mueller Hinton Broth (MHB) and filter-sterilized using a syringe-mounted membrane filter of 0.2 μm pore size prior to use. The BacLight stains were added directly to the leaf surfaces which were placed onto sterile glass slides in 250 μL aliquots before placing a coverslip on top of the stain. The stained leaf was then incubated in the dark for 30 min before viewing with a Confocal Scanning Laser Microscopy (Leica TCS SP2, Leica Microsystems, GMBH, Heidelberg, Germany). The samples were scanned with a 488 nm Argon laser for the SYTO®9-stained bacteria using emission wavelengths collected at 500–550 nm, whereas a 543 nm Helium/Neon laser was used for the propidium iodide-stained bacteria using emission wavelengths collected at 574–714 nm. The microscope was equipped with either 40× HCX Plan (numerical aperture – 0.85) or 63× oil immersion objective (numerical aperture – 1.32) to image the leaf surfaces.

2.2. Ozone fumigation system and optimization of ozone exposure levels to treat leafy salads

Ozone concentration and exposure time were optimized to treat 'ready-to-eat' organic baby spinach, Iceberg lettuce, wild rocket, coriander and watercress. The ozone fumigation system stainless steel container (35 cm in diameter) placed in a fume hood into which ozone gas was introduced (produced by an electric discharge ozone generator supplied with oxygen using a model SGA01 Pacific Ozone Technology Inc., Brentwood, California, USA). Stainless steel needle valves/gap flow meters were used to manually control the introduction of ozone. Produce was placed in the treatment chamber which was closed using a Pyrex cover (Wani et al., 2015). Targeted produce were exposed to 1, 10, 25, 50 $\mu L\,L^{-1}$ ozone or 'charcoal-filtered air' (control) for varying durations (from 1 to 60 min). A photometric analyzer (model 450, manufactured by Advanced Pollution Instrumentation Division, 9480 Carroll Park Drive, San Diego, CA 92121-5201) was used to accurately monitor the ozone concentration in the system. Following targeted ozone exposure, the produce was then placed in a sterile self-seal bag and maintained at 4 °C in the dark to mimic commercial storage conditions. The appearance of treated produce was assessed visually using a 5-point scale (5 being unaffected and 1 being the worst colour quality).

2.3. Direct enumeration of bacteria on leafy produce after ozone treatment using confocal microscopy

'Ready-to-eat' organic baby spinach, Iceberg lettuce, wild rocket, coriander and watercress were aseptically cut into discs using a sterile cork borer and placed onto sterile glass slides. Produce was treated with either 0 (charcoal-filtered air), 1 (spinach, lettuce and watercress) or 10 (rocket and coriander) $\mu L\,L^{-1}$ ozone for 10 min (results obtained from Section 3.2). The leaf surface bacterial staining procedure as described in Section 2.1 was then performed. Images were captured at 40× magnification. Three replicates (leaf discs) of each product per treatment were used for enumeration of viable cells (stained green). Bacteria from 20 microscopic fields were counted on each replicate leaf for each type of fresh produce using image J software (Selinummi et al., 2005), and results were expressed as average numbers of bacteria per square centimeter (cm^2) of leaf.

2.4. Investigating potential reasons for bacterial survival during ozone treatment

2.4.1. Isolation and identification of Pseudomonas sp.

The effect of stress on ozone resistance was determined on a *Pseudomonas* isolate from coriander. Samples (25 g) were stomached in Buffered Peptone Water (BPW) and the total viable count (TVC) determined after growth on Plate Count Agar (PCA) using standard spread plate technique. PCA agar plates were incubated at 30 °C for 3 days after serial dilution in minimum recovery diluent (MRD). Discrete colonies of one morphologically dominant microbial type were subsequently re-cultured for microbial identification using 16S rRNA gene sequence. The total DNA from agar grown cells was extracted using a QIAGEN kit and extracted DNA was stored at −20 °C. Using the universal prokaryotic primers, (27F) (5′-AGAGTTTGATCMTGGCTCAG-3′) and (1525R) (5′-AAGGAGGTGWTCCARCC-3′), a segment of the bacterial 16S rRNA gene was amplified using a Hybaid PCR Express thermal cycler; PCR cycles were performed at 94 °C for 3 min, 94 °C for 30 s, 55 °C for 30 s and 72 °C for 30 s. A total of 30 cycles were performed with a final extension step at 72 °C for 5 min. PCR amplification was performed using reaction mixtures (final volume 10 μL) consisting of 2 ng template, buffer incubation mix with 1.5 mM $MgCl_2$, 0.2 mM dNTP (Qiagen), 0.5 mM primer 27F, 0.5 mM primer 1525R, and 2.5 U of DreamTaq proof-reading DNA Polymerase (Fermentas). Amplification of PCR products was confirmed by 1.5% agarose gel electrophoresis with ethidium bromide staining and visualised using a UV transilluminator. PCR products were then purified using Exonuclease 1 & Alkaline phosphatase prior to sequencing (ABI 3730, 96 capillary array sequencer). The sequences were generated using Sanger sequencing and assembled by aligning the forward and reverse sequences using ABI MicroSeq software to form a consensus sequence. This consensus sequence was then compared with sequences in the ABI MicroSeq database v. 2.0 as well as with those in the BLAST nucleotide database (NCBI) to allow for genus/species matching. The nucleotide sequence for the isolate employed in this study has been deposited in GenBank (NCBI) under the accession number: KR067481.

2.4.2. Effect of temperature on ozone resistance of Pseudomonas sp. in vitro

Confocal microscopy images of ozone-treated leaves revealed that two/three cells often survived in micro-colonies surrounded by dead cells. Interestingly, individual survivors were also visible (see Section 3.3). This indicated that cells could be physically protected by other cells when present in small colonies but also that some invidual cells appear to display some type of inherent resistance to ozone exposure. To find potential reasons for the ozone resistance observed by individual bacteria, we hypothesised

that both previous stress exposure and cell age contribute to ozone resistance.

To determine the effect of prior cold exposure on ozone resistance in vitro, a colony of *Pseudomonas* sp. (isolated from coriander) was sub-cultured on to plates and incubated at optimum conditions i.e. 25 °C for 48 h (control) and 4 °C (test) to mimic produce storage conditions for 7 days. A colony of *Pseudomonas* sp. from each temperature plate was serially diluted to a standard concentration of 10^4 cells per mL (maintaining respective temperature conditions) in MRD and 100 μL of the cell suspension was spread on to Cephaloridin Fucidin Centrimide (CFC) agar plates. Each plate (containing either bacteria grown at 4 °C or 25 °C) was then treated with either 1 μL L^{-1} ozone concentration or 'clean air' for 10 min. Colony count was determined after incubating all plates at 25 °C for 48 h.

2.4.3. Colony age effects on ozone resistance of Pseudomonas *sp. in vitro*

To determine whether cell age affected the ozone resistance of bacteria, a colony of the *Pseudomonas* sp. (see Section 2.4.1) was sub-cultured on to CFC plates and incubated at 25 °C for up to 12 days. A single colony was isolated on the 2nd, 4th, 7th, 10th and 12th day of incubation and transferred to MRD. A volume of 10^4 cells per mL of each cell age was spread (100 μL) onto sterile CFC plates and these plates were then exposed to either 1 μL L^{-1} ozone or 'clean air' for 10 min (control). Colony count was determined after incubating CFC plates at 25 °C for 48 h. The% survival of *Pseudomonas* sp. was calculated by comparing the ozone treated colonies to the control colonies (not ozone treated).

2.5. Statistical analysis

Data were analysed using SPSS (IBM SPSS Statistics 19 64Bit) and graphs were produced using Microsoft Office Excel 2010 and SigmaPlot 12.5. Normal data distribution was tested using Normality test and significant differences between mean values were verified using LSD ($P < 0.05$) following one-way ANOVA.

3. Results

3.1. Confocal microscopy: visualization of bacteria on leaves

Spinach leaves were observed using confocal scanning laser microscopy together with LIVE/DEAD® BacLight™ Viability Kit to determine if the bacteria that survived ozone treatment were typically present in colonies or individual cells. Bacteria were attached mainly to the leaf epidermal cell margins, observed at 20× magnification, scale bar – 47.6 μm (Fig. 1).

3.2. Optimized ozone exposure levels to treat leafy produce

All treated leafy produce showed varying levels of discoloration, whereas non-exposed controls showed little to no discolouration. Non-exposed controls and all leaves treated with 1 μL L^{-1} ozone for duration time 10 min or less received a value of '5' on the 5-point scoring scale. All produce scored '1 to 4' with the score reciprocally related to ozone concentration * exposure time. Only coriander and rocket scored '5' when exposed to 10 μL L^{-1} ozone for up to 10 min. Table 1 shows maximum ozone exposure levels achievable to score '5' on the 5-point quality scale.

3.3. Direct enumeration of bacteria on leafy produce after ozone treatment using confocal microscopy

Bacterial viability on non-ozone exposed control leaves was nearly 90% (Fig. 2A and B), whereas only 10% of bacteria on ozone-

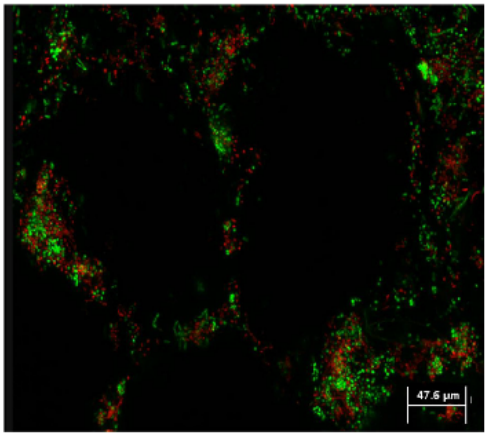

Fig. 1. Confocal microscopy image of a control (not exposed to ozone) baby spinach leaf. Bacteria appeared to attach preferentially to the epidermal cell margins. Scale bar – 47.6 μm.

treated leaf surfaces appeared viable. On control leaves, large aggregations of live cells stained green are visible (see Fig. 2A indicated by the blue arrow). Micro-colonies and cells in twos/threes, as indicated by the orange arrow (Fig. 2A—spinach leaf as an example), were frequent. Individual dead cells stained red are visible in Fig. 2A (indicated by a white arrow). Similar bacterial aggregates were also observed on watercress, coriander, rocket and lettuce leaf surfaces (results not shown). In Fig 2B, yellow arrows indicate individual bacteria surviving ozone treatment. Similar results were also observed on watercress, coriander, rocket and lettuce leaf surfaces (results not shown). Enumeration of bacterial viability after ozone exposure showed at least 1-log reduction in all targeted produce (Fig. 3).

3.4. Investigating potential reasons for bacterial survival on leaf surfaces after ozone treatment

3.4.1. Effect of temperature on ozone resistance of Pseudomonas *sp. in vitro*

Colony numbers (CFU) of *Pseudomonas* sp. grown in optimum conditions (25 °C) in vitro were significantly ($P < 0.05$) reduced by ozone treatment (Fig. 4). In contrast, colony numbers of *Pseudomonas* sp. maintained in cold conditions (i.e. stored at 4 °C) in vitro were not significantly ($P < 0.05$) reduced by ozone treatment (Fig. 4) implying that bacteria submitted to refrigerated conditions show enhanced resistance to ozone.

3.4.2. Effect of age on ozone resistance of the leaf surface bacteria in vitro

Pseudomonas cells derived from 7, 10 and 12 day old colonies showed approximately 40% greater survival to ozone treatment than those from 2 and 4 day old cells (Fig. 5), suggesting that cells from older bacterial colonies are more ozone resistant than cells from younger colonies. The increase in survival was statistically significant ($P < 0.05$).

4. Discussion

Confocal microscopy revealed that bacteria were mainly attached to the epidermal plant cell margins, consistent with the report by Romantschuk et al. (1996). SYTO®9/PI staining in

Table 1
Maximum ozone exposure levels of different types of leafy produce (ozone exposure levels that received a value of '5' on the 5-point quality scale).

Target produce	Ozone exposure limit	
	Concentration of ozone exposure ($\mu L L^{-1}$)	Duration of ozone exposure (min)
Baby spinach	1	10
Watercress	1	10
Coriander	10	10
Lettuce	1	10
Rocket	10	10

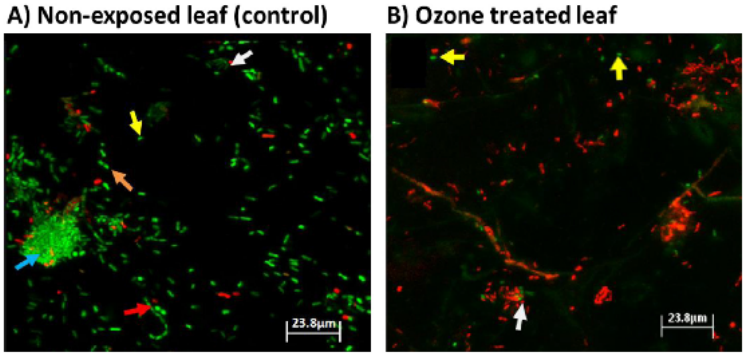

Fig. 2. Confocal microscopy image of a baby spinach leaf. Bacteria were stained with green-fluorescent SYTO®9 to label live bacterial cells green and with red-fluorescent propidium iodide to label dead bacterial cells red. Scale bar – 23.8 µm (A) Non-ozone exposed leaf (control). Blue arrow indicates large aggregates of live cells, orange arrow indicates small colonies in two/threes, red arrow indicates bacteria in chains, yellow arrow indicates individual cells present on a leaf surface and white arrow indicates individual dead cell (B) Leaf treated with 1 $\mu L L^{-1}$ ozone for 10 min. White arrow indicates live cells present in micro-colony of dead cells and yellow arrows indicate individual live cells surviving ozone treatment.

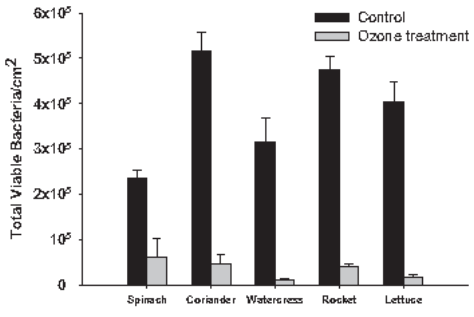

Fig. 3. Total viable bacterial counts from the surfaces of spinach, watercress, and lettuce leaves treated with 1 $\mu L L^{-1}$ ozone and coriander and rocket treated with 10 $\mu L L^{-1}$ (grey bars) versus leaves not treated with ozone and maintained in 'clean air' for an equivalent period (black bars) for 10 min. Data derived from microscopic counts of SYTO®9/PI stained bacteria on leaves. Values represent means (+/−Standard Error) of measurements made on three separate leaves per treatment.

conjunction with CSLM allowed in situ observation of bacteria on untreated leaf surfaces (control) and they appeared to be present as small micro-colonies and as individual cells. Similar observations were obtained by Carmichael et al. (1999) who used fluorescein isothiocyanate (FITC) staining together with confocal imaging techniques to observe both clusters and individual bacteria on the surface of lettuce leaves.

The visual appearance and freshness of leafy produce has been the main judging criteria for quality distinction at purchase or consumption (Rico et al., 2007). No visual discolouration was observed when leafy produce was treated with 1 $\mu L L^{-1}$ gaseous ozone but higher levels, e.g. 10 $\mu L L^{-1}$ for 10 min, caused discolouration to spinach, watercress and lettuce. Similar results were previously observed on fresh produce like lettuce, spinach, rocket leaves when treated with different ozone concentrations (Alexopoulos et al., 2013). Only coriander and rocket leaves retained their appearance when exposed to 10 $\mu L L^{-1}$ ozone treatment. This maybe related to differences in the physiology of the produce e.g., stomatal conductance (Kim et al., 1998; Alexopoulos et al., 2013). Discolouration was observed when high ozone dosages were applied. Bacterial colonization varies between leaves and largely depends on the properties of the leaf surface e.g., leaf surface morphology, hydrophobicity, waxiness, leaf surface chemistry etc (Golberg et al., 2011). Confocal microscopy revealed no obvious link between physical surface morphology and bacterial colonization.

The data presented here indicate that although ozone treatment significantly reduced bacterial viable counts on the leaf surface, approximately 10% of the bacterial flora exhibited resistance to the ozone treatment employed. Confocal images of ozone treated leaves revealed that two/three live cells survived in micro-colonies (surrounded by dead cells). Micro-colonies and biofilms are formed on leaf surfaces due to bacterial attachment and production of exopolymeric substances (Mah and O'Toole, 2001). This motivates microbial cells to stimulate activities unachievable alone or outside of micro-colonies and delivers added protection against UV, desiccation and predation. Moreover, biofilms potentially allow genetic exchange, gene transfer and synergistic interaction between cells (Morris and Monier, 2003). Biofilms allow microbes to remain in close contact and communicate by quorum sensing, and thus, combat anti-microbial treatments as a community (Jahid and Ha,

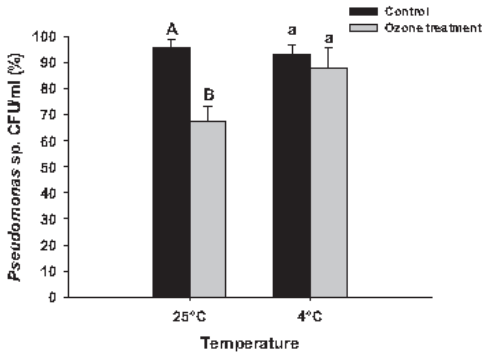

Fig. 4. Impacts of ozone-exposure on *Pseudomonas* sp. grown at 25 °C and 4° C and exposed to either 1 $\mu L\,L^{-1}$ ozone concentration (grey bar) or 'clean' air (black bar) for 10 min. After the treatment plates were incubated at optimum temperature i.e. 25° C for 48 h. Values represent means (±Standard Error) of measurements made on three independent plates per treatment. Bars with different letters are statistically significantly different ($P < 0.05$).

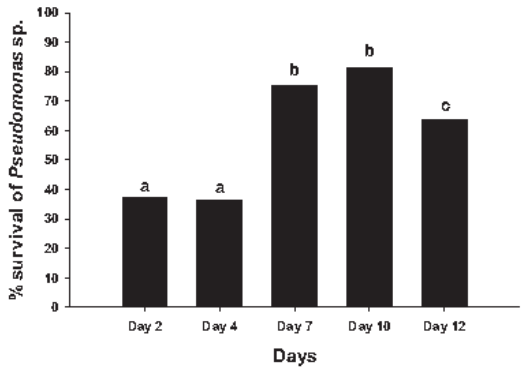

Fig. 5. Survival of cells obtained from different colony ages of *Pseudomonas* sp. exposed to 1 $\mu L\,L^{-1}$ ozone concentration for 10 min. After ozone exposure, the culture plates were maintained at 25 °C for 12 days. Bars with different letters are statistically significantly different ($P < 0.05$).

2012). The survival of bacteria to ozone exposure could also be due to the presence of a small sub-population of persister cells. These cells are invulnerable cells that neither grow nor die, which may enter a highly-protected state exhibiting intense resistance, and develop more commonly in micro-colonies or biofilm (Van Houdt and Michiels, 2010; Bridier et al., 2011). Therefore cells in micro-colonies/biofilms on leaf surfaces may resist ozone treatment by both physical protection (i.e., surrounding cells are killed but the cells in the centre of a colony are physically protected) or by the biofilm bacteria having inherent enhanced resistance mechanisms.

Interestingly, some individual cells on the leaf surface also survived ozone treatment suggesting that they also have inherent resistance mechanisms. We hypothesised that the survival of the individual bacteria on the leaf surface after ozone exposure is influenced by ageing and/or prior exposure to cold (Johnson, 2008; Wani et al., 2015).

During growth in the field, the bacteria present on the surface of leaves are continually subjected to changes in temperature, nutrient availability and osmotic pressure (Beattie and Lindow, 1995). In addition, to prevent microbial spoilage and contamination by pathogens, cumulative mild processing steps are employed during the production of fresh produce increasing chances of additional stress and potentially developing hardy bacteria that are able to resist any further applied treatments such as ozone exposure (Capozzi et al., 2009).

A number of stresses have been shown to induce such 'cross protection', and in this study, cold stress was used as a model to determine if prior stress exposure enhanced the ozone resistance of a typical leaf surface bacterium. Our results suggest that pre-exposure of bacteria (*Pseudomonas* sp.) to cold stress enhanced ozone resistance in vitro. Bacterial survival in stressed conditions requires a combination of cell responses designed to minimise the lethal effects or repair damage (Jozefczuk et al., 2010). When repairing damage, the presence of cold shock proteins in bacteria overcomes growth-limiting effects by either altering redox status or increasing stability of RNA and DNA secondary structures (Reva et al., 2006). Cold shock acclimation proteins are produced in high abundance during low temperature and have been identified in *Pseudomonas* sp. (Reva et al., 2006). Our results indicate that such stress-related temperature responses may also help bacteria to survive subsequent ozone exposure.

We also hypothesised that cell age is a factor contributing to the ozone resistance of individual leaf surface bacteria (Wani et al., 2015). Fresh produce typically takes weeks to grow and any cells present on the leaf surface could easily have been present and persisting for a prolonged period. Our results clearly demonstrated that cells derived from older colonies are more resistant to ozone than cells from younger colonies and this observation is strengthened by previous work showing that older biofilm cells of *Pseudomonas aeruginosa* are more resistant to biocides than younger cells (Bridier et al., 2011) and that the older cells had an increased expression of RpoS genes.

Therefore, further understanding of the molecular basis of ozone resistance of leaf surface bacteria is required. A detailed understanding of the resistance mechanisms involved may help to develop novel methods to control and combat the contamination of fresh produce.

5. Conclusions

This work focused on visualising microbes on leaf surfaces after ozone treatment by using confocal scanning microscopy and investigating potential reasons for ozone resistance in leaf surface bacteria. Confocal microscopy demonstrated that bacterial cells able to survive ozone exposure occurred both in micro-colonies and as individuals on the leaf surface. This suggested that bacterial ozone resistance was likely due to a number of factors e.g. physical protection in small colonies and inherent resistance of individual cells. Subsequent results suggested that cell (colony) age and prior exposure to cold stress of a typical leaf surface bacterium (*Pseudomonas* sp.) enhances ozone resistance in vitro. Therefore, further investigation of the mechanisms determining ozone resistance in aged and cold stressed bacterial cells is required, and this may lead to methods that can overcome resistance. Such applications could deliver significant potential benefits for commercial use.

Author contributions

The work presented is a part of a PhD project funded by the UK-ADHB/HDC (project number FV 386) and was also supported financially by Newcastle University Institute for Sustainability; the data were managed, designed, collected and analyzed by Shreya Wani, who took the lead on writing the manuscript. Ian Singleton and Jeremy Barnes supervised the work, assisted in experimental

design/ideas, data interpretation, manuscript writing and won the grant award.

Conflicts of interest

The authors declare no conflict of interest.

Acknowledgements

This work was supported by AHDB/Horticulture Development Company (HDC); project number PV 386 via award of a PhD studentship to Shreya Wani. The authors would like to thank Dr Matthew Peake for technical support; Dr Trevor Booth (Bio-Imaging services, William Leech Bldg, Newcastle University Medical School, NE2 4HH, UK) for assisting with CSLM; Alan Craig for maintaining and calibrating the ozone fumigation equipment; and Jagpreet K. Maker for editing the manuscript.

References

Alexopoulos, A., Plessas, S., Ceciu, S., Lazar, V., Mantzourani, I., Voidarou, C., Stavropoulou, E., Bezirtzoglou, E., 2013. Evaluation of ozone efficacy on the reduction of microbial population of fresh cut lettuce (*Lactuca sativa*) and green bell pepper (*Capsicum annuum*). Food Control 30, 491–496.

Beattie, G.A., Lindow, S.E., 1999. Bacterial colonization of leaves: a spectrum of strategies. Phytopathol 89, 353–359.

Bridier, A., Briandet, R., Thomas, V., Dubois-Brissonnet, F., 2011. Resistance of bacterial biofilms to disinfectants: a review. Biofouling 27, 1017–1032.

Capozzi, V., Fiocco, D., Amodio, M.L., Gallone, A., Spano, G., 2009. Bacterial stressors in minimally processed food. Int. J. Mol. Sci. 10, 3076–3105.

Carmichael, I., Harper, I.S., Coventry, M.J., Taylor, P.W.J., Wan, J., Hickey, M.W., 1999. Bacterial colonization and biofilm development on minimally processed vegetables. J. Appl. Microbiol. 85, 45s–51s.

Ferrando, M., Spiess, W.E.L., 2000. Review: confocal scanning laser microscopy. A powerful tool in food science revision: microscopia laser confocal de barrido. Una potente herramienta en la ciencia de los alimentos'. Food Sci. Tech. Int. 6, 267–284.

Finkel, S.E., 2006. Long term survival during stationary phase: evolution and the GSAP phenotype. Nat. Rev. Microbiol. 4, 113–120.

Golberg, D., Kroupitski, Y., Belausov, E., Pinto, R., Sela, S., 2011. *Salmonella typhimrium* internalization is variable in leafy vegetables and fresh herbs. Int. J. Food. Microbiol. 145, 250–257.

Goncalves, A.A., 2009. Ozone—an emerging technology for the seafood industry. Braz. Arch. Biol. Technol. 52, 1527–1539.

Jahid, I.K., Ha, S.-D., 2012. A review of microbial biofilms of produce: future challenge to food safety. Food Sci. Biotech. 21, 299–316.

Kim, J.-G., Yousef, A.E., Chism, G.W., 1998. Use of ozone to inactivate microorganisms on lettuce. J. Food Saf. 19, 17–34.

Johnson, L.R., 2008. Microcolony and biofilm formation as a survival strategy for bacteria. J. Theor. Biol. 251, 24–34.

Jozefczuk, S., Klie, S., Catchpole, G., Szymanski, J., Cuadros-Inostroza, A., Steinhauser, D., Selbig, J., Willmitzer, L., 2010. Metabolomic and transcriptomic stress response of *Escherichia coli*. Mol. Syst. Biol. 6, 364.

Beattie, G.A., Lindow, S.E., 1995. The secret life of foliar bacterial pathogens on leaves. Annu. Rev. Phytopathol. 33, 145–172.

Losio, M.N., Pavoni, E., Bilei, S., Bertasi, B., Bove, D., Capuano, F., Farneti, S., Blasi, G., Comin, D., Cardamone, C., Decastelli, L., Delibato, E., De Santis, P., Di Pasquale, S., Gattuso, A., Goffredo, E., Fadda, A., Pisanu, M., De Medici, D., 2015. Microbiological survey of raw and ready-to-eat leafy green vegetables marketed in Italy. Int. J. Food Microbiol. 210, 88–91.

Mah, T.F.C., O'Toole, G.A., 2001. Mechanisms of biofilm resistance to antimicrobial agents. Trends Microbiol. 9, 34–39.

Mahapatra, A.K., Muthukumarappan, K., Julson, J.L., 2005. Applications of ozone, bacteriocins and irradiation in food processing: a review. Crit. Rev. Food Sci. Nutr. 45, 447–461.

Morris, C.E., Monier, J.M., 2003. The ecological significance of biofilm formation by plant-associated bacteria. Annu. Rev. Phytopathol. 41, 429–453.

Naito, S., Takahara, H., 2006. Ozone contribution in food industry in Japan. Ozone Sci. Eng. 28, 425–429.

Olaimat, A.N., Holley, R.A., 2012. Factors influencing the microbial safety of fresh produce: a review. Food Microbiol. 32 (1), 1–19.

Palou, L.S., Smilanick, J.L., Crisosto, C.H., Mansour, M., Plaza, P., 2003. Ozone gas penetration and control of the sporulation of *Penicillium digitatum* and *Penicillium italicum* within commercial packages of oranges during cold storage. Crop Prot. 22, 1133–1134.

Reva, O.N., Weinel, C., Weinel, M., Bohm, K., Stjepandic, D., Hoheisel, J.D., Tummler, B., 2006. Functional genomics of stress response in *Pseudomonas putida* KT2440. J. Bacteriol. 188, 4079–4092.

Rico, D., Martín-Diana, A.B., Barat, J.M., Barry-Ryan, C., 2007. Extending and measuring the quality of fresh-cut fruit and vegetables: a review. Trends Food Sci. Technol. 18, 373–386.

Romantschuk, M., Roine, E., Bjorldof, K., Ojanen, T., Nurmiaho-Lassila, E.-L., Haatela, K., 1996. Microbial attachment to plant aerial surfaces. In: Morris, C.E., Nicot, P. C., Nguyen-The, C. (Eds.), Aerial Plant Surface Microbiology. Plenum Press, New York, pp. 45–57.

Saranraj, P., Stella, D., Reetha, D., 2012. Microbial spoilage of vegetables and its control measures: a review. Int. J. Nat. Prod. Sci. 2, 1–12.

Selinummi, J., Seppälä, J., Yli-Harja, O., Puhakka, J., 2005. Software for quantification of labeled bacteria from digital microscope images by automated image analysis. Biotechniques 39, 859–863.

Srey, S., Jahid, I.K., Ha, S.-D., 2013. Biofilm formation in food industries: a food safety concern. Food Control 31, 572–585.

Van Houdt, R., Michiels, C.W., 2010. Biofilm formation and the food industry, a focus on the bacterial outer surface. J. Appl. Microbiol. 109, 1117–1131.

Wani, S., Maker, J., Thompson, J., Barnes, J., Singleton, I., 2015. Effect of ozone treatment on inactivation of *E. coli* and *Listeria* sp. on spinach. Agriculture 5, 155–169.

Wei, K., Zhou, H., Zhou, T., Gong, J., 2007. Comparison of aqueous ozone and chlorine as sanitizers in the food processing industry: impact on fresh agricultural produce quality. Ozone Sci. Eng. 29, 113–120.

References

Abadias M, Usall J, Anguera M, Solsona C, Vinas I (2008) Microbiological quality of fresh, minimally-processed fruit and vegetables, and sprouts from retail establishments. International Journal of Food Microbiology 123 (1-2):121-129. doi:10.1016/j.ijfoodmicro.2007.12.013

Akbas MY, Ozdemir M (2008) Application of gaseous ozone to control populations of *Escherichia coli*, *Bacillus cereus* and *Bacillus cereus* spores in dried figs. Food Microbiology 25 (2):386-391. doi:10.1016/j.fm.2007.09.007

Alexopoulos A, Plessas S, Ceciu S, Lazar V, Mantzourani I, Voidarou C, Stavropoulou E, Bezirtzoglou E (2013) Evaluation of ozone efficacy on the reduction of microbial population of fresh cut lettuce (*Lactuca sativa*) and green bell pepper (*Capsicum annuum*). Food Control 30 (2):491-496. doi:10.1016/j.foodcont.2012.09.018

Alwi NA, Ali A (2014) Reduction of *Escherichia coli* O157, *Listeria monocytogenes* and *Salmonella enterica* sv. *Typhimurium* populations on fresh-cut bell pepper using gaseous ozone. Food Control 46:304-311. doi:10.1016/j.foodcont.2014.05.037

Arroqui C, Lopez A, Esnoz A, Virseda P (2003) Mathematical model of heat transfer and enzyme inactivation in an integrated blancher cooler. Journal of Food Engineering 58 (3):215-225. doi:10.1016/s0260-8774(02)00371-0

Artes F, and Allende, A. (2005) Processing lines and alternative preservation techniques to prolong the shelf-life of minimally fresh processed leafy vegetables. European Journal of Horticultural Science 70 (5):231 - 245.

Artés F, Gómez P, Aguayo E, Escalona V, Artés-Hernández F (2009) Sustainable sanitation techniques for keeping quality and safety of fresh-cut plant commodities. Postharvest Biology and Technology 51 (3):287-296. doi:10.1016/j.postharvbio.2008.10.003

Barth M, Hankinson TR, Zhuang H, Breidt F (2009) Microbiological Spoilage of Fruits and Vegetables.135-183. doi:10.1007/978-1-4419-0826-1_6

Beattie GA, Lindow SE (1995) The secret life of foliar bacterial pathogens on leaves. Annual Review of Phytopathology 33:145-172.

Beattie GA, Lindow SE. (1999) Bacterial colonization of leaves: A spectrum of strategies. The American Phytopathological Society 89 (5):353-359.

Beloin C, Ghigo JM (2005) Finding gene-expression patterns in bacterial biofilms. Trends in Microbiology 13 (1):16-19. doi:10.1016/j.tim.2004.11.008

Benjamini Y, Hochberg Y (1995) Controlling the false discovery rate: a practical and powerful approach to multiple testing. Journal of the Royal Statistical Society. Series B (Methodological): 289-300.

Bermúdez-Aguirre D, Barbosa-Cánovas GV (2013) Disinfection of selected vegetables under nonthermal treatments: Chlorine, acid citric, ultraviolet light and ozone. Food Control 29 (1):82-90. doi:10.1016/j.foodcont.2012.05.073

Bermúdez-Aguirre D, Wemlinger E, Pedrow P, Barbosa-Cánovas G, Garcia-Perez M (2013) Effect of atmospheric pressure cold plasma (APCP) on the inactivation of *Escherichia coli* in fresh produce. Food Control 34 (1):149-157. doi:10.1016/j.foodcont.2013.04.022

Berney M, Hammes F, Bosshard F, Weilenmann HU, Egli T (2007) Assessment and interpretation of bacterial viability by using the LIVE/DEAD BacLight Kit in combination with flow cytometry. Applied Environmental Microbiology 73 (10):3283-3290. doi:10.1128/AEM.02750-06

Bialka KL, Demirci A (2007) Decontamination of *Escherichia coli* O157:H7 and *Salmonella enterica* on blueberries using ozone and pulsed UV-light. Journal of Food Science 72 (9):M391-396. doi:10.1111/j.1750-3841.2007.00517.x

Bintsis T, Evanthia L-T, Robinson R (2000) Existing and potential applications of ultraviolet light in the food industry - a critical review. Journal of the Science of Food and Agriculture 80 (6):637-645.

Bower CK, Daeschel MA (1999) Resistance responses of microorganisms in food environments. International Journal of Food Microbiology 50:33 - 44.

Brandl MT (2006) Fitness of human enteric pathogens on plants and implications for food safety. Annual Review of Phytopathology 44:367 - 392. doi:10.1146/

Bridier A, Briandet R, Thomas V, Dubois-Brissonnet F (2011) Resistance of bacterial biofilms to disinfectants: a review. Biofouling 27 (9):1017-1032. doi:10.1080/08927014.2011.626899

British Leafy Salad Association (2014) Plough to plate. http://www.britishleafysalads.co.uk/plough/plough-plate.shtml. Accessed on 17/08/15

Burnett SL, Beuchat LR (2000) Human pathogens associated with raw produce and unpasteurized juices, and difficulties in decontamination. Journal of Industrial Microbiology & Biotechnology 25:281-287.

Caponigro V, Ventura M, Chiancone I, Amato L, Parente E, Piro F (2010) Variation of microbial load and visual quality of ready-to-eat salads by vegetable type, season, processor and retailer. Food Microbiology 27 (8):1071-1077. doi:10.1016/j.fm.2010.07.011

Capozzi V, Fiocco D, Amodio ML, Gallone A, Spano G (2009) Bacterial stressors in minimally processed food. International Journal of Molecular Sciences 10 (7):3076-3105. doi:10.3390/ijms10073076

Carmichael I, Harper IS, Coventry MJ, Taylor PWJ, Wan J, Hickey MW (1999) Bacterial colonization and biofilm development on minimally processed vegetables. Journal of Applied Microbiology Symposium Supplement, 85:45s-51s.

Chen G, Wang C, Shi T (2011) Overview of available methods for diverse RNA-Seq data analyses. Science China Life sciences 54 (12):1121-1128. doi:10.1007/s11427-011-4255-x

Coenye T (2010) Response of sessile cells to stress: from changes in gene expression to phenotypic adaptation. FEMS Immunology and Medical Microbiology 59 (3):239-252. doi:10.1111/j.1574-695X.2010.00682.x

Coia JE (1998) Clinical, microbiological and epidemiological aspects of *Escherichia coli* O157 infection. FEMS Immunology & Medical Microbiology 20:1-9.

Collins LJ, Moulton V, Penny D (2000) Use of RNA secondary structure for studying the evolution of RNase P and RNase MRP. Journal of Molecular Evolution 51 (3):194-204.

Corbo MR, Del Nobile MA, Sinigaglia M (2006) A novel approach for calculating shelf life of minimally processed vegetables. International Journal of Food Microbiology 106 (1):69-73. doi:10.1016/j.ijfoodmicro.2005.05.012

Critzer FJ, Doyle MP (2010) Microbial ecology of foodborne pathogens associated with produce. Current Opinion in Biotechnology 21 (2):125-130. doi:10.1016/j.copbio.2010.01.006

Cui X, Shang Y, Shi Z, Xin H, Cao W (2009) Physicochemical properties and bactericidal efficiency of neutral and acidic electrolyzed water under different storage conditions. Journal of Food Engineering 91 (4):582-586. doi:10.1016/j.jfoodeng.2008.10.006

Da Silva Felicio MT, Hald T, Liebana E, Allende A, Hugas M, Nguyen-The C, Johannessen GS, Niskanen T, Uyttendaele M, McLauchlin J (2015) Risk ranking of pathogens in ready-to-eat unprocessed foods of non-animal origin (FoNAO) in the EU: initial evaluation using outbreak data (2007-2011). International Journal of Food Microbiology 195:9-19. doi:10.1016/j.ijfoodmicro.2014.11.005

Davidson PM, Harrison MA (2002) Resistance and adaptation to food antimicrobials, sanitizers and other process controls. Food Technology 56 (1):69-78.

Dees MW, Lysoe E, Nordskog B, Brurberg MB (2015) Bacterial communities associated with surfaces of leafy greens: shift in composition and decrease in richness over time. Applied Environmental Microbiology 81 (4):1530-1539. doi:10.1128/AEM.03470-14

Dotsch A, Eckweiler D, Schniederjans M, Zimmermann A, Jensen V, Scharfe M, Haussler S (2012) The Pseudomonas aeruginosa transcriptome in planktonic cultures and static biofilms using RNA sequencing. PLoS one 7 (2):e31092

Dumont J, Spicher F, Montpied P, Dizengremel P, Jolivet Y, Le Thiec D (2013) Effects of ozone on stomatal responses to environmental parameters (blue light, red light, CO2 and vapour pressure deficit) in three Populus deltoides x Populus nigra genotypes. Environmental Pollution 173:85-96. doi:10.1016/j.envpol.2012.09.026

Engels C, Weiss A., Carle R., Schmidt H., Schieber A., Ganzle MG (2012) Effect of gallotannin treatment on attachment, growth and survival of *Escherichia coli* O157:H7 and *Listeria monocytogenes* on spinach and lettuce European Food Research and Technology 234:1081-1090. doi:10.1007/s00217-012-1727-6

Evans AA, Donahue RE (2008) Laser scanning confocal microscopy: a potential technique for the study of lithic microwear. Journal of Archaeological Science 35 (8):2223-2230. doi:10.1016/j.jas.2008.02.006

Fan L, Song J, McRae KB, Walker BA, Sharpe D (2007) Gaseous ozone treatment inactivates *Listeria innocua in vitro*. Journal of Applied Microbiology 103 (6):2657-2663. doi:10.1111/j.1365-2672.2007.03522.x

Farber JM Peterkin PI (1991) *Listeria monocytogenes*, a Food-Borne pathogen. American Society for Microbiology 55 (3):476 - 511.

Feller G (2013) Psychrophilic enzymes: from folding to function and biotechnology. Scientifica 2013:512840. doi:10.1155/2013/512840

Fernandez A, Shearer N, Wilson DR, Thompson A (2012) Effect of microbial loading on the efficiency of cold atmospheric gas plasma inactivation of *Salmonella enterica serovar Typhimurium*. International Journal of Food Microbiology 152 (3):175-180. doi:10.1016/j.ijfoodmicro.2011.02.038

Ferrando M, Spiess WEL (2000) Review: Confocal scanning laser microscopy. A powerful tool in food science Revision: Microscopia laser confocal de barrido. Una potente herramienta en la ciencia de los alimentos. Food Science and Technology International 6 (4):267-284. doi:10.1177/108201320000600402

Finkel SE (2006) Long-term survival during stationary phase: evolution and the GASP phenotype. Nature Reviews Microbiology 4 (2):113-120.

Fonseca JM, Fallon SD, Sanchez CA, Nolte KD (2011a) *Escherichia coli* survival in lettuce fields following its introduction through different irrigation systems. Journal of Applied Microbiology. doi:10.1111/j.1365-2672.2011.04942.x

Fonseca P, Moreno R, Rojo F (2011b) Growth of *Pseudomonas putida* at low temperature: global transcriptomic and proteomic analyses. Environmental microbiology reports 3 (3):329-339. doi:10.1111/j.1758-2229.2010.00229.x

Fonseca P, Moreno R, Rojo F (2013) *Pseudomonas putida* growing at low temperature shows increased levels of CrcZ and CrcY sRNAs, leading to reduced Crc-dependent catabolite repression. Environmental Microbiology 15 (1):24-35. doi:10.1111/j.1462-2920.2012.02708.x

Food Standards Agency (2004a) Aviation House, London, UK.

Francis GA, O'Beirne D (1998) Effects of the indigenous microflora of minimally processed lettuce on the surviavl and growth of *Listeria innocua*. International Journal of Food Science and Technology 33:477-488.

Frank S, Schmidt F, Klockgether J, Davenport CF, Gesell Salazar M, Volker U, Tummler B (2011) Functional genomics of the initial phase of cold adaptation of *Pseudomonas putida* KT2440. FEMS microbiology letters 318 (1):47-54. doi:10.1111/j.1574-6968.2011.02237.x

Gil MI, Selma MV, Lopez-Galvez F, Allende A (2009) Fresh-cut product sanitation and wash water disinfection: problems and solutions. International Journal of Food Microbiology 134 (1-2):37-45. doi:10.1016/j.ijfoodmicro.2009.05.021

Gil MI, Selma MV, Suslow T, Jacxsens L, Uyttendaele M, Allende A (2015) Pre- and postharvest preventive measures and intervention strategies to control microbial food safety hazards of fresh leafy vegetables. Critical Reviews in Food Science and Nutrition 55 (4):453-468. doi:10.1080/10408398.2012.657808

Gleeson E, O'Beirne D (2005) Effects of process severity on survival & growth of *Escherichia coli* & *Listeria innocua* on minimally processed vegetables. Food Control 16:677 - 685. doi:10.1016/j.foodcont.2004.06.004

Glowacz M, Colgan R, Rees D (2014) The use of ozone to extend the shelf-life and maintain quality of fresh produce. Journal of the Science of Food and Agriculture.. doi:10.1002/jsfa.6776

Gomez-Lozano M, Marvig RL, Molina-Santiago C, Tribelli PM, Ramos JL, Molin S (2015) Diversity of small RNAs expressed in *Pseudomonas* species. Environmental microbiology reports 7 (2):227-236. doi:10.1111/1758-2229.12233

Goncalves AA (2009a) Ozone - an Emerging Technology for the Seafood Industry. Brazilian Archives of Biology and Technology 52 (6):1527-1539.

Goncalves AA (2009b) Ozone an emerging technology for the seafood industry. Brazilian Archives of Biology and Technology 52 (6):1527-1539.

Goodburn C, Wallace CA (2013) The microbiological efficacy of decontamination methodologies for fresh produce: A review. Food Control 32 (2):418-427. doi:10.1016/j.foodcont.2012.12.012

Gopalan V, Baxevanis AD, Landsman D, Altman S (1997) Analysis of the functional role of conserved residues in the protein subunit of ribonuclease P from *Escherichia coli*. Journal of Molecular Biology 267 (4):818-829.

Gottesman S (2005) Micros for microbes: non-coding regulatory RNAs in bacteria. Trends in genetics : TIG 21 (7):399-404. doi:10.1016/j.tig.2005.05.008

Griffin PM, Tauxe RV (1991) The epidemiology of infections caused by *Escherichia coli* O157:H7, other enterohemorrhagic *E.coli*, and the associated Hemolytic Uremic Syndrome. Epidemiologic Reviews 13:60-99.

Gruegelsiepe H, Brandt O, Hartmann RK (2006) Antisense inhibition of RNase P: mechanistic aspects and application to live bacteria. The Journal of Biological Chemistry 281 (41):30613-30620. doi:10.1074/jbc.M603346200

Guzel-Seydim ZB, Greene AK, Seydim AC (2004) Use of ozone in the food industry. LWT - Food Science and Technology 37 (4):453-460. doi:10.1016/j.lwt.2003.10.014

Heaton JC, Jones K (2008) Microbial contamination of fruit and vegetables and the behaviour of enteropathogens in the phyllosphere: a review. Journal of Applied Microbiology 104 (3):613-626. doi:10.1111/j.1365-2672.2007.03587.x

Hems RS, Gulabivala K, Ng Y-L, Ready D, Spratt DA (2005) An *in vitro* evaluation of the ability of ozone to kill a strain of *Enterococcus faecalis*. International Endodontic Journal 38:22-29.

Hengge-Aronis R (2002) Stationary phase gene regulation:what makes an *Escherichia coli* promoter σ S-selective? Current Opinion in Microbiology 5 (6):591-595.

Holvoet K (2010) A quantitative microbial risk assessment of water in the fresh produce. http://www.enbichem.ugent.be/content/qmrafreshcut. Acessed on 17/08/15.

Horvitz S, Cantalejo MJ (2014) Application of ozone for the postharvest treatment of fruits and vegetables. Critical Reviews in Food Science and Nutrition 54 (3):312-339. doi:10.1080/10408398.2011.584353

Hutchison ML, Walters LD, Moore A, Crookes KM, Avery SM (2004) Effect of length of time before incorporation on survival of pathogenic bacteria present in livestock wastes applied to agricultural soil. Applied and Environmental Microbiology 70 (9):5111-5118. doi:10.1128/AEM.70.9.5111-5118.2004

Jacxsens L, Devlieghere F, Ragaert P, Vanneste E, Debevere J (2003) Relation between microbiological quality, metabolite production and sensory quality of equilibrium modified atmosphere packaged fresh-cut produce. International Journal of Food Microbiology 83 (3):263-280. doi:10.1016/s0168-1605(02)00376-8

Jacxsens L, Devlieghere F, Debevere J (2002) Temperature dependence of shelf-life as affected by microbial proliferation and sensory quality of equilibrium modified atmosphere packaged fresh produce. Postharvest Biology and Technology 26 (1):59-73.

Jahid IK, Ha S-D (2012) A review of microbial biofilms of produce: Future challenge to food safety. Food Science and Biotechnology 21 (2):299-316. doi:10.1007/s10068-012-0041-1

Jin-Gab K, Yousef AE, Chism GW (1998) Use of ozone to inactivate microorganisms on lettuce. Journal of Food Satefy 19 (1):17-34.

Johnson LR (2008) Microcolony and biofilm formation as a survival strategy for bacteria. Journal of theoretical biology 251 (1):24-34. doi:10.1016/j.jtbi.2007.10.039

Joshi K, Mahendran R, Alagusundaram K, Norton T, Tiwari BK (2013) Novel disinfectants for fresh produce. Trends in Food Science & Technology 34 (1):54-61. doi:10.1016/j.tifs.2013.08.008

Jozefczuk S, Klie S, Catchpole G, Szymanski J, Cuadros-Inostroza A, Steinhauser D, Selbig J, Willmitzer L (2010) Metabolomic and transcriptomic stress response of *Escherichia coli*. Molecular Systems Biology 6:364. doi:10.1038/msb.2010.18

Karaca H, Velioglu YS (2014) Effects of ozone treatments on microbial quality and some chemical properties of lettuce, spinach, and parsley. Postharvest Biology and Technology 88:46-53. doi:10.1016/j.postharvbio.2013.09.003

Karaca H, Velioglu YS (2007) Ozone applications in fruit and vegetable processing. Food Reviews International 23: 91-106.

Katz S, Hershberg R (2013) Elevated mutagenesis does not explain the increased frequency of antibiotic resistant mutants in starved aging colonies. PLoS genetics 9 (11):e1003968. doi:10.1371/journal.pgen.1003968

Khadre MA, Kim JG (2001) Microbiological aspects of ozone applications in food: A review. Journal of Food Science 66 (9):1242-1252.

Klockow PA, Keener KM (2009) Safety and quality assessment of packaged spinach treated with a novel ozone-generation system. Food Science and Technology 42:1047-1053. doi:10.1016/j.lwt.2009.02.011

Launders N, Byrne, L., Adams, N., Glen, K., Jenkins, C., Tubin-Delic, D., Locking, M., Williams, and C., Morgan, D. (2013) Outbreak of Shiga toxin-producing *E.coli* O157 associated with consumption of watercress, United Kingdom, August to September 2013. Eurosurveillance 18 (44):1-5.

Lee DH, Kim JB, Kim M, Roh E, Jung K, Choi M, Oh C, Choi J, Yun J, Heu S (2013) Microbiota on spoiled vegetables and their characterization. Journal of Food Protection 76 (8):1350-1358. doi:10.4315/0362-028X.JFP-12-439

Leuko S, Legat A, Fendrihan S, Stan-Lotter H (2004) Evaluation of the LIVE/DEAD BacLight kit for detection of extremophilic archaea and visualization of microorganisms in environmental hypersaline samples. Applied and Environmental Microbiology 70 (11):6884-6886. doi:10.1128/AEM.70.11.6884-6886.2004

Lindow SE, Brandl MT (2003) Microbiology of the Phyllosphere. Applied and Environmental Microbiology 69 (4):1875-1883. doi:10.1128/aem.69.4.1875-1883.2003

Little B, Wagner P, Ray R, Pope R, Scheetz R (1991) Biofilms: an ESEM evaluation of artifacts introduced during SEM preparation. Journal of Industrial Microbiology 8:213-222.

Little CL, Gillespie IA (2008) Prepared salads and public health. Journal of Applied Microbiology 105 (6):1729-1743. doi:10.1111/j.1365-2672.2008.03801.x

Lohse M, Bolger A, Nagel A, Fernie AR, Lunn JE, Stitt M, Usadel B (2012) RobiNA: a user-friendly, integrated software solution for RNA-Seq-based transcriptomics. Nucleic acids research gks540.

Lu Z, Yu Z, Gao X, Lu F, Zhang L (2005) Preservation effects of gamma irradiation on fresh-cut celery. Journal of Food Engineering 67 (3):347-351. doi:10.1016/j.jfoodeng.2004.04.038

Lucchetti-Miganeh C, Burrowes E, Baysse C, Ermel G (2008) The post-transcriptional regulator CsrA plays a central role in the adaptation of bacterial pathogens to different stages of infection in animal hosts. Microbiology 154 (Pt 1):16-29. doi:10.1099/mic.0.2007/012286-0

Luo Y, He Q, McEvoy JL (2010) Effect of storage temperature and duration on the behavior of *Escherichia coli* O157:H7 on packaged fresh-cut salad containing romaine and iceberg lettuce. Journal of Food Science 75 (7):M390-397. doi:10.1111/j.1750-3841.2010.01722.x

Mah TFC, O'Toole GA (2001) Mechanisms of biofilm resistance to antimicrobial agents. Trends in Microbiology 9 (1):34-39.

Mahapatra AK, Muthukumarappan K, Julson JL (2005) Applications of ozone, bacteriocins and irradiation in food processing: a review. Critical reviews in Food Science and Nutrition 45 (6):447-461. doi:10.1080/10408390591034454

Malone JH, Oliver B (2011) Microarrays, deep sequencing and the true measure of the transcriptome. BMC biology 9:34. doi:10.1186/1741-7007-9-34

Marles-Wright J, Lewis RJ (2007) Stress responses of bacteria. Current Opinion in Structural Biology 17 (6):755-760. doi:10.1016/j.sbi.2007.08.004

Martínez-Vaz BM, Fink RC, Diez-Gonzalez F, Sadowsky MJ (2014) Enteric Pathogen-Plant Interactions: Molecular Connections Leading to Colonization and Growth and Implications for Food Safety. Microbes and Environments 29 (2):123-135. doi:10.1264/jsme2.ME13139

Mattick JS, Makunin IV (2006) Non-coding RNA. Human molecular genetics 15 (suppl 1):R17-R29.

McCormick KP, Willmann MR, Meyers BC (2011) Experimental design, preprocessing, normalization and differential expression analysis of small RNA sequencing experiments. Silence 2 (1):2.

McDonald K, Sun D-W (2000) Vacuum cooling technology for the food processing industry: a review. Journal of Food Engineering 45:55-65.

Mercanoglu TB, Halkman AK (2011) Do leafy green vegetables and their ready-to-eat [RTE] salads carry a risk of foodborne pathogens? Anaerobe 17 (6):286-287. doi:10.1016/j.anaerobe.2011.04.004

Mercier J, Lindow SE (2000) Role of Leaf Surface Sugars in Colonization of Plants by Bacterial Epiphytes. Applied and Environmental Microbiology 66 (1):369-374. doi:10.1128/aem.66.1.369-374.2000

Miller FA, Silva CLM, Brandão TRS (2013) A Review on Ozone-Based Treatments for Fruit and Vegetables Preservation. Food Engineering Reviews 5 (2):77-106. doi:10.1007/s12393-013-9064-5

Mohamed MRM, Raja A, Mohamed HS, Sheik MA (2012) Screening of bacterial compost from spoiled vegetables and fruits and their physiochemical characterization. International Food Research Journal 19 (3):1193-1198.

Monier JM, Lindow SE (2005) Aggregates of resident bacteria facilitate survival of immigrant bacteria on leaf surfaces. Microbial Ecology 49:343-352.

Moreno R, Rojo F (2014) Features of pseudomonads growing at low temperatures: another facet of their versatility. Environmental Microbiology reports 6 (5):417-426. doi:10.1111/1758-2229.12150

Morris CE, Monier JM (2003) The ecological significance of biofilm formation by plant-associated bacteria. Annual Review of Phytopathology 41:429-453. doi:10.1146/annurev.phyto.41.022103.134521

Muller T, Ruppel S (2014) Progress in cultivation-independent phyllosphere microbiology. FEMS Microbiology Ecology 87 (1):2-17. doi:10.1111/1574-6941.12198

Naito S, Takahara H (2006) Ozone Contribution in Food Industry in Japan. Ozone: Science & Engineering 28 (6):425-429. doi:10.1080/01919510600987347

Navarro Llorens JM, Tormo A, Martinez-Garcia E (2010) Stationary phase in gram-negative bacteria. FEMS Microbiology Reviews 34 (4):476-495. doi:10.1111/j.1574-6976.2010.00213.x

Niemira BA (2012) Cold plasma decontamination of foods. Annual Review of Food Science and Technology 3:125-142. doi:10.1146/annurev-food-022811-101132

Nogales CG, Ferrari PH, Kantorovich EO, Lage-Marques JL (2008) Ozone Therapy in Medicine and Dentistry. The Journal of Contemporary Dental Practice 9 (4):1-9.

Olaimat AN, Holley RA (2012) Factors influencing the microbial safety of fresh produce: a review. Food Microbiology 32 (1):1-19. doi:10.1016/j.fm.2012.04.016

Ohlsson T, Bengtsson (2002) Minimal Processing of foods with non-thermal methods. Minimal Processing Technologies in the Food Industry: 34-60.

Ölmez H, Akbas MY (2009) Optimization of ozone treatment of fresh-cut green leaf lettuce. Journal of Food Engineering 90 (4):487-494. doi:10.1016/j.jfoodeng.2008.07.026

Ölmez H, Kretzschmar U (2009) Potential alternative disinfection methods for organic fresh-cut industry for minimizing water consumption and environmental impact. LWT - Food Science and Technology 42 (3):686-693. doi:10.1016/j.lwt.2008.08.001

Paddock SW (2000) Principles and practices of laser scanning confocal microscopy. Molecular Biotechnology 16 127-149.

Parish ME, Beuchat LR, Suslow TV, Harris LJ, Garrett EH, Farber JN, Busta FF (2003) Methods to reduce/eliminate pathogens from fresh and fresh-cut pathogens. Comprehensive Reviews in Food Science and Food Safety 2:161-173.

Park JS, Kihm KD (2006) Use of confocal laser scanning microscopy (CLSM) for depthwise resolved microscale-particle image velocimetry (μ-PIV). Optics and Lasers in Engineering 44 (3-4):208-223. doi:10.1016/j.optlaseng.2005.04.005

Perry JJ, Yousef AE (2011) Decontamination of raw foods using ozone-based sanitization techniques. Annual Review of Food Science and Technology 2:281-298. doi:10.1146/annurev-food-022510-133637

Pinto AC, Melo-Barbosa HP, Miyoshi A, Silva A, Azevedo V (2011) Application of RNA-seq to reveal the transcript profile in bacteria. Genetics and Molecular research : GMR 10 (3):1707-1718

Prakash A, Inthajak P, Huibregtse H, Caporaso F, Foley DM (2000) Effects of low-dose gamma irradiation and conventional treatments on shelf life and quality characteristics of diced celery. Journal of Food Science 65 (6):1070-1075.

Ragaert P, Devlieghere F, Debevere J (2007) Role of microbiological and physiological spoilage mechanisms during storage of minimally processed vegetables. Postharvest Biology and Technology 44 (3):185-194. doi:10.1016/j.postharvbio.2007.01.001

Ramos B, Miller FA, Brandão TRS, Teixeira P, Silva CLM (2013) Fresh fruits and vegetables—An overview on applied methodologies to improve its quality and safety. Innovative Food Science & Emerging Technologies 20:1-15. doi:10.1016/j.ifset.2013.07.002

Rastogi G, Sbodio A, Tech JJ, Suslow TV, Coaker GL, Leveau JH (2012) Leaf microbiota in an agroecosystem: spatiotemporal variation in bacterial community composition on field-grown lettuce. The ISME journal 6 (10):1812-1822. doi:10.1038/ismej.2012.32

Repoila F, Darfeuille F (2009) Small regulatory non-coding RNAs in bacteria: physiology and mechanistic aspects. Biology of the cell / under the auspices of the European Cell Biology Organization 101 (2):117-131. doi:10.1042/BC20070137

Reva ON, Weinel C, Weinel M, Bohm K, Stjepandic D, Hoheisel JD, Tummler B (2006) Functional genomics of stress response in Pseudomonas putida KT2440. Journal of Bacteriology 188 (11):4079-4092. doi:10.1128/JB.00101-06

Rico D, Martín-Diana AB, Barat JM, Barry-Ryan C (2007) Extending and measuring the quality of fresh-cut fruit and vegetables: a review. Trends in Food Science & Technology 18 (7):373-386. doi:10.1016/j.tifs.2007.03.011

Romeo T, Vakulskas CA, Babitzke P (2013) Post-transcriptional regulation on a global scale: form and function of Csr/Rsm systems. Environmental Microbiology 15 (2):313-324. doi:10.1111/j.1462-2920.2012.02794.x

Romling U, Balsalobre C (2012) Biofilm infections, their resilience to therapy and innovative treatment strategies. Journal of Internal Medicine 272 (6):541-561. doi:10.1111/joim.12004

Rubio M, Rodriguez-Moreno L, Ballester AR, de Moura MC, Bonghi C, Candresse T, Martinez-Gomez P (2015) Analysis of gene expression changes in peach leaves in response to Plum pox virus infection using RNA-Seq. Molecular Plant Pathology 16 (2):164-176. doi:10.1111/mpp.12169

Saint-Ruf C G-TM, Collin V, Cordier C, Franceschi C, Matic I (2014) Massive diversification in aging colonies of *Escherichia coli*. Journal of Bacteriology 196 (17):3059-3073. doi:10.1128/JB.01421-13

Saranraj P, Stella, D., and Reetha, D. (2012) Microbial spoilage of vegetables and its control measures: a review. International Journal of Natural Product Science 2 (2):1-12.

Sathe SJ, Nawani NN, Dhakephalkar PK, Kapadnis BP (2007) Antifungal lactic acid bacteria with potential to prolong shelf-life of fresh vegetables. Journal of Applied Microbiology 103 (6):2622-2628. doi:10.1111/j.1365-2672.2007.03525.x

Schluter O, Ehlbeck J, Hertel C, Habermeyer M, Roth A, Engel KH, Holzhauser T, Knorr D, Eisenbrand G (2013) Opinion on the use of plasma processes for treatment of foods. Molecular Nutrition & Food Research 57 (5):920-927. doi:10.1002/mnfr.201300039

Scifò GO, Randazzo CL, Restuccia C, Fava G, Caggia C (2009) *Listeria innocua* growth in fresh cut mixed leafy salads packaged in modified atmosphere. Food Control 20 (7):611-617. doi:10.1016/j.foodcont.2008.08.017

Selinummi J, Seppälä J, Yli-Harja O, Puhakka J (2005) Software for quantification of labeled bacteria from digital microscope images by automated image analysis. BioTechniques 39 (6):859-863. doi:10.2144/000112018

Selma MV, Allende A, Lopez-Galvez F, Conesa MA, Gil MI (2008) Disinfection potential of ozone, ultraviolet-C and their combination in wash water for the fresh-cut vegetable industry. Food Microbiology 25 (6):809-814. doi:10.1016/j.fm.2008.04.005

Seo KH, Frank JF (1998) Attachment of *Escherichia coli* O157:H7 to lettuce leaf surface and bacterial viability in response to chlorine treatment as demonstrated by using confocal scanning laser microscopy. Journal of Food Protection, 62:3-9.

Sharma M, Beuchat LR (2004) Sensitivity of *Escherichia coli* O157:H7 to Commercially Available Alkaline Cleaners and Subsequent Resistance to Heat and Sanitizers. Applied and Environmental Microbiology 70 (3):1795-1803. doi:10.1128/aem.70.3.1795-1803.2004

Singh N, Singh RK, Bhunia AK, Stroshine RL (2002) Efficacy of Chlorine Dioxide, Ozone, and Thyme Essential Oil or a Sequential Washing in Killing *Escherichia coli* O157:H7 on Lettuce and Baby Carrots. LWT - Food Science and Technology 35 (8):720-729. doi:10.1006/fstl.2002.0933

Song J-Y, An G-H, Kim C-J (2003) Color, texture, nutrient contents, and sensory values of vegetable soybeans [Glycine max (L.) Merrill] as affected by blanching. Food Chemistry 83 (1):69-74. doi:10.1016/s0308-8146(03)00049-9

Sorek R, Cossart P (2010) Prokaryotic transcriptomics: a new view on regulation, physiology and pathogenicity. Nature reviews Genetics 11 (1):9-16. doi:10.1038/nrg2695

Stepanyan K, Wenseleers T, Duenez-Guzman EA, Muratori F, Van den Bergh B, Verstraeten N, De Meester L, Verstrepen KJ, Fauvart M, Michiels J (2015) Fitness trade-offs explain low levels of persister cells in the opportunistic

pathogen *Pseudomonas aeruginosa*. Molecular Ecology 24 (7):1572-1583. doi:10.1111/mec.13127

Sun D-W, Zheng L (2006) Vacuum cooling technology for the agri-food industry: Past, present and future. Journal of Food Engineering 77 (2):203-214. doi:10.1016/j.jfoodeng.2005.06.023

Takayama K, Kjelleberg S (2000) The role of RNA stability during bacterial stress responses and starvation. Environmental Microbiology 2 (4):355-365.

Thaipisuttikul I, Hittle LE, Chandra R, Zangari D, Dixon CL, Garrett TA, Rasko DA, Dasgupta N, Moskowitz SM, Malmstrom L, Goodlett DR, Miller SI, Bishop RE, Ernst RK (2014) A divergent *Pseudomonas aeruginosa* palmitoyltransferase essential for cystic fibrosis-specific lipid A. Molecular Microbiology 91 (1):158-174. doi:10.1111/mmi.12451

Todd ECD, Notemans S (2011) Surveillance of listeriosis and its causative pathogen, *Listeria monocytogenes*. Food Control 22 (9):1484-1490. doi:10.1016/j.foodcont.2010.07.021

Tomas-Callejas A, Lopez-Velasco G, Camacho AB, Artes F, Artes-Hernandez F, Suslow TV (2011) Survival and distribution of *Escherichia coli* on diverse fresh-cut baby leafy greens under preharvest through postharvest conditions. International Journal of Food Microbiology 151 (2):216-222. doi:10.1016/j.ijfoodmicro.2011.08.027Tournas VH (2005a) Moulds and yeasts in fresh and minimally processed vegetables, and sprouts. International journal of food microbiology 99 (1):71-77. doi:10.1016/j.ijfoodmicro.2004.08.009

Tournas VH (2005a) Moulds and yeasts in fresh and minimally processed vegetables, and sprouts. International Journal of Food Microbiology 99 (1):71-77. doi:10.1016/j.ijfoodmicro.2004.08.009

Tournas VH (2005b) Spoilage of vegetable crops by bacteria and fungi and related health hazards. Critical Reviews in Microbiology 31 (1):33-44. doi:10.1080/10408410590886024

Tyrell DA, George KJ (2006) Finite Element Modelling of the Hydrodynamics and Water Quality of the Patos Lagoon System, Brazil. Journal of Coastal Research (2006): 1594-1599.

Tzortzakis N, Borland A, Singleton I, Barnes J (2007) Impact of atmospheric ozone-enrichment on quality-related attributes of tomato fruit. Postharvest Biology and Technology 45 (3):317-325. doi:10.1016/j.postharvbio.2007.03.004

Van Houdt R, Michiels CW (2010) Biofilm formation and the food industry, a focus on the bacterial outer surface. Journal of Applied Microbiology 109 (4):1117-1131. doi:10.1111/j.1365-2672.2010.04756.x

Vaz-Velho M, Silva, M., Pessoa, J., and Gibbs, P. (2006) Inactivation by ozone of *Listeria innocua* on salmon-trout during cold-smoke processing. Food Control 17 (8):609-619. doi:10.1016/j.foodcont.2005.03.007

Velusamy V, Arshak K, Korostynska O, Oliwa K, Adley C (2010) An overview of foodborne pathogen detection: in the perspective of biosensors. Biotechnology advances 28 (2):232-254. doi:10.1016/j.biotechadv.2009.12.004

Waite RD, Paccanaro A, Papakonstantinopoulou A, Hurst JM, Saqi M, Littler E, Curtis MA (2006) Clustering of *Pseudomonas aeruginosa* transcriptomes from planktonic cultures, developing and mature biofilms reveals distinct expression profiles. BMC Genomics 7:162. doi:10.1186/1471-2164-7-162

Wang Z, Gerstein M., Snyder M. (2009) RNA-Seq: a revolutionary tool for transcriptomics. Genetics 10:57-63.

Wani S, Barnes J, Singleton I (2016) Investigation of potential reasons for bacterial survival on 'ready-to-eat' leafy produce during exposure to gaseous ozone. Postharvest Biology and Technology 111:185-190. doi:10.1016/j.postharvbio.2015.08.007

Wani S, Maker J, Thompson J, Barnes J, Singleton I (2015) Effect of Ozone Treatment on Inactivation of *Escherichia coli* and *Listeria* sp. on Spinach. Agriculture 5 (2):155-169. doi:10.3390/agriculture5020155

Warning A, Datta AK (2013) Interdisciplinary engineering approaches to study how pathogenic bacteria interact with fresh produce. Journal of Food Engineering 114 (4):426-448. doi:10.1016/j.jfoodeng.2012.09.004

Wilhelm BT, Landry JR (2009) RNA-Seq-quantitative measurement of expression through massively parallel RNA-sequencing. Methods 48 (3):249-257. doi:10.1016/j.ymeth.2009.03.016#

WRAP (2012) Household food and drink waste in the UK. http://www.wrap.org.uk/sites/files/wrap/hhfdw-2012-main.pdf.pdf. Accessed on 17/08/2015.

Xia JH, Liu P, Liu F, Lin G, Sun F, Tu R, Yue GH (2013) Analysis of stress-responsive transcriptome in the intestine of Asian seabass (*Lates calcarifer*) using RNA-seq. DNA research : an international journal for rapid publication of reports on genes and genomes 20 (5):449-460. doi:10.1093/dnares/dst022

Yuk H-G, Yoo M-Y, Yoon J-W, Marshall DL, Oh D-H (2007) Effect of combined ozone and organic acid treatment for control of *Escherichia coli* O157:H7 and *Listeria monocytogenes* on enoki mushroom. Food Control 18 (5):548-553. doi:10.1016/j.foodcont.2006.01.004

Zhoa S, Fung-Leung W-P, Bittner A, Ngo k, Liu X (2014) Comparison of RNA-Seq and Microarray in Transcriptome Profiling of Activated T Cells. PLOS ONE 9 (1):e78644. doi:10.1371/journal.pone.0078644.g001

Zuma F, Lin J, Jonnalagadda SB (2009) Ozone-initiated disinfection kinetics of *Escherichia coli* in water. Journal of Environmental Science and Health Part A, Toxic/hazardous Substances & Environmental Engineering 44 (1):48-56. doi:10.1080/10934520802515335